Gondwana Research xxx (2013) xxx–xxx

Contents lists available at SciVerse ScienceDirect

Gondwana Research

journal homepage: www.elsevier.com/locate/gr

GR Focus Review

Phanerozoic continental growth and gold metallogeny of Asia

Richard J. Goldfarb [a,b,c,*], Ryan D. Taylor [a], Gregory S. Collins [d], Nikolay A. Goryachev [e], Omero Felipe Orlandini [f]

[a] U.S. Geological Survey, Box 25046, Mail Stop 973, Denver Federal Center, Denver, CO 80225-0046, USA
[b] Centre for Exploration Targeting, School of Earth and Geographical Sciences, University of Western Australia, Crawley, Western Australia 60094, Australia
[c] State Key Laboratory of Geological Processes and Mineral Resources, China University of Geosciences, Beijing 100083, China
[d] Eldorado Gold, Room 1001, West Tower, LG Twin Towers, B-12 Jianguomenwai Ave., Chaoyang District, Beijing 100022, China
[e] North East Interdisciplinary Science Research Institute N.A. Shilo, Far East Branch, Russian Academy of Sciences, ul. Portovaya 16, Magadan, 685000, Russia
[f] Department of Geological Sciences, University of Colorado, Boulder, CO 80309, USA

ARTICLE INFO

Article history:
Received 1 December 2012
Received in revised form 28 February 2013
Accepted 6 March 2013
Available online xxxx

Handling Editor: M. Santosh

Keywords:
Asia
Gold
Tectonics
Orogenic gold
Epithermal
Porphyry
Carlin-type

ABSTRACT

The Asian continent formed during the past 800 m.y. during late Neoproterozoic through Jurassic closure of the Tethyan ocean basins, followed by late Mesozoic circum-Pacific and Cenozoic Himalayan orogenies. The oldest gold deposits in Asia reflect accretionary events along the margins of the Siberia, Kazakhstan, North China, Tarim–Karakum, South China, and Indochina Precambrian blocks while they were isolated within the Paleotethys and surrounding Panthalassa Oceans. Orogenic gold deposits are associated with large-scale, terrane-bounding fault systems and broad areas of deformation that existed along many of the active margins of the Precambrian blocks. Deposits typically formed during regional transpressional to transtensional events immediately after to as much as 100 m.y. subsequent to the onset of accretion or collision. Major orogenic gold provinces associated with this growth of the Asian continental mass include: (1) the ca. 750 Ma Yenisei Ridge, ca. 500 Ma East Sayan, and ca. 450–350 Ma Patom provinces along the southern margins of the Siberia craton; (2) the 450 Ma Charsk belt of north-central Kazakhstan; (3) the 310–280 Ma Kalba belt of NE Kazakhstan, extending into adjacent NW Xinjiang, along the Siberia–Kazakhstan suture; (4) the ca. 300–280 Ma deposits within the Central Asian southern and middle Tien Shan (e.g., Kumtor, Zarmitan, Muruntau), marking the closure of the Turkestan Ocean between Kazakhstan and the Tarim–Karakum block; (5) the ca. 190–125 Ma Transbaikal deposits along the site of Permian to Late Jurassic diachronous closure of the Mongol–Okhotsk Ocean between Siberia and Mongolia/North China; (6) the probable Late Silurian–Early Devonian Jiagnan belt formed along the margin of Gondwana at the site of collision between the Yangtze and Cathaysia blocks; (7) Triassic deposits of the Paleozoic Qilian Shan and West Qinling orogens along the SW margin of the North China block developed during collision of South China; and (8) Jurassic(?) ores on the margins of the Subumusu block in Myanmar and Malaysia. Circum-Pacific tectonism led to major orogenic gold province formation along the length of the eastern side of Asia between ca. 135 and 120 Ma, although such deposits are slightly older in South Korea and slightly younger in the Amur region of the Russian Southeast. Deformation related to collision of the Kolyma–Omolon microcontinent with the Pacific margin of the Siberia craton led to formation of 136–125 Ma ores of the Yana–Kolyma belt (Natalka, Sarylakh) and 125–119 Ma ores of the South Verkhoyansk synclinorium (Nezhdaninskoe). Giant ca. 125 Ma gold provinces developed in the Late Archean uplifted basement of the decratonized North China block, within its NE edge and into adjacent North Korea, in the Jiaodong Peninsula, and in the Qinling Mountains. The oldest gold-bearing magmatic–hydrothermal deposits of Asia include the ca. 485 Ma Duobaoshan porphyry within a part of the Tuva–Mongol arc, ca. 355 Ma low-sulfidation epithermal deposits (Kubaka) of the Omolon terrane accreted to eastern Russia, and porphyries (Bozshakol, Taldy Bulak) within Ordovican to Early Devonian oceanic arcs formed off the Kazakhstan microcontinent. The Late Devonian to Carboniferous was marked by widespread gold-rich porphyry development along the margins of the closing Ob–Zaisan, Junggar–Balkhash, and Turkestan basins (Amalyk, Oyu Tolgoi); most were formed in continental arcs, although the giant Oyu Tolgoi porphyry was part of a near-shore oceanic arc. Permian subduction-related deformation along the east side of the Indochina block led to ca. 300 Ma gold-bearing skarn and disseminated gold ore formation in the Truong Son fold belt of Laos, and along the west side to ca. 250 Ma gold-bearing skarns and epithermal deposits in the Loei fold belt of Laos and Thailand. In the Mesozoic Transbaikal region, extension along the basin margins subsequent to Mongol–Okhotsk closure was associated with ca. 150–125 Ma formation of important auriferous epithermal (Balei), skarn (Bystray), and porphyry (Kultuminskoe) deposits. In northeastern Russia, Early Cretaceous Pacific margin subduction and Late Cretaceous extension were associated with epithermal gold-deposit formation in the Uda–Murgal (Julietta) and Okhotsk–Chukotka (Dukat, Kupol)

* Corresponding author at: U.S. Geological Survey, Box 25046, Mail Stop 973, Denver Federal Center, Denver, CO 80225-0046, USA. Tel.: +1 303 236 2441.
E-mail address: goldfarb@usgs.gov (R.J. Goldfarb).

1342-937X/$ – see front matter. Published by Elsevier B.V. on behalf of International Association for Gondwana Research.
http://dx.doi.org/10.1016/j.gr.2013.03.002

volcanic belts, respectively. In southeastern Russia, latest Cretaceous to Oligocene extension correlates with other low-sulfidation epithermal ores that formed in the East Sikhote–Alin volcanic belt. Other extensional events, likely related to changing plate dynamics along the Pacific margin of Asia, relate to epithermal–skarn–porphyry districts that formed at ca. 125–85 Ma in northeastmost China and ca. 105–90 Ma in the Coast Volcanic belt of SE China. The onset of strike slip along a part of the southeastern Pacific margin appears to correlate with the giant 148–135 Ma gold-rich porphyry–skarn province of the lower and middle Yangtze River. It is still controversial as to whether true Carlin-like gold deposits exist in Asia. Those deposits that most closely resemble the Nevada (USA) ores are those in the Permo-Triassic Youjiang basin of SW China and NE Vietnam, and are probably Late Triassic in age, although this is not certain. Other Carlin-like deposits have been suggested to exist in the Sepon basin of Laos and in the Mongol–Okhotsk region (Kuranakh) of Transbaikal.

Published by Elsevier B.V. on behalf of International Association for Gondwana Research.

Contents

1. Introduction

Asia represents one of the world's premier regions for giant gold deposits. Large gold deposits are presently being exploited, and the greenfield and brownfield exploration potentials are enormous. Because of the common political and resulting logistical and infrastructure hurdles facing major Western exploration companies in many countries of Asia, the region is often not viewed as being as prospective as other global regions with huge gold endowments, such as the western Australia and central Canada cratons and the young Andean orogen of South America. Nevertheless, some of the world's largest orogenic gold deposits and gold-bearing porphyry systems are being developed and mined throughout central Asia. The world's largest placer fields in eastern Russia define gold provinces that are now recognized to contain giant lode deposits amenable to large tonnage open-pit development. In 2007, China became

Please cite this article as: Goldfarb, R.J., et al., Phanerozoic continental growth and gold metallogeny of Asia, Gondwana Research (2013), http://dx.doi.org/10.1016/j.gr.2013.03.002

the largest gold-producing country in the world solely from deposits with defined resources nowhere greater than about 100–300 t of gold. Certainly a number of these deposits in China, with continued brownfield exploration and the rapidly improving mining technology, will develop into much greater resources.

The specifics of past production, measured reserves, and potential resources for the gold deposits in mainland Asia are very difficult to define with any degree of certainty. This reflects a number of problems that include: (1) published data in the literature and in company announcements are extremely variable; (2) historic records are poor; (3) under-estimates of tonnages in some goldfields may be advantageous for tax purposes; (4) over-estimations of tonnages in some goldfields may reflect relatively less stringent reporting rules for defined reserves and resources than are typical of Western countries; and (5) many reported tonnages are for an entire goldfield, rather than just single deposits within the goldfield. Also, many deposits with relatively small reported tonnages are being mined from high-grade orebodies just by underground operations. As modernization of the mining industry in Asia moves forward, many of these deposits will quickly become significantly larger because the focus will no longer solely be on high-grade orebodies. In Table 1 and Fig. 1, we list and locate some of the larger reported gold deposits in Asia. As stressed above, there is great uncertainty in many of these listed pre-mining tonnages of Table 1, which have been compiled from various company web sites and press releases, as well as from some of the more recent literature cited below in this paper for specific deposits.

Mainland Asia is dominated by orogenic gold belts in metamorphic rocks and auriferous porphyry–skarn–epithermal deposits in continental and oceanic arcs. Orogenic gold deposits (Goldfarb et al., 2005) are typically structurally hosted vein and disseminated ores formed between 3- and 20-km depth along major deep-seated faults in medium-grade metamorphic rocks. They are generally accepted to have formed from fluids produced during metamorphic devolatilization, with gold and sulfur in the fluids being derived from the breakdown of widely disseminated pyrite. Porphyry deposits are magmatic–hydrothermal deposits formed at shallow depth in oceanic and continental arcs and in association with oxidized dioritic to granitic porphyritic intrusions (Seedorff et al., 2005). They are commonly dominated by stockworks with copper or molybdenum resources, but many copper porphyry deposits can also be giant low-grade, bulk-tonnage gold resources. Where porphyry bodies intrude carbonate rocks, magmatic fluids reacting with these wallrocks may form auriferous skarn or calc–silicate assemblages (Meinert et al., 2005). Epithermal gold deposits form in the upper 1.5 km of the crust (Simmons et al., 2005). They may be low sulfidation types, which are adularia-sericite dominant vein assemblages formed from convection of meteoric waters above an intrusion, or they may be high sulfidation types, which are alunite–kaolinite assemblages typically located above large porphyry deposits. The relationship of globally uncommon sedimentary rock-hosted disseminated gold deposits (Carlin-type) to metamorphic (orogenic gold) or magmatic–hydrothermal (porphyry–epithermal) flow systems and resulting gold ores is unclear (Cline et al., 2005). Also, less common gold producers and targets are the so-called intrusion-related gold systems. These systems include a low-grade gold deposit consisting of sheeted auriferous veins in the cupola to a reduced felsic to intermediate causative intrusion, which is surrounded by an outward zoning of other lower temperature mineral deposit types in adjacent wallrocks (Goldfarb et al., 2005). Finally, other gold resources may be associated with base metal-rich volcanogenic massive sulfide (VMS) deposits formed by magmatism on the ocean floor (Franklin et al., 2005). All of these gold deposit types have been described in various parts of Asia and will be discussed below.

Although there are broad regions of Late Archean and Paleoproterozoic rocks throughout Asia, which are traditionally important age hosts for orogenic gold deposits, most such exposed rocks are of relatively high-metamorphic grade and define deeper crustal levels than those that would contain preserved Precambrian orogenic gold deposits. Rather than large cratons, the Asian rocks of these eras represent rifted fragments of supercontinents that may have lost enough of their subcontinental lithosphere, such that many relatively shallow parts of gold-favorable greenstone belts have been lost to erosion subsequent to rifting of the blocks. Thus, almost all orogenic gold deposits in Asia are Phanerozoic in age.

Epithermal and porphyry deposits of Asia also all formed in the Phanerozoic. Some of the exceptional gold endowments of resources in these deposit types are associated with the young oceanic arcs of Indonesia, the Philippines, and adjacent countries. The tectonics of the southwestern Pacific arcs have been well described in many other studies (e.g., Garwin et al., 2005) and thus we will restrict the material in this paper to mainland Asia. Much of the development to date of gold resources in these mainland gold deposits has been centered on gold-rich iron and/or copper skarns, which may define high-grade, low-tonnage systems. This is particularly true of the Yangtze River area in China, many belts in Southeast Asia, and parts of the Russian Transbaikal. But with the rapidly modernizing technologies of gold mining taking place in Asia, many large tonnage operations of associated porphyry systems will become more dominant in the future.

The exceptional gold endowment of Asia reflects that it is the one continent not built over billions of years around one or a few very large Precambrian craton nuclei. Rather, it is a composite of older blocks and Paleozoic–early Mesozoic terranes that were amalgamated to form this relatively young landmass, much of it during the so-called Central Asian orogen (e.g., Sengor and Natal'in, 1996; Jahn, 2004; Yakubchuk et al., 2005; Windley et al., 2007; Xiao et al., 2008, 2009). An abundance of active "continental" margins along the numerous Precambrian blocks rifted from Rodinia and Gondwana into the Panthalassa and Paleotethys Oceans provided many favorable settings for arc development and orogenesis as the various subbasins between each block were closed via terrane accretion and eventual collision. Thus, the Central Asian orogen represents a rather unique product of Cordilleran style tectonism, one with essentially multiple episodes of discreet accretionary and collisional events, rather than just a series of accretionary events and a single possible final continent–continent collision between major blocks.

The Cretaceous circum-Pacific tectonism is also exceptional, as it is characterized by typical Cordilleran style gold-forming events, as well as events that are globally unique. Many of the great gold resources in eastern Russia and southeastern China are products of deformation occurring soon after terrane collision or post-collisional extension in metasedimentary rocks or shallow volcanic arcs adjacent to the

Table 1
Estimated past gold production + reserves + resources for Asia's largest lode gold deposits.

Deposit	Location	Deposit Type	Tonnage Au
Muruntau	Southern Tien Shan	Orogenic	5246
Almalyk	Northern Tien Shan	Porphyry	2800
Natalka	Yana–Kolyma belt	Orogenic	1860
Olympiada	Yenisei Ridge	Orogenic	1300
Sukhoi Log	Baikal Mountains	Orogenic	1100
Jiaodong district	North China craton	Orogenic	>1000
Oyu Tolgoi	Kazakh–Mongol arc	Porphyry	>1000
Balei/Taseevo	Central Transbaikal	Epithermal	800
Nezhdaninskoe	South Verkhoyansk	Orogenic	640
Qinling Mts. district	North China craton	Orogenic	>600
Kumtor	Middle Tien Shan	Orogenic	570
Vasilkovskoe	Charsk belt	Orogenic	450
Bakyrchik	Irtysh–Zaisan basin	Orogenic	410
Bestobe	Charsk belt	Orogenic	400
Kuranakh	Central Transbaikal	Epithermal(?)	400
Zijinshan	Southeast China fold belt	Epithermal	>350
Zarmitan	Southern Tien Shan	Orogenic	340
Blagodatnoye	Yenisei Ridge	Orogenic	325

Please cite this article as: Goldfarb, R.J., et al., Phanerozoic continental growth and gold metallogeny of Asia, Gondwana Research (2013), http://dx.doi.org/10.1016/j.gr.2013.03.002

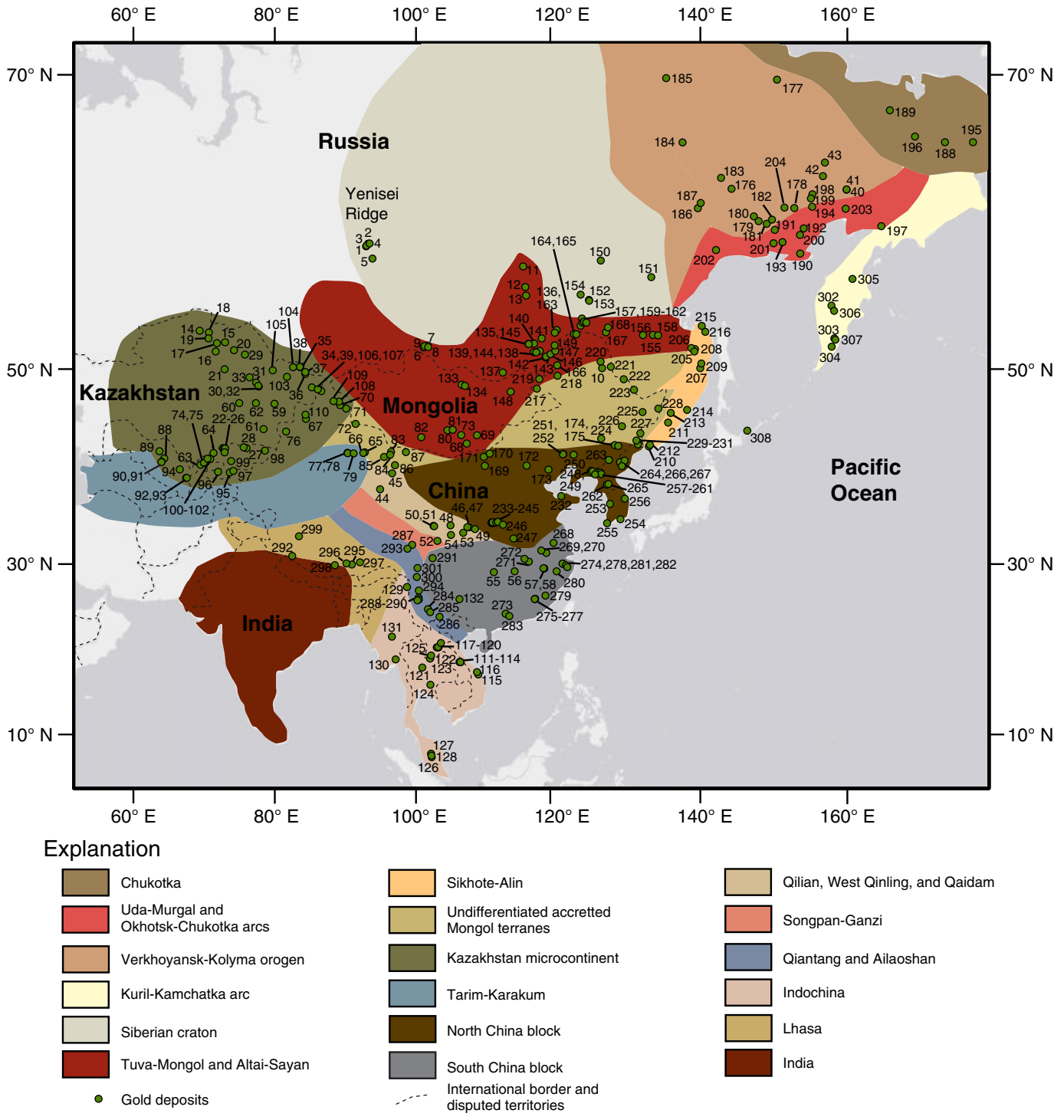

Fig. 1. Location of major gold deposits and districts in mainland Asia. Numbers refer to listings in Tables 2–13 throughout the text.

Precambrian blocks. However, the giant gold endowment along the northern, eastern, and southern margins of the eastern part of the North China block is characterized by Cretaceous orogenic gold deposits in Archean basement rocks, a scenario uncommon elsewhere.

Our aim in this paper is to synthesize the many major tectonic events that led to the Phanerozoic growth of Asia and how these define the spatial distribution of the continent's gold resources. Discussion will be restricted to mainland Asia that is north of India–Pakistan–Afghanistan and east of the Ural Mountains. We will show how specific tectonic events are best correlated with the major recognized gold-forming episodes throughout the continent. Such an understanding is significant because it should allow for an improved capability for prediction and discovery of new gold resources in specific deposit types in various parts of mainland Asia.

2. Panthalassa to Paleotethys gold

2.1. Late Proterozoic Siberia craton margin

The oldest recognized significant gold resources of Asia are those of the Yenisei Ridge region (Fig. 2, Table 2), a late Neoproterozoic Cordilleran-style orogenic belt along the southwestern margin of

Please cite this article as: Goldfarb, R.J., et al., Phanerozoic continental growth and gold metallogeny of Asia, Gondwana Research (2013), http://dx.doi.org/10.1016/j.gr.2013.03.002

the Siberia craton. The craton was an independent block for 500 m.y. within the Paleotethys and Panthalassa (or Paleo-Pacific) Oceans, subsequent to ca. 800 Ma rifting from its poorly constrained position within the Rodinian supercontinent (Cocks and Torvsik, 2007). Accretion of pericratonic terranes, oceanic arcs, turbidite sequences, and high-grade metamorphic continental fragments to the block, forming the 700-km-long Yenisei Ridge belt, took place between ca. 760 and 600 Ma (Vernikovsky et al., 2007). Fault zones and fold systems within medium-grade metasedimentary rocks of the Central Angara terrane host the gold ores.

Orogenic gold deposits at Olympiada, Blagodatnoye, Veduga, Sovetskoe, and Eldorado, as well as >1000 t of related historic placer mining (Yakubchuk et al., 2005), have a combined pre-mining resource of almost 2000 t Au. The >1000 t Olympiada deposit, mined at a variety of scales since the early 1980s, is the largest active mine of a gold-only deposit in Russia. The structurally controlled lode ores, dominated by pyrrhotite, arsenopyrite, and pyrite, along with commonly abundant stibnite, occur as veinlets and disseminations within the more argillaceous parts of the terrane. Absolute dates on the ores are imprecise, but generally indicate that they were deposited between 850 and 640 Ma (e.g., Gertner et al., 2011). Because much of the deformation and metamorphism of the Central Angara terrane took place from 760 to 720 Ma, the gold ores also most likely formed during this time. This timing would broadly overlap with the documented change in magmatism of the region from ca. 760 Ma syn-collisional granites to ca. 750–720 Ma post-collisional leucogranites (Vernikovsky et al., 2007). However, Yakubchuk (2010) indicates a Re–Os age of 512 Ma for pyrite from Olympiada, so a significantly younger ore-forming event cannot be ruled out. Localization of many of the schist-hosted deposits and occurrences in the region follow a NW-striking trend (Genkin et al., 2002), which could relate to shearing along older thrust faults, particularly adjacent to many granitoid bodies oriented along the same general trend. Thrusting of more inboard parts of the cratonic margin over rocks of the Central Angara terrane during accretionary orogenesis (Likhanov et al., 2006) led to development of an inverted Barrovian-like metamorphic sequence that hosts the gold lodes within Neoproterozoic greenschist facies units.

2.2. Early to middle Paleozoic Siberia craton margin

Other significant gold deposits also formed along the tectonically active, present-day southern margin to the Siberia craton during early and middle Paleozoic. To the south of Yenisei Ridge, along the present-day most southwestern part of the craton, the East Sayan region is dominated by a series of oceanic arcs that define the Altai–Sayan orogeny, a Vendian to Cambrian Cordilleran-style event. Proterozoic high-grade metamorphic rocks and earliest Paleozoic oceanic metasedimentary and metavolcanic rocks underlie the orogen. Nozhkin et al. (2007) define the Yenisei Ridge and East Sayan regions as a single, continuous Vendian accretionary belt. In East Sayan, deformation, thrusting, magmatism, regional metamorphism, and extensive strike-slip continued to about 500–450 Ma (Khain et al., 2003; Nozhkin et al., 2007). Orogenic gold deposits and occurrences, as well as numerous polymetallic VMS occurrences, are recognized in the southeastern part of the region. The early Paleozoic tellurium-rich gold lodes (e.g., Zun–Kholba, Zun–Ospa, Baroon–Holba; Fig. 3, Table 2) are predominantly hosted by Vendian–Early Cambrian carbonaceous shales. The most abundant resources, similar to the Yenisei Ridge region, are located in these metasedimentary units adjacent to sheared margins of granitoid masses, along fault zones marked by slices of ultramafic rocks situated to the northeast of the gneisses of the Precambrian Gargan block. Rubidium–Sr dating on a number of gold occurrences suggested gold deposition at 537 Ma (Damdinov et al., 2007), which overlaps a Re–Os date on molybdenum at the Tainsky prospect of ca. 550 Ma (Mironov et al., 2005). However, Neimark et al. (1995) presented a Pb date on ore-related galena of 450 Ma for the Zun–Kholba deposit, which

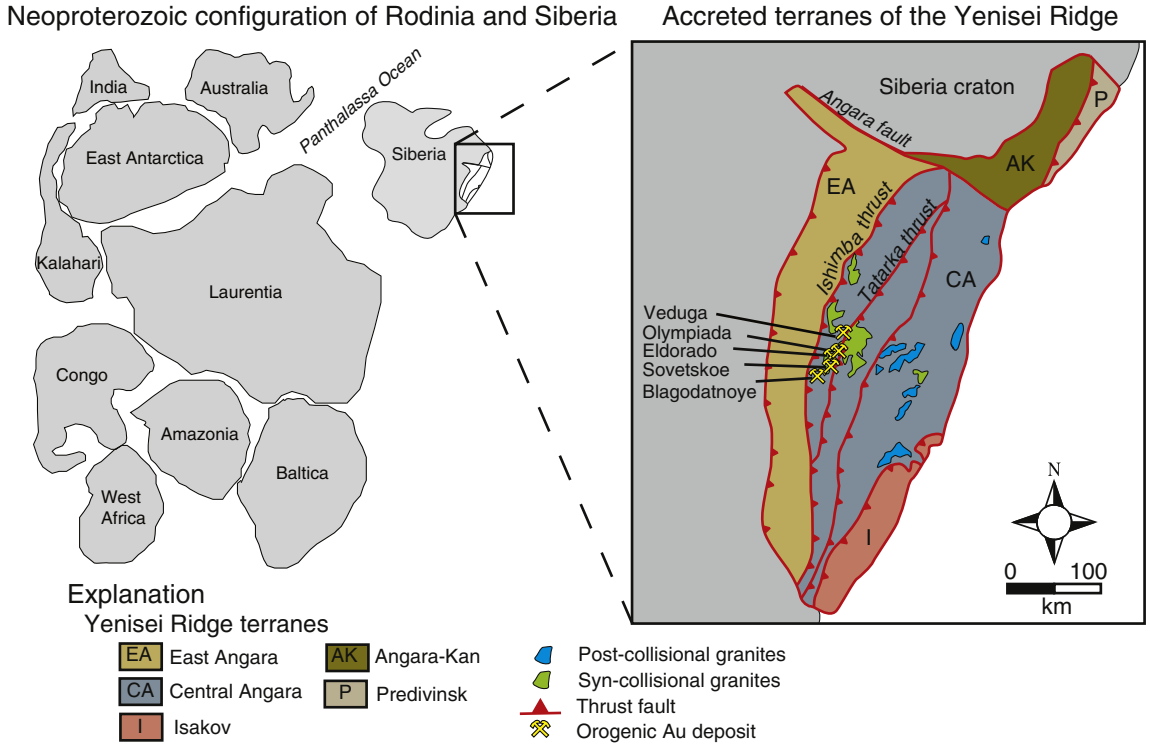

Fig. 2. Late Neoproterozoic orogenic gold deposits were formed in the central Angara terrane of the Yenisei Ridge province along the present-day southwestern margin of the Siberian craton. These are the oldest recognized gold deposits in Asia and include the giant Olympiada deposit, Russia's largest active lode gold producer. The deposits formed in Siberia when it was a fragmented block rifted from the Rodinia supercontinent into the Panthalassa Ocean. Rodinia configuration and Siberia orientation modified from Meert and Lieberman (2008). Yenisei Ridge plutonism and terrane boundary locations from Vernikovsky et al. (2003).

Please cite this article as: Goldfarb, R.J., et al., Phanerozoic continental growth and gold metallogeny of Asia, Gondwana Research (2013), http://dx.doi.org/10.1016/j.gr.2013.03.002

Table 2
Late Neoproterozoic to early Paleozoic gold deposits of the southern Siberian craton margin and adjacent blocks.

Deposit	Location in Fig. 1	Latitude	Longitude	Country	Tectonic location	Deposit type	Age (Ma)	Geochron. methodology	Geochron. reference
Olympiada	1	59.93	92.8	Russia	Yenisei Ridge	Orogenic	760-720 (?)	time of deformation	
							513-511	Re-Os (pyrite)	Yakubchuk (2010)
Blagodatnoye	2	60.12	93.07	Russia	Yenisei Ridge	Orogenic	698±13	Rb-Sr (biotite/muscovite/whole rock)	Gertner et al. (2011)
							364±7.2	Rb-Sr (late-stage fluorite)	Gertner et al. (2011)
							368±23	Sm-Nd (late-stage fluorite)	Gertner et al. (2011)
Veduga	3	59.07	93.68	Russia	Yenisei Ridge	Orogenic	760-720 (?)	time of deformation	
Sovetskoe	4	59.98	92.87	Russia	Yenisei Ridge	Orogenic	760-720 (?)	time of deformation	
Eldorado	5	60.13	93.28	Russia	Yenisei Ridge	orogenic	760-720 (?)	time of deformation	
Zun-Kholba	6	52.07	100.83	Russia	East Sayan	Orogenic	537±15	Rb-Sr (altered whole rock)	Damdinov et al. (2007)
							450	U-Pb (galena)	Neimark et al. (1995)
Zun-Ospa	7	52.23	101.38	Russia	East Sayan	Orogenic	early Paleozoic?	other gold ages in region	
Baroon-Holba	8	52.19	100.95	Russia	East Sayan	Orogenic	early Paleozoic?	other gold ages in region	
Tainsky	9	52.1	101.49	Russia	East Sayan	Orogenic	550	Re-Os (molybdenite)	Mironov et al. (2005)
Duobaoshan	10	50.25	125.78	China	Tuva-Mongol arc	Porphyry	486-482	Re-Os (molybdenite/pyrite/chalcopyrite)	Liu et al. (1995)
Sukhoi Log	11	58.5	114.75	Russia	Baikal Mountains	Orogenic	450-440	U-Th-Pb (zircon, monazite)	Yudovskaya et al. (2011)
							447±6	Rb-Sr (altered whole rock)	Laverov et al. (2007)
							345	Ar-Ar (sericite)	Goldfarb et al. (2001)
							329±13 to 313±10	K-Ar (sericite)	Laverov et al. (2007)
							508-477	Re-Os (pyrite)	Yakubchuk (2010)
Kamenny	12	56.96	115.06	Russia	Baikal-Muya terrane	Epithermal(?)	Late Riphean(?)		Mironov et al. (2008)
Irokinda	13	56.31	115.17	Russia	Baikal-Muya terrane	Orogenic	uncertain		
Kubaka	40	63.67	159.97	Russia	Kolyma-Omolon	Epithermal	337-334	Rb-Sr isochron	Kotlyar et al. (2001)
Birkachan	41	63.69	159.97	Russia	Kolyma-Omolon	Epithermal	uncertain		
Ol'cha	42	64.5	156.67	Russia	Kolyma-Omolon	Epithermal	Devonian	age of volcanic host	
Zet	43	65.3	156.95	Russia	Kolyma-Omolon	Epithermal	uncertain		

corresponds to the episode of regional shearing that is likely important to the gold-forming event.

East of the East Sayan, along the eastern edge of a growing Tuva–Mongol arc, either extending from or close to the Siberian craton, earliest Paleozoic oceanic arcs collided with the Gargan block (e.g., Windley et al., 2007), a fragment rifted from the Siberian craton. The Duobaoshan porphyry Cu–Mo–Au deposit, now in Heilongjiang province (China), is associated with such an arc. The deposit was previously considered to be no older than Permian and as young as Jurassic based on argon dating (Liu et al., 1995), but it is now generally accepted to be much older based on 486–482 Ma Re–Os dating of ore-stage sulfide minerals (Zhao et al., 1997; Liu et al., 2011a). The older age indicates that this early arc collision within the Central Asian Orogenic Belt (CAOB) was responsible for some of the oldest, significant magmatic hydrothermal gold resources being added through arc magmatism to the growing orogen; subsequently, more outboard accretions, including that responsible for the giant Oyu Tolgoi deposit in southern Mongolia (see below) and other magmatic ore systems, continued throughout the Paleozoic.

A giant middle Paleozoic gold endowment (Table 2) characterizes the northwestern Transbaikal region on the southeastern side of the Siberian craton. A 400-km-wide zone of uplifted late Mesoproterozoic through Neoproterozoic basement rocks and near-margin foredeep sediments is exposed to form the Baikal Mountains or Patom fold-and-thrust belt (Fig. 4). These rocks were deformed during the latest Proterozoic collision of the Barguzin–Vitim block and the late Paleozoic outboard collision of the Kazakhstan microcontinent (De Boisgrollier et al., 2009). To the south, ca. 630–580 Ma oceanic arc rocks define terranes accreted to the margin between the two blocks by the start of the Paleozoic (Makrygina et al., 2007). More than 75% of this Neoproterozoic–early Paleozoic active margin is now characterized by exposures of the massive ca. 340–270 Ma Angara–Vitim batholith, particularly within the Barguzin–Vitim block. Regional deformation is associated with the first half of the magmatic event, whereas post-collisional extension was dominant after about 320 Ma (Tsygankov et al., 2007).

Important gold resources occur both on the northern and eastern sides of the batholith (Bulgatov and Gordienko, 1999). To the north, more than 2200 t of placer gold have been recovered since 1864 from productive placers in the shelf sequence rocks. In addition, the Sukhoi Log orogenic gold deposit (Fig. 4) represents a major undeveloped lode resource (1100 t Au) about 5 km north of the Konstantinovsk massif (see Fig. 3 in Distler et al., 2005), probably part of the Angara–Vitim batholith; additional deposits or occurrences in the district include Chertovo Koryto, Ozherel'e, Pervenets–Verninskoe, and Vysochaishee (see Fig. 1 in Chugaev et al., 2010). The auriferous quartz–carbonate–pyrite stringers and disseminated ores at Sukhoi Log are located along the axis of a regional anticline in Riphean and Vendian carbonaceous slate and phyllite. On a regional scale, Sukhoi Log and adjacent gold occurrences are localized along fold axes within 10 km of the northern side of the WNW-trending Baikal–Bodaibo deep fault zone (Rusinov et al., 2008), which appears to define the boundary between the Baikal–Patom passive margin and the accreted Olokit oceanic arc (Lishnevskii and Distler, 2004; Makrygina et al., 2007). The age of gold ore formation remains highly debated, but may correspond to ca. 450–440 Ma U–Th–Pb SHRIMP dates on hydrothermal monazite and zircon (Yudovskaya et al., 2011). A series of other dates include a similar 447 ± 6 Ma Rb–Sr calculation on altered whole-rock samples, but

Please cite this article as: Goldfarb, R.J., et al., Phanerozoic continental growth and gold metallogeny of Asia, Gondwana Research (2013), http://dx.doi.org/10.1016/j.gr.2013.03.002

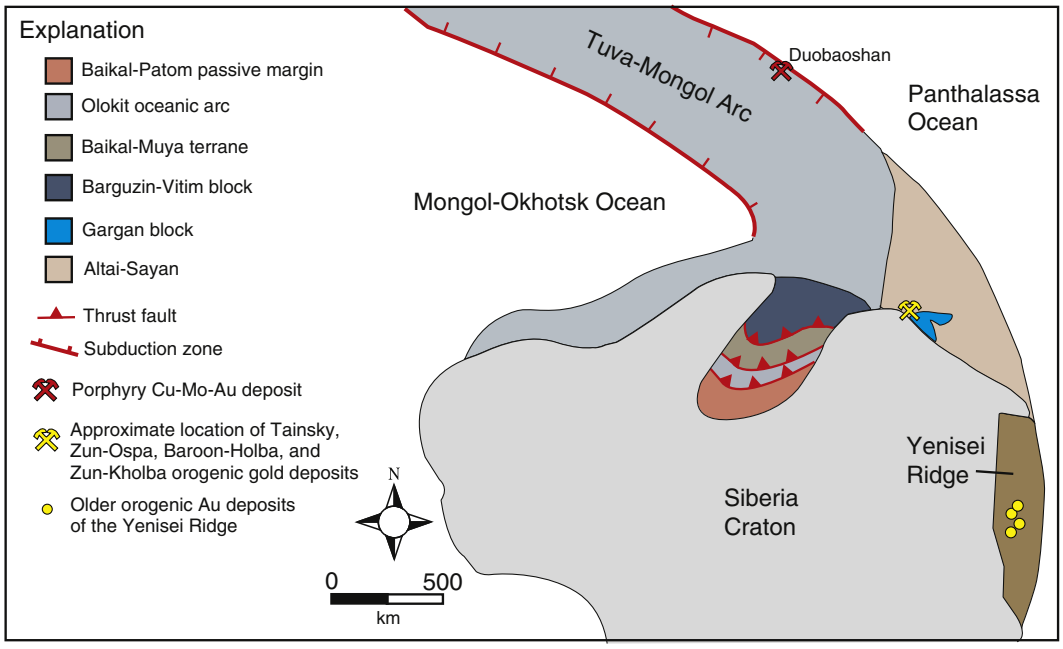

Fig. 3. Early Paleozoic gold deposits were formed along active margins of the Siberia craton within the Panthalassa Ocean as depicted during the Late Ordovician. These include the orogenic gold deposits of the East Sayan region of the Altai–Sayan tectonic province and the Duobaoshan Cu–Mo–Au deposit of the adjacent Tuva–Mongol arc, which is Asia's oldest recognized economic porphyry deposit.
Reconstruction based on Sengor and Natal'in (1996), Makrygina et al. (2007), Windley et al. (2007), and Wilhem et al. (2012).

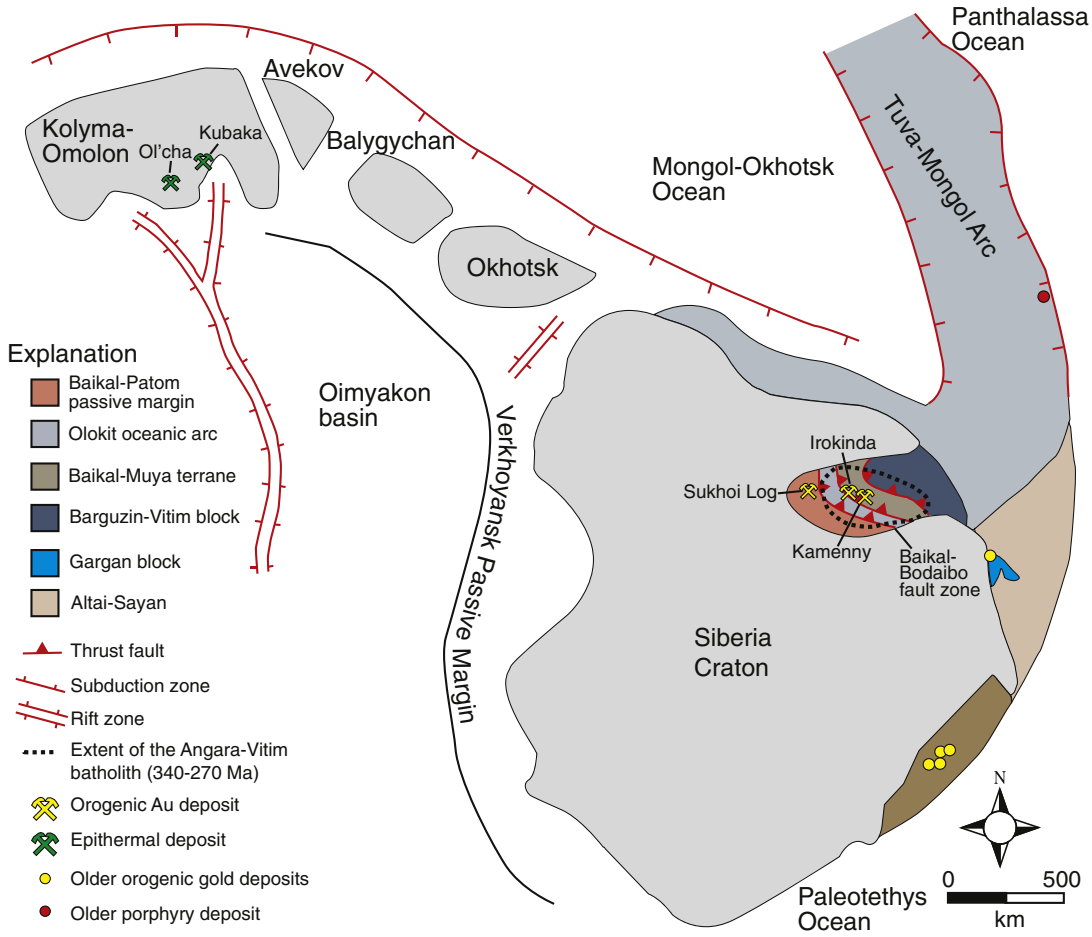

Fig. 4. Middle Paleozoic orogenic gold deposits were formed in the Patom fold-and-thrust belt of the northwestern Transbaikal region along the present-day southeastern margin of the Siberian craton. These include the giant undeveloped lode resource at Sukhoi Log and surrounding Lena placer fields. During Devonian rifting of blocks from the craton, epithermal gold deposits, such as Kubaka and Ol'cha, formed in resulting volcanic arcs of the Kolyma–Omolon microcontinent.
Reconstruction based on Sengor and Natal'in (1996), Makrygina et al. (2007), Windley et al. (2007), and Wilhem et al. (2012).

Please cite this article as: Goldfarb, R.J., et al., Phanerozoic continental growth and gold metallogeny of Asia, Gondwana Research (2013), http://dx.doi.org/10.1016/j.gr.2013.03.002

also 321 ± 14 Ma on hydrothermal quartz by Rb–Sr, and 329 ± 13, 313 ± 10, and 328 ± 6 Ma on hydrothermal sericite by K–Ar (Laverov et al., 2007), and a ca. 345 Ma Ar–Ar plateau age on hydrothermal white mica (Goldfarb et al., 2001). Some workers (e.g., Laverov et al., 2007) have argued that both the Late Ordovician and Early Carboniferous ages may be correct, with early disseminated ore deposition and subsequent vein formation; however, this is a very unlikely scenario. Given the uncertainties in gold deposition age, it is difficult to relate ore formation to a specific tectonic event. It is worth noting that the older SHRIMP date roughly correlates with regional metamorphism in the back-arc (e.g., Zorin et al., 2009), whereas the younger dates overlap batholith emplacement and transpressional deformation. In support of the latter younger Carboniferous age is the timing of the major regional folds, such as that hosting the Sukhoi Log deposit, which formed at 412 ± 15 Ma (Zorin et al., 2008) and, therefore, after the older suggested age.

About 300 km south of Sukhoi Log, hundreds of small gold occurrences define the Muya district. These are hosted within the mainly Mesoproterozoic to Neoproterozoic volcano-sedimentary rocks of the Baikal–Muya terrane (e.g., Makrygina et al., 2007). Whereas the occurrences show a spatial association with NE-trending regional faults, some of the deposits and occurrences, such as Kamenny and Irokinda (Fig. 4; Table 2), appear to be localized along north-trending thrust faults between these more regional lineaments (Abramov, 2006; Mironov et al., 2008). The few descriptions of these occurrences suggest that many may be classified as orogenic gold deposits. Although no absolute dates on gold formation are published, Mironov et al. (2008) suggest that Kamenny is Late Riphean and, in contrast to other deposits, perhaps an epithermal Ag–Au deposit, whereas Rytsk et al. (2007) suggest that many occurrences may be younger than Early Vendian.

2.3. Early to middle Paleozoic Kazakhstan microcontinent

A very similar tectonic scenario characterizes the formation of the Late Ordovician(?) orogenic gold deposits scattered through north-central Kazakhstan (Fig. 5; Table 3), which together have been referred to as the Charsk gold belt. The Kazakhstan microcontinent, in a similar history to the Siberian craton, was present as an isolated block within the Tethyan Oceans throughout the Paleozoic. The Precambrian nucleus of the block, the so-called Stepnyak–North Tien Shan terrane, moved away from fragmenting Rodinia and a series of oceanic arcs and flysch basin terranes were amalgamated with this older terrane to form the Kazakhstan microcontinent by the Late Silurian (Windley et al., 2007). The Silurian microcontinent has also been termed the Kipchak superterrane (Yakubchuk et al., 2005) or Kipchak arc collage (Sengor and Natal'in, 1996). Subduction-related continental margin batholiths were emplaced into the active margin of the microcontinent during Late Ordovician tectonism, which also is suggested as the approximate time of a major uplift episode along the margin (Spiridonov, 1996; Kroner et al., 2008). The magmatism affected both the Stepnyak–North Tien Shan terrane, as well as some of the

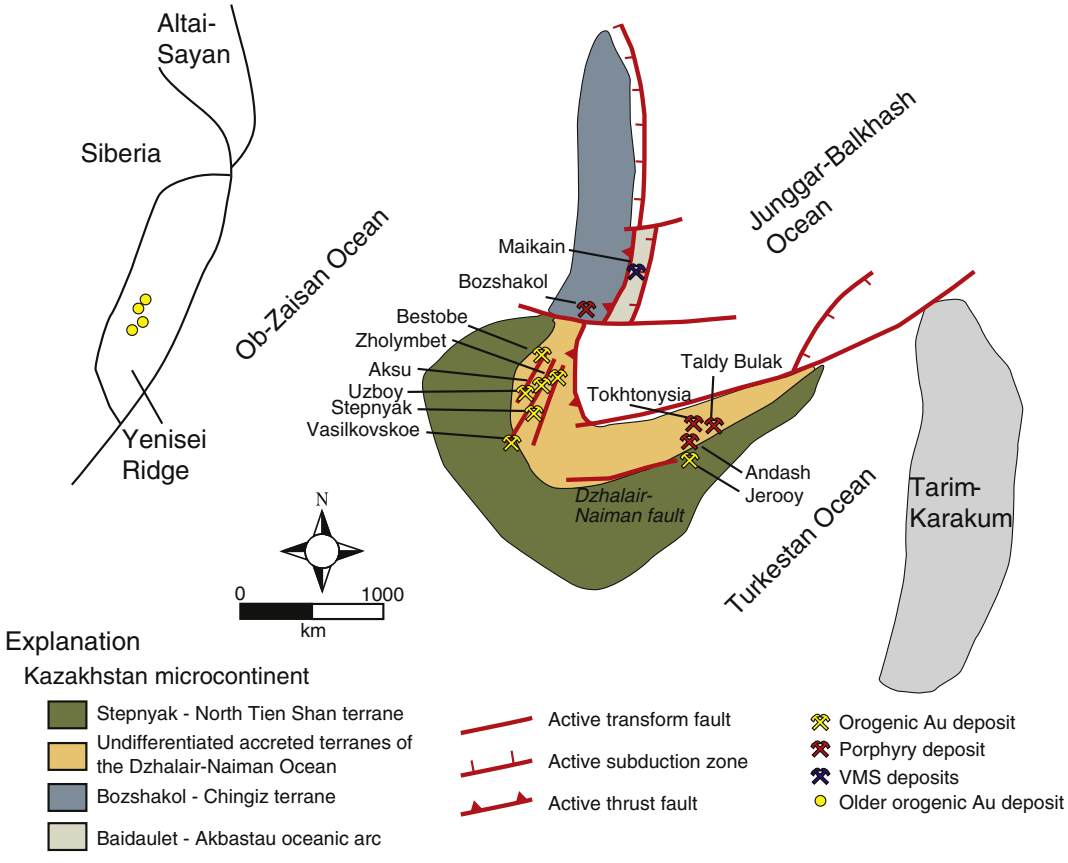

Fig. 5. Ordovician gold deposits were formed along the active margins seaward of the Stepnyak–North Tien Shan terrane, which was likely rifted from Rodinia at the end of the Neoproterozoic and formed the nucleus for Paleozoic terrane accretion to a growing Kazakhstan microcontinent (or Kipchak superterrane) within the Tethys Ocean. Orogenic gold deposits, such as Bestobe and Vasilkovskoe, form the Charsk gold belt of present-day north-central Kazakhstan. Arc-related magmatism was associated with important gold-rich porphyry formation at deposits such as Bozshakol and Taldy Bulak. The oldest large auriferous VMS deposits in Asia, such as Maikain, formed in the Baidaulet–Akbastau oceanic arc. Timing and processes of the oroclinal bending of this microcontinent remain uncertain.
Based on reconstruction of Filippova et al. (2001) and Windley et al. (2007).

Please cite this article as: Goldfarb, R.J., et al., Phanerozoic continental growth and gold metallogeny of Asia, Gondwana Research (2013), http://dx.doi.org/10.1016/j.gr.2013.03.002

Table 3
Early-middle Paleozoic gold deposits of the Kazakhstan microcontinent.

Deposit	Location in Fig. 1	Latitude	Longitude	Country	Tectonic location	Deposit type	Age (Ma)	Geochron. methodology	Geochron. reference
Vasilkovskoe	14	53.48	69.53	Kazakhstan	Charsk Au belt	Orogenic	Late Ordovician(?)	Syn-magmatic	
Bestobe	15	52.5	73.08	Kazakhstan	Charsk Au belt	Orogenic	Late Ordovician(?)	Syn-magmatic	
Zholymbet	16	51.72	71.77	Kazakhstan	Charsk Au belt	Orogenic	Late Ordovician(?)	Syn-magmatic	
Aksu	17	52.42	71.96	Kazakhstan	Charsk Au belt	Orogenic	Late Ordovician(?)	Syn-magmatic	
Uzboy	18	53.33	70.83	Kazakhstan	Charsk Au belt	Orogenic	Late Ordovician(?)	Syn-magmatic	
Stepnyak	19	52.83	70.75	Kazakhstan	Charsk Au belt	Orogenic	Late Ordovician(?)	Syn-magmatic	
Bozshakol	20	51.83	74.33	Kazakhstan	Bozshakol-Chingiz	Porphyry	481±23	Rb-Sr (host tonalite)	Kudryavtsev (1996)
Nurkazghan	21	50.15	73.02	Kazakhstan	Bozshakol-Chingiz	Porphyry	410	Unknown	Seltmann and Porter (2005)
Taldy Bulak	22	42.55	72.77	Kyrgyzstan	Stepnyak-N. Tien Shan	Porphyry	475-455	Unknown	Yakubchuk et al. (2010)
Andash	23	42.5	72.97	Kyrgyzstan	Stepnyak-N. Tien Shan	Porphyry	440±8	U-Pb (zircon on ore-related porphyry)	Jenchuraeva (2001)
Tokhtonysai	24	42.53	73.04	Kyrgyzstan	Stepnyak-N. Tien Shan	Porphyry	Ordovician	Unknown	Seltmann and Porter (2005)
Aktash	25	42.53	73.09	Kyrgyzstan	Stepnyak-N. Tien Shan	Skarn	Ordovician	Unknown	Seltmann and Porter (2005)
Jerooy	26	42.12	73.03	Kyrgyzstan	Stepnyak-N. Tien Shan	Orogenic	uncertain		
Solton Sary	27	42.55	76.08	Kyrgyzstan	Stepnyak-N. Tien Shan	Orogenic	395-390	Ar-Ar (muscovite)	Ispolatov et al. (2000)
							late Paleozoic	Spatial assoc with Carboniferous plutons	
Taldybulak Levoberezhny	28	42.65	75.67	Kyrgyzstan	Stepnyak-N. Tien Shan	Orogenic (?)	uncertain		Djenchuraeva et al. (2008)
Maikain	29	51.45	75.87	Kazakhstan	Baidaulet-Akbastau	VMS	Middle-Late Ordovician	Stratigraphy	
Kosmurun	30	48.59	77.79	Kazakhstan	Baidaulet-Akbastau	VMS	Middle-Late Ordovician	Stratigraphy	
Mizek	31	48.95	77.42	Kazakhstan	Baidaulet-Akbastau	VMS	Middle-Late Ordovician	Stratigraphy	
Akbastau	32	48.64	77.72	Kazakhstan	Baidaulet-Akbastau	VMS	Middle-Late Ordovician	Stratigraphy	
Abyz	33	49.42	76.52	Kazakhstan	Baidaulet-Akbastau	VMS	Middle-Late Ordovician	Stratigraphy	
Karchiga	34	48.5	85.21	Kazakhstan	Rudny Altai	VMS	Devonian	Stratigraphy	
Leninogorsk	35	50.33	83.61	Kazakhstan	Rudny Altai	VMS	Devonian	Stratigraphy	
Zyryanovsk	36	49.75	84.3	Kazakhstan	Rudny Altai	VMS	Devonian	Stratigraphy	
Maleevsky	37	49.89	84.31	Kazakhstan	Rudny Altai	VMS	Devonian	Stratigraphy	
Ridder Sokolnoye	38	50.36	83.54	Kazakhstan	Rudny Altai	VMS	Devonian	Stratigraphy	
Ashele	39	48.25	86.31	China	Rudny Altai	VMS	375±3	U-Pb (zircon on host rhyolite)	Wan et al. (2011)

more landward and earliest terranes accreted to the block. The accreted oceanic terranes and arcs were dominated by juvenile crust of the Junggar–Balkhash and Ob–Zaisan Oceans, smaller basins that existed in the early Paleozoic between the converging Siberian craton and Kazakhstan microcontinent (e.g., Bykadorov et al., 2003).

Districts of large orogenic gold deposits are scattered along a present-day NW-striking trend for about 350 km in the region of some of the most inboard terrane suture zones. The deposits exhibit a spatial relationship with regional faults that are also present-day NW-trending (Spiridonov, 1996), and which have been termed "post-metamorphic transcrustal shear zones" by Heinhorst et al. (2000). There are no detailed published data on fault kinematics. Important deposits include Vasilkovskoe (448 t Au), Bestobe (400 t Au), Zholymbet, Aksu, Uzboy, and Stepnyak (Fig. 5), all occurring as quartz veins, stockworks, and disseminations hosted by intrusions and clastic metasedimentary rocks (Spiridonov, 1996).

As with many of the gold deposits of the southern Siberian craton, these deposits of the Kazakhstan microcontinent similarly lack well-constrained age information. The deposits are most commonly locally sited along zones of shearing between intrusions and country rocks (Spiridonov, 1996; Heinhorst et al., 2000). These plutons have been dated at 481 ± 5 Ma and 441 ± 1 Ma at Stepnyak, 457 ± 7 Ma at Aksu, and 453 ± 6 and 447 ± 5 Ma at Zholymbet (Kroner et al., 2008; Letinov et al., 2008). Although no absolute dates exist for the gold deposits, various workers (e.g., Spiridonov, 1996; Yakubchuk et al., 2002) have suggested a broadly syn-magmatic Late Ordovician timing for the gold events. This also is a suggested time of extensive strike-slip events between the terranes of the drifting microcontinent (e.g., Sengor and Natal'in, 1996; Yakubchuk, 2008), a tectonic scenario particularly favorable for genesis of orogenic gold deposits (e.g., Goldfarb et al., 2005). Although not clear due to discrepancies between existing published maps, it appears that most of the deposits of the Charsk gold belt occur in a deformed early Paleozoic sedimentary rock-dominant sequence immediately seaward of the Stepnyak–North Tien Shan block; however, the large Vasilkovskoe deposit may be an exception that is located within Precambrian basement.

Please cite this article as: Goldfarb, R.J., et al., Phanerozoic continental growth and gold metallogeny of Asia, Gondwana Research (2013), http://dx.doi.org/10.1016/j.gr.2013.03.002

The gold-bearing Bozshakol Cu–Mo ± Au porphyry deposit (Fig. 5) is presently located 125 km east of the Charsk gold belt and is probably of approximately the same age as the orogenic gold deposits. Earliest Paleozoic oceanic volcanic rocks are intruded by Cambrian to Ordovician mafic to felsic bodies, with the auriferous Cu–Mo mineralization associated with tonalite dated at 481 ± 23 Ma (Kudryavtsev, 1996). The volcanic country rocks define the Bozshakol–Chingiz terrane of Windley et al. (2007), which is an oceanic arc accreted to the Kazakhstan microcontinent sometime between Middle Cambrian and Early Silurian. The Mo-rich nature of the ore deposit suggests the mineralization was post-collisional and thus related to continental magmatism within the microcontinent. The Nurkazghan porphyry Cu–Au deposit (Fig. 6), 240 km southwest of Bozshakol, formed at ca. 410 Ma within slightly older intermediate to mafic volcanic rocks (Seltmann and Porter, 2005) and is probably part of the magmatism of the extensive Kazak–Mongol arc (Yakubchuk, 2002).

Very poorly understood ore-forming events along the same continental margin, today located south of the above mentioned porphyry deposits within the north-central part of Kyrgyzstan, also appear to have been associated with Ordovician arc development along the active margin of the Stepnyak–North Tien Shan block. Gold-bearing Cu–Au–Mo porphyry (Taldy Bulak: 270 t Au, Andash, Tokhtonysai; Fig. 5) and associated skarn (Aktash) deposits and occurrences are associated with mainly Ordovician porphyry bodies that have intruded earliest Paleozoic volcanic and volcanoclastic units of the microcontinent (Seltmann and Porter, 2005). Dates on ore-stage monzonitic to monzodioritic intrusions and ore-related mineralization at the Andash deposit indicate ore formation sometime between 440 and 400 Ma (Jenchuraeva, 2001) and between 475 and 455 Ma at Taldy Bulak (Yakubchuk et al., 2010). Such timing, although imprecisely constrained, would generally temporally correlate with final accretion of the Dzhalair–Naiman terrane of Windley et al. (2007) on the seaward side of the arc.

There are a number of other deposits of uncertain age and even uncertain type in northern Kyrgyzstan that possibly could also be part of this early Paleozoic orogenesis/arc development along the same part of the Kazakhstan microcontinent. The Jerooy deposit (Fig. 5) occurs along NE-trending shear zones cutting quartz diorite and quartz syenite bodies of a large Cambrian–Ordovician batholith system. The gold-bearing quartz veins and stockworks are most characteristic of orogenic gold deposits (e.g., Oakes et al., 1998), but there is no available geochronology to indicate whether the hydrothermal event was related to the early Paleozoic tectonism or some younger event. The Solton Sary deposit (Fig. 6), additionally within the Stepnyak–North Tien Shan block, is hosted by Cambrian–Ordovician marine sedimentary and volcanic rocks, and is just south of a massive Ordovician batholith complex. Dating of the hydrothermal mineralization by $^{40}Ar/^{39}Ar$ indicates an age of 395–390 Ma (Ispolatov et al., 2000). Description of the ore veins and stockworks is consistent with classification as an orogenic gold deposit, but high fluid salinities and very shallow ore formation (i.e., Ispolatov et al., 2000) are atypical of such a deposit type. Furthermore, Carboniferous plutons in the area and the deposit's proximity to the major Nikolaev Line (see Fig. 1 in Seltmann et al., 2011), which is the terrane bounding fault that is

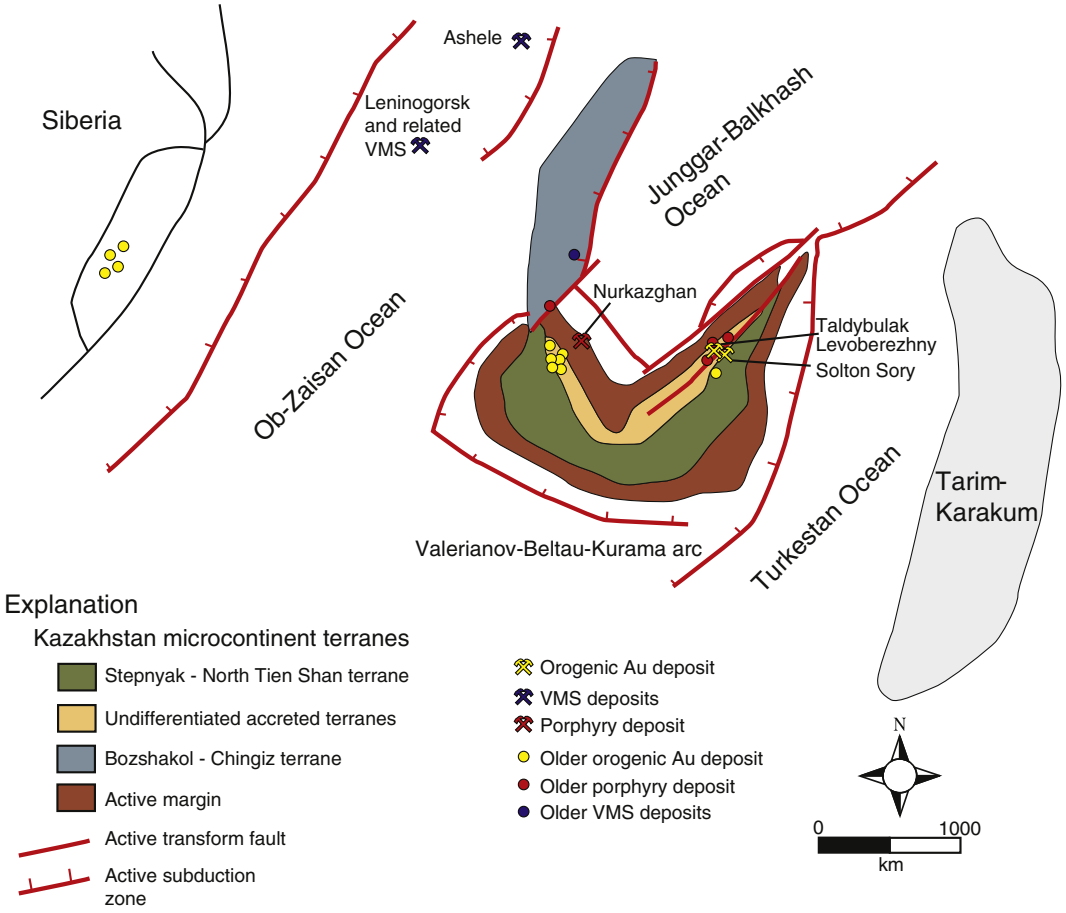

Fig. 6. Additional porphyry and orogenic gold deposits were formed along the active margins of the Kazakhstan microcontinent in the Devonian. Closure of the ocean basin between the Siberian craton and Kazakhstan microcontinent, forming the initial component to mainland Asia, included localization of the large VMS deposits of the Rudny Altai along the suture. Based on reconstruction of Filippova et al. (2001) and Windley et al. (2007).

Please cite this article as: Goldfarb, R.J., et al., Phanerozoic continental growth and gold metallogeny of Asia, Gondwana Research (2013), http://dx.doi.org/10.1016/j.gr.2013.03.002

associated with the late Paleozoic Kumtor deposit a few hundred kilometers to the east, suggest more robust dating of Solton Sary may be needed to confirm an early or late Paleozoic gold-forming event. The Taldybulak Levoberezhny deposit, located in the cluster of mainly magmatic Pb–Zn and REE deposits of the Aktiuz–Boordu district a few tens of kilometers north of Solton Sary, is the most cryptic of all these gold deposits. The undated deposit is hosted by shear zones in Proterozoic metasedimentary rocks and in spatial association with granitoids broadly dated between latest Silurian and Late Triassic (Djenchuraeva et al., 2008). Descriptions of the ores are most consistent with an orogenic deposit model, but some stated characteristics are more typical of epithermal and porphyry gold systems.

In addition to the above early to middle Paleozoic gold-bearing deposits related to regional metamorphism and magmatism within the growing Kazakhstan microcontinent, volcanogenic massive sulfide (VMS) ores define other gold resources that formed dominantly in adjacent oceanic arcs, but with some likely developing in rifted continental crust due to significant Pb accumulations. The VMS deposits in present-day northeastern Kazakhstan, mainly Cu–Pb–Zn–Au–Ag types, have been classified into Early–Middle Cambrian, Middle–Late Ordovician, and Devonian groups by Kudryavtsev and Popov (2000). The oldest group is comprised of small deposits (e.g., Yakubchuk et al., 2005) developed in the heterogeneous continental and oceanic rocks of the Bozshakol–Chingiz terrane. The Ordovician group, which includes the large Maikain deposit (Fig. 5) and many smaller deposits (i.e., Kosmurun, Mizek, Akbastau, Abyz), formed in intermediate to mafic volcanic rocks of the Baidaulet–Akbastau oceanic arc terrane. These terranes and their associated auriferous polymetallic ores were all accreted to the Kazakhstan microcontinent by the Silurian (e.g., Windley et al., 2007). The mid-Paleozoic collision of the Kazakhstan microcontinent with the Siberian craton occurred by closure of the Ob–Zaisan ocean basin (Windley et al., 2007). Rocks of the Rudny Altai, which form part of the suturing terranes, host a NW-striking belt of Devonian Cu–Zn VMS deposits in northeasternmost Kazakhstan (Karchiga, Leninogorsk, Zyryanovsk, Maleevsky, and Ridder Sokolnoye; Fig. 6) and adjacent western Xinjiang (Ashele). A variety of dates on the ores and the volcanic country rocks are generally ca. 380–360 Ma (Goldfarb et al., 2003). The oxide zones of these VMS deposits contain economic amounts of gold (Yakubchuk et al., 2005).

2.4. Paleozoic Kolyma–Omolon microcontinent

A number of Precambrian blocks rifted from the margin of the Siberian craton microcontinent in the Devonian (Shpikerman, 1998; Nokleberg et al., 2000; Sokolov, 2010). They occurred as isolated terranes and larger microcontinents within the Paleozoic–Mesozoic Panthalassa Ocean, and were responsible for the opening of the Carboniferous to Late Jurassic Oimyakon basin along the craton margin (Fig. 4). Two of the larger blocks were amalgamated in the Panthalassa Ocean to form the Kolyma–Omolon microcontinent or superterrane. Rifting of the Omolon terrane from this superterrane during Late Devonian and Early Carboniferous time was associated with deposition of the subaerial felsic to intermediate volcanic rock of the Kedon Group above the Archean to Paleoproterozoic basement of the terrane (Savva and Shakhtyrov, 2011).

The middle Paleozoic rocks of the Kedon Group, and associated subduction-related subvolcanic and granitic intrusions, are the hosts for the Devonian–Carboniferous Kedon metallogenic belt of Volkov et al. (2006). The volcanic–plutonic belt includes numerous low sulfidation epithermal Au–Ag deposits (e.g., Kubaka, Birkachan, Ol'cha, Zet; Table 3) and associated Cu–Mo-porphyry prospects. There are indications of Cretaceous overprints on some of the Paleozoic deposits (e.g., Sakharova et al., 1998; Volkov et al., 2006). Kubaka is hosted in Devonian trachydacitic subvolcanic rocks of a collapsed caldera (Savva et al., 2007) and formed ca. 335 Ma (Goryachev and Yakubchuk, 2008 and references therein; Goryachev et al., 2010). The Olcha deposit, hosted in Devonian trachyandesite that is now 200 km to the northwest, is commonly assumed to be middle Paleozoic (Savva and Shakhtyrov, 2011), although a Late Permian age is also suggested by Goryachev and Yakubchuk (2008). Taken as a whole, the epithermal gold resources are best defined as a preserved middle Paleozoic extension-related ore province.

2.5. Late Paleozoic–early Mesozoic southern margin of the North China block

The specifics of the Paleozoic history of the North China block, migrating across the Paleotethys Ocean, from somewhere along or near the Gondwanan continental margin to a northern hemisphere position along the southern side of Laurasia, is poorly understood. However, it is clear that subduction/accretion zones characterized much of the present-day southern margin of the block while it was within the same broad ocean as the above described Siberian craton and Kazakhstan microcontinent. The resulting Qilian and West Qinling orogenic belts that developed along the southwestern margin of the block (Fig. 7) contain significant gold resources formed before the craton collided with the CAOB (see below). The belts each contain distinct superterranes that were added to the southwestern margin of the North China block by closure of the Shangdan Ocean (see Li et al., 2007b), along what is now the Shangdan fault (Fig. 7).

2.5.1. Qilian Shan

The amalgamated terranes of the Qilian Shan, truncated by the Altyn Tagh fault and Tarim basin to the northwest, were accreted to the North China block by ca. 380–360 Ma (Xiao et al., 2009). The high-grade rocks of the Qaidam block were likely sutured to the southern side of these terranes by this time; this block may also have been part of a larger superterrane that included what is now the South Tarim and Pamir regions (e.g., Yin and Nie, 1996). Orogenic gold deposits (Fig. 7) include those hosted by Ordovician arc volcanic rocks in the North Qilian terrane (Mao et al., 2000), and the Tanjianshan deposit hosted by Mesoproterozoic phyllite and ca. 295 Ma felsic to intermediate igneous rocks (Holley et al., 2005) of the North Qaidam block (Table 4). Mao et al. (2000) report K–Ar ages for the Hanshan deposit in the former area between 224 and 214 Ma. This age suggests some gold formation in this poorly understood orogenic belt postdated accretion and associated deformation by at least 150 m.y., and may correlate with early strike-slip motion along the nearby, continental-scale Altyn Tagh fault system (e.g., Delville et al., 2001). Dates from the Tanjianshan deposit range from ca. 285 to 265 Ma (Zhang et al., 2009a), which indicates important ore formation to be late Paleozoic in the southern part of the orogen.

2.5.2. West Qinling

The western part of the Qinling orogen (W. Qinling of Fig. 7) reflects 300 m.y. of Paleozoic closure of the Shangdan and Mianlue Oceans between the North China and South China blocks within the broader Paleotethys Ocean. The North Qinling oceanic arc was accreted to the edge of the North China block immediately to the east of the Qaidam block by ca. 430 Ma; followed by Devonian closure of the Shangdan Ocean and accretion of the South Qinling terrane, a rifted piece of the northern edge of the South China block, and associated oceanic terranes; and then closure of the Mianlue Ocean and collision of the South China block by ca. 228 Ma (see Figs. 1 and 2 in Dong et al., 2011). Along the western side of the orogen, the southern Qilian Shan represents the backstop for the accretion of these West Qinling terranes.

Gold resources in the West Qinling (Fig. 7) consist of >500 t Au with more than ten >20 t Au deposits as summarized in Mao et al. (2002b). They were stated to include both important examples of orogenic gold within the oceanic rocks that were deformed in the middle to late Paleozoic between the North Qinling arc and South Qinling terrane, and, to the south, Carlin-like gold in carbonate-

Please cite this article as: Goldfarb, R.J., et al., Phanerozoic continental growth and gold metallogeny of Asia, Gondwana Research (2013), http://dx.doi.org/10.1016/j.gr.2013.03.002

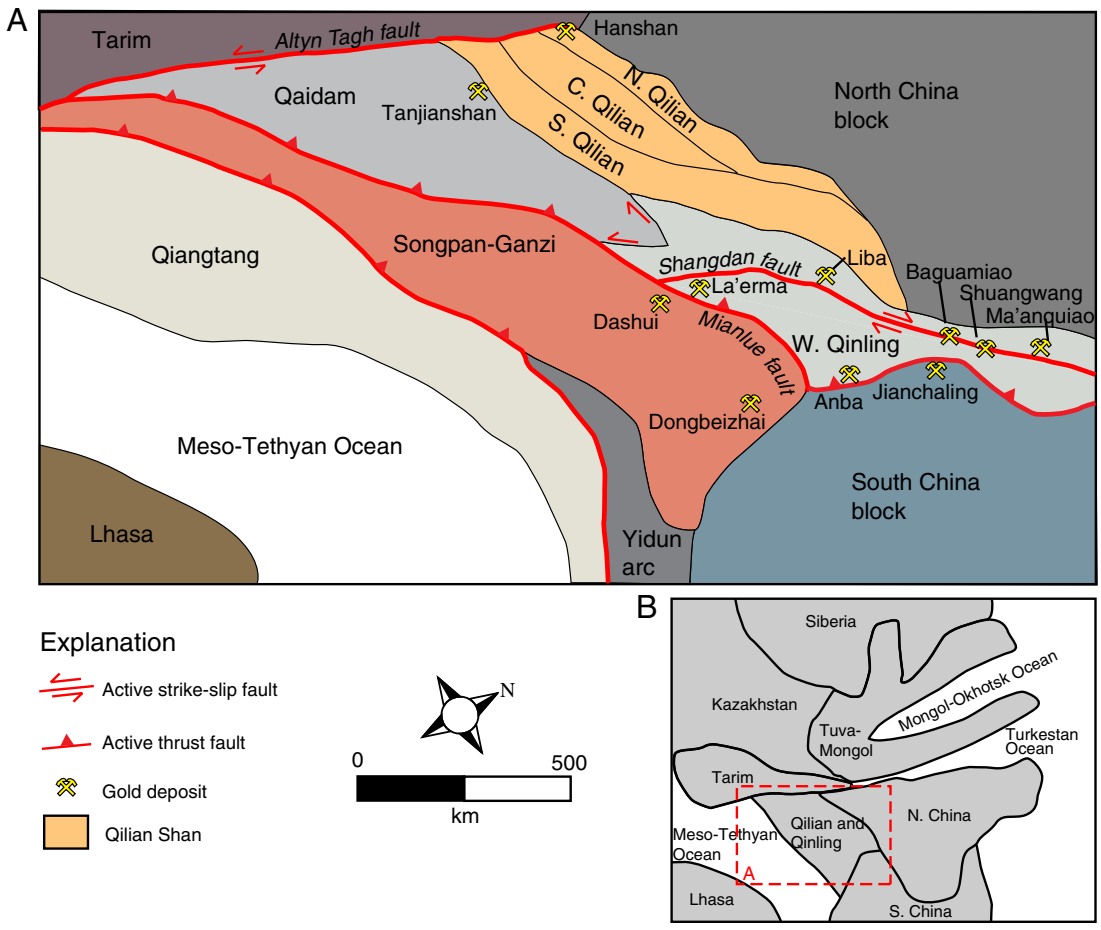

Fig. 7. (A) Terranes of the Qilian Shan and western side of the Qinling belt were accreted to the southwestern margin of the North China block in the Tethys Ocean throughout the Paleozoic. Permian and Triassic strike-slip events, typically along reactivated thrust faults defining terrane boundaries from older closing ocean basins, were associated with widespread formation of orogenic gold deposits. Much of the reactivation likely resulted from collision of the South China block. (B) Regional location of the southern margin of the North China block in the late Paleozoic–early Mesozoic. Not to scale. Panel A is adapted from Mao et al. (2000, 2002b) and Enkelmann et al. (2007).

bearing sequences of the South China block that are interbedded with overlapping Triassic Songpan–Ganzi turbidites shed from the west. The orogenic gold deposits (e.g., Shuangwang, Baguamiao, Liba, Ma'anqiao), hosted by brittle–ductile shear zones in mainly Devonian greenschist-facies metasedimentary rocks, are variably and poorly dated by many workers between 210 and 170 Ma (Mao et al., 2002b). Recent work on the Liba group of deposits suggests the older part to the range may be most accurate, with numerous high-precision dates of ca. 216 Ma defining ore formation along dilational jogs during a local transtentional event (Zeng et al., 2012b).

The Late Triassic dates (Table 4) suggest an important episode of gold introduction during the waning phases of NE–SW directed compression due to collision of the North and South China blocks. The WNW-trending, ore-hosting shear zones parallel the regional Shangdan fault, which is located a few tens of kilometers to the north and is a sinistral transpressive wrench fault system that defines the main suture between the early Paleozoic North Qinling accreted arc and the more seaward Shangdan oceanic terranes. Ratschbacher et al. (2003) document that these were reactivated in early Mesozoic as dextral systems during docking of the South China block, and we favor this timing to reflect the main ore-controlling event. Deposits such as Baguamiao developed synkinematically in sheared Late Devonian phyllite between more competent units of limestone and sandstone. Others, including some at Liba, formed along the margins of pre existing intrusions, which have U–Pb zircon dates between 225 and 210 Ma (Jingwen Mao, written commun., 2013). Little studied, massive Pb–Zn replacement bodies and complex, brittle copper-bearing quartz-vein systems are abundant in the area of the Baguamiao deposit near phyllite–limestone contacts. The timing of base metal mineralization seems to be identical to that of the gold, as suggested by a variety of mainly unpublished Re–Os and Rb–Sr Late Triassic dates (Yitian Wang, written commun., 2013).

The disseminated nature of some of the gold ores, the low temperature metallogeny of some deposits, and the interbedded carbonate units have historically led to classification of deposits, for 600 km along and adjacent to the 20- to 30-km-wide Mianlue fault system, as Carlin-like (e.g., Dashui, La'erma, Dongbeizhai, Jianchaling). Nevertheless, many of these deposits have features that suggest that they are more likely additional orogenic gold deposits of the West Qinling. The large auriferous quartz veins cutting fault-controlled serpentinized and greenschist-facies facies ultramafic rocks at the Jianchaling deposit (Vielreicher et al., 2003) and the anticlinal control to many of the deposits near the Mianlue fault system suggest to us similarities with the unequivocal orogenic gold deposits to the north. Age estimates for gold deposit formation along the Mianlue fault have been estimated by many workers to be between Late Triassic and Middle Jurassic (Mao et al., 2002b; Zeng et al., 2012a), similar to many of the above orogenic gold deposits, but are even more poorly constrained.

In the past few years, the Yangshan gold belt has been recognized along the northern side of the Mianlue fault system, mainly within Devonian phyllite sheared between more competent limestone units. Although deposits in this belt are commonly classified as Carlin types, they too are better defined as orogenic gold deposits. The Anba deposit

Table 4
Late Paleozoic-early Mesozoic gold deposits of the North China block.

Deposit	Location in Fig. 1	Latitude	Longitude	Country	Tectonic location	Deposit type	Age (Ma)	Geochron. methodology	Geochron. reference
Tanjianshan	44	38.17	94.75	China	Qilian Shan	Orogenic	269±4.3	K-Ar (sericite)	Zhang et al. (2009a)
							288±9.7	Rb-Sr (mixed hydrothermal mins.)	Zhang et al. (2009a)
Hanshan	45	39.91	96.43	China	Qilian Shan	Orogenic	224-214	K-Ar	Mao et al. (2000)
Shuangwang	46	33.88	107.24	China	West Qinling	Orogenic	202-198	Ar-Ar (feldspar)	Mao et al. (2002b)
Baguamiao	47	33.90	106.95	China	West Qinling	Orogenic	209	U-Pb	Mao et al. (2002b)
Liba	48	34.10	104.59	China	West Qinling	Orogenic	216	Ar-Ar	Zeng et al. (2012b)
							176	Rb-Sr	Shicai (2000)
Ma'anqiao	49	33.66	108.04	China	West Qinling	Orogenic	210-170	by association	Mao et al. (2002b)
Dashui	50	34.05	102.23	China	West Qinling	Orogenic or carlin	L. Triassic-M. Jurassic	by association	Mao et al. (2002b)
La'erma	51	34.01	102.32	China	West Qinling	Orogenic or carlin	L. Triassic-M. Jurassic	by association	Mao et al. (2002b)
Dongbeizhai	52	32.30	102.76	China	West Qinling	Orogenic	L. Triassic-M. Jurassic	by association	Mao et al. (2002b)
Jianchaling	53	33.25	106.37	China	West Qinling	Orogenic	L. Triassic-M. Jurassic	by association	Mao et al. (2002b)
Anba	54	32.98	104.67	China	West Qinling	Orogenic	E. Triassic	geologic	
Wulashan	169	40.70	109.40	China	N margin of N. China block	Orogenic	352	Ar-Ar (fuchsite)	Hart et al. (2002)
							297-296	Ar-Ar (sericite)	Nie et al. (2002)
Saiyinwusu	170	41.99	110.09	China	N margin of N. China block	Orogenic	253	Ar-Ar (mica)	Hart et al. (2002)
							249	Ar-Ar (sericite)	Nie et al. (2002)
217 (Chang Shan Hao)	171	41.66	109.26	China	N margin of N. China block	Orogenic	260-250	by association	Hart et al. (2002); Nie et al. (2002)
Dongping	172	40.73	115.25	China	N margin of N. China block	Orogenic	153	Ar-Ar isochron (sericite/illite)	Hart et al. (2002)
							147	Ar-Ar lowest plateau step	Hart et al. (2002)
Jinchangyu	173	40.30	118.30	China	N margin of N. China block	Orogenic	204-180	Ar-Ar (white mica)	Hart et al. (2002)
							196	K-Ar	Yu and Jia (1989)
Bajiazi	174	42.87	127.56	China	N margin of N. China block	Orogenic	204	Ar-Ar (sericite)	Miao et al. (2005)

(Fig. 7) is widely stated to contain 281 t Au, which would make it one of China's largest gold deposits (Nan Li, written commun., 2012), but this large stated resource remains poorly documented and could be much smaller. The shear system here developed during the Permian–Triassic and was reactivated during the Jurassic–Early Cretaceous (Du and Wu, 1998; Yan et al., 2010). It formed as a suture during final closure of the Mianlue Ocean and was reactivated during later tectonism, which Dong et al. (2011) relate to southward subduction of the North China block below the Paleozoic orogen. Gold is mainly disseminated with pyrite and arsenopyrite in the more deformed phyllite and within competent and rotated Late Triassic granite porphyry dikes (Nan Li, written commun., 2012). Although shearing and gold deposition are assumed to be Early Triassic based on geological relationships, absolute age constraints on the Yangshan deposits, or the other gold deposits along the Mianlue fault system, are lacking.

3. Early Paleozoic Yangzte block of the Gondwanan margin

The Proterozoic Jiangnan fold belt of present-day central China stretches for 1500 km from eastern Guizhou in the southwest to western Zhejiang in the east. The belt, and probably its associated gold resources, formed while the South China block was still a marginal part of the Rodinia and then Gondwana supercontinents. The fold belt initially developed during collision of the Yangtze and Cathaysia blocks along an active margin of Rodinia at ca. 830 Ma as a part of Jinning or Sibao orogeny, and then the belt rifted apart during the subsequent 100 m.y (Zhao et al., 2011), perhaps as part of the Rodinia break-up. After almost 300 m.y. of sedimentation within the aborted rift, renewed convergence, along the Gondwana margin, led to ca. 465–425 Ma Caledonian subduction of Cathaysia below Yangtze, thrusting along both sides of the suture, and late tectonic intrusions and doming (Charvet et al., 2010); locally this is referred to as the early Paleozoic Wuyi–Yunkai orogen (Fig. 8). Deep-seated faults paralleling the Yangtze active margin, such as the Jiangshan–Shaoxin, as well as those further inland in the orogen, underwent sinistral transpression during late stages of orogeny (Charvet et al., 2010).

Gold deposits of the Jiangnan fold belt (Fig. 8; Table 5) are located throughout the inboard side of the orogen and continue into adjacent parts of the Paleozoic foreland basin. They are predominantly Caledonian orogenic deposits, but with distinct differences in character from west to east. The west Jiangnan is predominantly underlain by lower greenschist-facies Mesoproterozoic and Neoproterozoic turbidites, with gold typically occurring along the margins of bedding-parallel saddle reef-style quartz veins, which are controlled by NE-striking shear zones interpreted to be of Caledonian origin (Lu et al., 2005a). These deposits are not well-studied, with a broad range of Rb–Sr ages from 514 to 370 Ma (Lu et al., 2005a). The central Jiangnan deposits are characterized by an Au–As–W association, with reported conflicting 410 Ma (Sm–Nd scheelite: Peng et al., 2003), 160–130 Ma (Rb–Sr quartz: Peng et al., 2003), or 199 Ma (Rb–Sr sphalerite: Peng and Frei, 2004) ages for the large Woxi deposit. Although ores are hosted by bedding-parallel quartz veins in greenschist-facies Neoproterozoic metasedimentary rocks at Woxi, 270 km to the east of Wangu, mineralization is controlled by E–W-striking thrust faults and proximal anticlinal hinges in subgreenschist-facies Mesoproterozoic rocks (Hu et al., 1996). Between Woxi and Wangu is the Xikuangshan Sb deposit, where lenses of stibnite-bearing quartz and calcite within a chert layer contained in a Late Devonian black shale represent the world's largest Sb resource (Fan et al., 2004). Within the eastern part of the Jiangnan fold belt, Jinshan, the largest gold deposit in the area,

Please cite this article as: Goldfarb, R.J., et al., Phanerozoic continental growth and gold metallogeny of Asia, Gondwana Research (2013), http://dx.doi.org/10.1016/j.gr.2013.03.002

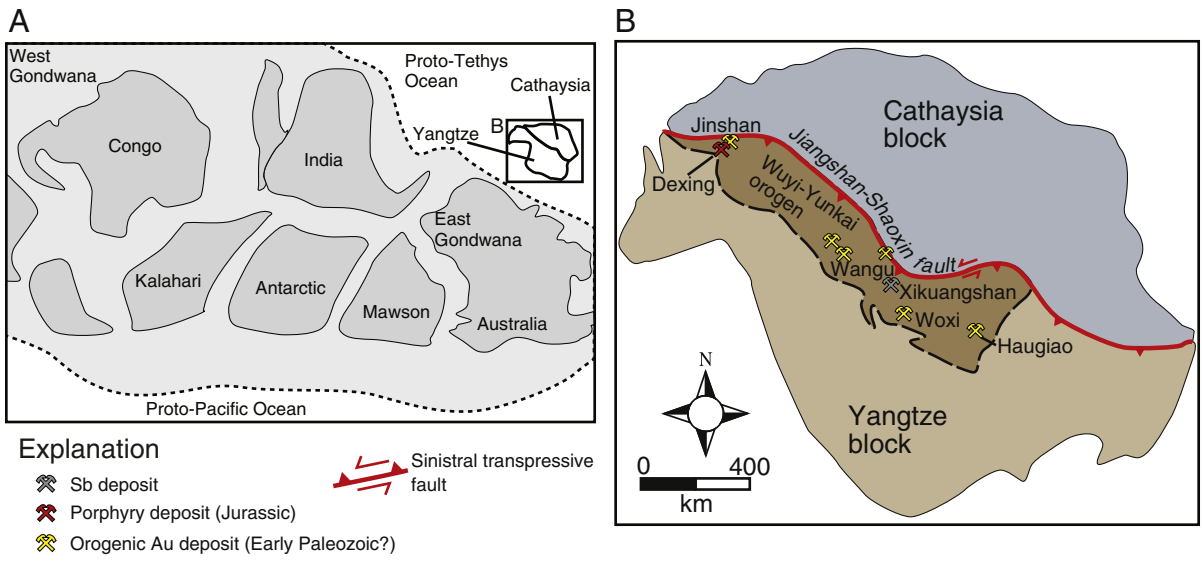

Fig. 8. Dozens of orogenic gold deposits of the Jiangnan fold belt (e.g., Jinshan, Woxi) are located along the Ordovician–Silurian suture between the Yangtze and Cathaysia blocks, termed the Wuyi–Yunkai orogen. The belt also includes the world's largest antimony deposit at Xikuangshan. Although controversial, if dates of the ores are also early Paleozoic, then these deposits formed while the South China block was a part of East Gondwana and prior to its rifting into the Tethys Ocean.
(A) Gondwana configuration in the Early Paleozoic after Cawood et al. (2007). (B) South China based largely from Yang et al. (2010) and Liu et al. (2012).

and many smaller gold deposits are hosted by mylonitic Mesoproterozoic metasedimentary rocks within the sub-horizontal Jinshan shear zone that links regional-scale thrust faults. Reported ages for Jinshan include an unspecified Neoproterozoic date ($^{40}Ar/^{39}Ar$: Li et al., 2010), 406 ±25 Ma (Rb–Sr quartz: Wang et al., 1999), 379 ± 49 Ma (Rb–Sr quartz: Mao et al., 2008) and 168 Ma (Rb–Sr illite: Mao and Wang, 2000). The Dexing porphyry deposit is located a couple of kilometers from Jinshan and is China's largest porphyry copper deposit, with an additional 300 t Au resource (Mao et al., 2012). The porphyry orebodies, however, have a Middle Jurassic age (Zhou et al., 2012) and likely define an early event in the evolution of the nearby Yangtze River province porphyry and skarn belt (see below), rather than having any relationship to the orogenic gold ores in the Jiangnan belt.

There is, for the most part, wide agreement that the time of gold formation was Caledonian, synchronous with final collision between the Yangtze and Cathaysia blocks. This is consistent with many published dates and the accepted timing of transpressional motion on the regional faults. However, a middle to late Mesozoic age cannot be ruled out for at least some of the ores. Almost all published absolute dates are problematic and some of these are younger than Caledonian and overlap with Yanshanian (late Mesozoic) magmatism in the belt. Charvet et al. (2010) documented left-lateral faulting along some of the regional NE-trending faults in the Early Cretaceous. Finally, although its relationship to the gold ores is unclear, the age of the Xikuangshan Sb deposit host rocks indicates that ore formation must be post-Caldeonian in age. But, if an early Paleozoic gold event is eventually fully confirmed by better geochronology, then it would suggest that the Jiangnan fold belt gold deposits formed within the Gondwana margin and were subsequently rifted and transported to Asia.

4. Middle–late Paleozoic Central Asian Orogenic Belt

The closure of the ocean basins between the Siberian craton, and the Kazakhstan, Tarim, and North China blocks, controlled the final amalgamation of the CAOB or the Altaid Orogen. Many parts of the orogen are particularly well endowed in gold resources. These include the above discussed (1) early Paleozoic districts formed along the margins of the Kazakhstan block and Siberian craton, within what could be defined as the mainly Caledonian component of the CAOB (Figs. 2–6); and the below discussed (2) Devonian and Carboniferous porphyry, and lesser epithermal, gold-bearing deposits developed predominantly within continental arcs or in near-shore oceanic arcs that formed as ocean basins closed (Fig. 9); (3) Permian orogenic gold deposits formed during post-collisional strike-slip between terranes (Figs. 10, 11); and (4) the Mesozoic Transbaikal gold deposits (Sections 6.1 and 6.2). The middle to late Paleozoic gold ores generally define part of the complex closure of the Turkestan Ocean, another basin developed along the northern Paleotethys Ocean, located between the Tarim–Karakum (e.g., Zonenshain et al., 1990) and Kazakhstan microcontinents during the Devonian to Early Permian (e.g., Heubeck, 2001). The closure was contemporaneous with subduction of Paleotethys oceanic crust beneath the length of the Tarim–Karakum block and the Turkestan Ocean crust below the Kazakhstan block.

The age relationships of the epigenetic gold ores, presented in detail below, are typical of what has been observed in other Cordilleran-style orogens (e.g., Kerrich et al., 2000; Goldfarb et al., 2001; Kerrich et al., 2005). Porphyry and epithermal gold deposits of this well-defined part of the accretionary orogen formed during a 100-m.y.-long

Table 5
Early Paleozoic(?) gold deposits of South China.

Deposit	Location in Fig. 1	Latitude	Longitude	Country	Tectonic location	Deposit type	Age (Ma)	Geochron. methodology	Geochron. reference
Woxi	55	28.53	110.67	China	Jiangnan fold belt	Orogenic	Unreliable		
Wangu	56	28.64	113.56	China	Jiangnan fold belt	Orogenic			
Jinshan	57	28.98	117.71	China	Jiangnan fold belt	Orogenic	Unreliable		
Dexing	58	29.02	117.58	China	Jiangnan fold belt	Porphyry	172–168	Re–Os (molybdenite)	Lu et al. (2005b)

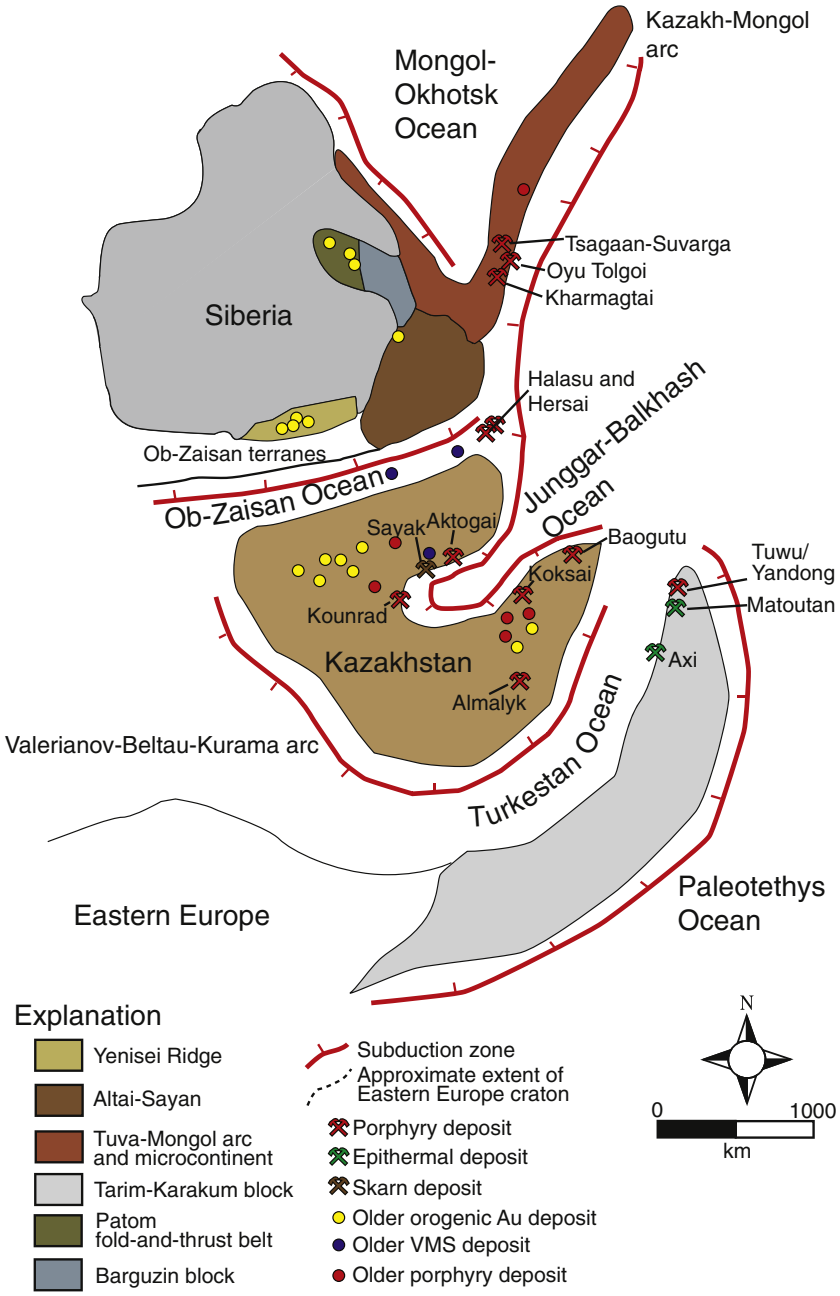

Fig. 9. One hundred million years of Devonian to Carboniferous continental margin and near-shore oceanic-arc magmatism was associated with closure of the ocean basins between the Siberian craton, Kazakhstan microcontinent, and Tarim–Karakum block. The magmatism was associated with formation of extensive porphyry development in the northern to middle Tien Shan and the southern Mongolian terranes, as depicted during the Carboniferous. These include some of the world's largest gold-bearing porphyry deposits in the Amalyk district of Uzbekistan and in the Oyu Tolgoi district in Mongolia.
Based on Filippova et al. (2001) and Yakubchuk (2002).

Devonian–Carboniferous time span, in both pre-accretionary oceanic-arc environments and post-accretionary continental margin settings. Almost all the orogenic gold deposits, from Uzbekistan east to southern Mongolia, formed during an extraordinarily brief 10- to 20-m.y.-long episode at roughly the Carboniferous–Permian time boundary. This episode reflects the well-defined cessation of compressional accretionary tectonics and the onset of large-scale strike-slip movement (Allen et al., 1995; Laurent-Charvet et al., 2003) along the many terrane suture zones of the Tien Shan, which were previously marked by thrust faulting. Such a massive ore-forming event is best visualized as an ancient analog to modern-day western North America, where seismic activity and crustal dewatering along the San Andreas and Queen Charlotte strike-slip fault systems are likely forming a gold province many thousands of kilometers long that will be exposed tens of millions of years in the future. Timing for this compressional to strike-slip transition in the CAOB, marking a change from subduction-related calc-alkaline to post-subduction more alkaline magmatism and overlapping broad regional metamorphism, is best placed at ca. 290–280 Ma (e.g., Ecomomos et al., 2012).

4.1. Northern Tien Shan

The porphyry and epithermal deposits associated with closure of the Turkestan Ocean (Fig. 9; Table 6) are associated with Middle

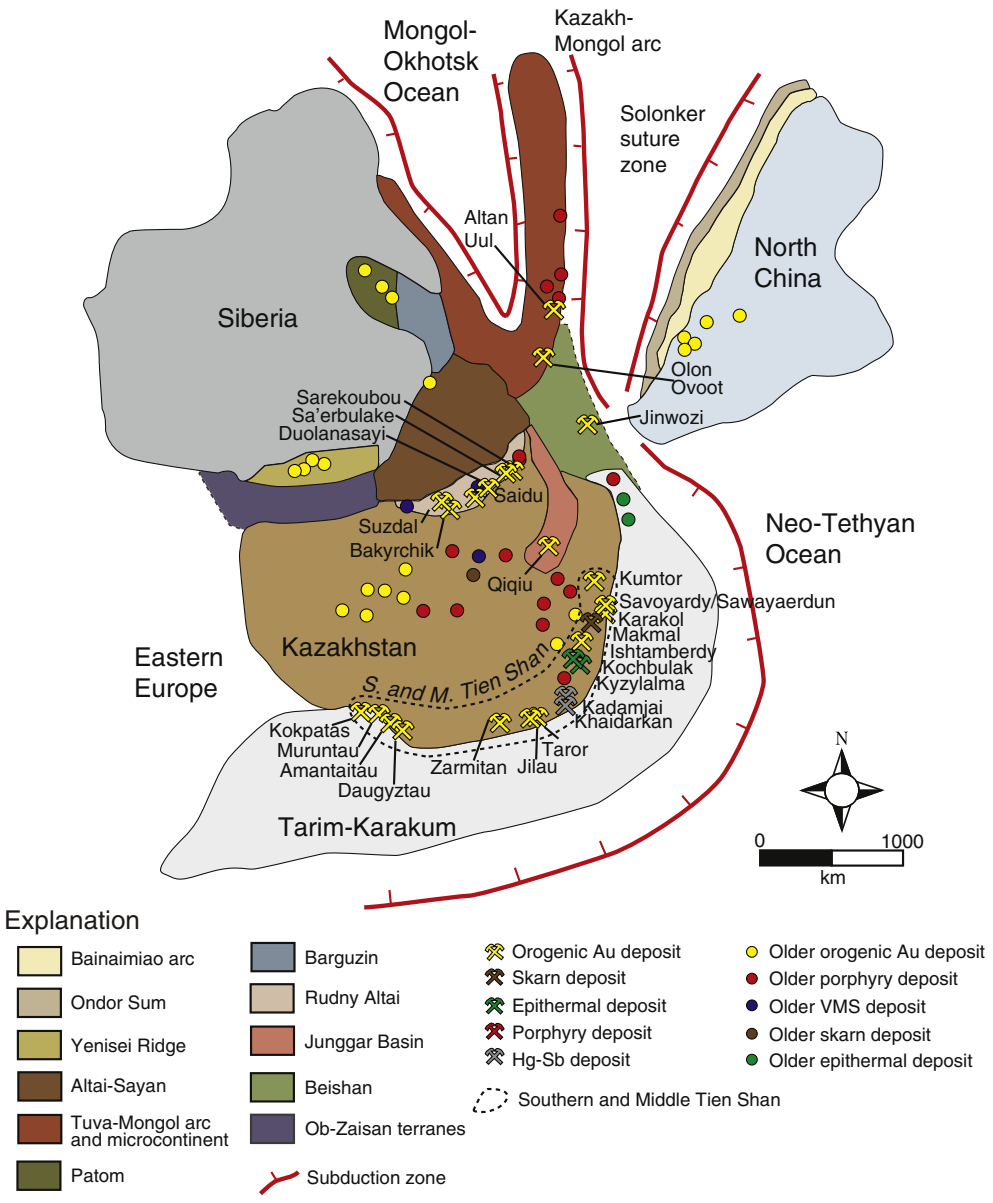

Fig. 10. A protracted ca. 30-m.y.-long latest Carboniferous to Early Permian period of strike-slip events along terrane-bounding sutures between older Paleozoic terranes led to widespread orogenic gold deposit formation across the southern margin of the Central Asia Orogenic Belt, as depicted during the Permian. These included formation of the orogenic gold deposits of the Charsk gold belt (e.g., Bakyrchik, Suzdol) at the site of closure of the Ob–Zaisan Ocean, of the southern to middle Tien Shan at the site of closure of the Turkestan Ocean (e.g., Muruntau, Kumtor, Zarmitan), and of the Junggar basin at the site of the Junggar–Balkhash Ocean (e.g., Qiqiu). Subduction and accretion along the northern margin to the North China block, mainly from Carboniferous through Triassic, was associated with formation of additional orogenic gold deposits within the reactivated Precambrian basement rocks of the block (see Fig. 15). Based on Filippova et al. (2001) and Yakubchuk (2002).

Devonian to latest Carboniferous arcs. Yakubchuk et al. (2002) have grouped these into the Kazakh–Mongol arc (also the Balkhash–Yili arc of Windley et al., 2007) in the region from Kazakhstan, through Xinjiang, and into southern Mongolia, and the Valerianov–Beltau–Kurama arc in Uzbekistan to the far west. Some of the porphyry ores contain giant gold resources, whereas in other deposits gold is more of a by product of copper mining.

Isotopic data indicate that many of the large Cu ± Au porphyry deposits and related skarns of both arcs (Fig. 9), in contrast to some of the above early Paleozoic porphyry deposits that formed in oceanic environments, are products of continental margin arc magmatism along the Kazakhstan microcontinent active margin (Heinhorst et al., 2000). Recent geochronology suggests a remarkably tight cluster on the ages of the deposits. Absolute dates on the northernmost of these deposits are ca. 327 Ma for Kounrad (55 t Au) and Aktogai (Fig. 9; Chen et al., 2012). Dates of ca. 330 Ma for ore-related granitoids at the Koksai porphyry and associated Sayak skarns (Seltmann and Porter, 2005) indicate an extensive porphyry belt along the Junggar–Balkhash Ocean, potentially coeval with the oroclincal bending of the microcontinent (Fig. 9).

An age of ca. 315 Ma for the giant Cu–Au porphyry orebodies at Almalyk (2800 t Au; Seltmann and Porter, 2005) reflects similar arc magmatism along the northern side of the Turkestan Ocean (Fig. 9). These auriferous magmatic systems also include the Kuru–Tegerek copper skarn in the Chandalash Ridge area of northwestern Kyrgyzstan, where middle Carboniferous diorites intrude Early Carboniferous carbonates of the middle Tien Shan (Jenchuraeva, 2001). The 322.7 ± 2.5 Ma Tuwu/Yandong porphyry prospects in the northern Tien Shan (Rui et al., 2002), as well as the ca. 312 Ma Baogutu Cu–Mo–Au porphyry deposit in the West Junggar (Shen et al., 2012), reflect additional subduction-related porphyry mineralization along the margins of the closing ocean basin.

Please cite this article as: Goldfarb, R.J., et al., Phanerozoic continental growth and gold metallogeny of Asia, Gondwana Research (2013), http://dx.doi.org/10.1016/j.gr.2013.03.002

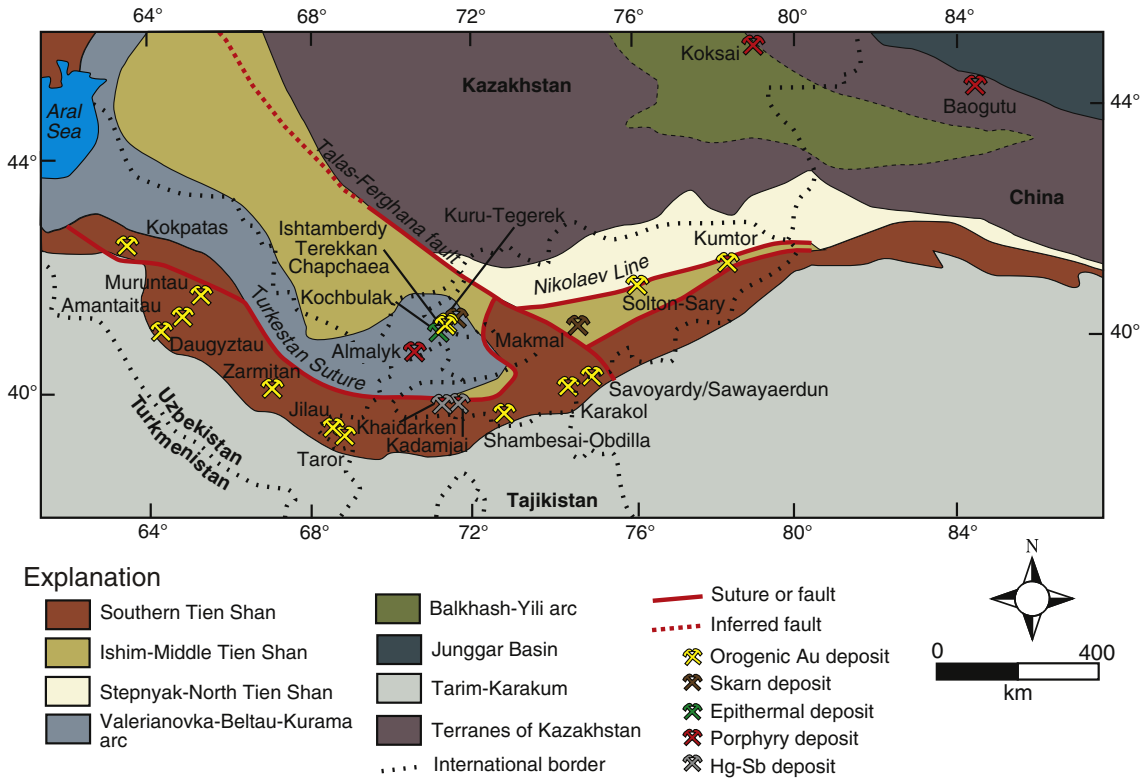

Fig. 11. Present day configuration of the geology of the Tien Shan, central Asia, showing the most significant late Paleozoic Au-bearing mineral deposits. Map based on Yakubchuk (2002), Konopelko et al. (2007), and Windley et al. (2007).

Formation of auriferous porphyry bodies continued far to the east within the Kazakh–Mongol arc, where there is a greater spread in ages and evidence for distinct Devonian and Carboniferous events. The enormous Oyu Tolgoi Cu–Au–Mo (1000 t Au) deposit and the nearby Tsagaan–Suvarga deposit (Fig. 9; Lamb and Cox, 1998; Kirwin et al., 2005a), both formed at ca. 380–370 Ma in rocks of the Gurvansayhan terrane of Badarch et al. (2002) in southern Mongolia, are products of an oceanic magmatic event during the early part of Kazak–Mongol arc development. Although oceanic in character, zircon data suggest Oyu Tolgoi was close to the Siberian craton margin during formation (Wainwright et al., 2011). The Xilekuduke–Halasu–Hersai group of porphyry Cu–Au–Mo deposits, located in the Chinese Altai–East Junggar, in an area sometimes referred to as the Kalatongke island arc, may also have developed in the disappearing Ob–Zaisan Ocean. Dates by Re–Os methods of 377 Ma for Halasu and 408 Ma for Hersai, reported by Xue et al. (2010) and Du et al. (2010), respectively, could be representative of ore-forming events within a broader province that also included Oyu Tolgoi. The ca. 330 Ma Kharmagtai deposit in southern Mongolia indicates youngest subduction-related Cu–Au porphyry formation along a more eastern part of the developing active continental margin (Kirwin et al., 2005b).

Gold-bearing epithermal deposits also host important resources within the middle to late Paleozoic arc environments. Kochbulak and Kyzylalma (Figs. 10, 11), within a few tens of kilometers of the Almalyk porphyry systems, formed in the Valerianov–Beltau–Kurama arc at ca. 290–280 Ma (Yakubchuk et al., 2002), a few tens of millions of years subsequent to the main recognized porphyry events. Conflicting absolute-age data characterize Axi (Fig. 9) and associated epithermal deposits in westernmost Xinjiang, with reported dates covering almost the entire Carboniferous (Rui et al., 2002). Nevertheless, similar to the Tuwu/Yandong porphyries, these were part of a series of Turkestan Ocean island arcs that were accreted to the northern margin of the Tarim–Karakum block. To the east, but also in the northern part of the Tien Shan in Xinjiang, small epithermal gold ores (e.g., Xitan) and Fe–Cu–Au replacement deposits (e.g., Kanggur, Matoutan) may be part of the same oceanic arc system (termed the Harlik–Dananhu arc by Xiao et al., 2008), or alternatively have been suggested to be post-accretionary ores (e.g., Mao et al., 2005).

Although the northern side of the Tien Shan is characterized by important arc-related porphyry and epithermal ores, orogenic gold deposits are uncommon. One exception is far to the east in southern Mongolia, where poorly exposed middle Paleozoic metasedimentary rocks of the Gobi Altai terrane are part of a Paleozoic back-arc sequence of the closing Turkestan Ocean. The quartz diorite-hosted Olon Ovoot orogenic gold deposit (Fig. 10) is located along the southern side of the Main Mongolian Lineament in rocks that define a back-arc basin trapped behind the Kazakh–Mongol arc (see Fig. 16 in Lamb and Badarch, 2001). Although a relatively small deposit, Olon Ovoot forms part of the little described 50 by 10 km, ENE-trending Khaniin Khets orogenic gold belt that terminates to the east at the jasperoid-hosted Unegen Del Au–Sb–Hg prospect. The Altan Uul orogenic gold prospect, located 500 km east of Olon Ovoot in a similar rock package, is hosted by a polydeformed jasperoid/schist, with gold occurring in post-peak metamorphic quartz veins. Little geochronology is available for these deposits, but K–Ar dates on granitoids near Olon Ovoot indicate a probable Early Permian age for magmatism (Japan International Cooperation Agency, 1992) that could be part of the same tectonism as the gold event.

4.2. Beishan

A series of Paleozoic small arcs and intervening ocean basins were accreted to the Tuva–Mongol microcontinent during Permian–Early Triassic and now define the Beishan (Fig. 10) located to the east of

Please cite this article as: Goldfarb, R.J., et al., Phanerozoic continental growth and gold metallogeny of Asia, Gondwana Research (2013), http://dx.doi.org/10.1016/j.gr.2013.03.002

Table 6
Middle-late Paleozoic gold deposits of the Central Asian Orogenic Belt (CAOB).

Deposit	Location in Fig. 1	Latitude	Longitude	Country	Tectonic location	Deposit type	Age (Ma)	Geochron. methodology	Geochron. reference
Aktogai	59	46.97	79.98	Kazakhstan	Northern Tien Shan	Porphyry	327		Chen et al. (2012)
Kounrad	60	47.02	75.08	Kazakhstan	Northern Tien Shan	Porphyry	327		Chen et al. (2012)
Koksai	61	44.48	78.47	Kazakhstan	Northern Tien Shan	Porphyry	330	unknown	Seltmann and Porter (2005)
Sayak	62	47.02	77.38	Kazakhstan	Northern Tien Shan	Skarn	330	unknown	Seltmann and Porter (2005)
Almalyk	63	40.81	69.65	Uzbekistan	Middle Tien Shan	Porphyry	315	unknown	Seltmann and Porter (2005)
Kuru-Tegerek	64	42.05	71.45	Kyrgyzstan	Middle Tien Shan	Skarn	Mid. Carboniferous(?)		
Tuwu	65	42.12	92.62	China	Northern Tien Shan	Porphyry	322.7±2.3	Re-Os (molybdenite)	Rui et al. (2002)
Yandong	66	42.06	92.39	China	Northern Tien Shan	Porphyry	341.2±4.9	K-Ar (sericite)	Zhang et al. (2004)
Baogutu	67	45.50	84.41	China	West Junggar	Porphyry	314-309	Re-Os (molybdenite)	Shen et al. (2012)
							313-312	U-Pb (zircon)	Shen et al. (2012)
Oyu Tolgoi	68	43.02	106.85	Mongolia	Kazakh-Mongol arc	Porphyry	372-366	U-Pb (zircon)	Wainwright et al. (2011)
Tsagaan-Suvarga	69	43.87	108.32	Mongolia	Kazakh-Mongol arc	Porphyry	371-369	Re-Os (molybdenite)	Watanabe and Stein (2000)
Xilekduke	70	46.84	89.15	China	Kazakh-Mongol arc	Porphyry			
Halasu	71	46.49	90.02	China	Kazakh-Mongol arc	Porphyry	377	Re-Os	Xue et al. (2010)
Hersai	72	45.00	91.32	China	Kazakh-Mongol arc	Porphyry	408	Re-Os	Du et al. (2010)
Kharmagtai	73	43.90	106.10	Mongolia	Kazakh-Mongol arc	Porphyry	330	Re-Os	Kirwin et al. (2005b)
Kochbulak	74	41.02	70.15	Uzbekistan	Valerianov-Beltau-Kirama arc	Epithermal	290-280		Yakubchuk et al. (2002)
Kyzylalma	75	41.06	70.13	Uzbekistan	Valerianov-Beltau-Kirama arc	Epithermal	290-280		Yakubchuk et al. (2002)
Axi	76	44.23	81.62	China	Valerianov-Beltau-Kirama arc	Epithermal	Carboniferous		Rui et al. (2002)
Xitan	77	42.09	90.20	China	Valerianov-Beltau-Kirama arc	Epithermal	288±7 to 244±9	Rb-Sr isochron	Zhang et al. (2004)
Kanggur	78	42.03	90.23	China	Valerianov-Beltau-Kirama arc	Fe-Cu-Au replacement	290.4±7.2	Sm-Nd isochron	Zhang et al. (2004)
							282.3±5 to 254±7	Rb-Sr isochron	Zhang et al. (2004)
Matoutan	79	42.02	91.07	China	Valerianov-Beltau-Kirama arc	Fe-Cu-Au replacement			
Olon Ovoot	80	44.38	104.17	Mongolia	Valerianov-Beltau-Kirama arc	Orogenic	Early Permian	K-Ar	Japan International Cooperation Agency (1992)
Unegen Del	81	~44.41	~104.9	Mongolia	Valerianov-Beltau-Kirama arc	Au-Sb-Hg			
Altan Uul	82	43.66	100.50	Mongolia	Valerianov-Beltau-Kirama arc	Orogenic			
Mazhuangshan	83	42.17	96.30	China	Beishan	Orogenic? Epithermal?	298±28	Rb-Sr (fluid inclusions)	Li et al. (1999)
Jinwozi	84	41.64	95.30	China	Beishan	Orogenic? Epithermal?	230±5.7	Rb-Sr (fluid inclusions)	Chen et al. (1999)
Nanjinshan	85	41.88	96.18	China	Beishan	Orogenic? Epithermal?	242.8±0.8	Ar-Ar (sericite)	Jiang et al. (2004)
Xiaoxigong	86	40.78	96.85	China	Beishan	Orogenic? Epithermal?	267±7, 284±4	K-Ar (sericite)	Jiang et al. (2004)
Liushashan	87	42.15	98.37	China	Beishan	Orogenic? Epithermal?	260±10	Re-Os (molybdenite)	Jiang et al. (2004)
Muruntau	88	41.48	64.58	Uzbekistan	Southern Tien Shan	Orogenic	287	Re-Os (arsenopyrite)	Morelli et al. (2007)
Kokpatas	89	42.23	63.90	Uzbekistan	Southern Tien Shan	Orogenic	Carboniferous/ Permian(?)		
Amantaitau	90	41.15	64.22	Uzbekistan	Southern Tien Shan	Orogenic	Carboniferous/ Permian(?)		
Daugyztau	91	41.10	64.20	Uzbekistan	Southern Tien Shan	Orogenic	Carboniferous/ Permian(?)		
Jilau	92	39.42	67.65	Tajikistan	Southern Tien Shan	Orogenic	Carboniferous/ Permian(?)		
Taror	93	39.41	67.74	Tajikistan	Southern Tien Shan	Orogenic	Carboniferous/ Permian(?)		
Zarmitan	94	40.33	66.77	Uzbekistan	Southern Tien Shan	Orogenic	286	Re-Os (pyrite)	R. Seltmann, oral commun. (2010)
Karakol	95	40.00	73.75	Kyrgyzstan	Southern Tien Shan	Orogenic	Carboniferous/ Permian(?)		
Shambesai-Obdilla	96	40.08	72.12	Kyrgyzstan	Southern Tien Shan	Carlin?			
Savoyardy/ Sawayaerdun	97	40.17	74.25	China/ Kyrgyzstan	Southern Tien Shan	Orogenic	213-206(?)	Ar-Ar (fluid inc., poor profiles)	Liu et al. (2007)
							288±50	Rb-Sr (fluid inc.)	Liu et al. (2007)

Please cite this article as: Goldfarb, R.J., et al., Phanerozoic continental growth and gold metallogeny of Asia, Gondwana Research (2013), http://dx.doi.org/10.1016/j.gr.2013.03.002

Table 6 (*continued*)

Deposit	Location in Fig. 1	Latitude	Longitude	Country	Tectonic location	Deposit type	Age (Ma)	Geochron. methodology	Geochron. reference
Kumtor	98	41.87	78.20	Kyrgyzstan	Middle Tien Shan	Orogenic	285	Ar-Ar (sericite)	Mao et al. (2004)
Makmal	99	41.22	73.93	Kyrgyzstan	Middle Tien Shan	Skarn	290-277 pluton		Jenchuraeva et al. (2001)
Ishtamberdy	100	41.41	70.80	Kyrgyzstan	Middle Tien Shan	Uncertain	Late Paleozoic (?)		
Terekkan	101	41.41	71.01	Kyrgyzstan	Middle Tien Shan	Orogenic			
Chapchaea	102	41.46	70.65	Kyrgyzstan	Middle Tien Shan	Orogenic			
Bakyrchik	103	49.47	81.73	Kazakhstan	Rudny Altai	Orogenic	310-280	Ar-Ar	Naumov et al. (2012)
Sekisovskoye	104	50.33	82.60	Kazakhstan	Rudny Altai	Orogenic	306±3.8	Ar-Ar (sericite)	Naumov et al. (2012)
Suzdal	105	50.05	79.75	Kazakhstan	Rudny Altai	Orogenic	281±3.3	Ar-Ar (sericite)	Naumov et al. (2012)
Duolanasayi	106	48.15	86.53	China	Xinjiang	Orogenic	289		Li and Chen (2004)
Saidu	107	48.32	86.05	China	Xinjiang	Orogenic	278		Li and Chen (2004)
Sa'erbulake	108	47.17	89.02	China	Xinjiang	Orogenic	320-285		Goldfarb et al. (2003)
Sarekoubou	109	47.20	88.25	China	Xinjiang	Orogenic	320.6±4	Ar-Ar (fluid inclusions)	Ding et al. (2004)
Qiqiu (Hatu)	110	45.91	84.32	China	Junggar-Balkhash basin	Orogenic	290-288	Rb-Sr (unspecified material)	Rui et al. (2002)

the northern Tien Shan. Xiao et al. (2010) argue that the Beishan represent part of the broad suture that includes the northern margin of the Tien Shan to the southwest and the Solonker suture of southern Mongolia to the east (see below). The suture represents the area of the main closure of the Turkestan Ocean, and related branches of the Paleoasian Ocean, between the North China and Tarim/Karakum blocks with the amalgamating Siberia and Kazakhstan blocks.

There are more than one hundred small gold deposits and prospects adjacent to the major east–west thrust faults and strike-slip faults in the Beishan. Most of these are concentrated near the western edge of the Beishan. Deposit types and ages remain contradictory. Available geochronology is of variable quality, but puts four dated deposits in an appoximate range between 300 and 230 Ma (Table 6; Jiang et al., 2004), which roughly overlap with Permian–Early Triassic accretionary deformation.

Gold deposit classification has been uncertain. Descriptions of the ores by Jiang et al. (2004) are consistent with classification as orogenic gold deposits, with many localized along margins of older intrusions. A Permian age is also consistent with deposits in the adjacent southern Tien Shan (see below). Yang et al. (2009a), however, favor classification of some of the larger gold deposits, such as Mazhuangshan and Jinwozi (Fig. 10), as low-sulfidation epithermal deposits associated with ca. 300 Ma Beishan oceanic arcs. If this scenario is correct, then these would be pre-accretionary gold ores that might correlate with the other small epithermal and replacement deposits immediately to the west in the eastern part to the northern Tien Shan (e.g., Matoutan and Axi of Fig. 9). At the ca. 298 Ma Mazhuangshan deposit (Rb–Sr fluid inclusions: Li et al., 1999), bladed carbonate, banded quartz-adularia, and other boiling textures clearly indicate the epithermal classification to be correct. However, the mineralization style at Jinwozi is definitely orogenic and it has a younger date of ca. 230 Ma (Rb–Sr fluid inclusions: Chen et al., 1999). Thus, the Beishan apparently hosts both pre-accretionary low-sulfidation epithermal ores and syn-accretionary orogenic gold deposits.

4.3. Southern Tien Shan

Late Paleozoic accretionary orogenesis on the southern side of the Kazakhstan block led to the formation of orogenic gold deposits mainly seaward of the Valerianov–Beltau–Kurama continental arc, although there are some exceptions noted below. Where the western part of the Turkestan Ocean basin was closed, numerous world-class deposits formed in the southern Tien Shan (Figs. 10, 11; Table 6), typically considered the most outboard part of the western part of CAOB. The rocks of the southern Tien Shan are dominated by carbonate platform sequences on the northwestern margin of the Tarim–Karakum block and clastic sedimentary rocks from the closing ocean basin, with lesser felsic to intermediate volcanic rocks; these early to late Paleozoic rocks of the southern Tien Shan are sometimes collectively referred to as the Altay microcontinent (e.g., Natal'in and Sengor, 2005), although they might be better viewed as a number of dismembered terrane fragments and not as a single cohesive block.

The largest of these orogenic gold deposits of the southern Tien Shan, and the largest gold deposit in the world after Witwatersrand, is the 287 Ma (Morelli et al., 2007), Muruntau deposit (>5200 t Au) situated in the westernmost part of the mountain range (Fig. 10). Iron-rich and carbonaceous Ordovician to Early Silurian marine clastic rocks host the gold-bearing quartz veins and veinlets. The reason for the extraordinary size of Muruntau remains highly debated, but a possible cause could be a very large crustal endowment of early Paleozoic gold, mainly hosted in disseminated syngenetic sulfides, which was mobilized and focused 200 m.y. later to form the ores during late Paleozoic regional metamorphism and tectonism. Other significant gold deposits of probably similar age in the Paleozoic of the southwestern Tien Shan include Kokpatas, Amantaitau, and Daugyztau. This important group of deposits, including Muruntau, is located to the south of a major offset along the main fault (e.g., Turkestan suture) between the Kazakhstan and Tarim–Karakum blocks (e.g., Fig. 1 in Natal'in and Sengor, 2005), which may have been critical for large-scale dilational focusing of auriferous ore fluids. A few hundred kilometers to the east, other deposits in the southern Tien Shan belt, such as Jilau, Taror, and Zarmitan (340 t Au), occur as large veins and stockworks often hosted by older, competent intrusive bodies or along the sheared margins of the intrusions. At Zarmitan, the ore-hosting Koshrabad massif, which intrudes Ordovician–Early Silurian flysch, has a reported K–Ar date of 269 ± 4.2 Ma (Bortnikov et al., 1996; Abzalov, 2007), which, if reliable, would give a maximum age to gold deposition. A Re–Os age on pyrite of 286 Ma (R. Seltmann, oral commun., 2010) is, however, older and similar to the Muruntau date. The Jilau deposit is hosted along shears within the eastern margin of the ca. 329–306 Ma Chinorsai granodiorite that intrudes Silurian to Devonian bituminous dolomite (Cole et al., 2000).

Less well-documented and little developed orogenic gold deposits occur farther east in the southern Tien Shan (Figs. 10, 11). A 280-km-long belt of mercury (e.g., Khaidarken) and antimony (e.g., Kadamjai) deposits extend along the southern side of the present-day Fergana Valley to the south and west of Osh (United Nations, 1998). The gold potential of these Hg–Sb resources is unclear, but the area also contains some orogenic gold deposits (e.g., Karakol) within Carboniferous argillites and could be part of a single metallogenic event in southwestern Kyrgyzstan. The Shambesai–Obdilla deposits (Fig. 11), also in this belt, exhibit some features in common with Carlin deposits.

Please cite this article as: Goldfarb, R.J., et al., Phanerozoic continental growth and gold metallogeny of Asia, Gondwana Research (2013), http://dx.doi.org/10.1016/j.gr.2013.03.002

The quartz veins and breccias of the Savoyardy/Sawayaerdun deposit, an orogenic gold deposit 300 km to the east along the Kyrgyzstan/Xinjiang border (Fig. 11), are hosted by Late Silurian–Early Devonian or younger phyllite. Although absolute dates exist for the deposit, their reliability is very uncertain. Liu et al. (2007) favored 213–206 Ma as being representative of the age of the Savoyardy/Sawayaerdun deposit, based upon saddle-shaped argon profiles of gold-bearing quartz samples and a Rb–Sr whole rock date on a diabase dike in the region, whereas they interpreted a Rb–Sr isochron age of 288 ± 50 Ma on the quartz to be from mixed sources.

The giant (570 t Au) Kumtor orogenic gold deposit (Figs. 10 and 11) is an anomaly in the region in that it is situated in the narrow (15–20 km) eastern arm of the Naryn basin of Windley et al. (2007), which appears to overlie the Ishim–Middle Tien Shan terrane, and not in the terranes of the southern Tien Shan. This basin is separated from the southern Tien Shan by the eastern continuation of the Turkestan suture, and from the Balkhash–Yili arc of the Stepnyak–North Tien Shan terrane to the north by the Nikolaev line, although plutons intruding rocks of the basin may also be a part of the same arc. Gold-bearing stockworks cut Vendian carbonaceous phyllites, perhaps basement to the basin, near the margin of a large batholith and close to a major offset along the Nikolaev line. A 285 Ma Ar–Ar date for hydrothermal sericite from Kumtor (Mao et al., 2004) indicates that orogenic gold formation was coeval on both sides of the Turkestan suture.

A few other gold resources define late Paleozoic hydrothermal events within the Ishim–Middle Tien Shan terrane. About 300 km west of Kumtor, the Makmal deposit is defined as a skarn adjacent to the ca. 290–277 Ma Chaartash porphyritic leucogranite that intrudes Early Carbonaceous sedimentary rocks of the Naryn basin (Jenchuraeva et al., 2001). Also, within the area of the Valerianov–Beltau–Kurama arc (Fig. 9), a number of Au–Sb quartz veins, some in saddle reef structures within Neoproterozoic to early Paleozoic schists, have characteristics most consistent with orogenic gold deposits (e.g., Ishtamberdy, Terekkan, Chapchaea; United Nations, 1998). Although absolute dates are not reported, Jenchuraeva (2001) suggests an association with Late Permian–Early Triassic tectonism for these deposits on the northeastern margin of the Fergana Valley. These observations would seem to further indicate late Paleozoic tectonism and related ore formation was widespread on both sides of the suture.

4.4. Rudny Altai/Chinese Altai/Junggar

Deformation during the final late Paleozoic closure of the Ob–Zaisan Ocean (Fig. 9), between the Siberia craton and Kazakhstan block, was associated with the formation of a second belt of giant late Paleozoic orogenic gold deposits in the Rudny Altai region. These less well-studied deposits, including Bakyrchik, Sekisovskoye, and Suzdal (Fig. 10), comprise what has been termed the Kalba gold belt or East Kazak orogenic gold province. The present-day NW-striking belt trends for more than 1000 km along the Irtysh–Zaisan system of regional faults in northeastern Kazakhstan and continues to the southeast into the adjacent Xinjiang Chinese Altai. The ore-hosting, sheared Carboniferous flyschoid rocks of the Irtysh–Zaisan basin define the southeasternmost part of the Chara suture along the edge of the Kazakhstanian collage of terranes (e.g., Fig. 6 in Windley et al., 2007); Devonian VMS deposits of the Rudny Altai, described above, occur just seaward of the flysch basin. Numerous $^{40}Ar/^{39}Ar$ dates of the orogenic gold deposits and prospects in the Kalba belt range between ca. 310 and 280 Ma (Naumov et al., 2012).

In Xinjiang, relatively imprecise dates are similarly spread between ca. 310 and 270 Ma for many deposits of the Habahe district, which include Duolanasayi and Saidu (Rui et al., 2002) that have more recently been dated at 289 Ma and 278 Ma, respectively (Li and Chen, 2004). The ores in Xinjiang are less refractory than those in Kazakhstan, perhaps indicating a deeper formation and/or reflecting the less carbonaceous host rocks and, significantly, may thus be intrinsically more amenable to future large-scale mining operations. The gold-bearing quartz veins and stockworks typically occur along faulted margins of Devonian plutons that intrude Silurian–Middle Devonian metasedimentary and metavolcanic units, and are adjacent to subsidiary faults of the Irtysh–Zaisan fault system. Continuing even farther to the southeast, other similar, but small orogenic gold occurrences along the NW-trending group of faults include Sa'erbulake and Sarekoubou in the Keketale district (Fig. 10), which have been dated between ca. 320 and 285 Ma (Goldfarb et al., 2003; Ding et al., 2004; Xu et al., 2005).

The Carboniferous–Permian time was also characterized by final closure of the Junggar–Balkhash basin (Xiao et al., 2008), an arm of the Turkestan Ocean located between the Northern Tien Shan on the margin of the Tarim–Karakum block and the Altai terranes. Devonian to Early Carboniferous metasedimentary and metavolcanic rocks of the western Junggar basin host more than 300 orogenic gold deposits and occurrences, which are particularly well-concentrated along a 70 by 20 km strike of the Dalabute fault zone. Quartz veins of the Qiqiu orebodies (Fig. 10) in the Hatu gold district contain >30 t Au and have been dated at ca. 290 Ma (Rui et al., 2002). Typically smaller orogenic gold deposits within similar age units of the eastern Jungger basin occur along the Kelameili fault system and were suggested by Rui et al. (2002) to also be latest Paleozoic in age.

5. Devonian–Triassic Cathaysialand

Cathaysialand formed within the eastern Paleotethys Ocean during the middle to late Paleozoic (e.g., Metcalfe, 2011). It involved gradual amalgamation of the South China, Indochina (also called Annamia), East Malaya, West Burma, and West Sumatra blocks (Fig. 12), which were all rifted from Gondwana in Devonian, and the Sibumasu block (Fig. 13; i.e., Southwest China–Burma–Malaya–Sumatra; Metcalfe, 1984), which was rifted from Gondwana in Early Permian. The resulting microcontinent or superterrane was sutured to North China and the Asian continent by the end of the Triassic. Mainly magmatic-related gold resources (Table 7) are associated with two subduction-related events during the growth of Cathaysialand, which took place while the superterrane was migrating across the Paleotethys. In addition, orogenic gold deposits (Table 7) most likely relate to transcurrent tectonics along the younger margin of the microcontinent.

5.1. Accretionary orogenesis

Many of the gold deposits in Cathaysialand are associated with late Paleozoic closing of ocean basins between the South China and Indochina–East Malaya (Fig. 12) blocks and subsequently the Indochina–East Malaya and Sibumasu blocks (Fig. 13). Subduction-related magmatism may have been important in both cases as subduction of a small ocean basin may have occurred below the eastern side of the Indochina block in late Paleozoic (Manaka et al., 2008) and the Paleotethyan Ocean was subducted below the western side of the same block through the Triassic (Metcalfe, 2011). All resulting gold deposits formed prior to docking of the superterrane with the southeastern margin of the growing Asian continent.

The Song Ma fault system represents the suture between the Indochina and South China blocks (Findlay and Trinh, 1997) that formed the first stages of Cathaysialand superterrane growth in Late Devonian–Early Carboniferous time (Metcalfe, 2011). Deformation of early to middle Paleozoic mainly shallow marine sedimentary rocks on the eastern side of the Indochina Block formed the NW-trending Truong Son fold belt (Fig. 12) that extends from present-day northeastern Laos through north-central Vietnam. Latest Carboniferous calc-alkaline magmatism is widespread within the belt.

The highly mineralized Sepon basin within the Truong Son fold belt in Laos contains gold-bearing copper skarn/replacement (e.g., Khanong, Thengkham) and disseminated gold (e.g., Discovery, Nalou) deposits, as well as copper porphyry deposits (Manini et al., 2001; Cromie et al.,

Please cite this article as: Goldfarb, R.J., et al., Phanerozoic continental growth and gold metallogeny of Asia, Gondwana Research (2013), http://dx.doi.org/10.1016/j.gr.2013.03.002

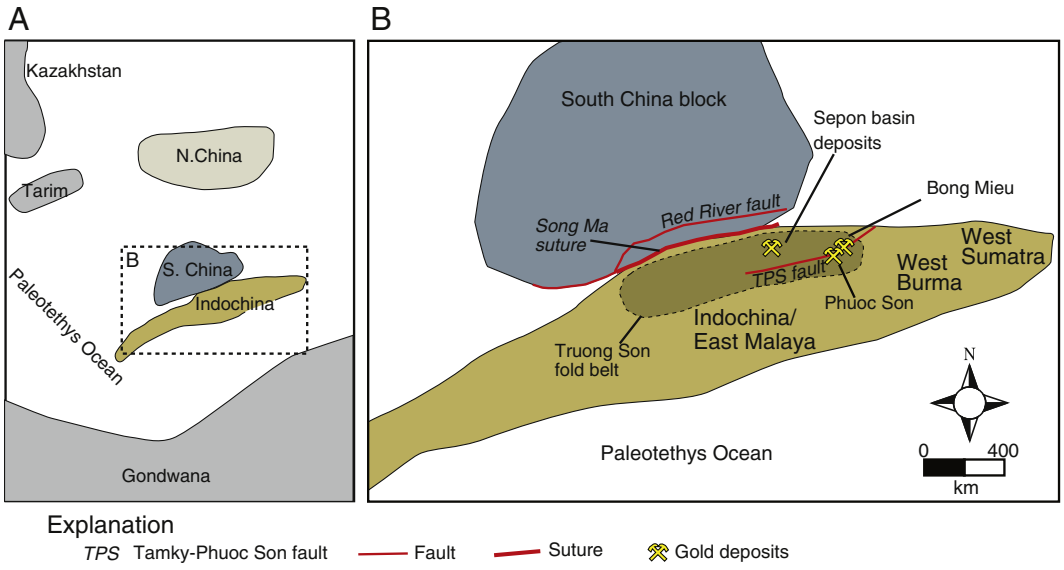

Fig. 12. The Song Ma fault zone defines the Late Devonian–Early Carboniferous suture between the South China and Indochina/East Malaya block in the Tethys Ocean. The Truong Son fold belt, formed during the collision-related deformation and part of present-day NE Laos and north-central Vietnam, hosts Late Carboniferous gold-bearing skarns and disseminated gold ores in the Sepon basin, and undated orogenic gold orebodies at Bong Mieu.
Modified from Metcalfe (2006, 2011).

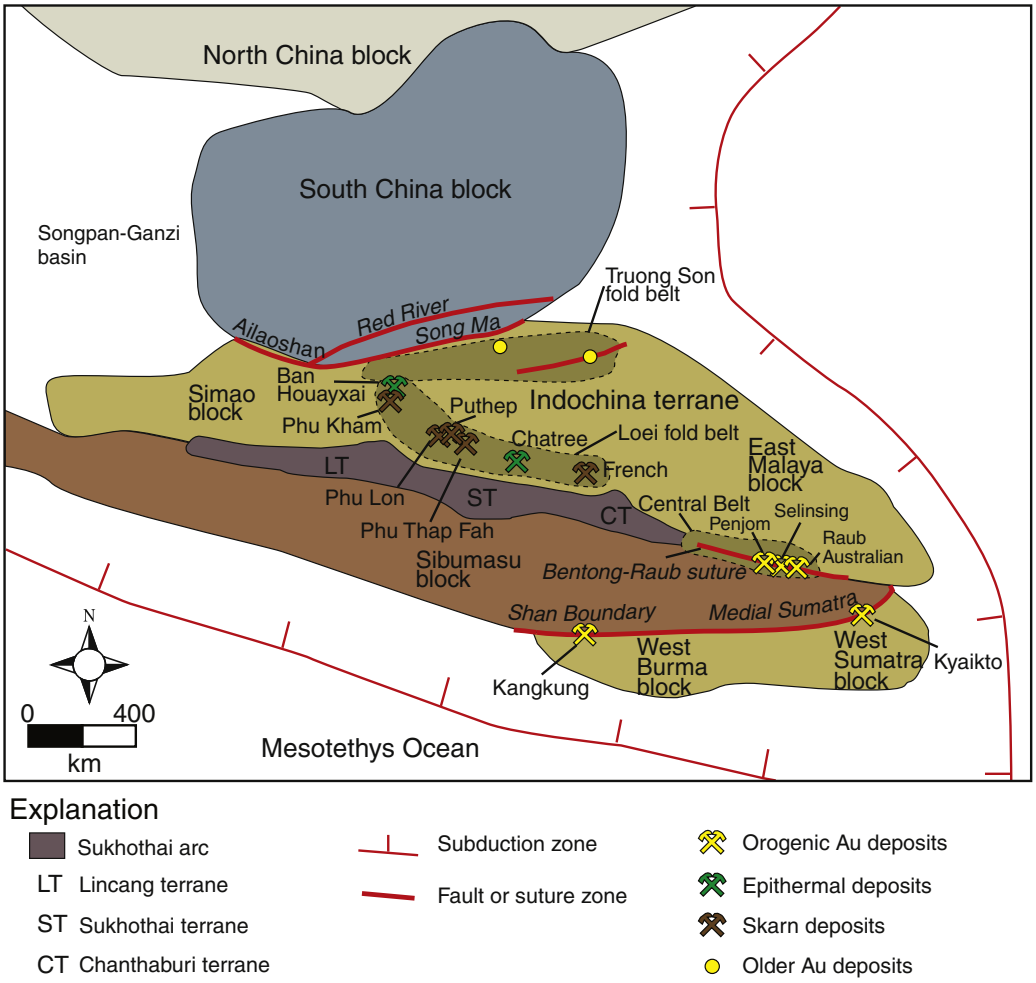

Fig. 13. The Permian–Triassic Loei–Phetchabun fold belt formed from the collision of the Sibumasu block with the Sukhothai arc, represented by the Lincang, Sukhothai, and Chanthaburi terranes. Deformation and magmatism resulted in epithermal and skarn mineralization. This collision also defines the Bentong–Raub suture, which hosts the Penjom, Selinsing, and Raub Australian orogenic gold deposits. Dextral movement along the Shan Boundary and the Medial Sumatra sutures began to translate the West Burma and West Sumatra blocks westward along the southern margin of the Sibumasu block.
Map based upon Metcalfe (2011).

Please cite this article as: Goldfarb, R.J., et al., Phanerozoic continental growth and gold metallogeny of Asia, Gondwana Research (2013), http://dx.doi.org/10.1016/j.gr.2013.03.002

Table 7
Devonian-Triassic gold deposits of Cathaysialand.

Deposit	Location in Fig. 1	Latitude	Longitude	Country	Tectonic location	Deposit type	Age (Ma)	Geochron. methodology	Geochron. reference
Khanong (Sepon)	111	16.97	106.01	Laos	Truong Son Fold Belt	Skarn	300		
Thongham (Sepon)	112	16.95	105.87	Laos	Truong Son Fold Belt	Skarn	300		
Discovery (Sepon)	113	16.97	106	Laos	Truong Son Fold Belt	Disseminated			
Nalou (Sepon)	114	16.96	105.97	Laos	Truong Son Fold Belt	Disseminated			
Bong Mieu	115	15.3	108.48	Vietnam	Truong Son Fold Belt	Orogenic			
Phuoc Son	116	15.6	108.3	Vietnam	Truong Son Fold Belt	Orogenic			
Phu Kham	117	18.92	102.93	Laos	Loei Fold Belt	Skarn	305	Re-Os (molybdenite); U-Pb (zircon)	Zaw et al. (2011)
Ban Houayxai	118	18.92	102.68	Laos	Loei Fold Belt	Epithermal			
Long Chieng Track	119	18.96	102.86	Laos	Loei Fold Belt	Epithermal			
Phu He	120	19.5	103.26	Laos	Loei Fold Belt	Epithermal			
Chatree	121	16.24	100.65	Thailand	Loei Fold Belt	Epithermal	251		Tangwattananukul et al. (2009)
Puthep	122	17.48	101.8	Thailand	Loei Fold Belt	Skarn	246	Re-Os (molybdenite); U-Pb (zircon)	Zaw et al. (2011)
							244-234	U-Pb (zircon)	Zaw et al. (2011)
							248-247	Ar-Ar (biotite)	Zaw et al. (2011)
Phu Thap Fah	123	17.43	101.72	Thailand	Loei Fold Belt	Skarn	245	U-Pb (zircon)	Zaw et al. (2011)
French	124	13.9	101.8	Thailand	Loei Fold Belt	Skarn			
Phu Lon	125	17.83	101.87	Thailand	Loei Fold Belt	Skarn	244	U-Pb (zircon)	Kamvong and Zaw (2009); Zaw et al. (2011)
Raub Australian	126	3.92	101.96	Malaysia	Bentong-Raub suture	Orogenic			
Selinsing	127	4.39	101.89	Malaysia	Bentong-Raub suture	Orogenic			
Penjom	128	4.12	101.95	Malaysia	Bentong-Raub suture	Orogenic			
Kangkung	129	26.69	98.53	Myanmar	Mogok Metamorphic Belt	Orogenic	L. Permian-M. Jurassic	geologic	Mitchell et al. (2004)
Kyaikto	130	17.31	96.93	Myanmar	Mogok Metamorphic Belt	Orogenic	L. Permian-M. Jurassic	geologic	Mitchell et al. (2004)
Modi Taung-Nankwe dist.	131	20.33	96.42	Myanmar	Mogok Metamorphic Belt	Orogenic			
Jinfeng	132	25.17	105.85	China	Youjiang basin	Orogenic or Carlin	193	Re-Os (pyrite)	Chen et al. (2007a)

2004). The deposits are spatially associated with ca. 300 Ma rhyodacite porphyry bodies. The disseminated gold deposits, defining the largest gold resource in Laos, are found throughout the Ordovician through Devonian sequence of clastic and calcareous sedimentary rocks (Cromie, 2010). Associated with widespread jasperoid formation and decalcification, they have been classified as classic Carlin-type deposits by Cromie (2010). Sillitoe (2010), however, defines the Sepon gold deposits as distal disseminated deposits to Cu–Au porphyry systems within carbonate-rich sequences. The actual relationship between distal disseminated gold deposits and true Carlin-like ores is controversial (Smith et al., 2005). Given the lack of many Carlin-like features and lack of porphyry-style mineralization in spatial association with the disseminated deposits, they may be presently best classified as some type of magmatic-related disseminated ores (Doug Kirwin, written commun., 2013).

Numerous small alluvial workings to the west along the fold belt in Vietnam (World Bank, 2006) suggest additional potential for magmatic–hydrothermal gold systems. The Bong Mieu gold deposit (Dzung, 1988; Banks et al., 2004), within the southeastern corner of the fold belt, is an orogenic gold deposit formed along one of many NW-trending shears that parallel the Song Ma suture. It is hosted in uplifted Precambrian basement rocks along what has been called the Kontun block, a large component of the Indochina terrane. The Phuoc Son gold deposits (Manaka et al., 2010), about 70 km west of Bong Mieu, are similar shear zone-related orogenic gold deposits. It is unclear whether these lode occurrences in metamorphic rocks are also late Paleozoic in age or formed at a different time than the above described magmatic hydrothermal gold deposits in Laos.

The continued subduction of the Paleotethys Ocean below Cathaysialand formed the Early Permian Sukhothai arc (Fig. 13) on the present-day western margin of the Indochina block. The arc was subsequently rifted from the microcontinent until latest Permian closure of the resulting back-arc basin, which is reflected as accretion of the narrow Lincang, Sukhothai, and Chanthaburi terranes via the Jinghong, Sra Kaeo, and Nan–Uttradit sutures (Metcalfe, 2011). This renewed convergence, which was terminated with the eventual Late Permian–Early Triassic docking of the Sibumasu block onto the seaward side of the arc, included a major episode of deformation (i.e., Loei–Phetchabun fold belt) and continental arc magmatism within the older Sukhothai arc terranes and adjacent western margin of the Indochina block (Sone and Metcalfe, 2008). Rocks of the fold belt are dominated by volcaniclastics and marine sedimentary rocks that range in age from Devonian through Early Triassic.

In present-day Laos and Thailand, the Loei fold belt or Loei–Phetchabun Volcanic Belt hosts ca. 300–250 Ma intrusion-related mineralization. The Phu Kham and adjacent Fe–Cu–Au skarn deposits

Please cite this article as: Goldfarb, R.J., et al., Phanerozoic continental growth and gold metallogeny of Asia, Gondwana Research (2013), http://dx.doi.org/10.1016/j.gr.2013.03.002

(Fig. 13) were formed within Late Carboniferous–Early Permian volcaniclastics and limestones in the northern part of the belt (Tate, 2005; Kamvong and Zaw, 2009; Circosta, 2011; Zaw et al., 2011). These are both oxidized (Phu Kham: 305 Ma; Puthep: 248–234 Ma; Phu Lon: 244 Ma) and reduced skarns (Phu Thap Fah: 245 Ma), which are stated as associated with I-type granites (Zaw et al., 2011). The Ban Houayxai, Long Chieng Track, and Phu He low-sulfidation epithermal gold deposits are also a part of the district (Manaka et al., 2007). Auriferous copper porphyry deposits are associated with many of the skarns, but to date, bulk mining of this type of low-grade porphyry mineralization has not taken place. The low-sulfidation Ag–Au epithermal deposit at Chatree (100 t Au), the largest gold deposit in Thailand, formed at 251 Ma in association with Late Permian to Late Triassic andesitic to rhyolitic volcanism near the center of the N–S trending fold belt (Tangwattananukul et al., 2009). In the south part of the fold belt, the oxidized Fe–Cu–Au skarn French deposit is hosted in ca. 247 Ma volcanic rocks adjacent to a ca. 203 Ma diorite (Zaw et al., 2011); the Early Triassic host rock age is interpreted to reflect the time of mineralization (e.g., Crow and Zaw, 2011).

To the south, the Late Permian–Early Triassic collision of the Sibumasu block defines the Bentong–Raub suture along the margin of Cathaysialand. Metcalfe (2011) suggests that the suture is likely the southern continuation of the Sukhothai arc, or Chanthaburi terrane, along the active margin of the superterrane. The Permo-Triassic fore-arc sedimentary rocks of the arc terrane are commonly referred to as the Central Belt domain of Malaysia. The suture contains mélange of Devonian through Permian oceanic sedimentary and mafic–ultramafic rocks. Granites within the suture zone were subsequently emplaced between 270 and 230 Ma (Barber and Crow, 2009). Perhaps significantly in regard to gold ore formation, the Bentong–Raub suture (Fig. 13) is the one zone of deformation between Cathaysialand and Sibumasu with considerable strike-slip (e.g., Flindell, 2003).

Malaysia's most abundant gold resources are orogenic gold deposits located within rocks of the Central Belt (Fig. 13), some of which have been mined for more than 100 years. Deposits such as Raub Australian and Selinsing are hosted along the main suture; others, such as Penjom, are along NE-trending splays off the suture (Ariffin and Hewson, 2007). Spatial association of the deposits with the Bentong–Raub fault system could indicate that orogenic gold formation is associated with the suggested strike-slip event, although there are no published details on such. Altered tonalite at the Penjom deposit has a K–Ar date of 194–191 Ma (Flindell, 2003), but the significance of such is not clear.

Metcalfe (2011) suggests that the West Burma and West Sumatra blocks were translated westward by latest Paleozoic transcurrent motion along the seaward margin of the Sibumasu block. The major deformation zones defining this tectonism are the Shan Boundary and Medial Sumatra sutures; the former correlates with the Mogok metamorphic belt (Metcalfe, 2011) and hosts numerous orogenic gold deposits. Rocks of the Mergui Group or the late Paleozoic "slate belt" of central Myanmar are located immediately east of the higher grade Mogok sequence, and together define a Barrovian metamorphic sequence about 1500 km in length. The affiliation of these rocks is controversial, but as Mitchell et al. (2004) point out, there is a late Paleozoic Gondwanan affinity of the metamorphic rocks. They would thus be the more landward part of the Sibumasu block that wasn't rifted from Gondwana until Early Permian.

Orogenic gold deposits and associated alluvial workings are recognized for more than 1000 km (Fig. 13), in a north–south trend along the length of present-day Myanmar, within rocks of the parallel Mogok and slate belts (Mitchell et al., 2004). They include Kangkung, now in the far north, to Kyaikto, now farthest south (see Fig. 13 in Mitchell et al., 2004). The 25 by 5 km Modi Taung–Nankwe orogenic gold district, in the central part of the slate belt, is underlain by Late Carboniferous–Early Permian argillaceous rocks and is the largest (>30 t Au) of the gold systems. Late Jurassic to Early Cretaceous calc-alkaline granites (Mitchell et al., 2007) bound the district to the west, north, and south. The age of gold formation is equivocal. Geological constraints place it between Late Permian and Middle Jurassic (Mitchell et al., 2004), so gold could have been deposited during either the Late Permian strike-slip event, or during later regional metamorphism associated with early stages of late Mesozoic magmatic arc evolution as suggested by Mitchell et al. (2004).

5.2. Foreland basin(?)

The large Permo-Triassic Youjiang (or Nanpanjing) basin developed as perhaps a foreland basin to the Cathaysialand accretionary margin. Alternatively, it could be a back-arc region to the initial Paleo-Pacific subduction below the South China block (Carter and Clift, 2008). Rocks of the basin now occupy the southwestern corner of the block in the areas of Guangxi province, southern Guizhou province, and eastern Yunnan province in China, as well as northeastern Vietnam to the east of the Red River fault zone. Until ca. 250 Ma, this was a sediment-starved, deep marine basin that was characterized by deposition of pelagic carbonates and shale. This was followed by deposition of siliclastic turbidites as the basin subsided in Middle and Late Triassic, and late continental sedimentation (Enos et al., 2006; Carter and Clift, 2008). In the Chinese part of the basin the only magmatism is the ca. 80 Ma granite stocks and mafic dikes at the basin margins (Mao et al., 2012); Permo-Triassic alkaline magmatism in parts of northeastern Vietnam is related to the giant Emeishan plume event situated in China's Sichuan province to the north (Lepvrier et al., 2011). In addition, early Mesozoic fold-and-thrust deformation is described in Vietnam (Lepvrier et al., 2011), but deformation is more limited farther inland from the Cathaysialand sutures within China. Nevertheless, scattered exposures of anticlinal domes of Permo-Triassic rocks are well-recognized in this part of China, and both SW–NE and SE–NW compressional deformation has been defined in the areas of the gold deposits (Ilchik et al., 2005).

Hundreds of gold deposits, as well as many deposits of mercury and antimony, are found throughout rocks of the basin (Fig. 14; Dzung, 1988; Kochetkov et al., 1997; Peters et al., 2007; Hoa et al., 2008). These are described in more detail from China, where they form the Dian–Qian–Gui metallogenic province. Hu et al. (2002) and Peters et al. (2007) have summarized many of the features of the deposits in the province. The metallogenic signature, alteration, and tectonic setting are somewhat characteristic of the Carlin-type gold deposits as defined in Nevada, USA (e.g., Cline et al., 2005). The ores are in an area of carbonate and clastic rocks, but in rocks that are generally more siliceous than those carbonate-dominant areas that host ores in Nevada. Many of the larger deposits are hosted in Triassic domes that are cored by Permian to Early Triassic carbonates and are overlain by later Triassic turbidites; the ores are often controlled by brittle fault systems that cut the turbidites on the outer margins of the domes. Our field observations suggest that much of the mineralization is associated with synkinematic veinlets in the more highly deformed parts of the domes. The relatively high CO_2 of the ore fluids and consistently heavy $\delta^{18}O$ of the gold-hosting quartz (e.g., Hu et al., 2002), as well as the common occurrence of coarse gold (e.g., Su et al., 2008), further suggest some differences from Carlin-like deposits in Nevada and some similarities to epizonal orogenic gold deposits. In fact, the metallogeny of the Youjiang basin province is not unlike that of the Kuskokwim basin in southwestern Alaska that hosts the giant epizonal orogenic gold deposit at Donlin Creek (e.g., Goldfarb et al., 2004). In both areas, Hg- and Sb-rich lodes were originally the widespread, easily visible economic metal targets; in fact, in the former, the large Jinfeng deposit was originally the site of a Hg–As mine (Ilchik et al., 2005).

The timing of mineralization in southwestern China and northeastern Vietnam is controversial. Many published K–Ar, Ar–Ar, and U–Pb dates for described ore-related phases range from >300 Ma to

Please cite this article as: Goldfarb, R.J., et al., Phanerozoic continental growth and gold metallogeny of Asia, Gondwana Research (2013), http://dx.doi.org/10.1016/j.gr.2013.03.002

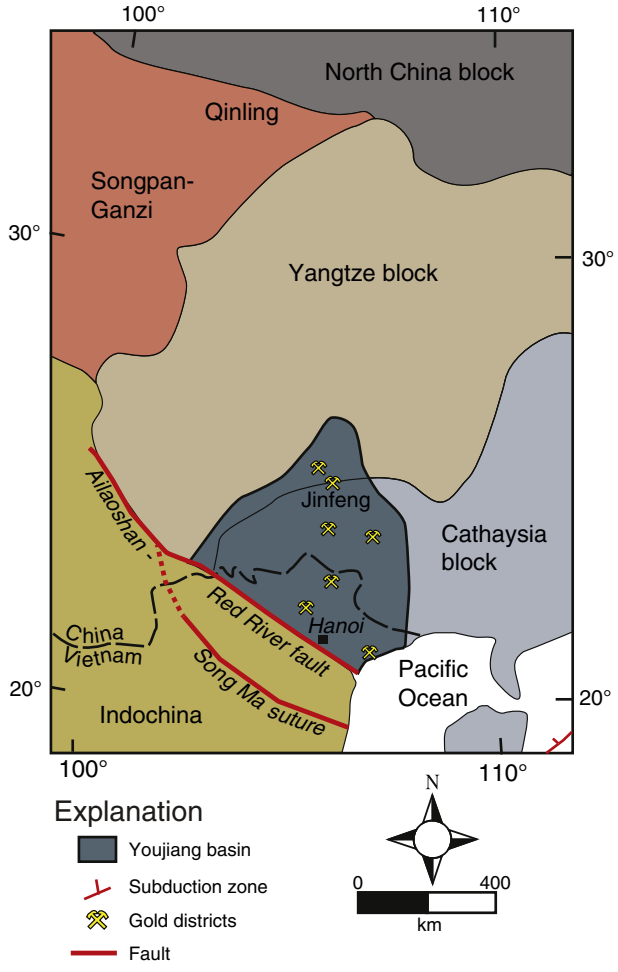

Fig. 14. The Permian–Triassic Youjiang basin in the southwestern South China block probably formed as a foreland basin during Indochina block collision along the Red River/Song Ma fault systems. Hundreds of poorly dated Hg, Sb, and Au deposits in southwestern China and northeastern Vietnam, many hosted in carbonate-clastic rock structural domes, are defined as either Carlin-like or orogenic gold deposits. Modified from Enos et al. (2006).

<15 Ma (Peters et al., 2007), and obviously evaluation of these data suggests many problems. The ores are hosted by turbidites as young as Late Triassic providing a broad maximum age constraint of Late Triassic. A Re–Os analysis of hydrothermal pyrite from the Jinfeng deposit (Chen et al., 2007a) gave a Late Triassic–Early Jurassic date of 193 ± 13 Ma, which we suggest is a reasonable estimate for ore formation in the basin. This also appears to be the time of regional exhumation in the basin (Lepvrier et al., 2011), which would have been important in facilitating the very regional hydrothermal fluid flow event.

6. Mesozoic Central Asia Orogenic Belt

6.1. Permian–late Mesozoic Mongol–Okhotsk basin and post-basin rifting

The closure of the Mongol–Okhotsk (Fig. 9) or Khangai–Khentii Ocean, forming the Mongol–Okhotsk orogenic belt (Fig. 15), formed the most seaward part of the eastern side to the CAOB. The 2500-km-long ocean basin closed diachronously from the southwest, in central Mongolia, to the northeast, near the present-day Okhotsk Sea, between Permian and Late Jurassic (Khanchuk, 2006). The basin developed between the oroclinal limbs of the complexly deformed Tuva–Mongol terranes (e.g., the Mongolian orocline of Yakubchuk et al., 2005), the high-grade metaigneous Precambrian block that extended from the Siberian Platform since at least the earliest Paleozoic (Sengor and Natal'in, 1996). The southern limb is often referred to as the 1500-km-long Argun terrane of the Amur block. The margins of the basin are marked by Devonian and Carboniferous volcanic arc systems, whereas the basin itself is dominated by turbidites of mainly the same age, but with also some older clastic units (Kelty et al., 2008). These turbidites define what is known as the Khangai–Khentii basin in north-central Mongolia (Badarch et al., 2002) and the central and eastern Transbaikal area in adjacent parts of Russia. In Mongolia, the turbidites have been subdivided into the Zag–Haraa, Asralt Hairhan, Harhorin, Tsetserleg, Ulaanbaatar, and South Khentii terranes by Tomurtogoo (2005). Gold ores formed during strike-slip and extensional events in the latter part of basin evolution (Table 8).

6.1.1. Khangai–Khentii and central Transbaikal

Gold deposition in the central Transbaikal region of Russia and adjacent parts to Mongolia (Fig. 15) appears to be associated with two periods of post-closure deformation focused within the late Paleozoic metasedimentary rocks. The first reflects formation of orogenic gold deposits, probably during episodes of sinistral strike-slip motion on terrane-bounding faults within the basin or adjacent parts of the CAOB (e.g., Cluer et al., 2005). The second is associated with subsequent extension and formation of epithermal and porphyry deposits, and may reflect some type of intra- or back-arc extension, or rollback, of a subducting Paleo-Pacific slab (e.g., Lin et al., 2013).

The North Khentii gold belt includes hardrock and significant alluvial gold occurrences in a NE-striking 400 by 100 km area of Mongolia that continues north into Siberia. The Zamar alluvial goldfields have yielded more than 600 t Au. The Boroo orogenic gold deposit, actively mined from 2004 to 2010, is the largest lode deposit of the gold belt and was the initial large-scale lode-gold producer in Mongolia (50 t Au). It is located along a flat-lying inferred thrust fault between early Paleozoic metasedimentary rocks and granitoids about 40 km to the west of one strand of the Yeroogol fault, a major regional structure traceable for several hundred kilometers. Argon dating indicates an age between ca. 210 and 185 Ma for Boroo, whereas the small Gatsuurt deposit, hosted within the first-order fault itself, has a date of ca. 178 Ma (Cluer et al., 2005).

In adjacent central Transbaikal, numerous similar orogenic gold deposits (e.g., Darasun, Klyuchevsk, Lubov, Kazakovka, Pogromnoe, Kara), as well as some gold-bearing Cu–Mo–porphyry deposits (e.g., Zhireken, Bugdaya, Shakhtama), occur along the boundary between the basin and Argun superterrane (Spiridonov et al., 2005). Dated orogenic gold deposits have a range of Ar–Ar and Re–Os ages between 168 and 154.5 Ma (Ponomarchuk et al., 2008; Borisenko et al., 2010). It is possible that the slightly younger latest Jurassic to earliest Cretaceous dates in Russia relative to the Mongolia dates reflect the diachronous Mongol–Okhotsk basin closure and thus the slightly later onset of strike-slip along terrane bounding faults in the basin in Russia.

About 100 km east of Klyuchevsk, the most significant accumulations of placer gold in northeastern China, within the upper Heilongjiang basin and mined for thousands of years (Lu et al., 1992; Zeng et al., 2011), defines a part of the region with additional important orogenic gold potential. Numerous small epizonal orogenic gold-stibnite deposits in the area include Shabaosi, Laogou, and Xiaoyinuogaigou. The deposits, generally located along a NE-trending ductile shear zone for 500 km along the Erguna River defining the Russia–China border, are hosted by Middle Jurassic clastic sedimentary rocks (Wu et al., 2006). Shabaosi (Fig. 15) formed at ca. 133.5 Ma (Song et al., 2007) indicating that these ores along the western side of the Argun block are part of the same Late Jurassic–Early Cretaceous metallogenic event as those in adjacent Russia.

The second period of deformation, characterized by later rifting/transtension within the Mongol–Okhotsk basin (e.g., Khanchuk, 2006;

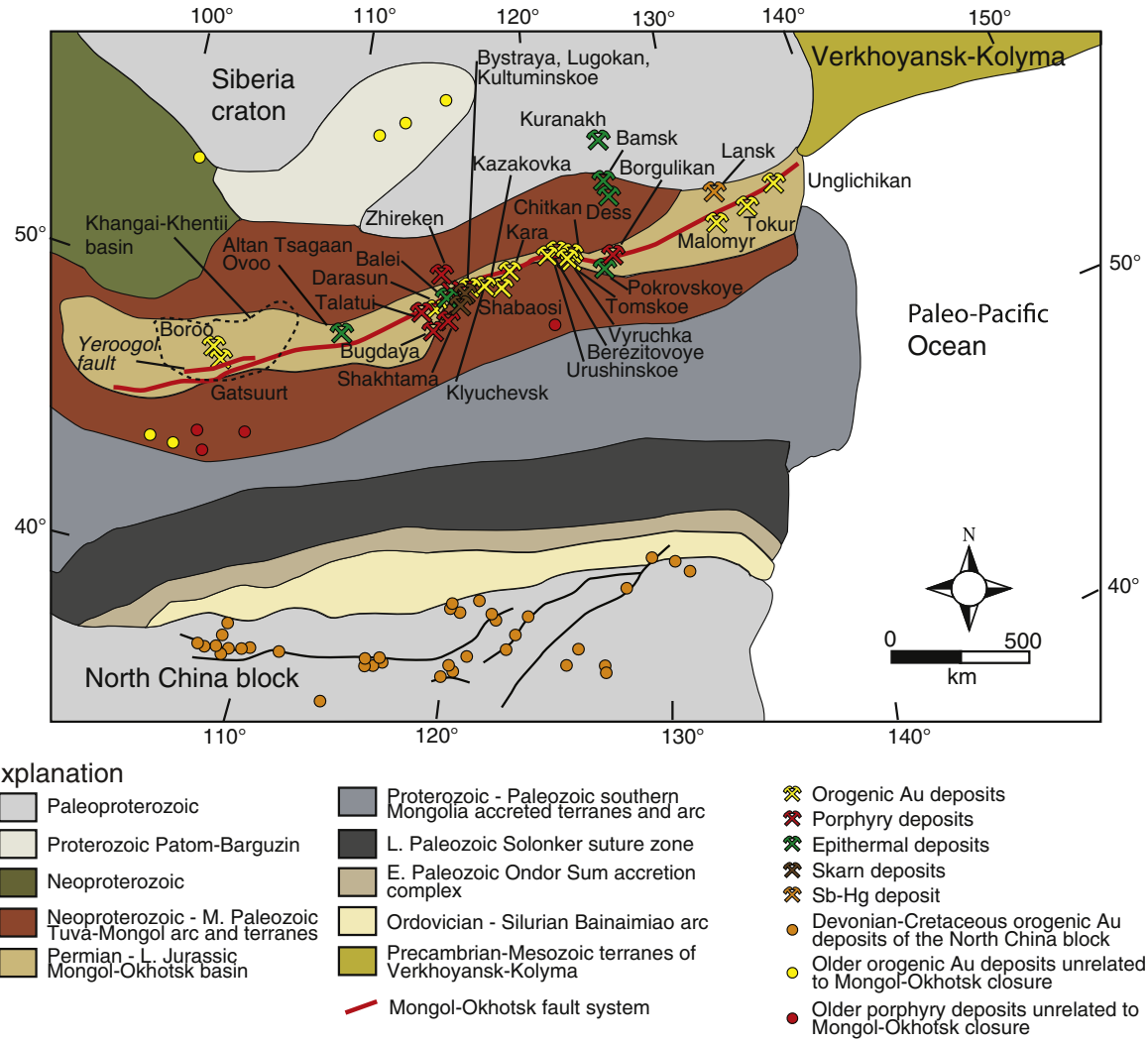

Explanation

- Paleoproterozoic
- Proterozoic Patom-Barguzin
- Neoproterozoic
- Neoproterozoic - M. Paleozoic Tuva-Mongol arc and terranes
- Permian - L. Jurassic Mongol-Okhotsk basin
- Proterozoic - Paleozoic southern Mongolia accreted terranes and arc
- L. Paleozoic Solonker suture zone
- E. Paleozoic Ondor Sum accretion complex
- Ordovician - Silurian Bainaimiao arc
- Precambrian-Mesozoic terranes of Verkhoyansk-Kolyma
- Mongol-Okhotsk fault system
- Orogenic Au deposits
- Porphyry deposits
- Epithermal deposits
- Skarn deposits
- Sb-Hg deposit
- Devonian-Cretaceous orogenic Au deposits of the North China block
- Older orogenic Au deposits unrelated to Mongol-Okhotsk closure
- Older porphyry deposits unrelated to Mongol-Okhotsk closure

Fig. 15. The Mongol–Okhotsk orogenic belt resulted from diachronous closure of the Mongol–Okhotsk basin between Permian and Jurassic within the geologically complex region between the Siberian craton and North China block. Orogenic gold deposits, younging from west to east, include those of the North Khentii gold belt (e.g., Boroo), central Transbaikal (e.g., Darasun, Kara, Shabaosi), and eastern Transbaikal (e.g., Berezitovoye, Tokur, Malomyr). In the latter two areas, extensional events slightly after deposition of orogenic gold, within and adjacent to the basinal rocks, was associated with formation of important epithermal (e.g., Balei, Kuranakh, Bamsk, Altan Tsagaan Ovoo), skarn (e.g., Bystraya, Lugokan), and porphyry deposit (Kultuminskoe) formation. Based largely on Sengor and Natal'in (1996) and Xiao et al. (2009).

Donskaya et al., 2008), was associated with significant bimodal volcanism in the same area as the central Transbaikal orogenic gold deposits and farther to the east. The period is imprecisely defined as between ca. 135 and 120 Ma (e.g., Lin et al., 2013), but the ca. 150-125 Ma age of magmatic–hydrothermal auriferous orebodies suggests the extensional period may have begun as early as the end of the Jurassic. It included formation of epithermal ores, such as the 149.2–143.6 Ma giant Balei low sulfidation epithermal deposit (345 t Au) just south of the southern basin margin (Borisenko et al., 2010). The Zhipkoshin Sb–Hg deposit is dated by $^{40}Ar/^{39}Ar$ on sericite at 142.5 Ma (Borisenko et al., 2010) and reflects a similar epithermal system, although without significant gold resources. There are also a series of deposits near Darasun and Balei (Fig. 15) termed porphyry-type systems (e.g., Talatui). These occur as veins and lenses in Paleozoic mafic intrusive complexes, and are stated to be characterized by a Au–Cu–Mo–W signature (Prokof'ev et al., 2007), but their temporal and genetic relationship to the epithermal and orogenic gold deposits is not fully clear.

There is some evidence that the epithermal and porphyry-like deposits, although the latter appear to be mainly hosted in Paleozoic intrusions, reflect sites of localized extension within an overall lengthy period of strike-slip orogenesis (Goryachev, 2010). The huge Bystraya (or Bystrinskoye) and Lugokan Fe–Cu–Au skarns (each 150–170 t Au) are located about 200 km to the northeast of Balei and the Kultuminskoe Cu–Au porphyry (300 t Au) a few tens of kilometers south of Balei within latest Proterozoic to early Paleozoic sedimentary rocks of the Argun superterrane. These clearly suggest a regional latest Jurassic–Early Cretaceous epithermal, porphyry, and skarn magmatic gold province, with perhaps a similar broad regional extensional control to that responsible for the Late Jurassic–Early Cretaceous epithermal gold deposits of northeastern China to the south (see below). The recently discovered Altan Tsagaan Ovoo intermediate-sulfidation epithermal Au–Ag–Pb–Zn deposit in the Mesozoic Onon graben region of northeasternmost Mongolia (Boris Kotlyar, unpub. presentation, PDAC 2012) may define extension of this late Mesozoic metallogenic event to the southeast.

On the northern side of the basin, a series of gold-rich ores are located in cover sequences of the Aldan–Stanovoy shield of the Siberia craton. They include the low-sulfidation epithermal deposits, such as Kuranakh (Fig. 15), and also some porphyry-type occurrences (e.g., Ryabinovoe) within the Central Aldan district. A genetic association of the ores appears to be clear with suggested, although undated, Early Cretaceous magmatism (Rodionov et al., 2005). At the Kuranakh

Table 8
Permian-Late Mesozoic gold deposits of the Mongol-Okhotsk basin and subsequent rifting.

Deposit	Location in Fig. 1	Latitude	Longitude	Country	Tectonic location	Deposit type	Age (Ma)	Geochron. methodology	Geochron. reference
Boroo	133	48.75	106.17	Mongolia	Khangai-Khentii	Orogenic	186.2±1.6, 195.6±1.3 188.0±2.3, 208,3±1.9	Ar-Ar (sericite)	Cluer et al. (2005)
Gatsuurt	134	48.64	106.63	Mongolia	Khangai-Khentii	Orogenic	178	Ar-Ar	Cluer et al. (2005)
Darasun	135	52.37	115.5	Russia	Central Transbaikal	Orogenic	158.5		
Klyuchevsk	136	53.53	119.43	Russia	Central Transbaikal	Orogenic(?)	Late Jurassic (?)		
Lubov	137	49.86	111.9	Russia	Central Transbaikal	Orogenic	Late Jurassic (?)		
Kazakovka	138	51.78	117.08	Russia	Central Transbaikal	Orogenic	Late Jurassic (?)		
Pogromnoe	139	51.65	116.25	Russia	Central Transbaikal	Orogenic	Late Jurassic (?)		
Kara	140	52.39	116.27	Russia	Central Transbaikal	Orogenic	157		
Zhireken	141	52.84	117.36	Russia	Central Transbaikal	Porphyry	163-162	Re-Os (molybdenite)	Berzina et al. (2003)
Bugdaya	142	51.2	117.88	Russia	Central Transbaikal	Porphyry	Late Jurassic		Laznica (1976)
Shakhtama	143	51.28	117.95	Russia	Central Transbaikal	Porphyry	159-158	Re-Os (molybdenite)	Berzina et al. (2003)
Balei	144	51.63	116.6	Russia	Central Transbaikal	Epithermal	149-143	Ar-Ar	Borisenko et al. (2010)
Talatui	145	52.36	115.56	Russia	Central Transbaikal	Porphyry			
Bystraya	146	51.48	118.57	Russia	Central Transbaikal	Skarn	Early Cretaceous		
Lugokan	147	51.75	119.25	Russia	Central Transbaikal	Skarn	Early Cretaceous		
Altan Tsagaan Ovoo	148	~48.1	~113	Mongolia	Central Transbaikal	Epithermal			
Kultuminskoe	149	52.25	119.15	Russia	Central Transbaikal	Porphyry	Early Cretaceous		
Kuranakh	150	58.92	125.62	Russia	Central Transbaikal	Epithermal			
Ryabinovoe	151	57.71	132.67	Russia	Central Transbaikal	Porphyry			
Bamsk	152	55.97	123.95	Russia	Central Transbaikal	Epithermal	130	Rb-Sr (muscovite)	Stepanov (2001)
							129-109	K-Ar (muscovite)	Stepanov (2001)
Dess	153	55.9	123.97	Russia	Central Transbaikal	Epithermal	128	Ar-Ar (sericite)	Buchko et al. (2010)
							127	Rb-Sr (muscovite)	Stepanov (2001)
Vykhodnoe	154	56.37	122.78	Russia	Central Transbaikal	Porphyry	125-122	Ar-Ar	Buchko et al. (2010)
Tokur	155	53.13	132.9	Russia	Eastern Transbaikal	Orogenic	122	Ar-Ar (adularia)	Sorokin et al. (2011)
Malomyr	156	53.12	131.52	Russia	Eastern Transbaikal	Orogenic	132	Ar-Ar	Buchko et al. (2011)
Berezitovoye	157	54.48	122.98	Russia	Eastern Transbaikal	Orogenic	132-127	Ar-Ar	Sorokin et al. (2008)
Unglichikan	158	53.1	133.6	Russia	Eastern Transbaikal	Orogenic	Early Cretaceous (?)		
Urushinskoe	159	53.9	122.8	Russia	Eastern Transbaikal	Orogenic			
Vyruchka	160	54.15	123.08	Russia	Eastern Transbaikal	Orogenic			
Chitkan	161	54.22	123.28	Russia	Eastern Transbaikal	Orogenic			
Tomskoe	162	54.15	123.6	Russia	Eastern Transbaikal	Orogenic			
Klyuchevsk	163	53.31	119.18	Russia	Eastern Transbaikal	Orogenic	104	K-Ar (muscovite)	Stepanov (2001)
Shabaosi	164	53.2	121.85	China	Eastern Transbaikal	Orogenic	133.5		Song et al. (2007)
Langou (Laogou)	165	53.19	122.19	China	Eastern Transbaikal	Orogenic			
Xiaoyinugaigou	166	50.51	119.53	China	Eastern Transbaikal	Orogenic			
Pokrovskoye	167	53.35	126.35	Russia	Eastern Transbaikal	Epithermal	130		
Borgulikan district	168	53.75	126.62	Russia	Eastern Transbaikal	Porphyry	126-122	Ar-Ar (porphyry)	Sotnikov et al. (2007)

deposit (400 t Au), orebodies within bituminous limestones and dolomites have led to its common classification as the one definite Carlin-like deposit in Russia, but most descriptions of the mineralization (e.g., Levitan, 2008) are more consistent with an epithermal model. To the southwest, a ca. 130 Ma Rb–Sr date also characterizes the Bamsk gold deposit, in the North Stanovoy or Apsakan district, that is hosted by an Early Cretaceous volcanoplutonic complex within Precambrian rocks along the southern margin of the Aldan–Stanovoy Shield (Stepanov, 2001). The deposit is typically defined as an epithermal gold deposit, although some features of the ores resemble many orogenic gold deposits, so definitive classification is uncertain. The adjacent ca. 128 Ma Dess epithermal gold occurrence and ca. 125 Ma Vykhodnoe molybdenum porphyry (Buchko et al., 2010), suggest that an epithermal gold province is the more likely scenario. In contrast, reported hydrocarbons in fluid inclusions and ore textures (Kazansky and Yanovsky, 2006) are more consistent with those of orogenic gold deposits (e.g., Goldfarb et al., 2007).

North of the Bamsk and Kuranakh deposits, numerous poorly described gold deposits are hosted in the Archean and Paleoproterozoic greenstone belts of the basement of the shield (e.g., Smelov and Timofeev, 2005). Descriptions of the ores are too vague to be certain as to whether they are orogenic gold deposits or epithermal gold deposits related to alkalic magmatism. There is a widespread and unusual gold and uranium correlation associated with much of this mineralization. Despite the favorable setting for Precambrian gold deposits, Kazansky and Yanovsky (2006) suggest that these are Mesozoic gold lodes.

Please cite this article as: Goldfarb, R.J., et al., Phanerozoic continental growth and gold metallogeny of Asia, Gondwana Research (2013), http://dx.doi.org/10.1016/j.gr.2013.03.002

To the south of the Bamsk and Kuranakh deposits, epithermal veins at the Pokrovskoye deposit (Gonzha district) are associated with a 130 Ma subvolcanic body, part of the Umelkan–Ogodzha volcano-plutonic belt, intruding Late Archean and Paleoproterozoic rocks along the northern edge of the Bureya massif, and immediately south of the Mongol–Okhotsk basin margin (Khomich and Vlasov, 2004). Adjacent 125 Ma Cu–Mo–Au porphyry bodies of the Borgulikan district (Sotnikov et al., 2007), emplaced within the Paleozoic sedimentary rocks of the Mongol–Okhotsk belt, may be part of the same event.

6.1.2. Eastern Transbaikal

Understanding the relationship between gold and tectonism in the eastern part of the Transbaikal region (Fig. 15), located between the Aldan–Stanovoy Shield and Argun block (e.g., Zonenshain et al., 1990), is complicated by overlapping deformation associated with both basin closure and circum-Pacific influences. Some gold provinces within the Precambrian blocks likely relate to circum-Pacific tectonics (e.g., Khanchuk, 2006). However, we favor the model of Yakubchuk and Edwards (1999) that relates much of the gold formation in the intervening basin, hosted in mainly greenschist facies units of the Paleozoic black shales of the Selemdzha, Niman, and Kerbi terranes, to late Mesozoic strike-slip along the regional E–W Mongol–Okhotsk fault system.

In addition to 1000 t of historic placer production, major orogenic gold deposits in the eastern Mongol–Okhotsk terranes, also enriched in Sb and W, include Tokur, Malomyr, Berezitovoye, and Unglichikan. The gold-bearing quartz veins in middle Paleozoic sediments at Tokur have a $^{40}Ar/^{39}Ar$ date on adularia of ca. 122 Ma (Sorokin et al., 2011). Hydrothermal K-feldspar from the Malomyr deposit hosted in middle Carboniferous metasedimentary rocks is dated by $^{40}Ar/^{39}Ar$ at ca. 132 Ma (Buchko et al., 2011). The Berezitovoe deposit (Vakh et al., 2008), located about 400 km east of Sukhoi Log and hosted in a Paleoproterozoic gneiss–porphyritic granite basement uplift along the southern edge of the Siberia craton, has been dated at ca. 132–127 Ma by an $^{40}Ar/^{39}Ar$ analysis of sericite (Sorokin et al., 2008). Taken together, these age data indicate the orogenic gold ores of eastern Transbaikal formed during Late Jurassic to early Early Cretaceous. Many other significant gold deposits in eastern Transbaikal, possibly orogenic types that formed along the margins of Permian plutons, are characterized by very limited published information and include Urushinskoe, Vyruchka, Chitkan, and Tomskoe (Krivolutskaya, 1997; Buchko and Sorokin, 2005); the latter deposit may contain a significant resource (Yakubchuk et al., 2005). Numerous mercury deposits 50 km north of Malomyr (Stepanov, 1998), including the Lansk deposit, may reflect shallow level products of the same orogenic hydrothermal systems within the Mongol–Okhotsk sedimentary rocks.

6.2. Carboniferous–middle Mesozoic northern margin of North China block

Many of the oldest known gold deposits in China are located along the northern margin of the North China block (Fig. 16; Table 4) and are temporally spread across 200 m.y. of Paleotethyan history. These

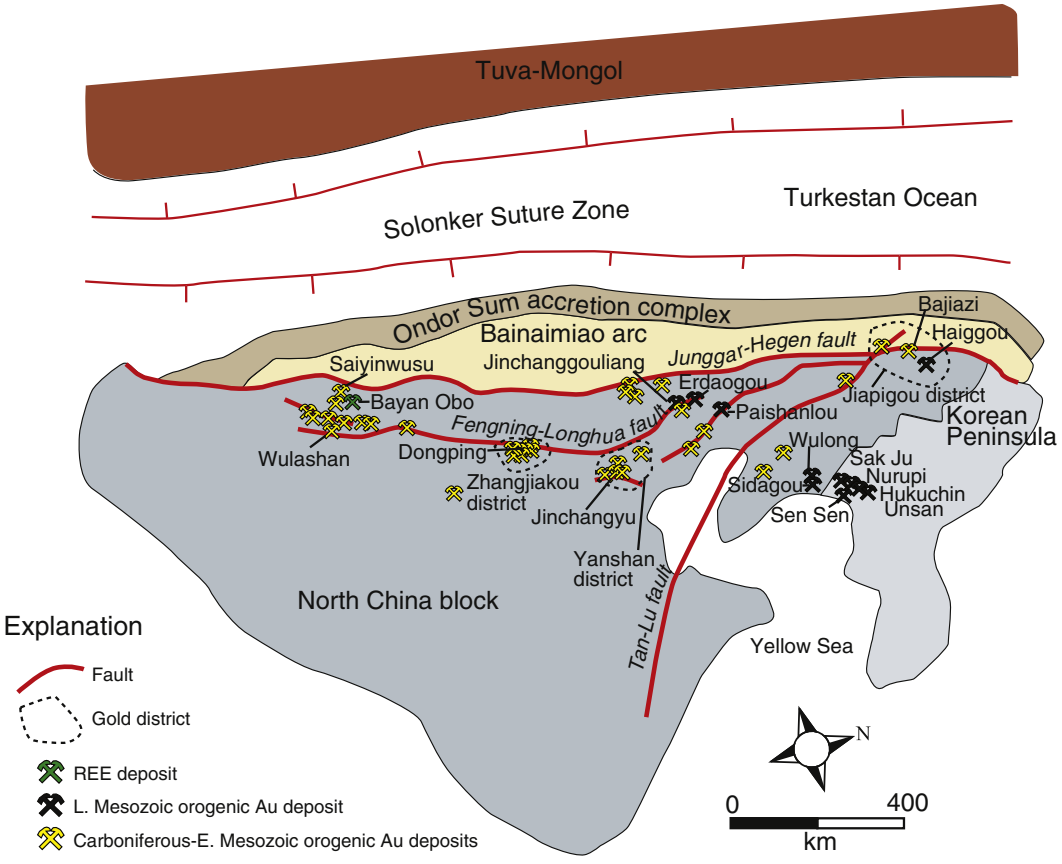

Fig. 16. Abundant, yet scattered districts of Carboniferous through Triassic orogenic gold deposits occur along the entire reworked northern margin of the North China block (NCB). Oldest deposits, such as the ca. 350 Ma Wulashan deposit, may have formed while the NCB was still along the Gondwana margin. Younger deposits formed during subduction/accretion events along the NCB margin as it migrated across the Tethys Ocean from ca. 350 to 250 Ma, and eventually closed the Turkestan Ocean marked by the Solonker suture zone, as well as during later early Mesozoic deformation (e.g., Dongping, Jinchangyu, Jiapigou). Many deposits in the northeastern corner of the block (e.g., Jinchanggouliang, Paishanlou, Wulong, Sidagou, Haiggou) reflect later Yanshanian (late Mesozoic) tectonism associated with lithosphere delamination along the eastern edge of the NCB (see Fig. 19). Based largely on Hart et al. (2002) and Xiao et al. (2003).

Please cite this article as: Goldfarb, R.J., et al., Phanerozoic continental growth and gold metallogeny of Asia, Gondwana Research (2013), http://dx.doi.org/10.1016/j.gr.2013.03.002

mainly orogenic gold deposits formed as early as Carboniferous, when the North China block was migrating away from Gondwana, to as recently as Jurassic, after the block partly closed the Paleoasian Ocean with Siberia and the trapped Mongolian arc terranes (i.e., the Northern Orogen of Jian et al., 2008).

The North China block may have been a part of Gondwana that started to rift between Early Devonian and Early Carboniferous, and subsequently moved northward across the Paleotethys Ocean (Li and Powell, 2001). Prior to rifting, subduction below and accretion to these Precambrian rocks of the Gondwanan margin developed the Ordovician–Silurian Bainaimiao continental margin magmatic arc and addition of oceanic volcanic rocks, cherts, and other early Paleozoic marine rocks of the Ondor Sum complex to the margin of the North China block (De Jong et al., 2006). From about 350 Ma, until the collision with Asia between 290 and 250 Ma, the North China block migrated across the Paleotethys Ocean. Approximately coeval with closure of the Mongol–Okhotsk Ocean to the north, the Solonker basin or Turkestan Ocean, located between the Tuva–Mongol massif, with its seaward accreted terranes of present-day southern Mongolia, and the northern margin of the North China block, was closed. The 900 by 60 km Solonker suture zone consists of late Paleozoic mélange, turbidites, and volcanic rocks to the north of the Ondor Sum complex, and these are collectively termed the Erdaojing accretionary complex (Xiao et al., 2003, 2009). Late Carboniferous S-type magmatism and Late Permian to Middle Triassic post-collisional magmatism impacted both the accreted margin and the adjacent outermost 200 km of the North China block margin (Windley et al., 2007; Zhang et al., 2009b), with resulting plutons and batholiths best exposed within Archean and Paleoproterozoic basement uplifts. The older group of igneous rocks was, therefore, emplaced while the North China craton was distal to Siberia.

Orogenic gold deposits cluster in a number of regions within the northern margin of the North China block (Nie, 1997; Miller et al., 1998; Hart et al., 2002). The deposits tend to be associated with areas of Late Archean and Paleoproterozoic basement uplifts, many of which are also characterized by abundant pre- and syn-ore igneous bodies. Significant deposits are not found north of these basement uplifts within younger rocks of the Ondor Sum or Erdaojing accretionary sequences. There is a general spatial association of the gold districts with the east–west regional fault zones, particularly the Fengning–Longhua fault, located a couple of hundred kilometers into the ancient cratonic block, and, to a lesser degree, the Junggar–Hegen (or Chifeng–Obo) fault system that marks the edge of the Precambrian block (Fig. 3 in Hart et al., 2002). Gold ores formed pre-, syn-, and post-closure of the Turkestan Ocean basin. A lack of comprehensive regional tectonic data makes it difficult to relate these gold ores to specific episodes of major fault motion, basement uplift, and (or) lithospheric erosion within the cratonic block margin.

The oldest deposits are concentrated in the northwestern corner of the North China block, between Bayan Obo in the north and Baotou in the south, with veins generally hosted by the high-grade Archean rocks. The southernmost large deposit, Wulashan, is interpreted to have formed at ca. 350 Ma (Hart et al., 2002) or ca. 300 Ma (Nie et al., 2002). The older of these two ages overlaps emplacement of a biotite granite batholith a few kilometers to the west. Deposits young to the north, for about 200 km and thus toward the edge of the block, and some of these are hosted by younger Neoproterozoic slate cover rocks. The youngest of these, which includes the Saiyinwusu gold deposit within a few kilometers of the Bayan Obo REE–Nb–Fe deposit, have dates of ca. 260–250 Ma ($^{40}Ar/^{39}Ar$: Hart et al., 2002; Nie et al., 2002). This group also includes the 217 (or Chang Shan Hao) deposit that is hosted along a ductile shear within Mesoproterozoic to Neoproterozoic carbonaceous phyllite. This 112 t Au deposit is being developed by open-pit mining and represents one of the largest reported gold resources in China. The vein type ore has a reported grade of 0.83 g/t gold, which is exceptionally low for such deposit types being mined in Asia. A clear younging of ages seaward toward the paleo-subduction zone is most consistent with some type of slab-rollback or similar tectonic scenario controlling the mineralization event. The presence of both late Paleozoic hydrothermal events and subduction-related magmatism within Archean basement of the northwestern corner of the Precambrian block suggests a relatively early loss of some parts of the subcontinental lithospheric mantle keel in this area of the craton, at least 100 m.y. before the much more well-documented Mesozoic lithospheric erosion below the present-day eastern side of the block (see below).

Two other large groups of gold deposits occur in the Zhangjiakou and Yanshan districts (Hart et al., 2002), about 500 and 700 km east, respectively, of these westernmost deposits. The former district is centered along the margins of the 55 by 8 km, east–west trending, alkalic, Devonian Shiquangou batholith complex, which was emplaced along the boundary of Late Archean and Neoproterozoic units. Although the large (>100 t Au) Dongping deposit has a well-defined date of ca. 150 Ma, other orogenic gold deposits hosted within the margin of the complex may be Triassic in age (Hart et al., 2002). Deposits in the Yanshan district occur in an east–west trending uplift of high-grade basement rocks surrounded by Mesoproterozoic and Neoproterozoic cover. The large (90 t Au) Jinchangyu deposit has been dated at ca. 196 Ma (Hart et al., 2002), although some of the other deposits in the district may be 20 m.y. older or younger (Miao et al., 2008).

Far to the east, a few tens of kilometers east of a large splay of the NE-trending, continental-scale Tan–Lu fault zone, the Jiapigou district consists of gold-bearing quartz veins along ductile shears within uplifted Late Archean basement. This is the most northeasterly basement uplift zone within the craton. The NW-trending group of orogenic deposits occurs along the southern margin of the massive, ca. 166 Ma Huangnihe granite batholith. Miao et al. (2005) define a ca. 204 Ma gold-forming event based upon argon dating of the Bajiazi deposit. They note, however, that the Haigou deposit is hosted by rocks of the batholith and has been dated as Early Cretaceous. This fact, as well as the structural setting of most of the gold deposits within a linear belt along the batholith margin, are not particularly consistent with a Triassic ore-forming event. Additional geochronological work is critical before gold ores this far to the east within the craton margin can also be related to the Turkestan Ocean closure.

7. Jurassic–Cenozoic Pacific margin orogenesis

7.1. Late Jurassic–Cretaceous Verkhoyansk–Kolyma orogen

One of the major gold forming episodes in eastern Asia is that associated with the evolution of the Yana–Kolyma/South Verkhoyansk and Oloi–Chukotka (Arctic) orogenic belts and the Late Jurassic–Early Cretaceous Uda–Murgal and Late Cretaceous Okhotsk–Chukotka arcs (Khanchuk, 2006; Sokolov, 2010; Goryachev et al., 2011). Together these define the late Mesozoic Verkhoyansk–Kolyma orogeny, which includes the formation of major late Mesozoic gold resources (Fig. 17; Table 9). This orogeny consists of three stages, marked by terrane accretion on the western, southern, and northern sides, respectively, of easternmost Russia. The first of these is reflected by collision of the Kolyma–Omolon microcontinent with the Verkhoyansk fold-and-thrust belt and it was the main stage in the formation of the Yana–Kolyma fold belt (Parfenov, 1995; Parfenov and Kuzmin, 2001; Oxman, 2003; Khanchuk, 2006; Sokolov, 2010). The fold-and-thrust belt developed during the resulting deformation of passive margin carbonate and terrigeneous sediments along the platform on the eastern side of the Siberia craton. The microcontinent represents older pieces of the continental margin that, as discussed above, were rifted into the Panthalassa Ocean in the middle Paleozoic. The resulting Oimyakon basin (Fig. 4) was subsequently closed during the redocking of the microcontinent beginning in the Middle Jurassic; whether the craton was subducted below the microcontinent or vice versa is still

Please cite this article as: Goldfarb, R.J., et al., Phanerozoic continental growth and gold metallogeny of Asia, Gondwana Research (2013), http://dx.doi.org/10.1016/j.gr.2013.03.002

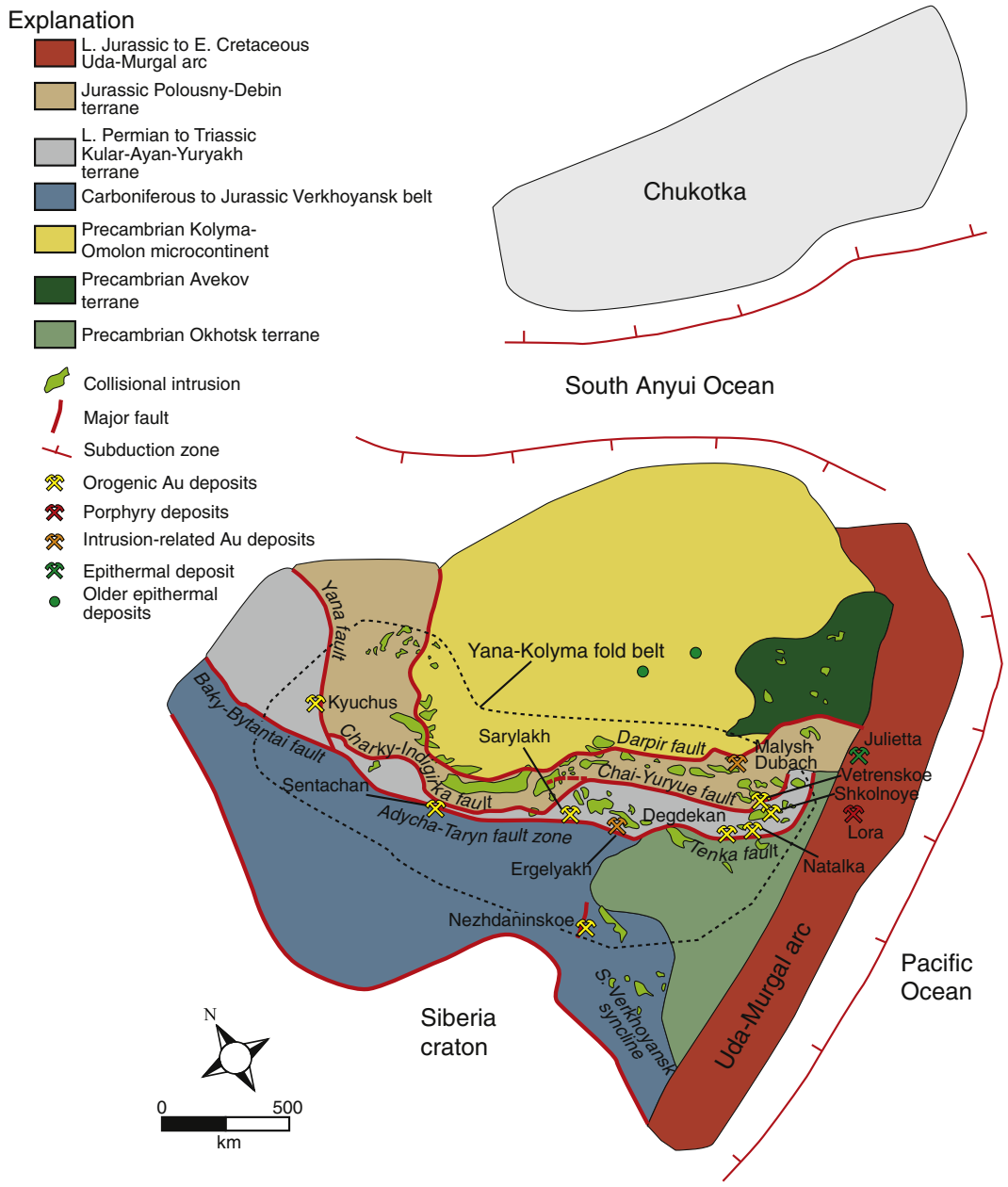

Fig. 17. The Yana–Kolyma fold belt, formed during the Late–Jurassic–Early Cretaceous collision of the Kolyma–Omolon terrane along the Pacific margin, includes the deformed Permian to Jurassic oceanic terranes and adjacent seaward margin of the Verkhoyansk passive margin to the Siberian craton. Giant Early Cretaceous orogenic gold deposits, such as Natalka and its associated widespread placer fields, Sarylakh, Sentachan, and Kyuchus formed in the terranes of the fold belt, as well as in the adjacent South Verkhoyansk synclinorium (e.g., Nezhdaninskoe). The Early Cretaceous subduction-related granitoids of the continental margin Uda–Murgal arc are associated with epithermal gold (e.g., Julietta) and other magmatic hydrothermal mineral deposits.
Based mainly on Konstantinovsky (2007) and Sokolov et al. (2009).

unclear. The >1500-km-long, Late Permian to Triassic Kular–Ayan–Yuryakh terrane adjacent to the fold-and-thrust belt and Jurassic Polousny–Debin terrane immediately to the east (Konstantinovsky, 2007) represent the main suture between the cratonic margin and microcontinent. The major boundaries include: (1) the 40-km-wide regional Adycha–Taryn fault zone between the craton margin and Kular–Ayan–Yuryakh terrane, which includes the Tenka fault to the south; (2) the Chai–Yuryue and Charky–Indigirka thrust faults between the two turbidite terranes; and (3) the Darpir thrust fault along the seaward side of the Polousny–Debin terrane.

The second stage of orogeny reflected Late Jurassic to early Early Cretaceous accretion of the Okhotsk and additional Paleozoic–early Mesozoic oceanic arc terranes, as well as small Precambrian terrane fragments, to the south (e.g., Prokopiev et al., 2004; Bortnikov et al., 2010) and led to formation of the 3500-km-long Uda–Murgal arc along the margin of northeastern Asia within the accreted block (Sokolov et al., 2009). The arc is best defined as a series of oceanic terrane fragments that were added to the southwestern side of the craton during Izanagi plate subduction, with some syn-accretionary arc magmatism. The terrane accretion episode also led to reactivation of the first-stage suturing faults as left lateral strike-slip faults at ca. 140–120 Ma.

The third stage of orogeny, forming the Oloy–Chukotka (Arctic) fold belt along the present-day northern margin of the Siberia craton

Please cite this article as: Goldfarb, R.J., et al., Phanerozoic continental growth and gold metallogeny of Asia, Gondwana Research (2013), http://dx.doi.org/10.1016/j.gr.2013.03.002

Table 9
Late Jurassic-Cretaceous gold deposits of northeast Russia.

Deposit	Location in Fig. 1	Latitude	Longitude	Country	Tectonic location	Deposit type	Age (Ma)	Geochron. methodology	Geochron. reference
Ergelyakh	176	63.72	143.88	Russia	Verkhoyansk-Kolyma orogen	Intrusion-related	149-140	Ar-Ar	Goryachev and Gamyanin (2006); Goryachev (2006)
Chistoye	177	69.72	150.25	Russia	Verkhoyansk-Kolyma orogen	Intrusion-related	149-140	Ar-Ar	Goryachev and Gamyanin (2006); Goryachev (2006)
							136	K-Ar	Goryachev and Yakubchuk (2008)
Malysh-Dubach	178	62.51	152.67	Russia	Verkhoyansk-Kolyma orogen	Intrusion-related	147-146	Ar-Ar	Goryachev and Gamyanin (2006); Goryachev (2006)
Natalka	179	61.65	147.68	Russia	Verkhoyansk-Kolyma orogen	Orogenic	135		
Degdekan	180	61.97	147	Russia	Verkhoyansk-Kolyma orogen	Orogenic	137-133		
Shkolnoye	181	61.47	148.8	Russia	Verkhoyansk-Kolyma orogen	Orogenic	135		
Vetrenskoe	182	61.75	149.55	Russia	Verkhoyansk-Kolyma orogen	Orogenic	125		
Sarylakh	183	64.4	142.41	Russia	Verkhoyansk-Kolyma orogen	Orogenic	124		
Sentachan	184	66.45	137.05	Russia	Verkhoyansk-Kolyma orogen	Orogenic	Early Cretaceous		
Kyuchus	185	69.8	134.75	Russia	Verkhoyansk-Kolyma orogen	Orogenic	Early Cretaceous		
Nezhdaninskoe	186	62.5	139.17	Russia	Verkhoyansk-Kolyma orogen	Orogenic	119		
Levo-Dybinskoye	187	62.83	139.58	Russia	Verkhoyansk-Kolyma orogen	Intrusion-related	125		
Mayskoye	188	66.47	173.73	Russia	Verkhoyansk-Kolyma orogen	Orogenic	115-107		
Karalveem	189	68.18	166.01	Russia	Verkhoyansk-Kolyma orogen	Orogenic	130-100	K-Ar	
Lora	190	59.42	153.48	Russia	Uda-Murgal	Porphyry	103-102		
Teutedjak	191	61.06	149.95	Russia	Uda-Murgal	Intrusion-related	100	K-Ar	Mirgorodskaya (2008)
Julietta	192	61.17	153.98	Russia	Uda-Murgal	Epithermal	136	Rb-Sr (adularia)	Struzhkov et al. (1996)
Karamken	193	60.23	151	Russia	Okhotsk-Chukotka	Epithermal	73		Newberry et al. (2000)
Dukat	194	62.6	155.18	Russia	Okhotsk-Chukotka	Epithermal	82-79	Ar-Ar	Newberry et al. (2000)
Valunistoye	195	66.47	177.63	Russia	Okhotsk-Chukotka	Epithermal	84-72		Layer et al. (1994); Newberry et al. (2000)
Kupol	196	66.78	169.55	Russia	Okhotsk-Chukotka	Epithermal	L. Cretaceous		
Ametistovoye	197	61.32	164.82	Russia	Okhotsk-Chukotka	Epithermal	L. Cretaceous		
Lunnoye	198	63.38	155.2	Russia	Okhotsk-Chukotka	Epithermal	87	Rb-Sr	Konstantinov et al. (1998)
Arylakh	199	63.13	154.97	Russia	Okhotsk-Chukotka	Epithermal	81.5	Ar-Ar	Newberry et al. (2000)
Nyavlenga	200	60.73	153.47	Russia	Okhotsk-Chukotka	Epithermal	90	Ar-Ar	Newberry et al. (2000)
Oira	201	60.15	149.75	Russia	Okhotsk-Chukotka	Epithermal	93		
Yurievka	202	59.68	141.73	Russia	Okhotsk-Chukotka	Epithermal	97		
Evenskoye	203	62.47	159.83	Russia	Okhotsk-Chukotka	Epithermal	82	Ar-Ar	Newberry et al. (2000)
Utesnoye	204	62.54	151.29	Russia	Okhotsk-Chukotka	Epithermal	81		
Agnie-Afanas'evskoe	205	51.93	138.78	Russia	Sikhote-Alin	Orogenic	Cretaceous(?)		
Albazinskoye	206	52.02	138.25	Russia	Sikhote-Alin	Orogenic	Cretaceous(?)		
Oemku	207	50.25	139.5	Russia	Sikhote-Alin	Orogenic	Cretaceous(?)		
Uchaminskoye	208	51.72	138.68	Russia	Sikhote-Alin	Orogenic	Cretaceous(?)		
Dzhegdag	209	50.67	139.67	Russia	Sikhote-Alin	Intrusion-related	Cretaceous(?)		
Askol'd	210	42.73	132.33	Russia	Sikhote-Alin	Orogenic? Intrusion?	83.8	K-Ar	Sayadyan (2004)
Malinovoye	211	45.13	135.03	Russia	Sikhote-Alin	Orogenic? Intrusion?	Cretaceous(?)		
Krinichnoye	212	42.9	132.48	Russia	Sikhote-Alin	Orogenic? Intrusion?	76.2	K-Ar	Sayadyan (2004)
Glukhoye	213	~46.07	~135.38	Russia	Sikhote-Alin	Orogenic? Intrusion?	Cretaceous(?)		
Salyt	214	46.37	137.68	Russia	Sikhote-Alin	Orogenic? Intrusion?	Cretaceous(?)		
Mnogovershinnoe	215	53.88	139.73	Russia	Sikhote-Alin	Epithermal	69-66	K-Ar	
Belaya Gora	216	53.38	140.23	Russia	Sikhote-Alin	Epithermal			

(Khanchuk, 2006), took place also during Late Jurassic–Early Cretaceous (Katkov et al., 2007; Akinin et al., 2009). The resulting South Anyui suture (Fig. 18) marks the docking of the Arctic Alaska–Chukotka terrane (Miller et al., 2009; Sokolov, 2010). The post-accretionary Okhotsk–Chukotka volcanic arc, mainly ca. 105–77 Ma (Akinin and Miller, 2011), overprints all the terranes in this part of the Russian Far East.

7.1.1. Yana–Kolyma fold belt

The NW-trending Yana–Kolyma fold belt includes an orogen-parallel belt of subduction-related I-type granitic batholiths and collision-related S-type granitic bodies. The intrusions were emplaced for more than 1100 km along the length of the turbidite terranes, mainly between 153 and 147 Ma, although a few intrusions are also dated at 160–155 and 146–143 Ma (Khanchuk, 2006; Akinin et al., 2009). Numerous

Please cite this article as: Goldfarb, R.J., et al., Phanerozoic continental growth and gold metallogeny of Asia, Gondwana Research (2013), http://dx.doi.org/10.1016/j.gr.2013.03.002

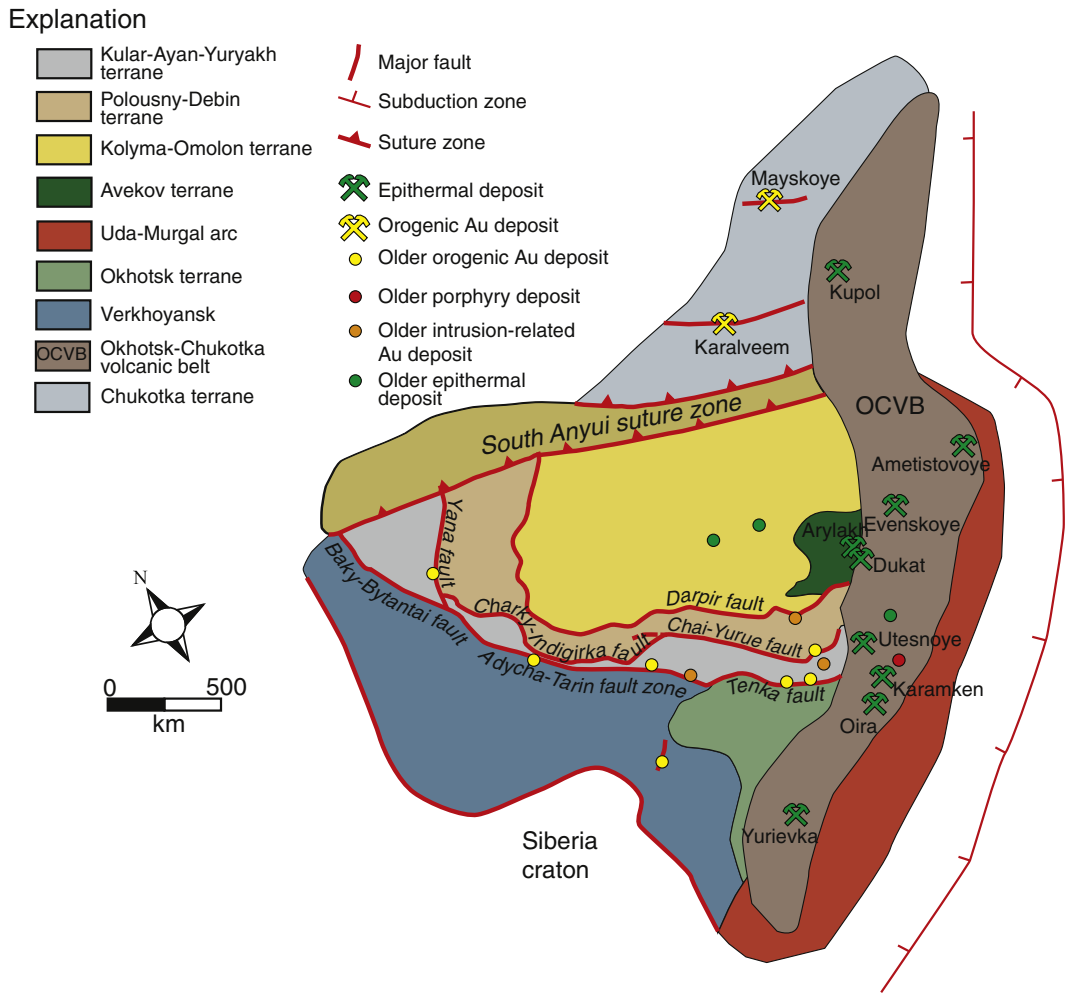

Fig. 18. Final closure of the South Anyui Ocean between the Arctic Alaska–Chukotka terrane and the Kolyma–Omolon terrane occurred in the Early Cretaceous. The Mayskoye and Karalveem orogenic gold deposits, as well as others to the east in northwestern Alaska, formed during associated Early Cretaceous deformation. The Middle to Late Cretaceous Okhotsk–Chukotka volcanic arc overprinted the entire northeastern Pacific margin of Russia. Magmatic hydrothermal deposits of the arc include low-sulfidation epithermal Au–Ag ores (e.g., Dukat, Kupol, Karamkem).
Based mainly on Konstantinovsky (2007) and Parfenov et al. (2009).

gold deposits (e.g., Ergelyakh, Chistoye, Malysh-Dubach) of uncertain economic significance and characterized by anomalous concentrations of As, Bi, Te, and W, appear to be closely associated with intrusions of both types. Argon geochronology indicates gold deposition at 149–140 Ma and these are considered to be intrusion-related gold systems (Fig. 17; Goryachev and Gamyanin, 2006; Goryachev, 2006), similar to the Fort Knox gold deposit in eastern Alaska (e.g., Goldfarb et al., 2005).

Orogenic gold deposits throughout the Yana–Kolyma region host the most significant gold resources (Fig. 17). They formed during both thrust and strike-slip events, and subsequent to the easterly growth of the continental margin and the subduction-related magmatism (e.g., Konstantinovsky, 2007). Orogenic gold deposits occur along much of the length of the Adycha–Taryn and Chai–Yuryue fault zones and appear to have formed during the onset of (1) thrust events reflecting the final collision of the Kolyma–Omolon superterrane with the Siberia craton and (2) strike-slip events reflecting changes in Pacific margin plate subduction and formation of the Uda–Murgal accretionary arc. Argon data for several orogenic gold deposits at ca. 136 ± 3 and 125 Ma correspond to the two events.

The economically most important gold region of the Russian Far East is that of the 375 by 75 km Ayan–Yuryak anticlinorium to the west of the Tenka fault system. Gold deposits are hosted by mainly Permian greenschist-facies rocks within a Permian to Jurassic clastic sequence deformed along the edge of the Siberian craton. The most significant of these are adjacent to the 200-km-long Tenka fault system within the Degdekan–Tokichan, Omchak, and Rodinovskoe districts (e.g., Eremin et al., 1994). The largest of the deposits, Natalka within the Omchak district (Fig. 17), has historically produced about 260 t of both lode and placer gold, yet has a remaining giant bulk minable resource of 1760 t Au (Goryachev et al., 2008). Atypical platinum and palladium enrichments in the orogenic gold deposits are interpreted to reflect a mafic to ultramafic protolith for the metasedimentary host rocks and thus local contributions of the noble metals (Gamyanin et al., 2007; Goryachev et al., 2011). Estimates for ages of gold formation are 137–133 Ma for Degdekan and 135 Ma for Natalka and Shkolnoye, as well as 125 Ma for Vetrenskoe deposit of the Sanga–Talon district 100 km to the east of Natalka along the Chai–Yuryue fault system (Fig. 17; Newberry et al., 2000; Voroshin and Newberry, 2001; Akinin et al., 2003; Voroshin et al., 2004; Volkov et al., 2011).

Two of the most significant deposits within the Adycha–Taryn metallogenic zone include Sarylakh and Sentachan (Fig. 17), which also grade 20–30% Sb and are estimated to contain about 5% of the global antimony reserve. The two deposits, 350 km apart, are hosted by Late Triassic greywacke of the Kular–Ayan–Yuryakh terrane. Bortnikov et al. (2010) suggest from K–Ar dates in the available literature a ca. 120–115 Ma gold event, followed by a subsequent antimony event about 30–40 million years later. A ca. 120 Ma quartz diorite porphyry 2 km north of the Sarylakh deposit (Levitan, 2008)

Please cite this article as: Goldfarb, R.J., et al., Phanerozoic continental growth and gold metallogeny of Asia, Gondwana Research (2013), http://dx.doi.org/10.1016/j.gr.2013.03.002

indicates magmatism could be coeval with the gold deposition. But given the inherent uncertainty with K–Ar systematics and slightly older dates of other orogenic gold deposits in the region (see Natalka above), it is also possible that both gold and antimony could be slightly older than the 120 Ma estimate and closer in age to the onset of the strike-slip event.

Farther north, the Kular Au–Hg–Sb district is mainly located within the Late Permian to Middle Triassic rocks of the Kular uplift, in the center of the northernmost part of the Kular–Ayan–Yuryakh terrane (e.g., Konstantinovsky and Lipchanskaya, 2011); a few Hg occurrences continue into the Polousnyi–Debin accretionary prism to the east (Berzon et al., 1999). This uplift is bounded by the Baky–Bytantai fault to the west, which is the northern strand of the Adycha–Taryn fault zone, and the Lower Yana fault to the east, with ca. 105–103 Ma granitoids in the center of the anticlinorium (Fig. 17; Layer et al., 2001). Both fault zones were originally thrusts reactivated as left-lateral strike-slip zones. A series of NE-striking 2nd order strike-slip faults offset NW-trending thrusts throughout the uplifted basin. The district resembles that of the Bridge River district in western Canada (e.g., Goldfarb et al., 2008) in that different crustal levels exposed throughout a series of associated transform faults host orogenic gold, or related antimony or mercury deposits. Kyuchus represents the major gold resource within the district (e.g., Berzon et al., 1999) and it is likely that mineralization throughout the Kular district relates to the Late Cretaceous evolution of the strike-slip system in the Okhotsk–Chukotka back-arc region (e.g., Nokleberg et al., 2005).

7.1.2. South Verkhoyansk synclinorium

The South Verkhoyansk synclinorium (Fig. 17) is located landward of the Yana–Kolyma belt within the deformed craton margin strata. The largest gold district, Allakh–Yun, is located in the synclinorium that defines the most outward part of the South Verkhoyansk fold belt west of the accreted terranes. Extensive lodes, including the giant (640 t Au) Nezhdaninskoe orogenic gold deposit (Fig. 17; Gamyanin et al., 2000; Chernyshev et al., 2011), and related placers of the district are associated with the north-striking Kideriki regional fault system (Konstantinovsky, 2007). The stringer and disseminated ores are mainly hosted in the crests of anticlines within Late Carboniferous–Early Permian carbonaceous turbidites that were metamorphosed to lower greenschist facies in the eastern side of the fold belt. The metamorphic rocks along the southern flank of the synclinorium are dated at ca. 120–119 Ma (Prokopiev et al., 2006). The Nezhdaninskoe deposit is dated at ca. 119 Ma and is coeval with much of the magmatism near the goldfields (Chernyshev et al., 2011; Borisenko et al., 2012). Right-lateral reactivation of the regional fault system is broadly coeval with the collision of the Okhotsk terrane to the south. The ores are slightly younger than the other orogenic gold deposits associated with the left-lateral events to the east in the Yana–Kolyma part of the orogen, but are likely similarly related to regional N–S trending fault reactivations during seaward continental margin tectonism. In addition to the orogenic gold deposits in the Allakh–Yun area, several I-type granitoids within the synclinorium host small 125 Ma gold deposits (i.e., Levo–Dybinskoye) that may be intrusion-related gold systems (Gamyanin et al., 2003; Borisenko et al., 2012) and/or orogenic gold (i.e., Zaderzhnoye; Kondratieva et al., 2010).

7.1.3. Oloi–Chukotka belt

The Chukotka district (Fig. 18) is located in the Oloi–Chukotka (or Anyui–Chukotka) fold belt of northeastern Russia. This belt extends far to the east from the Kular area to eastern Chukotka and then continues into the Nome gold district of the Seward Peninsula area of northwestern Alaska, USA (Goryachev, 1998, 2003; Nokleberg et al., 2005). It was formed as result of closure of the South Anyui Ocean during Late Jurassic and Early Cretaceous opening of the Arctic Canada basin. The largest deposits in the Russian part of this belt are the Mayskoye and Karalveem orogenic gold deposits, which contain significant resources as disseminations in sedimentary country rocks. All of the orogenic gold deposits show a close relationship to regional anticlinal structures in mainly deformed early Mesozoic metamorphic rock sequences.

At Karalveem (Goryachev, 1998; Nokleberg et al., 2005), gold-bearing veins and disseminations are hosted by Early Triassic clastic sediments and diabase sills. Potassium–Ar dates of hydrothermal sericite range from 130 to 100 Ma and thus broadly correspond to granite doming and regional metamorphism dated as ca. 117–103 Ma by SHRIMP (Katkov et al., 2007; Miller et al., 2009; Polzunenkov et al., 2011), and ca. 110 Ma orogenic gold events in the Nome district (e.g., Goldfarb et al., 1997). The Mayskoye deposit, with gold associated with disseminated arsenopyrite and pyrite and later stibnite-bearing quartz veins, is hosted by Middle Triassic clastic sedimentary rocks and numerous granite and granodiorite porphyry dikes dated at 118–107 Ma (Volkov and Sidorov, 2001; Bortnikov et al., 2004). The ca. 100 Ma right-lateral displacement along the South Anyui fault system (e.g., Bortnikov et al., 2004) may relate to the orogenic gold deposition in the Russian arctic region.

7.1.4. Uda–Murgal and Okhotsk–Chukotka arcs

The Uda–Murgal subduction-related magmatic belt, mainly comprising a complex group of accreted terranes, hosts several epithermal Au–Ag deposits within shallowly preserved volcanic rock sequences (Fig. 18; Goryachev, 2003, 2005). The largest of these, Julietta, is dated at 136 Ma by Rb–Sr on adularia (Struzhkov et al., 1994, 1996) and is closely related to the Early Cretaceous andesite and dacite sequences. The epithermal Au–Ag deposits of Uda–Murgal volcanic belt are also spatially associated with Cu-porphyry (Lora, Fig. 17) and intrusion-related Au (Teutedjak) deposits; the latter is suggested to be ca. 100 Ma based on K–Ar of ore minerals (Mirgorodskaya, 2008). The younger middle Cretaceous dates correlate with a broad period of east–west extension in this part of the Russian Far East (Layer et al., 2001), and thus may actually be an early part of the Okhotsk–Chukotka magmatism (see below). However, the K–Ar dating is questionable and these other deposits could also have similar ages to the gold ores at Julietta.

The immense post-accretionary Late Cretaceous extension-related Okhotsk–Chukotka volcanic belt (OCVB) extends for more than 3000 km in a NE–SW direction. Regional metallogeny resembles that described for the Bolivian Andes (e.g., Arce-Burgoa and Goldfarb, 2009). The 105–77 Ma OCVB (Akinin and Miller, 2011) defines the late Mesozoic active continental margin of northeastern Asia (Parfenov, 1995). This belt includes many low-sulfidation epithermal Au–Ag deposits, including Karamken, Dukat, Valunistoye, Kupol, and Ametistovoye (Fig. 18; Konstantinov et al., 1993; Nokleberg et al., 2005); Dukat is the largest epithermal deposit in Russia. These deposits are associated with large caldera complexes formed during late-stage Late Cretaceous dacitic to rhyolitic volcanism and associated subvolcanic plutonism. Epithermal deposits vary in Au–Ag ratio from gold-dominant at Kupol, to relatively equal amounts of gold and silver at Karamken, Valunistoye, and Ametistovoye, to silver-rich at Dukat. The Dukat deposit and some smaller epithermal deposits (Lunnoye, Arylakh) are located in the back-arc part of the OCVB. They occur in the local Omsukchan rift-like depression and are spatially associated with numerous tin- and argentiferous base metal-rich deposits. The ore-forming event at Dukat at 86–80 Ma appears to be episodic and associated with two distinct magmatic stages (Konstantinov et al., 1998; Nokleberg et al., 2005). Other Au–Ag epithermal deposits are located along the length of the OCVB and show middle Cretaceous (100–91 Ma: Karamken, Nyavlenga, Oira, Yurievka) and Late Cretaceous (84–72 Ma: Valunistoye, Evenskoye, Utesnoye) formation ages (Layer et al., 1994; Newberry et al., 2000). Many of the epithermal gold ores are associated with small Late Cretaceous Mo and Cu–Mo porphyry deposits in the center and seaward parts of the OCVB.

Please cite this article as: Goldfarb, R.J., et al., Phanerozoic continental growth and gold metallogeny of Asia, Gondwana Research (2013), http://dx.doi.org/10.1016/j.gr.2013.03.002

7.2. Cretaceous Sikhote–Alin orogen

The Sikhote–Alin or North Sakhalin–Sikhote Alin orogen is located in the southern part of the Russian Far East, to the south of the eastern part of eastern Transbaikal (Fig. 19). This orogen extends in a north-to-south direction from the Sea of Okhotsk to the Japan Sea (Khanchuk, 2001, 2006). Terranes along the eastern side of the Bureya–Jiamusi block are dominated by Jurassic and Early Cretaceous accretionary prisms containing late Paleozoic through Mesozoic sedimentary rocks, Early Cretaceous turbidites, and Early Cretaceous oceanic arcs; they are overprinted by the post-accretionary Late Cretaceous–Paleogene East Sikhote–Alin volcanic arc belt (ESAVB; Kemkin, 2008). The main orogenic event was in late Early Cretaceous and was dominated by left-lateral strike-slip movements. These movements were along the Central Sikhote–Alin strike-slip fault system, >1000 km in length, and likely resulted in the giant "S-form" tectonic structure of the Sikhote–Alin orogeny (Khanchuk, 2001). This fault system, along with the giant Tan–Lu fault system that is associated with much of the orogenic gold in eastern China and parallels the Central Sikhote–Alin fault 500 km to the west, are the two giant strike-slip structures along the east Asian Pacific margin.

The northern part of this orogen hosts several orogenic gold deposits (Agnie–Afanas'evskoe, Albazinskoye, Oemku, Uchaminskoye) and an intrusion-related gold system (Dzhegdag) that contains the rare palladium-bearing sudberite (Molchanov et al., 2000). The deposits are located in Cretaceous clastic sedimentary rocks near middle to Late Cretaceous I-type granodiorite intrusions. Many of these are located near the intersection of the Central Sikhote–Alin fault system and the Ilan–Itun fault, which is a northern continuation of the Tan–Lu regional fault system (Fig. 19). The southeastern side of the orogen hosts gold deposits defined as orogenic and intrusion-related (Askol'd, Malinovoye, Krinichnoye, Glukhoye, Salyt), which are closely related to Central Sikhote–Alin fault system (Utkin et al., 2004; Goryachev et al., 2012). These include gold-bearing quartz veins (Askol'd, Krinichnoye) in granitoids dated at 97–82.5 Ma and in Jurassic–Early Cretaceous sandstones and conglomerates (Sayadyan, 2004). The age of mineralization of the Askol'd deposit is estimated as 83.8 Ma and Krinichnoye is 76.2 Ma based on K–Ar analyses of hydrothermal muscovite (Sayadyan, 2004). The reduced nature of the central Sikhote–Alin granitoids and their Sn–W association (e.g., Sato et al., 2006), suggesting favorability for intrusion-related gold systems (e.g., Hart et al., 2004), is consistent with the classification by Russian workers. However, the abundance of sulfides, the Pd at Djegdak, and the young age at Krinichnoye are problematic with an intrusion-related gold system classification. Historical placer operations have been recognized for more than 100 years along the northern side of the Amur River, yielding more than 900 t Au (Ratkin, 1995), and are certainly associated with much of the orogenic gold mineralization.

The >1000-km-long ESAVB is very similar to the OCVB and also hosts numerous Au–Ag low-sulfidation epithermal deposits. It is located in the area near the two regional strike-slip faults associated with the orogenic gold ores (Fig. 19). Volcanism and ores of the belt may be associated with extensional features that developed between the regional faults (e.g., Utkin, 2012). The largest deposit in the ESAVB, Mnogovershinnoe, located in the north of this belt, includes 3-km-long ore zones that consist of numerous adularia–quartz and rodonite–quartz veins and veinlets in altered volcanic rocks (Nokleberg et al., 2005; Khanchuk, 2006). Host rocks for the gold-, silver-, and telluride-rich mineralization are andesite and dacite. A K–Ar age for the mineralization is reported as 69–66 Ma. The Belaya Gora Au–Ag deposit is located 120 km to the south of the Mnogovershinnoe deposit. Stockwork-like and disseminated orebodies are located in rhyolite–dacite extrusive rocks and explosive breccia of an Eocene–Oligocene magmatic complex (Nokleberg et al., 2005).

7.3. Late Jurassic–Cretaceous Yanshanian orogen

7.3.1. Northeastern China

As emphasized by Zhou et al. (2009), the tectonic evolution of northeastern China, to the north of the margin of the North China block (Fig. 19), is complex and controversial. Allochthonous blocks, such as Argun (or Erguna) and Songliao, were accreted to the growing Tuva–Mongol throughout the Paleozoic. This was followed by Paleo-Asian ocean closure to the south, during the same Late Permian–Triassic closure of a part of the Mongol–Okhotsk Ocean to the north. Final closure of the oceans was coeval with the Jurassic onset of west-directed Izanagi plate subduction below northeastern China (Zhou et al., 2009). This convergence included the Early Jurassic redocking of the Bureya–Jiamusi block on the eastern margin of the CAOB, which may have been a part of a larger Songliao block that rifted into the late Paleozoic Mongol–Okhotsk Ocean (Zhou et al., 2009). Although ultimate controls are uncertain, latest Jurassic to Early Cretaceous extensional structures developed within the convergent regime throughout the region (e.g., Daoudene et al., 2009), with the majority of dates on the extension concentrated between 134 and 110 Ma (Lin et al., 2013). Zhang et al. (2010a) relate the extension to a more oblique subduction of the Izanagi plate, which would have lead to back-arc extension.

Middle Jurassic to Early Cretaceous volcanic rocks of variable composition are widespread in the Great Xing'an Range (e.g., Wu et al., 2005). A felsic- to intermediate-dominated suite of volcanic rocks is notably voluminous in the Huolinhe area of the southern Great Xing'an Range (Guo et al., 2009; Zhang et al., 2010b). This area is defined as the south segment of the Hercynian fold belt by Zeng et al. (2011) or Solon terrane collage of Parfenov et al. (2009). Marine sedimentary and volcanic rocks were accreted to the CAOB in late Paleozoic–early Mesozoic, and then overprinted by the Mesozoic continental arc. The arc rocks are genetically associated with a cluster of epithermal and porphyry deposits of the Manzhouli polymetallic belt that include the Ereentolgoi intermediate-sulfidation epithermal Ag ± Au deposit and the Au–Cu high-sulfidation epithermal deposits at Siwumuchang and Daba (Table 10; Fig. 19; Mao et al., 2007). Zeng et al. (2011) indicate that the epithermal ores are associated with Middle to Late Jurassic andesites and rhyolites. Thus, ore formation relates to the earlier period of subduction and convergence.

Other epithermal deposits (Table 10), farther northeast near the Heilongjiang/Amur River and at the northeastern end of the Great Xing'an Range, and within the north segment of the Hercynian fold belt (Guo et al., 2009) or South Mongolia–Khingan arc terranes (Parfenov et al., 2009), include the low-sulfidation Guliku Au ± Ag, intermediate-sulfidation Sandaowanzi Au–Te, and the previously undocumented Tianwangtai high-sulfidation gold (G. Collins, Eldorado Gold, internal memo, 2012) systems. These volcanic-related gold ores are slightly younger than in the Hinggan Mountains, as evidenced by an association with Early Cretaceous andesite at Guliku (Zeng et al., 2011) and by geological constraints placing gold deposition at Sandaowanzi between ca. 125 and 116 Ma (Liu et al., 2011b). The Great Xing'an deposits are spatially associated with the large Duobaoshan Cu–Mo–Au porphyry (see above), but the latter has been suggested to be part of a much older, unrelated magmatic event. We interpret the epithermal deposits as being related to the shift to oblique subduction and regional extension.

A few tens of kilometers to the southeast of the town of Heihe, the recently developed Eastern Dragon (or Dong'an) low-sulfidation Au–Ag deposit, within the Zuolun–Heihe metallogenic belt, indicates continuation of the extension-related epithermal province into the center of the Songliao block. Argon dating of sericite from the rhyolite porphyry-hosted breccias and veins indicates an age of ca. 107 Ma (Zhang et al., 2010b). The Tuanjiegou epithermal deposit is located 140 km southeast of Eastern Dragon, where mineralized veins and breccias cut a ca. 110 Ma granodiorite porphyry (G. Collins, Eldorado Mining, unpub. company report, 2012). The intrusion was emplaced

Please cite this article as: Goldfarb, R.J., et al., Phanerozoic continental growth and gold metallogeny of Asia, Gondwana Research (2013), http://dx.doi.org/10.1016/j.gr.2013.03.002

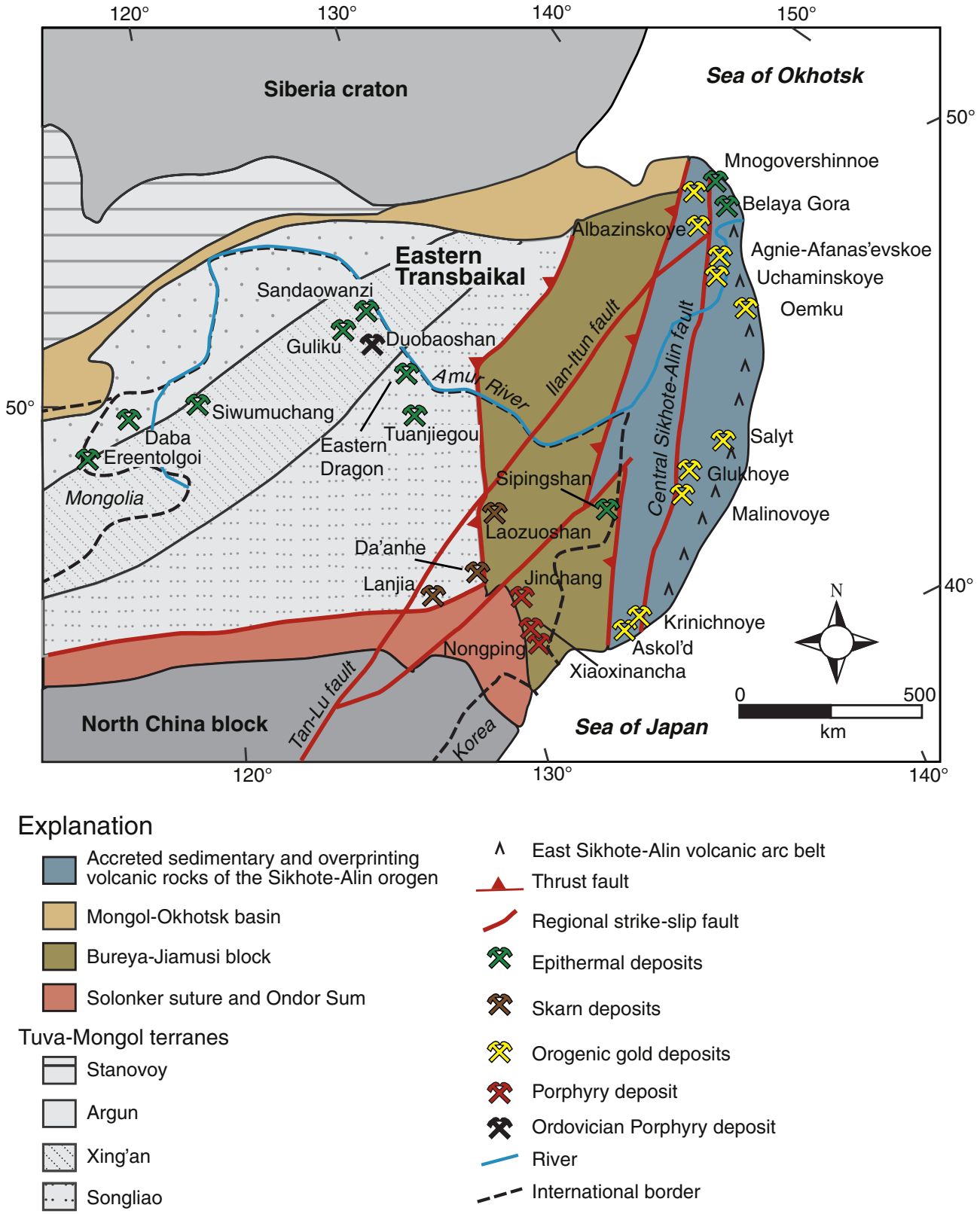

Explanation

- Accreted sedimentary and overprinting volcanic rocks of the Sikhote-Alin orogen
- Mongol-Okhotsk basin
- Bureya-Jiamusi block
- Solonker suture and Ondor Sum

Tuva-Mongol terranes

- Stanovoy
- Argun
- Xing'an
- Songliao

- East Sikhote-Alin volcanic arc belt
- Thrust fault
- Regional strike-slip fault
- Epithermal deposits
- Skarn deposits
- Orogenic gold deposits
- Porphyry deposit
- Ordovician Porphyry deposit
- River
- International border

Fig. 19. Jurassic and Early Cretaceous accretionary prisms of the Sikhote–Alin orogen with Late Cretaceous orogenic and intrusion-related gold deposits mainly formed along the Central Sikhote–Alin fault system, likely during a period of oblique subduction. Epithermal Ag–Au deposits, such as Mnogovershinnoe, are associated with the overprinting Late Cretaceous–Paleogene East Sikhote–Alin volcanic arc. Farther inland, regional extension in the Songliao, Xing'an, and Argun allochthonous blocks, which were accreted through Early Jurassic, was associated with widespread magmatism and formation of epithermal deposits (e.g., Ereentolgoi, Siwumuchang, Guliku, Sandaowanzi, Eastern Dragon). Adapted from Utkin (2012) and Zhou and Wilde (2013).

Table 10
Middle Jurassic-Cretaceous gold deposits of eastern China.

Deposit	Location in Fig. 1	Latitude	Longitude	Country	Tectonic location	Deposit type	Age (Ma)	Geochron. methodology	Geochron. reference
Ereentolgoi	217	48.38	116.67	China	Great Xing'an Range	Epithermal	Mid-L. Jurassic		Zeng et al. (2011)
Siwumuchang	218	49.56	119.56	China	Great Xing'an Range	Epithermal	Mid-L. Jurassic		Zeng et al. (2011)
Daba	219	49.27	117.01	China	Great Xing'an Range	Epithermal	Mid-L. Jurassic		Zeng et al. (2011)
Guliku	220	50.83	125.58	China	Great Xing'an Range	Epithermal	Early Cretaceous		Zeng et al. (2011)
Sandaowanzi	221	50.36	127.01	China	Great Xing'an Range	Epithermal	125-116	geologic	JL Liu et al. (2011b)
Eastern Dragon	222	49.25	128.8	China	Songliao block	Epithermal	107	Ar-Ar (sericite)	Zhang et al. (2010b)
Tuanjiegou	223	48.28	130.25	China	Yanshanian orogen- NE China	Epithermal	Early Cretaceous		Sinclair (2007)
Lanjia	224	43.53	125.67	China	Yanshanian orogen- NE China	Skarn	Late Triassic		Meinert et al. (2005)
Laozuoshan	225	46.16	131.45	China	Yanshanian orogen- NE China	Skarn	146-123	K-Ar	Chen et al. (2007b)
Da'anhe	226	44.76	128.56	China	Yanshanian orogen- NE China	Skarn	L. Triassic-E. Cretaceous		Meinert et al. (2005)
Jinchang	227	44.07	131.13	China	Yanshanian orogen- NE China	Epithermal	123.1	Ar-Ar (sericite)	Han et al. (2013)
Sipingshan	228	46.49	133.64	China	Yanshanian orogen- NE China	Epithermal	122(?)		Zhang et al. (2013)
Xiaoxinancha	229	43.18	130.82	China	Yanshanian orogen- NE China	Porphyry	104.6-102.1	geologic	Sun et al. (2008)
Nongping	230	42.94	130.79	China	Yanshanian orogen- NE China	Porphyry	100	U-Pb	Ren et al. (2012)
Duhuangling	231	~43.33	~130.59	China	Yanshanian orogen- NE China	Porphyry	107	fluid inclusions	Han et al. (2013)
Jiaodong deposits	232	~37.42	~120.07	China	Jiaodong	Orogenic	126-117	U-Pb; Ar-Ar, Rb-Sr; K-Ar	
Dahu	233	34.44	110.63	China	Qinling orogen	Porphyry	133-123	Re-Os (molybdenite)	Li et al. (2007a)
Q875	234	34.43	110.58	China	Qinling orogen	Orogenic	128-126	Ar-Ar (biotite)	Wang et al. (2002)
Yagzhaiyu (Xiaoqinling dist.)	235	34.4	110.57	China	Qinling orogen	Orogenic			
Wenyu (Xiaoqinling dist.)	236	34.43	110.44	China	Qinling orogen	Orogenic	127	K-Ar	Chao (1988)
							130	Ar-Ar (sericite and biotite)	Li et al. (2012a)
Qiangma (Xiaoqinling dist.)	237	34.38	110.42	China	Qinling orogen	Orogenic	125-120	Ar-Ar (sericite and biotite)	Li et al. (2012a)
Chen'er (Xiaoqinling dist.)	238	34.38	110.37	China	Qinling orogen	Orogenic	130-127	Ar-Ar (sericite and biotite)	Li et al. (2012a)
Dongtongyu (Xiaoqinling dist.)	239	34.45	110.39	China	Qinling orogen	Orogenic	144, 125-119	Ar-Ar (sericite)	Li et al. (2012a)
Shancheyu (Xiaoqinling dist.)	240	34.39	110.32	China	Qinling orogen	Orogenic	130-127	Ar-Ar (sericite)	Li et al. (2012a)
Dongchuang (Xiaoqinling dist.)	241	34.41	110.44	China	Qinling orogen	Orogenic	131	Ar-Ar (sericite)	Li et al. (2012a)
Fancha (Xiaoqinling dist.)	242	34.38	110.68	China	Qinling orogen	Orogenic	135-130	Ar-Ar (sericite)	Li et al. (2012a)
Simuyu (Xiaoqinling dist.)	243	34.47	110.49	China	Qinling orogen	Orogenic	134-131	Re-Os (molybdenite)	Li et al. (2012a)
Baishuling (Xiaoqinling dist.)	244	34.43	110.99	China	Qinling orogen	Orogenic	134-131	Re-Os (molybdenite)	Li et al. (2012a)
Xiaoshan district	245	34.5	111.25	China	Qinling orogen	Orogenic	Jurassic-E. Cretaceous		Mao et al. (2002a)
Qiyugou	246	34.18	111.93	China	Qinling orogen	Orogenic	125-115	geologic	Fan et al. (2011)
Weishancheng district	247	32.57	113.4	China	Qinling orogen	Orogenic	unreliable		
Haiggou	170	42.77	128.05	China	N margin of N. China block	Orogenic	144-120	Ar-Ar (sericite)	Shen et al. (1999)

(continued on next page)

Please cite this article as: Goldfarb, R.J., et al., Phanerozoic continental growth and gold metallogeny of Asia, Gondwana Research (2013), http://dx.doi.org/10.1016/j.gr.2013.03.002

Table 10 (*continued*)

Deposit	Location in Fig. 1	Latitude	Longitude	Country	Tectonic location	Deposit type	Age (Ma)	Geochron. methodology	Geochron. reference
Wulong	248	40.18	124.23	China	Eastern N. China block	Orogenic	135-125	geologic	Hart et al. (2002); Zhang et al. (2005a)
Sidagou	249	40.01	124.25	China	Eastern N. China block	Orogenic	135-125	geologic	Hart et al. (2002); Zhang et al. (2005a)
Paishanlou	250	41.88	121.8	China	Eastern N. China block	Orogenic	126-124	Ar-Ar (biotite); U-Pb (zircon)	Hart et al. (2002); Zhang et al. (2005a)
Erdaogou	251	41.95	120.35	China	Eastern N. China block	Orogenic	129-124	geologic	Hart et al. (2002); Zhang et al. (2005a)
Jinchanggouliang	252	41.93	120.33	China	Eastern N. China block	Orogenic	129-124	geologic	Hart et al. (2002); Zhang et al. (2005a)
Samgwang	253	36.54	126.89	South Korea	Korean Peninsula	Orogenic	127	K-Ar	Choi et al. (2005a) references within
Tongyeong	254	34.8	128.35	South Korea	Korean Peninsula	Epithermal			
Eunsan	255	34.35	126.5	South Korea	Korean Peninsula	Epithermal			
Geodo	256	37.13	128.97	South Korea	Korean Peninsula	Skarn	98		Meinert et al. (2005)
Sak Ju	257	~40.12	~124.47	North Korea	Korean Peninsula	Orogenic			
Nurupi	258	~40.03	~125.17	North Korea	Korean Peninsula	Orogenic			
Hukuchin	259	~40	~125.55	North Korea	Korean Peninsula	Orogenic			
Unsan	260	~39.83	~125.66	North Korea	Korean Peninsula	Orogenic			
Sen Sen	261	~39.8	~124.81	North Korea	Korean Peninsula	Orogenic			
Suan district	262	38.67	126.45	North Korea	Korean Peninsula	Skarn	Jurassic		Meinert et al. (2005)
Tomg Jom district	263	~41.33	~126.73	North Korea	Korean Peninsula	Skarn			
Kapsan district	264	~41.09	~128.29	North Korea	Korean Peninsula	Skarn			
Holdong	265	38.75	126.68	North Korea	Korean Peninsula	Skarn			
Hyesan	266	41.25	128.95	North Korea	Korean Peninsula	Skarn	Cretaceous		Meinert et al. (2005)
Sangnong	267	40.68	128.58	North Korea	Korean Peninsula	Skarn			
Ningzhen district	268	32.06	119	China	Yangtze River Province	Porphyry-Skarn	148-135	U-Pb (zircon); Re-Os (molybdenite)	Mao et al. (2006, 2011); Yang et al. (2011)
Tonling district	269	30.86	118	China	Yangtze River Province	Porphyry-Skarn	148-135	U-Pb (zircon); Re-Os (molybdenite)	Mao et al. (2006, 2011); Yang et al. (2011)
Anqing-Guichi district	270	31.14	117.28	China	Yangtze River Province	Porphyry-Skarn	148-135	U-Pb (zircon); Re-Os (molybdenite)	Mao et al. (2006, 2011); Yang et al. (2011)
Jiurui district	271	29.81	115.55	China	Yangtze River Province	Porphyry-Skarn	148-135	U-Pb (zircon); Re-Os (molybdenite)	Mao et al. (2006, 2011); Yang et al. (2011)
Edong district	272	30.14	114.93	China	Yangtze River Province	Porphyry-Skarn	148-135	U-Pb (zircon); Re-Os (molybdenite)	Mao et al. (2006, 2011); Yang et al. (2011)

into Proterozoic schists and gold formation is stated to be 105 Ma (Mao et al., 2007). The belt of Early Cretacous deposits extends 250 km south of the Eastern Dragon, to the Lanjia, Laozuoshan (Chen et al., 2007b), and Da'anhe Fe–Cu–Au skarns, and then is buried under Tertiary cover of the Songliao basin.

Continuing far to the east, within eastern Heilongjiang and within 100 km of the Russian border, the gold-rich veins and breccias hosted within altered granites, granodiorites, monzogranites, and porphyritic bodies, define the Jinchang copper–gold porphyry district (Jia et al., 2008; Han et al., 2013), with Banjiegou being the most significant porphyry deposit. The presence of adularia flooding of the breccia body is supportive of overprinting epithermal gold mineralization. The ore-hosting granitoids intrude Neoproterozoic rocks along the southeastern edge of the Bureya–Jiamusi block. Recent U–Pb SHRIMP dating of many granitoids in the area of the Jinchang deposit suggests a ca. 200 Ma episode of intrusion throughout the region (Wu et al., 2011). H.-F. Zhang (Santosh, written commun., 2012) has dated by U–Pb most of the intrusions at Jinchang and reports consistent ages of ca. 200 Ma; however, an age of 110 ± 3 Ma characterizes the granite porphyry. The Yanshanian younger age overlaps Zhang et al.'s (2008) 110 ± 3 and 104 ± 6 Ma mineralization dates (Rb–Sr sericite), but is younger than the age of mineralization estimated by Han et al. (2013) of 123.1 Ma ($^{40}Ar/^{39}Ar$ sericite). These are consistent with other extension-related late Yanshanian magmatic gold deposits in northeastern China, but are 40–50 m.y. older than similar deposit types to the east in the above described ESAVB. The ca. 120 Ma Sipingshan deposit, often described as a 'hot spring-type' (Zhang et al., 2013), is located 330 km NNE along strike from the Jinchang deposit (Fig. 19), in neighboring Heilongjiang province and, although similarly epithermal in character, appears to be formed at a much higher level as evidenced by the presence of mineralized sinters.

The Yanbian group of porphyry copper–gold deposits lies 100 km south of Jinchang, extending for more than 125 km in an E–W direction and localized along the northern edge of the North China block (see Fig. 1 in Han et al., 2013), which was likely reactivated during subduction of the Izanagi plate. The largest in the group is the Xiaoxinancha deposit (Fig. 19), geologically constrained between 104.6 and 102.1 Ma (Sun et al., 2008). The nearby Nongping deposit, dated at 100.04 ± 0.88 Ma (U–Pb zircon: Ren et al., 2012), shows similar gold-rich porphyry type characteristics. A gold-rich porphyry

Please cite this article as: Goldfarb, R.J., et al., Phanerozoic continental growth and gold metallogeny of Asia, Gondwana Research (2013), http://dx.doi.org/10.1016/j.gr.2013.03.002

deposit at Duhuangling is dated at 107 ± 6 Ma ($^{40}Ar/^{39}Ar$ fluid inclusions in quartz: Han et al., 2013).

7.3.2. North China block

The uplifted Precambrian basement rocks of the eastern, southern and northern margins of the eastern half of the North China block host both widespread Yanshanian granitoids and large resources in orogenic gold deposits (Fig. 20, Table 10). The Jiaodong province on the east of the North China block, as well as basement uplifts north of the eastern part of the Qinling orogen on the south of the North China block, represent the two largest gold provinces in China. These districts are also atypical, as significant Phanerozoic gold accumulations are rarely hosted in Precambrian rocks.

The Jiaodong Peninsula orogenic gold province covers less than 0.3% of China's total landmass, yet it accounts for 30% of the total national gold reserves and contributes more than 25% of its total gold production per annum (Qiu et al., 2002; Fan et al., 2007). Total estimates of past production and remaining resources exceed 1000 t Au, and these are likely modest given the relatively slow development of many of the gold systems. Gold has been recovered from some of the deposits in the province since the Ming dynasty, or for more than 1000 years.

The Jiaodong gold districts (Fig. 21) are bounded about 20–30 km to the west by the regionally extensive NNE-striking Tan–Lu fault system (see above), with NE-trending 2nd-order brittle–ductile faults splaying off the main system and controlling much of the lode gold. The majority of deposits in the district are hosted by Mesozoic granitoids or, less commonly, in basement rocks adjacent to the granitoids. The granitoids have intruded Late Archean and Paleoproterozoic high-grade metamorphic basement rocks episodically at ca. 160–150 and 130–126 Ma; the former bodies are mainly crustal melt monzogranites and biotite granite, whereas the latter are porphyritic granodiorites suggested to have been derived from underplated basalt (Qiu et al., 2002; Li et al., 2003). The intrusions are widespread and underlie about two-thirds of the peninsula. Gold mineralization occurs either as extensional massive gold–quartz–pyrite veins (Linglong-type) that can continue for more than 1 km along strike or as shear zone-hosted disseminated sulfides in granitoids (Jiaojia-type).

The timing of movement on the major faults of the Jiaodong Peninsula area remains controversial. Detailed $^{40}Ar/^{39}Ar$ geochronology of regional structures supports the development of thrusts and nappes ca. 210–180 Ma, extensional movement ca. 180–130 Ma, slip-thrust movement ca. 130–120 Ma, and extensional movement ca. 120 Ma (Zhang et al., 2007). Mercier et al. (2007), discussing the Tan–Lu fault system to the south of Jiaodong, noted sinistral transcurrent motion beginning on the system at ca. 127 Ma. Such transcurrent movement appears to correlate with the onset of widespread extension and the development of core complexes within the uplifting basement rocks and intrusions in Jiaodong and elsewhere in eastern Asia (e.g., Yang et al., 2007; Wang et al., 2011).

Gold mineralization is broadly constrained at 126–117 Ma from SHRIMP U–Pb zircon dating on host rocks, as well as by Ar–Ar, Rb–Sr, and K–Ar dating of hydrothermal alteration minerals (e.g., Wang et al., 1998; Chen et al., 2005; Fan et al., 2007), although there are a few possible outliers at ca. 110 Ma (Li et al., 2006) and ca. 130 Ma (Dayingezhuang: L-Q. Yang, written commun., 2012). It broadly correlates with changing motions along the Tan–Lu fault system and the above extension-related uplift. Smaller orogenic gold deposits in structurally less favorable areas to the south along the Tan–Lu fault system have similar Aptian ages in the Fengyang and Zhangbaling areas (Huang et al., 2011). The ca. 125–117 Ma age range for most of the Jiaodong gold deposits is much more restrictive than the lengthy period of Yanshanian magmatism in the Jiaodong Peninsula. It has been well-documented that 80–140 km of subcontinental lithospheric mantle (SCLM) was removed from the base of the eastern half of the cratonic block in Jurassic–Early Cretaceous time (Griffin et al., 1998; Windley et al., 2010). Basement uplifts and magmatism within the uplifts, driven by the upwelling of hotter asthenosphere, define the resulting Yanshanian orogeny and thus the decratonization of the North China block. The narrower window for gold mineralization is suggested to reflect major changes in plate kinematics in the Pacific basin and the onset of seismicity along the Tan–Lu fault system during Aptian time (Fig. 22; Goldfarb et

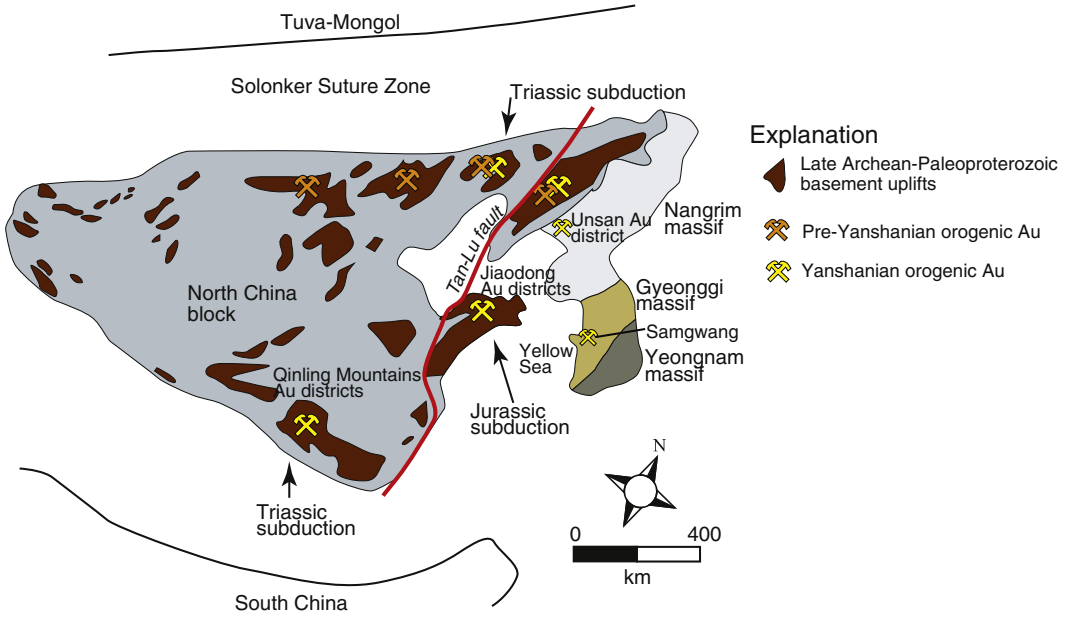

Fig. 20. The largest gold resources in China are the Early Cretaceous orogenic gold deposits within Late Archean–Early Proterozoic basement rocks that were uplifted along the eastern margins of the North China block during Jurassic–Cretaceous Yanshanian orogeny. These include deposits of the Jiaodong Peninsula, the eastern Qinling Mountains, and the northeastern corner of the block extending into adjacent North Korea. Mesozoic plate subduction from the north, south, and west may have been critical in causing delamination of thick subcontinental mantle lithosphere and thus consequent uplift of the thinned lithosphere. Similar, but much smaller orogenic gold deposits ("Korean-type") in basement uplifts of the Gyeonggi massif in South Korea formed in Middle to Late Jurassic.
Based on Metcalfe (2006) and Goldfarb et al (2007).

Please cite this article as: Goldfarb, R.J., et al., Phanerozoic continental growth and gold metallogeny of Asia, Gondwana Research (2013), http://dx.doi.org/10.1016/j.gr.2013.03.002

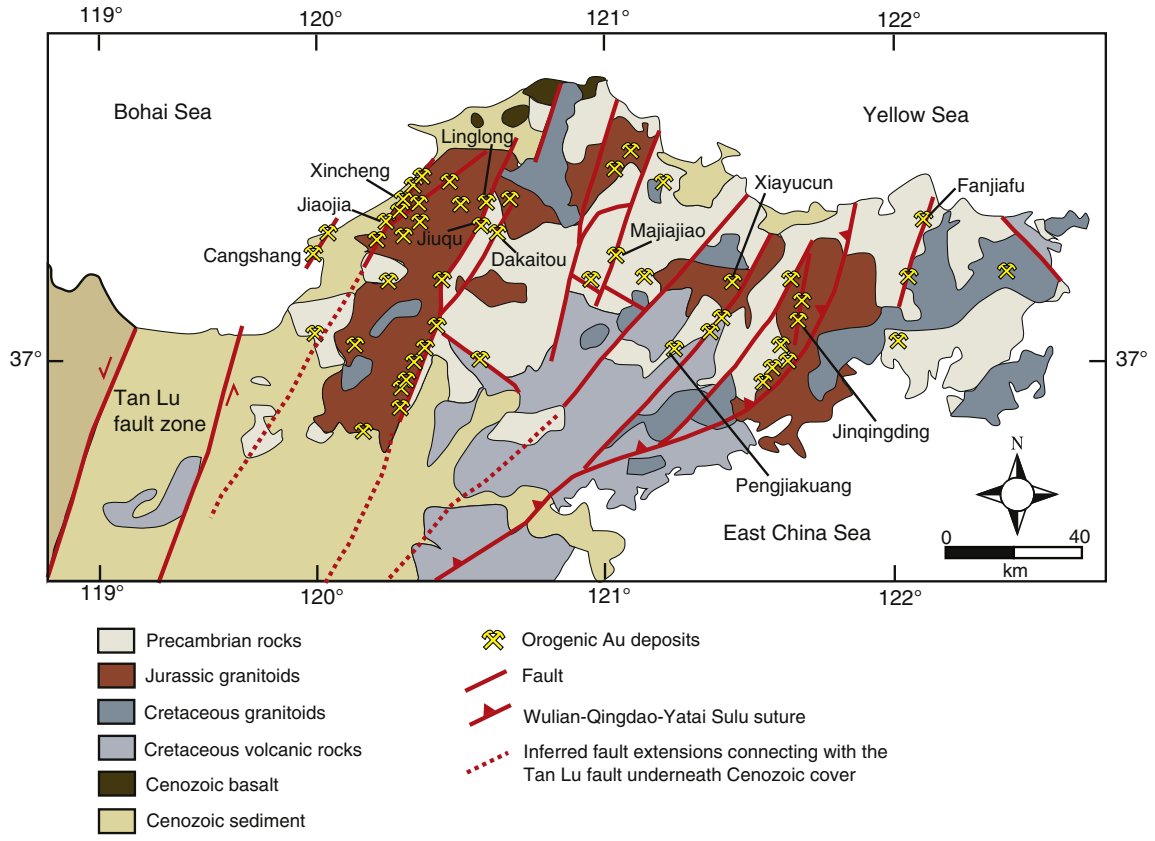

Fig. 21. The largest gold resource in China is that of the Jiaodong Peninsula. Orogenic gold deposits, all ca. 130–120 Ma, are located along second-order faults to the continental-scale Tan–Lu fault system. The second-order faults occur along the boundaries of ca. 160–150 and 130–126 Ma granitoids that were emplaced into Late Archean uplifted basement gneiss. Adapted from Li et al. (2003, 2006).

al., 2007), with fluids and metals perhaps being derived from sediment volatilization above the downgoing Izanagi slab.

With at least 600 t of mined and defined gold resources, the basement uplifts in the Qinling Mountains (Fig. 20) define the second most significant gold province of China (e.g., Mao et al., 2002a). The deposits are located about 30–50 km north of the southern margin of the block. The uplifts are characterized by the emplacement of numerous granitic stocks of mainly Early Cretaceous age, although some are also Late Triassic. However, in contrast to the Jiaodong province, the gold ores are hosted by the Precambrian basement rocks, rather than the much younger intrusions.

Most deposits cluster in three areas: the Xiaoqinling district to the west, the Xiaoshan district in the center, and the Xiong'ershan district to the east (see Fig. 1 in Mao et al., 2002a). In the economically most important 75 by 10–15 km Xiaoqinling district, deposits are clearly associated with east–west folds in the Precambrian rocks and associated faults that follow fold hinges. Additional gold deposits of probably the same broad ore-forming event continue to the southeast,

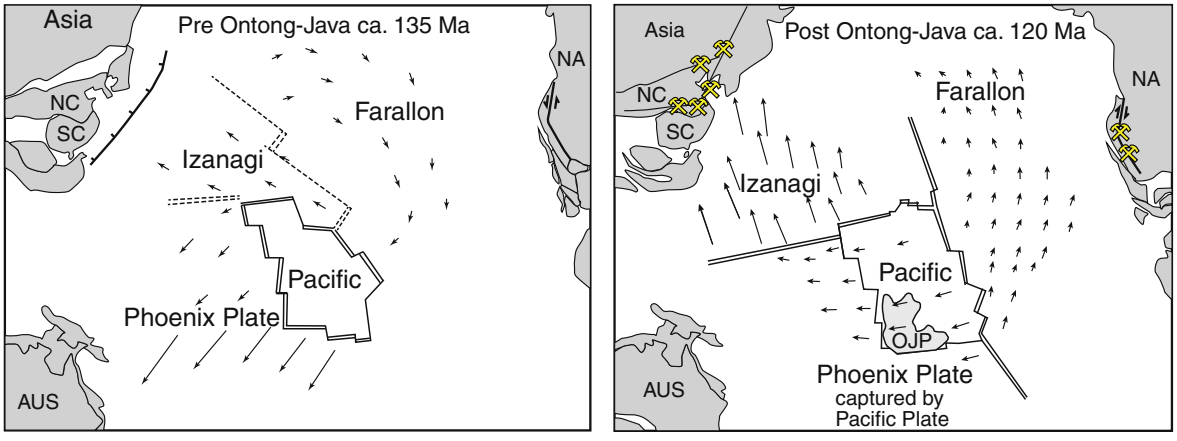

Fig. 22. Major changes in plate dynamics in the northern Pacific basin, which was caused by the capture of the Phoenix Plate by the Pacific Plate during the ca. 125 Ma Ontong–Java plume event, included a shift to a more northerly subduction of the Izanagi and Farallon plates. Associated seismicity along major continental margin faults on both sides of the Pacific Ocean was responsible for a broad-scale fluid-flow event and formation of giant orogenic gold provinces in the North China block and California, USA. NC: North China block; SC: South China block; NA: North America; Aus: Australia; OJP: Ontong–Java Plateau.
Adapted from Ratcliff et al. (1998) and Goldfarb et al. (2007).

Please cite this article as: Goldfarb, R.J., et al., Phanerozoic continental growth and gold metallogeny of Asia, Gondwana Research (2013), http://dx.doi.org/10.1016/j.gr.2013.03.002

where deposits of the Weishancheng district (Zhang et al., 2011) are localized in a narrow part of the Qinling orogen deformed between the North China and South China blocks.

Whereas most deposits in the Qinling Mountains districts are best classified as orogenic, there are some atypical features in the region. Numerous Late Triassic and Cretaceous molybdenum-rich porphyry and skarn deposits occur through the uplifted basement rocks. Mao et al. (2011a) also note significant molybdenum in the large Dahu gold deposit in the Xiaoqinling district, yet they show the economic gold- and molybdenum-rich orebodies to be in different parts of the deposit. Much of the molybdenum may have been Triassic in age and reworked during Yanshanian orogenesis and gold formation, as suggested by Ni et al. (2012). There are also numerous structurally controlled silver-, lead-, and/or zinc-rich Coeur d'Alene-type vein deposits in the districts (e.g., Chen et al., 2004; Zhang et al., 2011). These could be part of the same metallogenic event as that which was responsible for the gold, but such is uncertain. Finally, in the Xiong'ershan district a number of gold deposits are reported to occur in low-sulfidation epithermal-like volcanic breccia bodies (e.g., Zhang et al., 2005b), but more recent studies show that these too have many features characteristic of orogenic gold deposits (e.g., Fan et al., 2011).

The timing of gold formation in the eastern Qinling Mountains is broadly the same as that in the Jiaodong Peninsula. In the Xiaoqinling district, Wang et al. (2002) showed well-formed 128–126 Ma argon plateaus for hydrothermal biotite at the Q875 deposit, consistent with an older 127 Ma K–Ar date on hydrothermally altered host rock from the nearby Wenyu deposit (Chao, 1988). Molybdenum in the above mentioned Dahu gold deposit was dated by Re–Os between 133 and 123 Ma (Li et al., 2007a). Fan et al. (2011), evaluating all existing data of variable quality, suggested the Qiyugou deposit in the Xiong'ershan district formed sometime between 125 and 115 Ma. Data are even more difficult to interpret from the Weishanchang district, leading Zhang et al. (2011) to suggest that a 150 Ma gold event was possible, but more reliable data are critical before a definitive age is possible. Most recently, Li et al. (2012a) presented Re–Os and $^{40}Ar/^{39}Ar$ data for ten deposits throughout the Xiaoqinling district. Excluding the small Luzhougou deposit to the south of the main district-bounding fault and one discordant argon date, all dates range between ca. 135 and 120 Ma. In summary, most data suggest the gold events in the uplifts of the Qinling Mountains were coeval with those of Jiandong Peninsula, and both may reflect the same broad circum-Pacific plate changes (e.g., Goldfarb et al., 2007). As Wang et al. (2011) pointed out, both of these areas underwent the same top-to-the-northwest shearing during core-complex evolution at this time.

The northern margin of the North China block is complex, reflecting both Paleotethyan and younger Pacific margin subduction processes. As mentioned above, many deposits, particularly in uplifted basement rocks of the western and central parts of the margin, are characterized by Carboniferous through Jurassic gold deposits (Fig. 16) that relate to closure of the Turkestan Ocean. The ca. 150 Ma Dongping deposit may be one such deposit (Fig. 16) or it could be one of the westernmost deposits related to younger circum-Pacific tectonism.

Early Cretaceous orogenic gold deposits occur in basement uplifts in a number of areas to the east along the northern margin of the Precambrian block (Fig. 20); they are hosted both by Mesozoic granitoids and Precambrian basement, and appear, to a large extent, to be controlled by movement along NE- to NNE-trending fault systems. Zhang et al. (2003b) indicate sinistral strike-slip, extensional faulting, and core-complex unroofing along regional NNE-trending ductile shear zones in this area to have occurred ca. 130–115 Ma. The deposits in the region include the ca. 135–125 Ma Wulong and Sidagou deposits (Fig. 16) east of the Tan–Lu fault and within a few tens of kilometers of the North Korea border, and to the west of and along NW-trending regional faults parallel to the Tan–Lu fault, the ca. 124 Ma Paishanlou deposit and the ca. 129–124 Ma Erdaogou and Jinchanggouliang deposits (Fig. 16; Hart et al., 2002; Zhang et al., 2005a). Also, although as stated above, the Jiapigou group of deposits are Triassic in age, the large Haiggou deposit to the southwest of these deposits (Fig. 16), formed sometime between 144 and 120 Ma (Miao et al., 2005). Therefore, deposition of a giant gold endowment in the eastern half of the North China block was relatively coeval along the different margins of the block, and reflects a period of continental-scale extension and fault movement (e.g., Wang et al., 2011).

7.3.3. Korean Peninsula

The tectonic history of the Korean Peninsula is still unclear. There is general agreement that during much of the Precambrian the basement rocks of Korea were connected in some manner to the North and South China blocks, but the Phanerozoic relationship among the three blocks is unclear. Although unclear, it seems certain that transtensional stresses during the Late Cretaceous to Tertiary (Ren et al., 2002) produced the Bohaiwan Basin and North and South Yellow Sea Basins, effectively pulling apart the Korean Peninsula–Shandong Peninsula land mass.

From north to south, the Korean Peninsula includes the Nangrim, Gyeonggi, and Yeongnam Precambrian massifs (Fig. 20), which are respectively separated by the Pyeongnam basin/Imjingang belt and Okcheon belt. Like many of the Precambrian blocks in eastern Russia, the Korean massifs also have a poorly understood history, and may have been connected to the North China block (e.g., Chang and Zhao, 2012) or the South China block (Jeon et al., 2007) within the Paleotethys Ocean. Much of the peninsula is intruded by ca. 248–201, 200–158, and 110–50 Ma granitoids. The most widespread granitoids are those associated with the ca. 200–150 Ma Daebo orogeny.

Historically, much of the recognized gold production on the Peninsula, including perhaps 185 t of production from 1886 to 1934, has been in present-day North Korea (e.g., Emmons, 1937). Unfortunately, there are few modern data about the geology of any of these deposits. Deposits in present-day South Korea are much better known, although they are generally <10 t Au. These include orogenic, epithermal, and skarn deposit types. As with many other countries in Asia, most likely many of these may be much larger resources that have yet to be defined during the relatively small-scale mining operations.

Orogenic gold deposits are well dated mainly between ca. 170 and 140 Ma (Choi et al., 2005a), thus overlapping the latter stages of emplacement of the voluminous, I-type, NE-trending Jurassic batholith that cuts across much of South Korea. Many workers have referred to these deposits as “Korean-type” gold deposits, and have related these genetically to the batholith (e.g., Shelton et al., 1988; Choi et al., 2005a). The deposits show a spatial association to deep-crustal, dextral strike-slip shear zones, which are major ductile features associated with a shift from E–W to N–S compression during the second phase of the Daebo orogeny (e.g., Lim and Cho, 2012). Many are located in Precambrian basement rocks and Jurassic intrusions along the NE-trending Gongju–Eumseong fault zone between the Gyeonggi massif and Okcheaon belt; others are localized near other similarly-trending faults to the north and south, including the large Honam system between the Okcheaon belt and southerly Yeongnam massif (Fig. 1 in Choi et al., 2005a). The Samgwang deposit in the Gyeonggi basement gneisses (Fig. 20) in the Cheongyang district is possibly the largest deposit in South Korea (40 t Au: Yoo et al., 2010).

A major shift in Izanagi plate dynamics at ca. 160 Ma, from NW-trending orthogonal to N-trending oblique subduction, is suggested to have led to a 50-m.y.-long magmatic lull and the Middle to Late Jurassic gold event (Choi et al., 2005a). The shift correlates with a change from dextral to sinistral strike-slip on the NE-trending faults (Choi et al., 2005a) and probably rapid uplift of crystallized parts of the batholith as supported by the formation of some of the younger gold ores in extensional fractures in the slightly older igneous rocks. Although slightly older than the gold deposits of the Yanshanian orogenesis in the North China block, these gold ores of the Daebo orogen represent another east Asian example where significant young gold

Please cite this article as: Goldfarb, R.J., et al., Phanerozoic continental growth and gold metallogeny of Asia, Gondwana Research (2013), http://dx.doi.org/10.1016/j.gr.2013.03.002

resources are hosted by high-grade metamorphic rocks billions of years older.

About two-thirds of South Korea's gold endowment is hosted by Cretaceous–early Tertiary high- and low-sulfidation epithermal deposits (see Fig. 1 in Choi et al., 2005a) that developed in NE-trending pull-apart basins formed along the NE-striking faults during sinistral deformation (Choi et al., 2005b) under a more tensional regime (Lim and Cho, 2012). These include the presently mined Eunsan deposit in the southern part and the historically worked Tongyeong deposit in the southwestern part of South Korea, both low-sulfidation epithermal deposits associated with Late Cretaceous volcanic rocks (Kirwin et al., 1999; Yang et al., 2012). The majority of the gold- and silver-rich ores formed ca. 110–60 Ma during the young period of volcanic and subvolcanic magmatism in sedimentary-dominant basins to the north near the Gongju–Eumseong fault and volcanic-dominant basins to the south near the Yeongdong–Gwangju fault in South Korea (Choi et al., 2005b). In addition to epithermal deposits, many ca. 110 Ma gold-bearing skarns are located in the Taebaeksan basin on the eastern side of the peninsula. Host rocks include early Paleozoic carbonates that disconformably overlie the northeastern margin of the Yeongnam massif. Many of these, such as Geodo, were originally developed as Fe- and/or Cu deposits, and have only recently been recognized for their gold potential (Kim et al., 2012).

The Late Cretaceous shift to orthogonal NW-subduction of the Pacific plate below the Korean Peninsula has been suggested as a cause of the widespread calc-alkaline magmatism and associated epithermal and skarn mineralization on the Korean Peninsula (Choi et al., 2005b). Subduction of the spreading ridge between the Pacific and Izanagi plates may also have played a role in these events. Much of the older part of the metallogenic event temporally overlaps the above-mentioned widespread ca. 110 Ma epithermal/porphyry event in northeastern China. Whether the shallow magmatism and ore formation in the two adjacent regions are related is not certain, but is a possibility. Also, if indeed there is a South China block connection to the Korean Peninsula (e.g., Jeon et al., 2007), then the gold-bearing skarns in the Taebaeksan district may reflect the same favorable host lithologies that are present on the leading edge of the Yangtze block and host the slightly older Yangtze River province skarns (see below).

Descriptions of the historic gold producers in the northern part of the Korean Peninsula (Emmons, 1937; Gallagher, 1963) suggest at least past development of orogenic gold and gold-rich skarn deposits, as well as significant associated placers, all of which have been worked for many centuries. Large orogenic gold deposits (e.g., Sak Ju, Nurupi, Hukuchin, Unsan, Sen Sen) are located north of the Yellow Sea and are present along the border with China to 100 km inland into North Korea (Fig. 16). Like those in South Korea, they are hosted by Precambrian gneiss (e.g., Nangrim massif) and Mesozoic granitoids. These deposits seemingly form part of a single province with the above-mentioned 135–125 Ma Wulong and Sidagou deposits. If correct, then the orogenic gold deposits in North Korea would be somewhat younger than those in South Korea and the hosting Nangrim Massif is certainly what has been defined as North China block in northeastern China. Other historic gold resources in North Korea, including those of the Suan district in the Pyeongnam basin 150 km north of Seoul (Higgins, 1918), Tong Jom in the northwest, and Kapsan in the northeast, are probably best defined as Cu–Au skarns, likely similar to Geodo in South Korea. Active gold mines at Holdong, Hyesan, and Sangnong (Choi, 2011) could also be gold skarns. Hyesan, near the border with China, contains resources of Ag, Au, Cu, Pb, and Zn, is North Korea's largest copper producer, and could be an important area of middle Cretaceous porphyry, epithermal, and skarn resources. The district is located about 100 km southwest of ca. 119–116 Ma intermediate intrusions in China (Wu et al., 2011).

7.3.4. Yangzte River province

The Lower to Middle Yangtze metallogenic province hosts more than 200 skarn, porphyry, and magmatic vein deposits (Fig. 23; Table 10), containing significant resources of copper, iron, gold, and

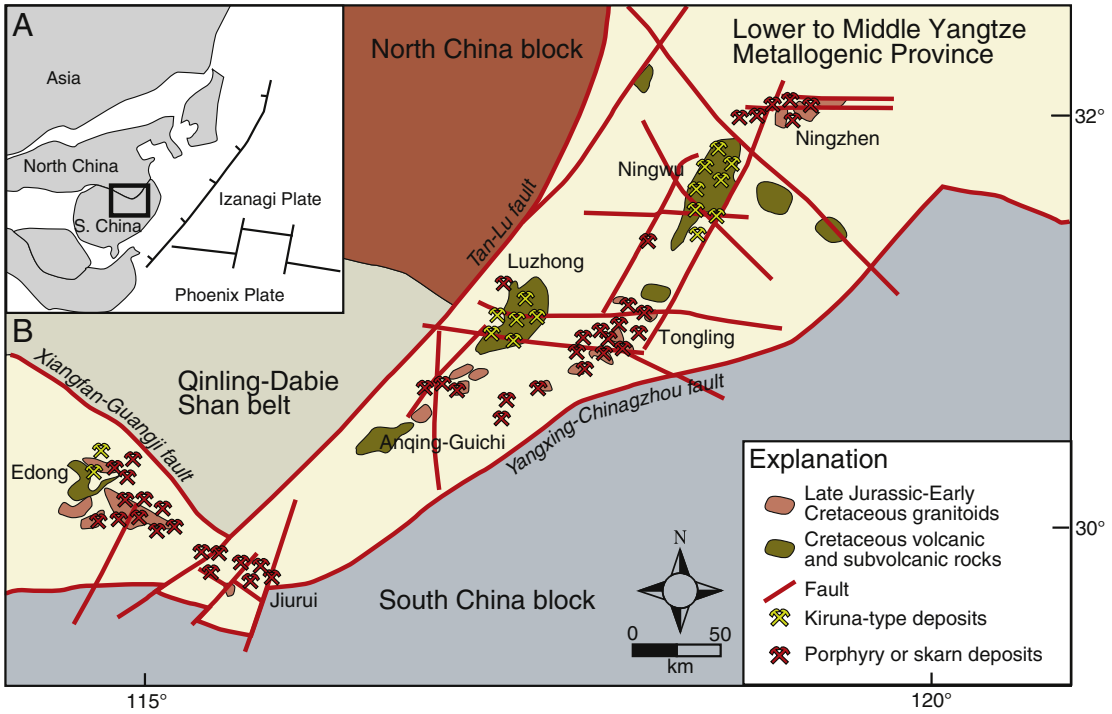

Fig. 23. Carbonate units along the northern passive margin of the South China block host a number of districts along the Middle and Lower Yangtze River with gold-bearing Fe and Cu skarn and Cu–Mo porphyry systems. (A) Most of these auriferous ores formed between ca. 148 and 135 Ma, subsequent to the North China block–South China block collision and perhaps during the onset of circum-Pacific oblique subduction. (B) Present-day configuration of the Middle and Lower Yangtze Metallogenic Province.
Adapted from Pan and Dong (1999) and Mao et al. (2011b).

Please cite this article as: Goldfarb, R.J., et al., Phanerozoic continental growth and gold metallogeny of Asia, Gondwana Research (2013), http://dx.doi.org/10.1016/j.gr.2013.03.002

molybdenum (Pan and Dong, 1999; Zhao et al., 1999; Mao et al., 2011b). The deposits are located within the Lower Yangtze region, and are defined by a 300-km-long northeast trend in Anhui Province, and, in the Middle Yangtze region, a 150-km-long northwest trend predominantly in Hubei and northern Jiangxi Provinces. Thick sequences of Neoproterozoic to Early Triassic marine sediments onlap the Yangtze block Paleoproterozoic basement in this area. They are covered by younger continental clastic rocks.

The region was deformed into the Northern Yangtze fold-and-thrust belt beginning during the late Middle Triassic collision of the Yangtze block with the Qinling–Dabie Shan belt that had formed along the southern margin of the North China block. The geometrically complex northeast to northwest bend in the Yangtze River Valley and the associated regional structures are poorly understood; the features likely relate to a complex Late Triassic–Early Cretaceous clockwise rotation of the region due to the northward indentation of the South China block into the Qinling–Dabie Shan belt (Wang et al., 2003). This resulted in the left-lateral slip developed on the Tan–Lu fault system, perhaps a reactivated Triassic thrust between terranes in the Dabieshan, which today forms the boundary between the Yangtze cover rocks hosting the NE-trending ore districts and the Dabie Shan and North China block to the north. The eastern part to the Qinling–Dabie Shan orogen was offset left-laterally 500 km during ca. 200–125 Ma rotation and is now part of the Jiaodong Peninsula (Wang et al., 2003).

Seven mining districts, from northeast to southwest, include Ningzhen, Ningwu, Tongling, Luzhong, Anqing–Guichi, Jiurui, and Edong (Fig. 23; Pan and Dong, 1999; Mao et al., 2011b). The dominant deposits are Cu–Mo–Au-bearing porphyry deposits and associated gold-rich Cu and/or Fe skarns that are located in uplifted areas in all districts, except in Ningwu and Luzong (see below). In many cases the two deposit types are mined together, but it appears that the bulk of the gold resource is in garnet- and pyroxene-rich copper skarns that developed in carbonates of all ages (Chang, 2005). Estimates of total production and resources for the province range from 625 t Au (Chen et al., 2007b) to >800 t Au (Zhou et al., 2002), including at least seven skarns each containing 30–100 t Au. The relatively small (<5 km), ore-related I-type intrusions exhibit a wide range in compositions, but the most important are granodiorites and diorites, which are often shallow porphyries. Ore-related igneous rocks have been suggested to have been emplaced along the Changjiang or Yangtze River regional brittle fault zone, an ancient deep crustal shear that was reactivated many times within the basement rocks and overlying sediments, and follows the Yangtze River. Intersections of E–W faults with the main northeast and northwest trends of the ore belts have been considered as important locations for porphyry emplacement (Mao et al., 2011b).

The causative intrusions for the gold-bearing skarns have been extensively dated, with most ages concentrated between 148 and 135 Ma (e.g., Mao et al., 2006, 2011b; Yang et al., 2011). Magnetite–apatite Kiruna-type deposits, which lack gold enrichment and are associated with mantle-generated shoshonitic porphyry intrusions and related volcanic rocks, are dominant in the basins of the Luzong and Ningwu districts (e.g., Hou et al., 2009a). They formed between 135 and 123 Ma (Mao et al., 2006, 2011b; Yang et al., 2011), and their specific relationship to the slightly older gold-rich magmatic deposits in the other five districts is unclear.

Whereas there is general agreement about the earliest Cretaceous age of most Yangtze province gold deposits, mechanisms to explain the age and localization remain controversial. Although the geochemistry of the felsic intrusions is characteristic of most adakites, it is not consistent with typical slab melts. This led Wang et al. (2007) to suggest delamination of the lower eclogitic crust along the northern edge of the subducting Yangtze block and then ascension of resulting melts through the subcontinental lithospheric mantle, with some contamination, leading to the metalliferous magmas. Zircon studies by Yang and Zhang (2012) suggest that lower crustal Neoproterozoic sediments or subducted ocean crust was an important component in the magmas. Deng et al. (2011) related the magmatism to mantle magmatism. A ridge-subduction model between the spreading Izanagi and Pacific plates (Fig. 23) has also been proposed (e.g., Ling et al., 2009), but it is unproven as to whether such a broad magmatic metallogenic event can be produced in such a manner and the variable northeast and northwest trends of the ore districts would seem to cause difficulties with such a model. No matter what the specific model for development of one of the world's premier gold-bearing skarn provinces, two critical broad controls must include: (1) the voluminous amount of favorably reactive carbonate units along the leading edge of the Yangtze block, which were intruded by the mass of volatile-rich plutons, and (2) the timing of a major change from South China–North China block convergence to oblique westward subduction and the associated left-slip regime of the circum-Pacific continental margin (e.g., Ratschbacher et al., 2000). The post-subduction, strike-slip setting of the Early Cretaceous Yangtze River porphyry/skarn systems thus may be similar to that described for the giant Pebble and related middle Cretaceous porphyry gold deposits along the northwestern margin of the North American Cordillera (Goldfarb et al., 2013).

7.3.5. Southeast China Fold Belt

The Southeast China Fold Belt (SCFB) of Hong et al. (1998) and Pirajno and Bagas (2002) represents an area of late Mesozoic basin and range deformation and magmatism to the southeast of the Jiangnan fold belt (Fig. 24; e.g., Wang and Shu, 2012). The tectonism was associated with the change, also noted above for the Yangtze River province, from north–south convergence between the North and South China blocks in the Triassic to a NW–SE Pacific plate subduction below the South China block in the Jurassic. About two-thirds of the Cathaysian block of southeastern China subsequently now exposes felsic igneous rocks and large coeval basins that reflect areas of back-arc extension above the subducting slab (Wang and Shu, 2012), perhaps due to initiation of some type of slab rollback in the Middle Jurassic (e.g., Li and Li, 2007; He and Xu, 2012). Felsic granitoids range in age from ca. 176–90 Ma, with associated bimodal volcanic rocks being widespread during the first 25 m.y. of the magmatism and at ca. 110–90 Ma. Country rocks for the magmatism and for late Mesozoic sedimentation were the Proterozoic to Devonian metamorphic rocks of the Cathaysian block and overlying Devonian–Triassic carbonates. Pirajno and Bagas (2002) noted that uplifted blocks of Precambrian basement material host orogenic gold deposits in the SCFB, whereas the Coastal Volcanic belt to the southeast of the uplift contains important epithermal ores associated with Mesozoic volcanic rocks (Fig. 24, Table 11). The Yuao–Macao or Zhenge–Dapu fault zone, a steeply SE-dipping normal fault (Wang and Shu, 2012), separates these two zones with the generally different gold-deposit types.

The Hetai–Gaocun group of orogenic gold deposits is located along the 480-km-long, NE-striking Hepu–Hetai dextral shear zone, one of a series of well-defined crustal-scale discontinuities in the uplifted part of the Cathaysia block (Zhang and Cai, 2009). Mineralization is associated with steeply dipping, NE-trending mylonitic shears within Neoproterozoic mica schists, feldspar–mica schists, and micaceous gneisses (Pirajno and Bagas, 2002). Although gold mineralization at the Gaocun deposit is hosted entirely within strongly ductily deformed mylonite, textural evidence suggests that some gold deposition occurred within a more brittle regime post-dating ductile deformation (Zhang et al., 2001; Pirajno and Bagas, 2002). Hydrothermal zircons have reported ages of ca. 152 Ma (U–Pb SHRIMP: Zhai et al., 2006), which could indicate that the brittle regime may be the result of stress relaxation during uplift of the basement (e.g., the Chencai–Suichang uplift of Pirajno and Bagas, 2002). Alternatively, dextral motion along the ore-hosting shear zone is dated at ca. 195 Ma ($^{40}Ar/^{39}Ar$ muscovite: Zhang and Cai, 2009), which is consistent with the ductile style of some mineralization and a possible Early Jurassic gold event (e.g., Wang et al.,

Please cite this article as: Goldfarb, R.J., et al., Phanerozoic continental growth and gold metallogeny of Asia, Gondwana Research (2013), http://dx.doi.org/10.1016/j.gr.2013.03.002

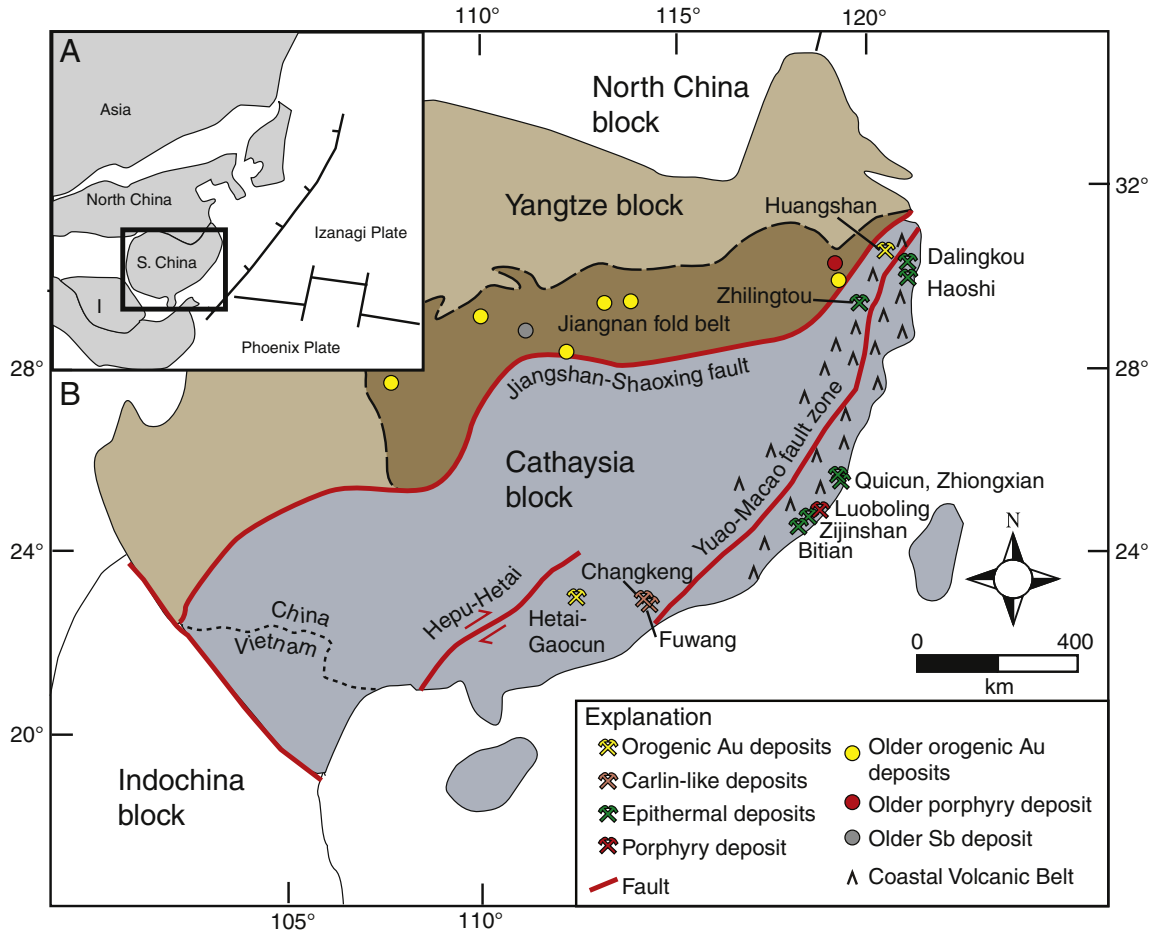

Fig. 24. Circum-Pacific tectonism along the margin of the Cathaysia block in late Mesozoic led to widespread magmatism and deformation in SE China. Uplifted Precambrian basement hosts orogenic gold deposits in the Hetai district and Huangshan district, but these may pre-date the tectonism. Development of the Coastal Volcanic Belt in the late Mesozoic is associated with formation of numerous epithermal deposits and gold-bearing porphyry ores at ca. 105–90 Ma (e.g., Zijinshan, Luoboling, Qiucun, Haoshi). (A) Configuration during the Cretaceous. (B) Geology and coordination are in the present location.
Adapted from Pirajno and Bagas (2002), Zhang and Cai (2009), and Liu et al. (2012).

1997). Zhang and Cai (2009) related the major dextral movement to the earlier described South China–Indochina suturing.

Approximately 1000 km to the northeast of Hetai, the Huangshan group of gold deposits (Pirajno and Bagas, 2002), similarly orogenic in character, are hosted within the uplifted Neoproterozoic Huangshan Complex, which is an intermediate to mafic–ultramafic layered intrusion. The highly sheared complex is located along the Jiangshan–Shaoxing fault system suturing the Yangtze craton and Cathaysia blocks. The 397±34.5 Ma date reported for the Huangshan deposit (Rb–Sr quartz: Chen and Xu, 1997) itself is broadly synchronous with collision of the Yangtze and Cathaysia blocks and earlier described Wuyi–Yunkai orogenesis. Thus, we would argue that the Huangshan goldfield may be a part of the early Paleozoic Jiangnan gold belt and unrelated to the other younger gold deposits in the SCFB.

Widespread late Mesozoic Yanshanian magmatism, particularly defining the Coastal Volcanic belt, is widespread from Guangdong in the southwest to Shanghai in the northeast. Significant extension at shallow levels is evident in the development of at least 17 large-scale volcano-tectonic depressions (Zhou et al., 2006) and calderas along the belt and associated syenitic bodies, which were produced via mixing between depleted asthenospheric melts and subduction-related enriched mantle melts (e.g., He and Xu, 2012). Several of these have been the focus for significant Au, Au–Ag, and Au–Cu mineralization in the porphyry–epithermal spectrum of ores, particularly concentrated between ca. 105 and 90 Ma.

The best developed examples of this are within the Zijinshan mining district in southern Fujian, which hosts the 104.5–102.5 Ma Zijinshan Au–Cu (>350 t Au) high-sulfidation epithermal deposit (Zhang et al., 2003a), 105 Ma Luoboling Cu–Mo porphyry (Liang et al., 2012), and 95 Ma Bitian (Zhang et al., 2003a) low-sulfidation epithermal Au deposit. The Zijinshan district is localized within the Mesozoic Shangchang–Bitian volcanic basin, bounded by NE-striking extensional faults. Mineralization at Zijinshan, defining the largest gold resource defined at a single deposit in China, is hosted by a series of NW-striking hydrothermal breccias that intrude a 125 Ma dacitic dome (So et al., 1998). We speculate that this northwest structural control is fundamental to both the location and distribution of mineralization at Zijinshan and reflects reactivation of deep crustal transfer structures, a common secondary control on arc-related porphyry and epithermal deposits (e.g., Richards, 2003; Cooke and Hollings, 2005).

The Daiyunshan–Shiniushan caldera, located along the coast of central Fujian province is approximately 80-km-wide and hosts dominantly epithermal Ag and Au–Ag deposits (Zhu, 2000), such as the Qiucun and Zhiongxian deposits (Fig. 24), that are localized along the caldera rim. The high-sulfidation ores are hosted by 92.5 Ma dacitic porphyries (Chen et al., 2008).

To the north, the coastal parts of northern Zhejiang province define a 300 km by 300 km region of epithermal gold deposits that extends to both sides of the Zhenge–Dapu fault zone. Many of these gold deposits contain significant volumes of base metals and manganese

Table 11
Mesozoic gold deposits of the Southeast China fold belt.

Deposit	Location in Fig. 1	Latitude	Longitude	Country	Tectonic location	Deposit type	Age (Ma)	Geochron. methodology	Geochron. reference
Gaocun	273	23.3	112.3	China	Yunkai uplift	Orogenic	152	U–Pb	Zhai et al. (2006)
							195	Ar–Ar	Zhang and Cai (2009)
Huangshan	274	29.57	120.31	China	Huangshan Complex	Orogenic	397	Rb–Sr (quartz)	Chen and Xu (1997)
Zijinshan	275	25.18	116.41	China	Coastal volcanic belt	Epithermal	105–102		Zhang et al. (2003a)
Luoboling	276	25.2	116.43	China	Coastal volcanic belt	Porphyry	105	Re–Os (molybdenite)	Liang et al. (2012)
Bitian	277	25.17	116.37	China	Coastal volcanic belt	Epithermal	95		
Qiucun	278	29.56	120.26	China	Chencai–Suichang uplift	Epithermal			
Zhiongxian	279	25.61	117.87	China	Chencai–Suichang uplift	Epithermal			
Zhilingtou	280	28.62	119.43	China	Chencai–Suichang uplift	Epithermal	141–82		Mao et al. (2007)
Haoshi	281	29.36	120.74	China	Coastal volcanic belt	Epithermal	104	Rb–Sr (fluid inclusions)	Chen and Xu (1997)
Dalingkou	282	29.13	120.92	China	Coastal volcanic belt	Epithermal			
Changkeng	283	22.98	112.84	China	Shanshui basin	Carlin?			

carbonates, and might best be classified as intermediate-sulfidation deposits; Zhilingtou is the largest of the deposits (Mao et al., 2007). A broad spread of dates exists for Zhilingtou from Late Triassic to latest Cretaceous. We favor an ore-forming age similar to the 104 Ma Haoshi (Chen and Xu, 1997) and Dalingkou intermediate-sulfidation deposits located 150 km to the northeast.

The southernmost and probably youngest significant gold deposit in the SCFB is the Changkeng deposit, about 45 km southwest of Guangzhou. It is adjacent to the latest Cretaceous–earliest Tertiary (68.6 ± 6 Ma: Rb–Sr; 64.3 Ma: Ar–Ar) Fuwang silver deposit (Liang et al., 2007). A great deal of debate is associated with these deposits, as they share many characteristics with Carlin-type deposits, such as an association with carbonate rocks and jasperoids, and a mineral assemblage with stibnite, realgar, orpiment, and pyrite. Unlike the older epithermal deposits described above in the SCFB, young igneous rocks are not associated with mineralization hosted in late Paleozoic sedimentary rocks.

8. Cenozoic gold

8.1. Himalayan orogen

The Tibetan–Himalayan orogen is part of the Alpine–Himalayan Belt, a continuous belt of Mesozoic and Cenozoic deformation marking the closure of the Tethys oceans. The orogen is a direct consequence of collision between the Indian and Asian continents beginning in the early Cenozoic, subsequent to Meso-Tethys accretionary orogenesis on the southwestern edge of the amalgamated North China, South China, and Tarim cratonic blocks. This orogenesis is built on a collage of at least three earlier terranes accreted onto southern Eurasia since the early Paleozoic (e.g., Allégre et al., 1984; Sengor and Natal'in, 1996; Yin and Nie, 1996). From north to south these are the Songpan–Ganzi, Qiangtang, and Lhasa terranes (Fig. 25).

The Jinsha fault zone is the Middle to Late Triassic suture between the Qiangtang terrane and the western side of the South China block, the Songpan–Ganzi turbidites, and the southern side of the Tarim block. The Bangong suture defines the Late Jurassic–Early Cretaceous docking between the Qiangtang and Lhasa terranes (e.g., Dewey et al., 1988; Yin and Harrison, 2000). These Paleozoic–Mesozoic terranes were fragments of Gondwana that rifted into the Paleo-Tethys Ocean in Late Devonian (Zhu et al., 2011). Closing of the Tethyan Ocean between the Himalayan Tethyan assemblages and the outboard Lhasa terrane of the growing Asian continent, along the Indus–Yarlong suture, followed at ca. 65–50 Ma. The Jinsha fault system can be traced into southeastern Asia, along the boundary area between the Yangtze craton and Indochina, where it links up with the continental-scale Red River fault zone and Ailaoshan shear zone. This system of major, continental-scale strike-slip faults underwent almost 1000 km of left-lateral movement, which was associated with metamorphism and upward extrusion of mid-crustal rocks (i.e., Xuelong Shan, Diancang Shan, Ailao Shan, Day Nui Con Voi) along the faults in southwestern China and adjacent Vietnam, in the middle Tertiary (Tapponnier et al., 1990; Burchfiel et al., 2008).

Although not widely developed as large resources, numerous orogenic gold and gold-bearing porphyry provinces are located within the Himalayan orogen (Fig. 25; Table 12; Hou et al., 2007; Hou and Cook, 2009). The most economically significant of the orogenic gold provinces is the Ailaoshan gold belt, which is located along strands of the Ailaoshan shear zone. The belt is dominated by three districts (Laowangzhai, Jinchang, and Daping–Chang'an) that occur over an area of about 400 by 60 km. Ores are hosted in mylonitized Neoproterozoic basement rocks and Paleozoic units (e.g., Ailao Shan metamorphic complex), which represent one of the extruded mid-crustal zones along the left-lateral shear zone (e.g., Burchfiel et al., 2008); some of the deposits are associated with mafic and ultramafic rocks that are localized along the faults. Sun et al. (2009) report an $^{40}Ar/^{39}Ar$ date of ca. 34 Ma for hydrothermal sericite at the Daping deposit, one of the largest gold deposits recognized to date in the Himalayan orogen (>150 t Au). This date is essentially identical to the ca. 32 Ma age for initiation of left-lateral ductile motion along the Ailaoshan shear zone (Searle et al., 2010) and indicates a correlation of gold formation with the metamorphism, deformation, and crustal extrusion along the zone.

Other deposits along the same Ailaoshan–Jinsha system, also likely best classified as orogenic, include Gala and a number of deposits (e.g., Shihuangchang, Zhacun, Bijiashan) south of the city of Dali (Hou et al., 2007) as well as the Daduhe group. Gala is hosted by sheared mafic rocks associated with ophiolitic assemblages developed foreland to the Yidun arc emplacement and along the suture. The Shihuangchang–Zhacun–Bijiashan group of deposits consists of veins cutting Triassic(?) metasedimentary rocks in the Lanping basin. The deposits in the basin are located a few tens of kilometers southwest of the Diancang Shan metamorphic complex and could have formed during the associated metamorphic and extrusion event, in a manner similar to the deposits of the Ailao Shan complex. The Lanping basin was one of a number of pull-apart basins near the Ailaoshan–Jinsha fault system that opened by ca. 23 Ma (Hou et al., 2007), and extensional offset of the deposits from a location originally nearer the suture and core complex should be examined. The exposed Late Triassic(?) host rocks reported at some deposits (e.g., Hou et al., 2007) suggest an association with the extrusive doming, as the Jurassic to Miocene sediments in the region (e.g., Fig. 2 in Searle et al., 2010) apparently are missing.

Similar to the Ailoashan–Jinsha deposits, the 25–21 Ma Daduhe group of deposits (Li et al., 2004b, 2007c) is localized along the regional Xiangshuihe fault zone, another structural zone of mainly strike-slip faulting. It is broadly parallel to, but east of the Jinsha suture. Mineralization is hosted within mylonitic shear zones transgressing migmatitic diorite, plagioclase–amphibolite, and granite of the Mesoproterozoic Kangding Complex.

Please cite this article as: Goldfarb, R.J., et al., Phanerozoic continental growth and gold metallogeny of Asia, Gondwana Research (2013), http://dx.doi.org/10.1016/j.gr.2013.03.002

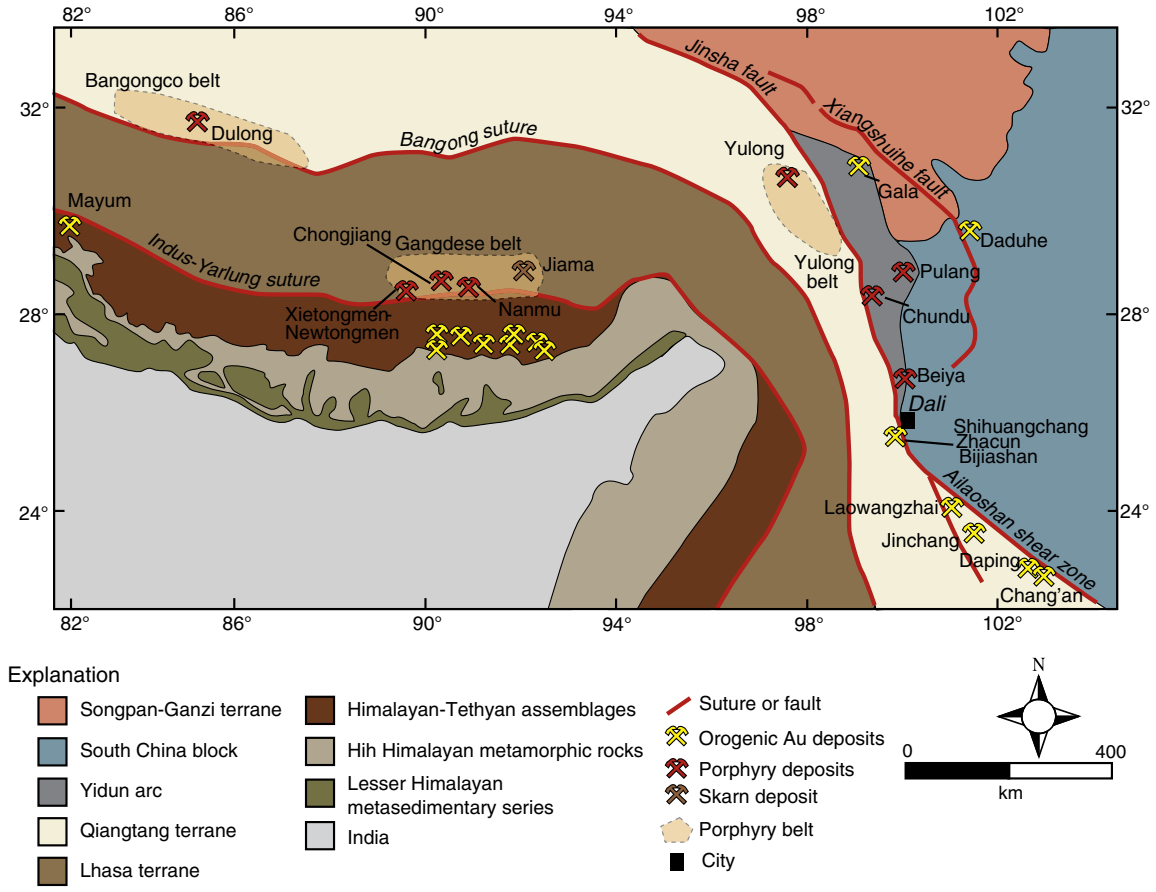

Fig. 25. Cenozoic lode gold deposits in Asia are mainly concentrated in the Tibetan–Himalayan orogen, developed on the southwestern side of the earlier amalgamated North China, South China, and Tarim blocks. The most important orogenic gold deposits are those of the Ailaoshan gold belt (e.g., Laowangzhai, Daping) formed at ca. 34 Ma in Yunnan during a period of escape tectonics. Large Cu–Au porphyry deposits include those of the 18–13 Ma Cu–Au Gangdese extension-related belt in central Tibet; the 40–36 Ma Yulong Cu–Mo porphyry belt in eastern Tibet, also extension related, lacks significant gold resources. Older Cretaceous subduction-related Cu–Mo–Au porphyry deposits define the Bangongco belt in western Tibet.
Adapted from Yin and Harrison (2000), Hou et al. (2007), and Hou and Cook (2009).

Cenozoic orogenic gold deposits, consistently enriched in antimony, also cluster in two areas within the Tethyan rocks on the leading edge of the Indian continent to the south of the Lhasa terrane and Indus–Yarlung suture. To the west, the Mayum deposit occurs within thrust faults in Neoproterozoic–Cambrian schists and limestone near the suture (Jiang et al., 2009). An argon step-heating profile for

Table 12
Cenozoic gold of the Himalayan orogen.

Deposit	Location in Fig. 1	Latitude	Longitude	Country	Tectonic location	Deposit type	Age (Ma)	Geochron. methodology	Geochron. reference
Laowangzhai district	284	23.9	101.45	China	Ailaoshan gold belt	Orogenic			
Jinchang district	285	23.5	101.75	China	Ailaoshan gold belt	Orogenic			
Daping–Chang'an district	286	22.9	103.08	China	Ailaoshan gold belt	Orogenic	34	Ar–Ar (sericite)	Sun et al. (2009)
Gala	287	31.83	99.25	China	Ailaoshan gold belt	Orogenic			
Shihuangchang	288	25.32	100.15	China	Ailaoshan gold belt	Orogenic			
Zhacun	289	25.12	100.17	China	Ailaoshan gold belt	Orogenic			
Bijiashan	290	25.00	100.00	China	Ailaoshan gold belt	Orogenic			
Daduhe group	291	30.23	102.11	China	Himalayan Orogen	Orogenic	25–21	K–Ar (sericite)	Li et al. (2004b, 2007c)
Mayum	292	30.48	82.46	China	Himalayan Orogen	Orogenic	59	Ar–Ar (sericite)	Jiang et al. (2009)
Yulong belt	293	31.36	98.57	China	Himalayan Orogen	Porphyry	40–36	Re–Os (molybdenite), U–Pb (host zircon)	Hou et al. (2006)
Beiya	294	26.25	100.17	China	Himalayan Orogen	Porphyry/Skarn	37–34	U–Pb (zircon)	Lu et al. (2010)
Nanmu (Gangdese belt)	295	29.45	90.8	China	Gangdese arc	Skarn	14.8	Re–Os (molybdenite)	Li et al. (2004a); Qu et al. (2007)
Chongjiang (Gangdese belt)	296	29.6	90.05	China	Gangdese arc	Skarn	14	Re–Os (molybdenite)	Li et al. (2004a); Qu et al. (2007)
Jiama (Gangdese belt)	297	29.73	91.96	China	Gangdese arc	Skarn	15.4	Re–Os (molybdenite)	Li et al. (2005)
Xietongmen–Newtongmen	298	29.38	88.42	China	Gangdese arc	Porphyry	174	Re–Os (molybdenite)	Tafti et al. (2009)
Dulong (Bangongco belt)	299	32.82	83.41	China	Qiangtang terrane	Porphyry	115	Ar–Ar (hydrothermal kspar)	Li et al. (2011a)
Chundu	300	27.94	99.89	China	Zhongdian–Yidun arc	Porphyry	220	U-Pb (zircon in porphyry)	Leng et al. (2012)
Pulang	301	29.04	99.99	China	Songpan–Garze basin	Porphyry	213	Re–Os (molybdenite)	Li et al. (2011b)

hydrothermal sericite is rather poor, and suggests, at best, an age for gold formation of ≥59 Ma. This is reasonable given that such timing would be consistent with the collisional deformation in the region. A relatively large tonnage (>80 t Au) reported by Jiang et al. (2009) is likely not justified (Sun Xiaoming, oral commun., 2009). To the east, more than 50 gold deposits and prospects in Triassic through Cenozoic sedimentary rocks are scattered within an area dominated by widespread mid-Miocene extrusive domes, which are intruded by Miocene leucogranites (Yang et al., 2009b). A few of these gold occurrences are within the domes, likely developed during extension in the period between 21 to 12 Ma and 8 to 4 Ma, although most of the occurrences are located on local north–south or east–west normal faults that are not within the domes (e.g., Fig. 1 in Yang et al., 2009b).

Three main belts of porphyry deposits in the Himalayan orogeny contain gold resources of variable significance: Gangdese, Yulong, and Bangongco. The ca. 18–13 Ma Miocene Gangdese Cu–Au porphyry belt is located south of Lhasa, in the Lhasa terrane, and is associated with a 1500-km-long belt of 26–8 Ma potassic to ultrapotassic syenites and granites emplaced during widespread extension (e.g., Williams et al., 2004; Hou et al., 2009b). Medium- and large-scale, gold-bearing copper skarn deposits are distributed along the belt, and are typically localized along N–S striking arc-normal faults and associated with the potassic intrusions. Occurrences include the 14.8 Ma Nanmu and 14.0 Ma Chongjiang (Li et al., 2004a; Qu et al., 2007) Cu–Mo porphyries, which contain minor gold resources, but the 15.4 Ma Jiama Cu–Mo–Au–Pb–Zn skarn and porphyry deposits have an estimated 150 t Au (Jingwen Mao, written commun., 2013).

In eastern Tibet, the 41–36 Ma Yulong Cu–Mo alkaline porphyry belt is associated with extension, small pull-apart basins, and post-collisional strike-slip along the Jinsha regional fault system (e.g., Yin and Harrison, 2000). These deposits stretch for more than 300 km in a NNW trend within the eastern part to the Qiangtang (Indochina) terrane (Hou et al., 2003), to the west of the Jinsha suture. They are composed of more than 20 monzonite to monzogranite porphyry bodies characterized by high K_2O contents and REE patterns suggestive of shoshonitic affinities. The largest deposit, Yulong, is associated with 41 Ma post-collisional adakitic monzogranite porphyries emplaced into Triassic sediments and then exhumed during ca. 33–30 Ma Tibetan uplift (Li et al., 2012b). Luddington et al. (2010) report almost 300 t Au in the Yulong deposit, but this seems to be an order of magnitude greater than any other estimate.

To the south in western Yunnan, and also along the Jinsha fault system, but to the east, ca. 37–33 Ma alkaline granite porphyries, with associated skarns and polymetallic veins, are also present. Although generally not gold-rich systems, the Bengge area within the South China block is a notable exception with significant gold (Xu et al., 2007; Lu et al., 2010). The Beiya deposit (Fig. 25), dominated by Cu–Au porphyry-style mineralization and auriferous Fe skarns, is the largest of these with likely >150 t Au.

Older and more classic subduction-related adakitic-related Cu–Mo–Au porphyry deposits formed prior to final Tertiary collision; these are subduction-related ore systems developed over 100 m.y., and before final ocean closure and continent collision. Within the above-mentioned Gangdese belt, Jiang et al. (2012) noted Jurassic to early Tertiary diorite and quartz monzonite associated with ca. 90 Ma Cu–Au–Mo porphyry mineralization in the same area that was later affected by the Miocene potassic event. The older Gangdese subduction-related arc also hosts the 174 Ma Xietongmen (or Xiongcun)–Newtongmen Cu–Au–Mo porphyry deposits (Tafti et al., 2009), which company data suggest contain >200 t Au. The Bangongco copper belt is located just north of the Bangong suture in the western Qiangtang terrane. A major gold resource is associated with the 115 Ma Dulong porphyry deposit (Li et al., 2011a), another significant subduction-related granodiorite porphyry body in the belt.

Possibly the oldest significant gold-bearing system formed during initial subduction related to the early Cenozoic Himalayan collisional orogen is the 213 Ma Pulang porphyry copper deposit (Li et al., 2011b). It is located in the Songpan–Garze turbidite basin terrane, broadly adjacent to the Yulong belt. The associated Zhongdian–Yidun volcanic arc was initiated as a result of westward subduction of the Garze–Litang oceanic basin during Indosinian time (Hou, 1991; Mo et al., 1993), producing distinctive western and eastern porphyry belts, separated by the Shudu ophiolite belt. The western belt hosts several small porphyries including Chundu, and is dominated by ca. 249 Ma andesitic volcaniclastic rocks and flows (Zeng et al., 2003, 2004), in addition to coeval dioritic intrusions. Although compositionally similar, the eastern porphyry belt that hosts the Pulang deposit is considered younger as constrained by dating of the Langdu quartz monzonite porphyry at 217 Ma (Zeng et al., 2003).

8.2. Cenozoic Kuril Island–Kamchatka volcanic arc

The Neogene to Quaternary Kuril Island–Kamchatka volcanic arc (Fig. 1) extends along the northwestern coast of the Pacific Ocean, to the east of the mainly Late Cretaceous Okhotsk–Chukotka volcanic arc. This Cenozoic arc is a modern volcanic belt forming the Kamchatka peninsula and Kuril Islands. It was built upon mainly middle Mesozoic accreted sedimentary and volcanic terranes of the Koryak–Kamchtaka fold and thrust belt. These were the most outboard accreted terranes of eastern Russia, were added to the margin between Late Cretaceous and late Eocene (Sokolov, 2010), and host numerous young epithermal gold orebodies (Table 13).

The Aginskoye, Rodnikovoye, and Asachinskoye low-sulfidation epithermal deposits are hosted in subduction-related paleovolcanic centers of the central (Aginskoye) and eastern (Rodnikovoye, Asachinskoye) parts of the Kamchatka peninsula (Nokleberg et al., 2005; Khanchuk, 2006; Goryachev et al., 2010). In central Kamchatka, epithermal deposits are dated at 22–14 Ma (Ozernovskoye) and 12–5 Ma (Aginskoye); in eastern Kamchatka, reported ages are 5–2.5 Ma (Asachinskoye, Baran'evskoye) and <2.5 Ma (Rodnikovoye, Mutnovskoye) (Khanchuk, 2006). Two large N- and NNE-trending normal faults, in central and eastern Kamchatka, respectively, regionally controlled the epithermal systems (Okrugin and Zelensky, 2004). At a more local scale, the ores are located in NW-trending secondary faults. Late Miocene and Pliocene basalt–andesite–rhyolite volcanic rocks and co-magmatic gabbro and diorite intrusions host the Rodnikovoye and Asachinskoye epithermal deposits. The Aginskoye deposit is located in Miocene andesitic basalt flows and tuffs.

Table 13
Cenozoic gold deposits of northeastern Russia.

Deposit	Location in Fig. 1	Latitude	Longitude	Country	Tectonic location	Deposit type	Age (Ma)	Geochron. methodology	Geochron. reference
Aginskoye	302	55.52	157.87	Russia	Kamchatka	Epithermal	12–5	K–Ar	Khanchuk (2006)
Rodnikovoye	303	52.83	158.27	Russia	Kamchatka	Epithermal	1.1–0.9	K–Ar	Khanchuk (2006)
Asachinskoye	304	52.13	157.9	Russia	Kamchatka	Epithermal	5–2.5	K–Ar	Khanchuk (2006)
Ozernovskoye	305	57.58	160.78	Russia	Kamchatka	Epithermal	22–14	K–Ar	Khanchuk (2006)
Baran'evskoye	306	55.1	158.22	Russia	Kamchatka	Epithermal	3.9–2.4	K–Ar	Khanchuk (2006)
Mutnovskoye	307	52.73	158.4	Russia	Kamchatka	Epithermal	3.3–1.3	K–Ar	Khanchuk (2006)
Prasolovskoye	308	44.32	146.08	Russia	Kuril Island	Epithermal	Neogene		Kovalenker and Plotinskaya (2005)

Please cite this article as: Goldfarb, R.J., et al., Phanerozoic continental growth and gold metallogeny of Asia, Gondwana Research (2013), http://dx.doi.org/10.1016/j.gr.2013.03.002

The Kuril Islands metallogenic belt includes the Prasolovskoye deposit with a young age of Au–Ag mineralization (Khanchuk, 2006). This belt, in addition to several Au–Ag epithermal deposits, also contains several relatively small volcanic sulfur, Kuroko massive sulfide, base metal vein, Mo porphyry, and Sn-bearing vein deposits (Nokleberg et al., 2005). The Prasolovskoye deposit is suggested to have formed in two stages, an early Sn–Au event is related to a late Miocene intrusion, and late Te-rich Ag–Au ores are related to a small Pliocene granitoid (Nokleberg et al., 2005).

9. Summary

The gold endowment of mainland Asia arguably defines the most significant gold resource in the world today. China has been the world's leading gold producer since 2007, vast gold resources remain undeveloped throughout eastern Russia, and central Asia is the location of a number of the world's largest gold deposits. The bulk of the endowment is hosted in orogenic gold belts associated with major structures and in magmatic auriferous porphyry–skarn–epithermal belts. The deposits reflect ca. 800–150 Ma Paleothys to Mesotethys tectonism, dominated by (1) the rifting of large Precambrian blocks from Rodinia and Gondwana, (2) terrane accretion along the margins of the blocks throughout the Paleozoic, (3) closure of numerous small oceans between the blocks, and (4) late Paleozoic–early Mesozoic amalgamation of the blocks and their marginal terranes into the present day Asian landmass. During the past 150 m.y., shifting trajectories of circum-Pacific plate subduction has lead to a massive gold endowment along the eastern margin of the new continental mass. Final collision of India with Asia was responsible for additional Cenozoic gold resources in many areas of the Himalayan orogen.

Accretionary orogens along the present-day southern margins to the Siberia craton were responsible for formation of orogenic gold deposits at ca. 750 Ma in the Yenisei Ridge province, which hosts Russia's largest lode gold deposit at Olympiada; at ca. 550–450 Ma in the East Sayan region; and at either ca. 450 Ma or 350 Ma in the Patom fold-and-thrust belt, which includes a significant unmined resource at the Sukhoi Log deposit. Accretionary events along the margins of the Kazakhstan microcontinent or Kipchuk superterrane were associated with relatively inboard formation of the orogenic gold deposits of the Charsk belt at ca. 450 Ma. At about the same time until ca. 350 Ma, gold-rich porphyry Cu ± Mo deposits, such as Bozshakol, Nurkazghan, and Taldy Bulak, developed in preserved oceanic and continental margin magmatic arcs. Gold-bearing polymetallic VMS ores were formed in some of the adjacent oceanic arcs and in rifted margins of the Kazakhstan microcontinent throughout the early and middle Paleozoic. Large Devonian VMS deposits of the Rudny Altai define the closing Ob–Zaisan basin and collisional zone between the Kazakhstan and Siberia blocks.

Subduction/accretion events along the present-day southwestern margin of the North China block are represented by the Qilian Shan and West Qinling orogenic belts. Terranes of the Qilian Shan were in place by the end of the Devonian and those of the West Qinling reflect 300 m.y. of accretion prior to Late Triassic collision of the South China block and closure of the Mianlue Ocean basin. Orogenic gold deposits formed in both belts mainly in the Late Triassic. Those along the Mianlue suture have been termed Carlin-like by some workers, but most more closely resemble orogenic gold deposits.

Early Paleozoic deformation within the South China block, along the ancient boundary representative of the colliding Cathaysia and Yangtze blocks, defines the location of the Jiangnan Au–Sb–W belt that includes mainly orogenic gold deposits formed along the margin of Gondwana. Subsequent to Devonian rifting of the South China block from Gondwana and during its collision with the North China block a couple of hundred million years later, Late Triassic deformation within the Youjiang basin, in a region now to the east of the Red River shear zone, led to widespread development of Au, Sb, and Hg lodes and defines the one possible Carlin-like gold province in Asia. Devonian to Triassic accretion of the Indochina, East Malaya, West Burma, West Sumatra, and Sibumasu blocks, also all rifted from Gondwana, to the seaward margin of the South China block formed much of the Late Paleozoic–Early Mesozoic gold endowment of southeastern Asia. Important subduction-related Fe–Cu–Au skarns and low-sulfidation epithermal deposits formed in Laos at ca. 300 Ma and in Laos and Thailand at ca. 250 Ma. Orogenic gold deposits, now in Malaysia and Myanmar, formed along major faults on both sides of the Sibumasu block during Late Permian and Triassic.

Closure of the ocean basins between the China blocks and the amalgamated Siberia–Kazakhstan blocks led to formation of much of the present-day Asia continent land mass and to development of much of the enormous Carboniferous through Jurassic gold endowment of the Central Asian Orogenic Belt (CAOB). As the Tarim–Karakum block approached Kazakhstan and the Turkestan basin was closed, ca. 380–315 Ma gold-rich copper porphyries (e.g., Oyu Tolgoi, Almalyk, Kharmagtai), copper porphyries with minor gold (e.g., Kounrad), and less significant epithermal gold deposits formed in oceanic and continental arcs along the margin of both blocks from what is now Uzbekistan through southern Mongolia. Subsequent strike-slip events along the southernmost seaward terrane boundaries of the orogen were associated with formation of some of the world's giant orogenic gold deposits (e.g., Muruntau, Kumtor, Zarmitan) that formed between ca. 300 and 280 Ma; in addition, similar fault motion along the more inboard suture of the closed Ob–Zaisan basin was associated with the 310–280 Ma formation of the Kalba orogenic gold belt.

The Mongol–Okhotsk basin, on the southeastern side of the CAOB, closed diachronously from Permian to Late Jurassic as the North China block was sutured to the Siberia craton. This was associated with formation of important orogenic gold deposits in the Early Jurassic in the Khangai–Khentii basin (e.g., Boroo), Middle and Late Jurassic in central Transbaikal (e.g., Darasun), and Early Cretaceous in eastern Transbaikal. Slightly later extension along the closed basin suture in central and eastern Transbaikal was associated with formation of gold-bearing epithermal, porphyry and skarn deposits, such as the Balei and Kuranakh low-sulfidation epithermal deposits in central Transbaikal.

The shift to Circum-Pacific tectonism led to major Early Cretaceous gold-forming events throughout eastern Asia. The collision of the Kolyma–Omolon microcontinent with Siberia and associated Late Jurassic–Early Cretaceous Verkhoyansk–Kolyma orogeny, led to widespread early Early Cretaceous orogenic gold formation within deformed sediments along the main suture zones (e.g., Natalka, Nezhdaninskoe). To the south, giant early Early Cretaceous orogenic gold provinces developed in uplifted Precambrian basement above regions of delaminated subcontinental mantle lithosphere within the North China block in northeastern China/adjacent North Korea, the Jiaodong Peninsula, and the Qinling Mountains. The deposits were ultimately related to major changes in plate kinematics in the Pacific basin and seismic events along the continental-scale Tan–Lu fault system. The deformational history along the northern margin of the South China block during the shift to an active Pacific continental margin is poorly understood, and thus the ultimate controls on the generation of the major gold-rich belt of porphyry and skarn deposits along the Lower and Middle Yangtze River at ca. 148–135 Ma remains unclear. Extension in late Early Cretaceous along the Pacific margin was associated with epithermal gold formation in the Okhotsk–Chukotka volcanic belt along the eastern Russia margin, in northeastern China, and in the Southeast China foldbelt.

The youngest gold resources of mainland Asia are located within the Himalayan belts of southwest China. Relatively small Tertiary orogenic gold deposits are located along major strike-slip fault systems in Tibet and Yunnan. Gold-rich 18–13 Ma porphyry copper deposits in the Gangdese belt of the Lhasa terrane and 40–36 Ma porphyry

Please cite this article as: Goldfarb, R.J., et al., Phanerozoic continental growth and gold metallogeny of Asia, Gondwana Research (2013), http://dx.doi.org/10.1016/j.gr.2013.03.002

Cu–Mo deposits in the Yulong belt of eastern Tibet formed during extensional episodes within the orogen. Older subduction-related porphyry deposits formed in the pre-Cenozoic, before final collision of India, and include the ca. 115 Ma gold-rich copper porphyries of the Bangongco belt in northwestern Tibet.

Acknowledgments

We thank Santosh, *Gondwana Research* chief editor, for the encouragement to conduct and the invitation to publish this synthesis, as well as for his patience in awaiting the final product. Nikolay Goryachev thanks the FEB RAS for support of this research (grant 12-II-CO-08-30) and IGCP-592. Rich Goldfarb thanks IGCP-592 and IGCP-600 for support and introducing him to some areas described in this manuscript, as well as the field support of the geological investigation work project of China Geological Survey (project no. 1212011121090), the National Natural Science Foundation of China (project no. 41230311), and the National Science and Technology Support Program (project no. 2011BAB04B09). We thank Jingwen Mao, Erin Marsh, Doug Kirwin, and Wenjiao Xiao for their thorough reviews of this paper and Janet Slate for final comments.

References

Abramov, B.N., 2006. Formation conditions of deposits of the gold–quartz formation in the Muya zone (North Transbaikal region). Doklady Earth Sciences 411, 1171–1173.
Abzalov, M., 2007. Zarmitan granitoid-hosted gold deposit, Tian Shan belt, Uzbekistan. Economic Geology 102, 519–532.
Akinin, V.V., Miller, E.L., 2011. Evolution of calc-alkaline magmas of the Okhotsk–Chukotka Volcanic Belt. Petrology 19, 237–277.
Akinin, V.V., Voroshin, S.V., Gelman, M.L., Leonova, V.V., 2003. SHRIMP data of metamorphic xenolites from lamprophyre on gold deposit Degdekan to history of reworking of continental crust in Ayan–Yurak anticlinorium (Yana–Kolyma folded system). Geodynamics, Magmatism and Mineralogy of Continental Margins of North Pacific. Proceedings of XII Annual Meeting of North-East Branch of All-Russian Mineralogy Society, 2. North-East Interdisciplinary Science Research Institute, Far East Branch, Russian Academy of Sciences, Magadan, pp. 142–146 (in Russian).
Akinin, V.V., Prokopiev, A.V., Toro, J., Miller, E.L., Wooden, J., Goryachev, N.A., Alshevsky, A.V., Bakharev, A.G., Trunilina, V.A., 2009. U–Pb SHRIMP age of granitoids from the main batholith belt (North East Asia). Doklady Earth Sciences 426, 605–610.
Allégre, C.J., Courtillot, V., Tapponnier, A., Hirn, A., Mattauer, M., Coulon, C., Jaeger, J.J., Achache, J., Schärer, U., Marcoux, J., Burg, J.P., Girardeau, J., Armijo, R., Gariépy, C., Göpel, C., Tindong, L., Xuchang, X., Chenfa, C., Guangqin, L., Baoyu, L., Jiwen, T., Naiwen, W., Guoming, C., Tonglin, H., Xibin, W., Wanming, D., Huaibin, S., Yougong, C., Ji, Z., Hongrong, Q., Peisheng, B., Songchan, W., Bixiang, W., Yaoxiu, Z., Xu, R., 1984. Structure and evolution of the Himalaya–Tibet orogenic belt. Nature 307, 17–22.
Allen, M.B., Sengor, A.M.C., Natal'in, B.A., 1995. Junggarm Turfan, and Alakol basins as Late Permian to Early Triassic extensional structures in a sinistral shear zone in the Altaid orogenic collage, Central Asia. Journal of the Geological Society of London 152, 327–338.
Arce-Burgoa, O.R., Goldfarb, R.J., 2009. Metallogeny of Bolivia. Society of Economic Geologists Newsletter 79 (1), 8–15.
Ariffin, K.S., Hewson, N.J., 2007. Gold-related sulfide mineralization and ore genesis of the Penjom gold deposit, Pahang, Malaysia. Resource Geology 57, 149–169.
Badarch, G., Cunningham, W.D., Windley, B.F., 2002. A new terrane subdivision for Mongolia: implications for the Phanerozoic crustal growth of Central Asia. Journal of Asian Earth Sciences 21, 87–110.
World Bank, 2006. Final Report For Economic Geology—FR-2: Sector Plan for Sustainable Development of the Mining Sector in the Lao PDR (97 pp.).
Banks, M.J., Murfitt, R.H., Quynh, N.-N., Hai, L.-V., 2004. Gold exploration of the Phuoc Son–Tam Ky suture, central Vietnam: a case study. PACRIM 2004, Conference Proceedings.Australasian Institute of Mining and Metallurgy 94–107.
Barber, A.J., Crow, M.J., 2009. The structure of Sumatra and its implications for the tectonic assembly of Southeast Asia and the destruction of Paleotethys. Island Arc 18, 3–20.
Berzina, A.N., Stein, H.J., Zimmerman, A., Sotnikov, V.I., 2003. Re–Os ages for molybdenite from porphyry and greisen Mo–W deposits of Southern Siberia (Russia) preserve metallogenic record. In: Eliopoulos, D., et al. (Ed.), Mineral exploration and sustainable development. Millpress, Rotterdam, pp. 231–234.
Berzon, R.O., Bryzgalov, I.A., Konyshev, V.O., Meshcherina, T.V., Nekrasova, A.N., 1999. Geological setting, mineral composition, and formation conditions of the Kyuchus gold–mercury deposit (Sakha, Russia). Geology of Ore Depoits 41, 440–459.
Borisenko, A.S., Zhmodik, S.M., Naumov, E.A., Spiridonov, A.M., Berzina, A.N., 2010. The age interval of East Transbaikalia gold mineralization formation: native gold–typomorphism of mineral assemblages, origin of deposits, problem of applied investigations. Abstracts of All-Russian Conference Moscow, Institute of Ore Geology, Petrography, Mineralogy, and Geochemistry, Russian Academy of Sciences, March 29–31, 2010, pp. 82–83 (in Russian).
Borisenko, A.S., Spiridonov, A.M., Izokh, A.E., Prokopiev, A.V., Lebedev, V.I., Gas'kov, I.V., Zorina, L.D., Kostin, A.V., Naumov, E.A., Tretiakova, I.G., 2012. High-productivity stage of mafic and granitoid magmatism of Northern Asia, resources potential estimation, scientific reasons of large deposits (Cu–Ni–Pt, Co, Au, Ag, and rare metal) exploration criteria. Minerageny Problems of Russia, Special Issue of Vestnik ONZ RAS, pp. 227–252 (in Russian).
Bortnikov, N.S., Prokof'ev, V.Y., Razdolina, N.V., 1996. Origin of the Charmitan gold–quartz deposit (Uzbekistan). Geology of Ore Deposits 38, 208–226.
Bortnikov, N.S., Bryzgalov, I.A., Krivitskaya, N.N., Prokof'ev, V.Y., Vikentieva, O.V., 2004. The Maiskoe multimegastage disseminated gold-sulfide deposit (Chukotka, Russia): mineralogy, fluid inclusions, stable isotopes (O and S), history, and conditions of formation. Geology of Ore Deposits 46, 409–440.
Bortnikov, N.S., Gamynin, G.N., Vikent'eva, O.V., Prokof'ev, V.Yu., Prokop'ev, A.V., 2010. The Sarylakh and Sentachan gold–antimony deposits, Sakha–Yakutia: a case of combined mesothermal gold–quartz and epithermal stibnite ores. Geology of Ore Deposits 52, 339–372.
Buchko, I.V., Sorokin, A.A., 2005. Late Paleozoic magmatic arc on the northern periphery of the Argun terrane and associated gold mineralization. Russian Geology and Geophysics 46, 617–624.
Buchko, I.V., Sorokin, A.A., Ponomarchuk, V.A., Travin, A.V., 2010. Age and geodynamic setting of the formation of the Dess gold–silver deposit (North Stanovoi Metallogenic Zone, southeastern fringes of the North Asian craton). Doklady Earth Sciences 435, 1560–1563.
Buchko, I.V., Sorokin, A.A., Ponomarchuk, V.A., Travin, A.V., 2011. The age of metasomatites of the gold ore Malomyr deposit. Abstracts of the Geology and Mining Conference of the II International Geology and Mining Forum on Gold of the North Pacific Rim.Far East Branch, Russian Academy of Sciences, Magadan 67–68.
Bulgatov, A.N., Gordienko, I.V., 1999. Terrains of the Baikal Mountain Range and the location of gold deposits. Geology of Ore Deposits 41, 204–213.
Burchfiel, B.C., Chen, L., Wang, E., Swanson, E., 2008. Preliminary investigations into the complexities of the Ailao Shan and Day Nui Con Voi shear zones of SE Yunnan and Vietnam. In: Burchfiel, B.C., Wang, E. (Eds.), Investigations into the Tectonics of the Tibetan Plateau: Geological Society of America Special Paper, 444, pp. 45–58.
Bykadorov, V.A., Bush, V.A., Fedorenko, O.A., Filippova, I.B., Miletenko, N.V., Puckkov, V.N., Smirnov, A.V., Uzhkenov, B.S., Volozh, Y.A., 2003. Ordovician–Permian palaeogeography of central Eurasia: development of Palaeozoic petroleum-bearing basins. Journal of Petroleum Geology 26, 325–350.
Carter, A., Clift, P.D., 2008. Was the Indosinian orogeny a Triassic mountain building or a thermotectonic reactivation event? Comptes Rendus Geoscience 340, 83–93.
Cawood, P.A., Johnson, M.R.W., Nemchin, A.A., 2007. Early Palaeozoic orogenesis along the Indian margin of Gondwana: tectonic response to Gondwana assembly. Earth and Planetary Science Letters 255, 70–84.
Chang, Z.-S., 2005. World skarn deposits: China. In: Meinert, L.D., Dipple, G.P., Nicolescu, S. (Eds.), Supplement to World Skarn Deposits: Electronic Appendix, 100th Anniversary of Economic Geology (9 pp.).
Chang, K.-H., Zhao, X.-X., 2012. North and South China suturing in the east end: what happened in Korean Peninsula? Gondwana Research 22, 493–506.
Chao, Y., 1988. Occurrence variation and mechanical property evolution of the vein-bearing faults in Xiaoqinling area and its relationship with gold-bearing veins. Symposium on Geology of Gold Deposits. Geological Publishing House, Beijing, pp. 114–122 (in Chinese).
Charvet, J., Shu, L.-S., Faure, M., Choulet, F., Wang, B., Lu, H.-F., Le Breton, N., 2010. Structural development of the lower Paleozoic belt of South China: genesis of an intracontinental orogen. Journal of Asian Earth Sciences 39, 309–330.
Chen, H., Xu, B., 1997. Isotope tracing and prospecting assessment of gold–silver deposits in Zhejiang province. Acta Geologica Sinica 71, 293–304 (in Chinese).
Chen, F.-W., Li, H.-Q., Cai, H., Liu, H.-Q., 1999. The origin of the Jinwozi gold deposit in eastern Xinjiang: evidence from isotope geochronology. Geology Review 45, 247–254 (in Chinese with English abstract).
Chen, Y.-J., Pirajno, F., Sui, Y.-H., 2004. Isotope geochemistry of the Tieluping silver deposit, Henan, China: a case study of orogenic silver deposits and related tectonic setting. Mineralium Deposita 39, 560–575.
Chen, Y.-J., Pirajno, F., Qi, J.-P., 2005. Origin of gold metallogeny and sources of ore-forming fluids, Jiaodong Province, eastern China. International Geology Review 47, 530–549.
Chen, M.-H., Mao, J.-W., Qu, W.-J., Wu, L.-L., Uttley, P.J., Norman, T., Zheng, J.-M., Qin, Y.-H., 2007a. Re–Os dating of arsenian pyrites from the Lannigou gold deposit, Zhenfeng, Guizhou Province, and its geological significances. Geological Review 53, 371–382 (in Chinese with English abstract).
Chen, Y.-J., Chen, H.-Y., Zaw, K., Pirajno, F., Zhang, Z.-J., 2007b. Geodynamic setting and tectonic model of skarn gold deposits in China: an overview. Ore Geology Reviews 31, 139–169.
Chen, C.-H., Lee, C.-Y., Lu, H.-Y., Hsieh, P.-S., 2008. Generation of Late Cretaceous silicic rocks in SE China: age, major element and numerical simulation constraints. Journal of Asian Earth Sciences 31, 479–498.
Chen, X.-H., Chen, Z.-G., Han, S.-Q., Yang, Y., 2012. Late Paleozoic tectonics, magmatism and metallogenesis and Late Mesozoic exhumation of Balkhash–west Junggar metallogenic belt in central Asia. 34th International Geological Congress, Brisbane, Australia, p. 54 (Abstract 1051).
Chernyshev, I.V., Bortnikov, N.S., Chugaev, A.V., Gamyanin, G.N., Bakharev, A.G., 2011. Metal sources of the large Nezhdaninsky orogenic gold deposit, Yakutia, Russia-results from high-precision MC-ICP-MS analysis of lead isotopic composition supplemented by data on strontium isotopes. Geology of Ore Deposits 53, 353–373.

Please cite this article as: Goldfarb, R.J., et al., Phanerozoic continental growth and gold metallogeny of Asia, Gondwana Research (2013), http://dx.doi.org/10.1016/j.gr.2013.03.002

Choi, K.-S., 2011. The mining industry of North Korea. The Korean Journal of Defense Analysis 23, 211–230.

Choi, S.-G., Kwon, S.-T., Ree, J.-H., So, C.-S., Pak, S.-J., 2005a. Origin of Mesozoic gold mineralization in South Korea. The Island Arc 14, 102–114.

Choi, S.-G., Ryu, I.-C., Pak, S.-J., Wee, S.-M., Kim, C.-S., Park, M.-E., 2005b. Cretaceous epithermal gold–silver mineralization and geodynamic environment, Korea. Ore Geology Reviews 26, 115–135.

Chugaev, A.V., Chernyshov, I.V., Safonov, Y.G., Saroyan, M.R., 2010. Lead isotopic characteristics of sulfides from large gold deposits of the Baikal–Patom Highland (Russia): evidence from high-precision MC–ICP-MS isotopic analysis of lead. Doklady Earth Sciences 434, 1366–1369.

Circosta, G., 2011. Gold (and copper) exploration and mining potential of the Loei–Phetchabun volcanic belt. International Conference on Geology, Geotechnology and Mineral Resources of Indochina (Geoindo 2011), Khon Kaen, Thailand, pp. 1–2.

Cline, J.S., Hofstra, A.H., Muntean, J.L., Tosdal, R.M., Hickey, K.A., 2005. Carlin type gold deposits in Nevada: critical geologic characteristics and viable models. Economic Geology 100th Anniversary Volume. 451–484.

Cluer, J.K., Kotlyar, B., Gantsetseg, O., Togtokh, D., Wood, G., Ullrich, T., 2005. Geology of the Boroo gold deposit, northern Mongolia. In: Seltmann, R., Gerel, O., Kirwin, D.J. (Eds.), Geodynamics and Metallogeny of Mongolia With a Special Emphasis on Copper and Gold Deposits. : IAGOD Guidebook Series, vol. 11. CERCAMS (Centre for Russian and Central EurAsian Mineral Sudies), Natural History Museum, London, United Kingdom, pp. 105–117.

Cocks, L.R.M., Torvsik, T.H., 2007. Siberia, the wandering northern terrane, and its changing geography through the Paleozoic. Earth-Science Reviews 82, 29–74.

Cole, A., Wilkinson, J.J., Halls, C., Serenko, T.J., 2000. Geological characteristics, tectonic setting and preliminary investigations of the Jilau gold–quartz vein deposit, Tajikistan. Mineralium Deposita 35, 600–618.

Cooke, D.R., Hollings, P., 2005. Giant porphyry deposits: characteristics, distribution, and tectonic controls. Economic Geology 100, 801–818.

Cromie, P.W., 2010. Geological setting, geochemistry, and genesis of the Sepon gold and copper deposits, Laos. Unpub. PhD thesis, U. of Tasmania.

Cromie, P.W., Manini, A.J., Zaw, K., 2004. Geological setting and characteristics of the Au and Cu deposits in the Sepon Mineral District, Lao PDR. In: Muhling, J., Goldfarb, R., Vielreicher, N., Bierlein, F., Stumpfl, E., Groves, D.I., Kenworthy, S. (Eds.), SEG 2004, Predictive Mineral Discovery Under Cover, Extended Abstracts. Publication, 33. Centre for Global Metallogeny, The University of Western Australia, p. 411.

Crow, M., Zaw, K., 2011. Metalliferous minerals. In: Ridd, M.F., Barber, A.J., Crow, M.J. (Eds.), The Geology of Thailand. The Geological Society of London, Bath, UK, pp. 459–492.

Damdinov, B.B., Mironov, A.G., Borovikov, A.A., Guntypov, B.B., Karmanov, N.S., Borisenko, A.S., Garmaev, B.L., 2007. Composition and conditions of formation of gold-telluride mineralization in the Tissa–Sarkhoi gold-bearing province (East Sayan). Russian Geology and Geophysics 48, 643–655.

Daoudene, Y., Gapais, D., Ledru, P., Cocherie, A., Hocquet, S., Donskaya, T.V., 2009. The Ereendavaa Range (north-eastern Mongolia): an additional argument for Mesozoic extension throughout eastern Asia. International Journal of Earth Sciences 98, 1381–1393.

De Boisgrollier, T., Petit, C., Fournier, M., Leturmy, P., Ringenbach, J.C., San'kov, V.A., Anisimova, S.A., Kovalenko, S.N., 2009. Palaeozoic orogeneses around the Siberian craton: structure and evolution of the Patom belt and foredeep. Tectonics 28, TC1005. http://dx.doi.org/10.1029/2007TC002210 (18 pp.).

De Jong, K., Xiao, W.-J., Windley, B.F., Masago, H., Lo, C.-H., 2006. Ordovician $^{40}Ar/^{39}Ar$ phengite ages from the blueschist-facies Ondor Sum subduction–accretion complex (Inner Mongolia) and implications for the early Paleozoic history of continental blocks in China and adjacent areas. American Journal of Science 306, 799–845.

Delville, N., Arnaud, N., Montel, J.-M., Roger, F., Brunnel, M., Tapponnier, P., Sobet, E., 2001. Paleozoic to Cenozoic deformation along the Altyn Tagh fault in the Altun Shan massif area, eastern Qilian Shan, northeastern Tibet. Geological Society of America Memoir 194, 269–292.

Deng, J., Wang, Q.-F., Xiao, C.-H., Yang, L.-Q., Liu, H., Gong, Q.-J., Zhang, J., 2011. Tectonic–magmatic–metallogenic system, Tongling ore cluster region, Anhui Province, China. International Geology Review 53, 449–476.

Dewey, J.F., Shackleton, R.M., Chang, C., Sun, Y., 1988. The tectonic evolution of the Tibetan Plateau. Philosophical Transactions of the Royal Society of London. Series A 327, 379–413.

Ding, R.-F., Wang, J.-B., Zhao, L.-S., Ma, Z.-M., Zhang, J.-H., 2004. Dating of fluid geochemistry of the Sarekoubu gold deposit in Altay, Xinjiang, China. Acta Geologica Sinica 78, 392–395.

Distler, V.V., Yudovskaya, M.A., Mitrofanov, G.L., Prokof'ev, V.Y., Lishnevskii, E.N., 2005. Geology, composition, and genesis of the Sukhoi Log noble metals deposit, Russia. Ore Geology Reviews 24, 7–44.

Djenchuraeva, R.D., Borisov, F.I., Pak, N.T., Malyukova, N.N., 2008. Metallogeny and geodynamics of the Aktiuz–Boordu mining district, northern Tien Shan, Kyrgyzstan. Journal of Asian Earth Sciences 32, 280–299.

Dong, Y.-P., Zhang, G.-W., Neubauer, F., Liu, X.-M., Genser, J., Hauzenberger, C., 2011. Tectonic evolution of the Qinling orogen, China: review and synthesis. Journal of Asian Earth Sciences 41, 213–237.

Donskaya, T.V., Windley, B.F., Mazukabzov, A.M., Kroner, A., Sklyarov, E.V., Gladkochub, D.P., Ponomarchuk, V.A., Badarch, G., Reichow, M.K., Hegner, E., 2008. Age and evolution of late Mesozoic metamorphic core complexes in southern Siberia and northern Mongolia. Journal of the Geological Society of London 165, 405–421.

Du, Z., Wu, G., 1998. Tectonic Dynamics and Tectono-metallogenic Dynamics of Gold Deposits in Western Qinling. Geological Publishing House, Beijing (145 pp. (in Chinese with English abstract)).

Du, S.-J., Qu, X., Zhang, Y., Cheng, S.-L., Lu, H., Wu, Q., Xu, X., 2010. Geochronology and tectonic setting of the intrusive bodies and associated porphyry copper deposits in the Hersai area, eastern Junggar. Acta Petrologica Sinica 26, 2981–2996.

Dzung, D.-H., 1988. Gold deposits of Viet Nam. United Nations Economic and Social Commission for Asia and the Pacific, Epithermal Gold in Asia and the Pacific, 6 204–226.

Ecomomos, R.C., Paterson, S.R., Said, L.O., Ducea, M.N., Anderson, J.L., Padilla, A.J., 2012. Gobi–Tianshan connections: field observations and isotopes from an early Permian arc complex in southern Mongolia. Geological Society of America Bulletin 124, 1688–1701.

Emmons, W.H., 1937. Gold Deposits of the World. McGraw-Hill Book Company, New York 353–361.

Enkelmann, E., Weislogel, A., Ratschbacher, L., Eide, E., Renno, A., Wooden, J., 2007. How was the Triassic Songpan–Ganzi basin filled? A provenance study. Tectonics 26, TC4007. http://dx.doi.org/10.1029/2006TC002078 (24 pp.).

Enos, P., Lehrmann, D.J., Wei, J.-Y., Yu, Y.-Y., Xiao, J.-F., Chalkin, D.H., Minzoni, M., Berry, A.K., Montgomery, P., 2006. Triassic evolution of the Yangtze Platform in Guizhou Province, People's Republic of China. Geological Society of America Special Paper 417 (105 pp.).

Eremin, R.A., Voroshin, S.V., Sidorov, V.A., Shakhtyrov, V.G., Pristavko, V.A., 1994. Geology and genesis of the Natalka gold deposit, Northeast Russia. International Geology Review 36, 1113–1138.

Fan, D.-L., Zhang, T., Ye, J., 2004. The Xikuangshan Sb deposit hosted by Upper Devonian black shale series, Hunan, China. Ore Geology Reviews 24, 121–133.

Fan, H.-R., Hu, F.-F., Yang, J.-H., Zhai, M.-G., 2007. Fluid evolution and large-scale gold metallogeny during Mesozoic tectonic transition in the Jiaodong Peninsula, eastern China. Geological Society London, Special Publication 280, 303–316.

Fan, H.-R., Hu, F.-F., Wilde, S.A., Yang, K.-F., Jin, C.-W., 2011. The Qiyugou gold-bearing breccia pipes, Xiong'ershan region, central China: fluid-inclusion and stable-isotope evidence for an origin from magmatic fluids. International Geology Review 53, 25–45.

Filippova, I.B., Bush, V.A., Didenko, A.N., 2001. Middle Paleozoic subduction belts: the leading factor in the formation of the Central Asian fold-and-thrust belt. Russian Journal of Earth Sciences 3, 405–426.

Findlay, R.H., Trinh, P.T., 1997. The structural setting of the Song Ma region, Vietnam and the Indochina–South China plate boundary problem. Gondwana Research 1, 11–33.

Flindell, P., 2003. Avocet Mining: exploration and development across Central and South East Asia. SMEDGE-AIG Symposium on Asian Update on Mineral Exploration and Development.Australian Institute of Geoscientists.

Franklin, J.M., Gibson, H.L., Jonasson, I.R., Galley, A.G., 2005. Volcanogenic massive sulfide deposits. Economic Geology 100th Anniversary Volume. 523–560.

Gallagher, D., 1963. Gold: mineral resources of Korea, volume III. Mining Branch Industry and Mining Division USOM/Korea in Cooperation With Geologic Survey, Republic of Korea, Volumes IIIA and IIIB.

Gamyanin, G.N., Bortnikov, N.S., Alpatov, V.V., 2000. The Nezhdaninskoye Gold Ore Deposit: A Unique Deposit of the Northeastern Russia. GEOS Publishing, Moscow (230 pp. (in Russian)).

Gamyanin, G.N., Goryachev, N.A., Bakharev, A.G., Kolesnichenko, P.P., Zaitsev, A.I., Diman, E.N., Berdnikov, N.V., 2003. Conditions of Origin and Evolution of Granitoid Gold-ore-magmatic Systems in Mesozoides of North East Asia. NEISRI FEB RAS, Magadan (196 pp. (in Russian)).

Gamyanin, G.N., Goryachev, N.A., Savva, N.E., 2007. Ore-magmatic systems and metallogeny of gold and silver in Northeastern Asia. Russian Geology and Geophysics 48, 913–922.

Garwin, S., Hall, R., Watanabe, Y., 2005. Tectonic setting, geology, and gold and copper mineralization in Cenozoic magmatic arcs of Southeast Asia and the West Pacific. Economic Geology 100th Anniversary Volume. 891–930.

Genkin, A.D., Wagner, F.E., Krylova, T.L., Tsepin, A.I., 2002. Gold-bearing arsenopyrite and its formation condition at the Olympiada and Veduga gold deposits (Yenisei Range, Siberia). Geology of Ore Deposits 44, 52–68.

Gertner, I., Tishin, P., Vrublevskii, V., Sazonovg, A., Zvyagina, E., Kolmakov, Y., 2011. Neoproterozoic alkaline igneous rocks, carbonatites and gold deposits of the Yenisei Ridge, central Siberia: evidence of mantle plume activity and late collision shear tectonics associated with orogenic gold minerlization. Resource Geology 61, 316–343.

Goldfarb, R.J., Miller, L.D., Leach, D.L., Snee, L.W., 1997. Gold deposits in metamorphic rocks in Alaska. In: Goldfarb, R.J., Miller, L.D. (Eds.), Mineral Deposits of Alaska: Economic Geology Monograph, 9, pp. 151–190.

Goldfarb, R.J., Groves, D.I., Gardoll, S., 2001. Orogenic gold and geologic time: a synthesis. Ore Geology Reviews 18, 1–75.

Goldfarb, R.J., Mao, J.W., Hart, C., Wang, D.H., Anderson, E., Wang, Z.L., 2003. Tectonic and metallogenic evolution of the Altay Shan, northern Xinjiang Uygur Autonomous Region, northwestern China. In: Mao, J., Goldfarb, R.J., Seltmann, R., Wang, D., Xiao, W., Hart, C. (Eds.), Tectonic Evolution and Metallogeny of the Chinese Altay and Tianshan: IAGOD Guidebook Series, vol. 10. CERCAMS (Centre for Russian and Central EurAsian Mineral Sudies), Natural History Museum, London, United Kingdom, pp. 17–30.

Goldfarb, R.J., Ayuso, R., Miller, M.L., Ebert, S., Marsh, E.E., Petsel, S.A., Miller, L.D., Bradley, D., Johnson, C., McClelland, W., 2004. The Late Cretaceous Donlin Creek gold deposit, southwestern Alaska: geological and geochemical controls on epizonal ore formation. Economic Geology 99, 643–672.

Goldfarb, R.J., Baker, T., Dube, B., Groves, D.I., Hart, C.J.R., Robert, F., Gosselin, P., 2005. Distribution, character, and genesis of gold deposits in metamorphic terranes. Economic Geology 100th Anniversary Volume. 407–450.

Goldfarb, R.J., Hart, C.J.R., Davis, G., Groves, D.I., 2007. East Asian gold: deciphering the anomaly of Phanerozoic gold in Precambrian cratons. Economic Geology 102, 341–346.

Goldfarb, R.J., Hart, C.J.R., Marsh, E.E., 2008. Orogenic gold and evolution of the Cordilleran orogen. In: Spencer, J.E., Titley, S.R. (Eds.), Circum-Pacific Tectonics, Geologic Evolution, and Ore Deposits. Digest, 22. Arizona Geological Society, Tucson, pp. 311–323.

Goldfarb, R.J., Anderson, E.D., Hart, C.J.R., 2013. Tectonic setting of the Pebble and other copper-gold-molybdenum porphyry deposits within the evolving middle Cretaceous continental margin of Northwestern North America. Economic Geology 108, 405–419.

Please cite this article as: Goldfarb, R.J., et al., Phanerozoic continental growth and gold metallogeny of Asia, Gondwana Research (2013), http://dx.doi.org/10.1016/j.gr.2013.03.002

Goryachev, N.A., 1998. Geology of Mesozoic Gold Quartz Vein Belts in Northeastern Asia. NEISRI FEB RAS, Magadan (210 pp. (in Russian)).
Goryachev, N.A., 2003. Origin of Gold Quartz Vein Belts Throughout the Northern Pacific Area. NEISRI FEB RAS, Magadan (143 pp. (in Russian)).
Goryachev, N.A., 2005. The Uda–Murgal magmatic arc: geology, magmatism, metallogeny. Problems of Metallogeny of Ore Regions in North-East of Russia, Proceedings. NEISRI FEB RAS, Magadan, pp. 17–38 (in Russian).
Goryachev, N.A., 2006. Gold ore forming systems of orogenic belts. Vestnik NESC FEB RAS, 1 2–16 (in Russian).
Goryachev, N.A., 2010. Orogenic gold deposits as metallogenic indicators of folded belts origin: main problems of mineral deposit geology and metallogeny. Proceedings of XXI International Scientific Conference Dedicated 100th Anniversary Academician V.I. Smirnov, Moscow State University, 2010 January 26–28, vol. 1. MAKS Press, Moscow, pp. 81–92 (in Russian).
Goryachev, N.A., Gamyanin, G.N., 2006. Gold–bismuth (gold–rare metal) deposits of North East Russia: types, and exploration perspectives. Gold Ore Deposits of East Russia. NESC FEB RAS, Magadan, pp. 50–62 (in Russian).
Goryachev, N., Yakubchuk, A., 2008. Gold deposits of Magadan region, northeastern Russia: yesterday, today, and tomorrow. SEG Newsletter 74 (1), 9–15.
Goryachev, N.A., Vikent'eva, O.V., Bortnikov, N.S., Prokof'ev, V.Yu., Alpatov, V.A., Golub, V.V., 2008. The world class Natalka gold deposit, northeast Russia: REE patterns, fluid inclusions, stable oxygen isotopes, and formation conditions of ore. Geology of Ore Deposits 50, 362–380.
Goryachev, N.A., Volkov, A.V., Sidorov, A.A., Gamyanin, G.N., Savva, N.E., Okrugin, V.M., 2010. The epithermal Au–Ag-mineralization in volcanic belts of northeast Asia. Lithosphera 3, 36–50 (in Russian).
Goryachev, N.A., Sotskaya, O.T., Goryacheva, E.M., Mikhalitsyna, T.I., Man'shin, A.P., 2011. The first discovery of platinum group minerals in black shale gold ores of the Degdekan deposit, northeast Russia. Doklady Earth Sciences 439, 902–905.
Goryachev, N., Gvozdev, V., Vakh, A., 2012. Orogenic lode gold deposits in the southern part of the Russian Far East. 34th International Geological Congress, Brisbane, Australia (Abstract 2676).
Griffin, W.L., Zhang, A.-D., O'Reilley, S.Y., Ryan, C.G., 1998. Phanerozoic evolution of the lithosphere beneath the Sino-Korean craton. American Geophysical Union Monograph 27, 107–128.
Guo, F., Fan, W.-M., Li, C.-W., Gao, X.-F., Miao, L.-C., 2009. Early Cretaceous highly positive ε_{Nd} felsic volcanic rocks from the Hinggan Mountain, NE China: origin and implications for Phanerozoic crustal growth. International Journal of Earth Sciences 98, 1395–1411.
Han, S.-J., Sun, J.-G., Bai, L.-A., Xing, S.W., Chai, P., Zhang, Y., Yang, F., Men, L.-J., Li, Y.-X., 2013. Geology and ages of porphyry and medium- to high-sulphidation epithermal gold deposits of the continental margin of Northeast China. International Geology Review 55, 287–310.
Hart, C.J.R., Goldfarb, R.J., Qiu, Y.M., Snee, L., Miller, L.D., Miller, M.L., 2002. Gold deposits of the northern margin of the North China Craton: multiple late Paleozoic–Mesozoic mineralizing events. Mineralium Deposita 37, 326–351.
Hart, C.J.R., Mair, J.L., Goldfarb, R.J., Groves, D.I., 2004. Source and redox controls of intrusion-related ore systems, Tombstone–Tungsten belt, Yukon Territory, Canada. In: Ishiahara, S., Stephens, W.E., Harley, S.L., Arima, M., Nakajima, T. (Eds.), Fifth Hutton Symposium Volume on the Origin of Granites and Related Rocks: Geological Society of America Special Paper, 389, pp. 339–356.
He, Z.-Y., Xu, X.-S., 2012. Petrogenesis of the Late Yanshanian mantle-derived intrusions in southeastern China: response to the geodynamics of paleo-Pacific plate subduction. Chemical Geology 328, 208–221.
Heinhorst, J., Lehmann, B., Ermolov, P., Serykh, V., Zhurutin, S., 2000. Paleozoic crustal growth and metallogeny of Central Asia: evidence from magmatic–hydrothermal ore systems of Central Kazakhstan. Tectonophysics 328, 69–87.
Heubeck, C., 2001. Assembly of central Asia during the middle and late Paleozoic. In: Hendrix, M.S., Davis, G.A. (Eds.), Paleozoic and Mesozoic Evolution of Central Asia: From Continental Assembly to Intercontinental Deformation: Geological Society of America Memoir, 194, pp. 1–22.
Higgins, D.F., 1918. Geology and ore deposits of the Collbran contact of the Suan mining concession, Korea. Economic Geology 13, 1–34.
Hoa, T.T., Izokh, A.E., Polyakov, G.V., Borisenko, A.S., Anh, T.T., Balykin, P.A., Phuong, N.T., Rudnev, S.N., Van, V.V., Nien, B.A., 2008. Permo-Triassic magmatism and metallogeny of Northern Vietnam in relation to the Emeishan plume. Russian Geology and Geophysics 49, 480–491.
Holley, K., Skayman, P., Zhiwei, H., 2005. Geotechnical design for open pits at Tanjianshan, China. The South African Institute of Mining and Metallurgy, International Symposium on the Stability of Rock Slopes in Open Pit Mining and Civil Engineering, pp. 483–507.
Hong, D., Xie, X., Zhang, J., 1998. Deep structural setting of granitoids and their metallogeny in South China. Global Tectonics and Metallogeny 6, 181–186.
Hou, Z.-Q., 1991. Characteristics of tectono-magmatic evolution of Yidun island arc in Sanjiang region. Geological Collected Works of Qinghai–Tibet Plateau, 21. Geological Publishing House, Beijing 153–156 (in Chinese with English abstract).
Hou, Z.-Q., Cook, N.J., 2009. Metallogenesis of the Tibetan collisional orogen: a review and introduction to the special issue. Ore Geology Reviews 36, 2–24.
Hou, Z.-Q., Ma, H., Zaw, K., Zhang, Y., Wang, M., Wang, Z., Pan, G., Tang, R., 2003. The Himalayan Yulong porphyry copper belt: product of large-scale strike-slip faulting in eastern Tibet. Economic Geology 98, 125–145.
Hou, Z.-Q., Zeng, P., Gao, Y., Du, A., Fu, D., 2006. Himalayan Cu–Mo–Au mineralization in the eastern Indo-Asian collision zone: constraints from Re–Os dating of molybdenite. Mineralium Deposita 41, 33–45.
Hou, Z.-Q., Pan, G.-T., Mo, X.-X., Xu, Q., Hu, Y.-Z., Li, X.-Z., 2007. The Sanjiang Tethyan metallogenesis in S.W. China: tectonic setting, metallogenic epoch and deposit type. Ore Geology Reviews 31, 48–87.
Hou, T., Zhang, Z.-C., Du, Y.-S., Li, S.-T., 2009a. Geology of the Gushan iron oxide deposit associated with dioritic porphyries, eastern Yangzte craton, SE China. International Geology Review 51, 520–541.
Hou, Z.-Q., Yang, Z.-M., Qu, X.-M., Meng, X.-J., Li, Z.-Q., Beaudoin, G., Rui, Z.-Y., Gao, Y.-F., 2009b. The Miocene Gangdese porphyry copper belt generated during post-collisional extension in the Tibetan orogeny. Ore Geology Reviews 36, 25–51.
Hu, X.-W., Murao, S., Huang, X.-C., 1996. Genetic model of gold–antimony–tungsten mineralization: evidence from geology and mineralization of the Woxi deposit, Hunan, China. Bulletin of the Geological Survey of Japan 47 (11), 577–597.
Hu, R.-Z., Su, W.-C., Bi, X.-W., Tu, G.-C., Hofstra, A., 2002. Geology and geochemistry of Carlin-type gold deposits in China. Mineralium Deposita 37, 378–392.
Huang, D.-Z., Wang, X.-Y., Yang, X.-Y., Li, G.-M., Huang, S.-Q., Liu, Z., Peng, Z.-H., Qiu, R.-L., 2011. Geochemistry of gold deposits in the Zhangbaling tectonic belt, Anhui province, China. International Geology Review 53, 612–634.
Ilchik, R.P., Uttley, P.J., Corben, R., Zhang, A.-Y., Ham, A., Hodkiewicz, P., 2005. The Jinfeng gold deposits: mining the new frontier of China. Geological Society of Nevada Symposium 2005.Windows to the World, Reno, Nevada 887–898.
Ispolatov, V.O., Heizler, M.T., Norman, D.I., 2000. Geology and tectonic setting of the Solton Sary gold district, Kyrgyzstan. In: Cluer, J.K., Price, J.G., Struhsacker, E.M., Hardyman, R.F., Morris, C.L. (Eds.), Geology and Ore Deposits 2000: The Great Basin and Beyond: Geological Society of Nevada Symposium Proceedings, Reno, pp. 507–511.
Jahn, B.-M., 2004. The Central Asian Orogenic Belt and growth of the continental crust in the Phanerozoic. In: Malpas, J., Fletcher, C.J.N., Ali, J.R., Aitchison, J.C. (Eds.), Aspects of the Tectonic Evolution of China: Geological Society London Special Publication, 226, pp. 73–100.
Japan International Cooperation Agency, 1992. Report on the mineral exploration in the Uudum–Tal area Mongolian People's Republic (Phase 1). Metal Mining Agency of Japan, MPN CR, 3 92-055, 124 pp.
Jenchuraeva, R.J., 2001. Paleozoic geodynamics, magmatism, and metallogeny of the Tien Shan. In: Seltmann, R., Jenchuraeva, R.J. (Eds.), Paleozoic Geodynamics and Gold Deposits in the Kyrgyz Tien Shan: IGCP-373 Field Conference in Bishkek and the Kyrgyz Tien Shan, Excursion Guidebook, pp. 29–70.
Jenchuraeva, R.J., Pak, N.T., Usmanov, I.A., 2001. The Makmal gold deposit. In: Seltmann, R., Jenchuraeva, R.J. (Eds.), Paleozoic Geodynamics and Gold Deposits in the Kyrgyz Tien Shan: IGCP-373 Field Conference in Bishkek and the Kyrgyz Tien Shan, Excursion Guidebook, pp. 82–96.
Jeon, H.-J., Cho, M.-S., Kim, H.-C., Horie, K., Hidaka, H., 2007. Early Archean to Middle Jurassic evolution of the Korean peninsula and its correlation with Chinese cratons: SHRIMP U–Pb zircon age constraints. Journal of Geology 115, 525–539.
Jia, G.-Z., Chen, J.-R., Yang, Z.-G., Bian, H.-Y., Wang, Y.-Z., Liang, H.-J., Jin, T.-H., Li, Z.-H., 2008. Geology and genesis of the superlarge Jinchang gold deposit, NE China. Acta Geologica Sinica 82, 750–761.
Jian, P., Liu, D.-Y., Kroner, A., Windley, B.F., Shi, Y.-R., Zhang, F.-Q., Shi, G.-H., Miao, L.-C., Zhang, W., Zhang, Q., Zhang, L.-Q., Ren, J.-S., 2008. Time scale of an early to mid-Paleozoic orogenic cycle of the long-lived Central Asian Orogenic Belt, Inner Mongolia of China: implications for continental growth. Lithos 101, 233–259.
Jiang, S.-H., Nie, F.-J., Liu, Y., 2004. Gold deposits in the Beishan Mountain, northwestern China. Resource Geology 54, 325–340.
Jiang, S.-H., Nie, F.-J., Hu, P., Lai, X.-R., 2009. Mayum: an orogenic gold deposit in Tibet, China. Ore Geology Reviews 36, 160–173.
Jiang, Z.-Q., Wang, Q., Li, Z.-X., Wyman, D.A., Tang, G.-J., Jia, X.-H., Yang, Y.-H., 2012. Late Cretaceous (ca. 90 Ma) adakitic intrusive rocks in the Kelu area, Gangdese Belt (southern Tibet): slab melting and implications for Cu–Au mineralization. Journal of Asian Earth Sciences 53, 67–81.
Kamvong, T., Zaw, K., 2009. The origin and evolution of skarn-forming fluids from the Phu Lon deposit, northern Loei Fold Belt, Thailand: evidence from fluid inclusion and sulfur isotope studies. Journal of Asian Earth Sciences 34, 624–633.
Katkov, S.M., Strickland, A., Miller, E.L., Toro, J., 2007. Age of granitic intrusions of Anui–Chukotka folded system. Doklady of Earth Sciences 414, 515–518.
Kazansky, V.I., Yanovsky, V.M., 2006. The correlation of Mesozoic gold ore districts at the Sino-Korean and Aldan–Stanovoi shields. Geology of Ore Deposits 48, 51–70.
Kelty, T.A., Yin, A., Dash, B., Gehrels, G.E., Ribeiro, A.E., 2008. Detrital-zircon geochronology of Paleozoic sedimentary rocks in the Hangay–Hentey basin, north-central Mongolia: implications for the tectonic evolution of the Mongol–Okhotsk Ocean in central Asia. Tectonophysics 451, 290–311.
Kemkin, I.V., 2008. Structure of terranes in a Jurassic accretionary prism in the Sikhote–Alin–Amur area: implications for the Jurassic geodynamic history of the Asian eastern margin. Russian Geology and Geophysics 49, 759–770.
Kerrich, R., Goldfarb, R.J., Groves, D.I., Garwin, S., 2000. The geodynamics of world class gold deposits: characteristics, space–time distribution, and origins. Society of Economic Geologists Reviews 13, 501–551.
Kerrich, R., Goldfarb, R.J., Richards, J., 2005. Metallogenic provinces in an evolving geodynamic framework. Economic Geology 100th Anniversary Volume. 1097–1136.
Khain, E.V., Bibikova, E.V., Salnikova, E.B., Kroner, A., Gibsher, A.S., Didenko, A.N., Degtyarev, K.E., Fedotova, A.A., 2003. The Paleo-Asian ocean in the Neoproterozoic and early Paleozoic: new geochronologic data and paleotectonic reconstructions. Precambrian Research 122, 329–358.
Khanchuk, A.J., 2001. Pre-Neogene tectonics of the Sea-of-Japan region: a view from the Russian side. Earth Science (Chikyu Kagaku) 55, 275–291.
Khanchuk, A.J. (Ed.), 2006. Geodynamics, Magmatism and Metallogeny of the Russian East, 1. Dalnauka, Vladivostok, 572 pp. [in Russian].
Khomich, V., Vlasov, N.G., 2004. The Pokrovka epithermal gold deposit. In: Khanchuk, A.I., Gonevchuk, G.A., Seltmann, R. (Eds.), Metallogeny of the Pacific Northwest

Please cite this article as: Goldfarb, R.J., et al., Phanerozoic continental growth and gold metallogeny of Asia, Gondwana Research (2013), http://dx.doi.org/10.1016/j.gr.2013.03.002

(Russian Far East): Tectonics, Magmatism and Metallogeny of Active Continental Margins. Excursion Guidebook, Interim IAGOD Conference. Dalnauka Publishing House, Vladivostok, pp. 72–86.
Kim, E.-J., Park, M.-E., White, N.C., 2012. Skarn gold mineralization at the Geodo mine, South Korea. Economic Geology 107, 537–551.
Kirwin, D.J., Spadafora, M.J., Sennitt, C.M., 1999. High and low sulphidation epithermal gold mineralization in South Korea. Proceedings PACRIM '99. Australasian Institute of Mining and Metallurgy 469–472.
Kirwin, D.J., Forster, C.N., Kavalieris, I., Crane, D., Orssich, C., Panther, C., Garamjav, D., Munkhbat, T.O., Niislelkhuu, G., 2005a. The Oyu Tolgoi copper–gold porphyry deposits, south Gobi, Mongolia. In: Seltmann, R., Gerel, O., Kirwin, D.J. (Eds.), Geodynamics and Metallogeny of Mongolia With a Special Emphasis on Copper and Gold Deposits: IAGOD Guidebook Series, vol. 11. CERCAMS (Centre for Russian and Central EurAsian Mineral Sudies), Natural History Museum, London, United Kingdom, pp. 155–168.
Kirwin, D.J., Wilson, C.C., Turmagnai, D., Wolfe, R., 2005b. Exploration history, geology, and mineralization of the Kharmagtai gold–copper porphyry district, south Gobi region, Mongolia. In: Seltmann, R., Gerel, O., Kirwin, D.J. (Eds.), Geodynamics and Metallogeny of Mongolia With a Special Emphasis on Copper and Gold Deposits: IAGOD Guidebook Series, vol. 11. CERCAMS (Centre for Russian and Central EurAsian Mineral Sudies), Natural History Museum, London, United Kingdom, pp. 193–201.
Kochetkov, A., Gatinsky, G., Epshtein, A., Chi, C.-V., 1997. The gold–antimonite formation in southeastern Asia. Doklady Earth Sciences 355, 687–690.
Kondratieva, K.A., Anisimova, G.S., Bakharev, A.G., Travin, A.V., Prokopiev, A.V., Borisenko, A.S., 2010. Gold ore deposit Zaderzhnoye (South Verkhoyan): geologic setting, mineralogy, age. New and Non-traditional Types of Mineral Deposits of Pribaykalia and Transbaikalia, Proceedings of Conference, Ulan–Ude, ECOS, pp. 105–106 (in Russian).
Konopelko, D., Biske, G., Seltmann, R., Eklund, O., Belyatsky, B., 2007. Hercynian post-collisional A-type granites of the Kokshaal Range, Southern Tien Shan, Kyrgyzstan. Lithos 97, 140–160.
Konstantinov, M.M., Rosenblum, I.S., Struzhkov, S.F., 1993. Types of epithermal gold–silver deposits, northeastern Russia. Economic Geology 88, 1797–1801.
Konstantinov, M.M., Natalenko, V.E., Kalinin, A.I., Struzhkov, S.F., 1998. Gold–Silver Deposit Dukat. Nedra Publishing, Moscow (203 pp.).
Konstantinovsky, A.A., 2007. Structure and geodynamics of the Verkhoyansk fold-thrust belt. Geotectonics 41, 337–354.
Konstantinovsky, A.A., Lipchanskaya, L.N., 2011. Structure and sedimentary formations of the northern Yana–Kolyma fold system, Yakutia. Geotectonics 2011, 453–468.
Kotlyar, I.N., Zhulanova, I.L., Rusakova, T.B., Gagieva, A.M., 2001. Isotope Systems of Magmatic and Metamorphic Complexes of the Russian Northeast. NEISRI FEB RAS, Magadan (220 pp. (in Russian)).
Kovalenker, V.A., Plotinskaya, O.Y., 2005. Te and Se mineralogy of Ozernovskoe and Prasolovskoe epithermal gold deposits, Kuril–Kamchatka volcanic belt. Geochemistry, Mineralogy and Petrology 43, 118–123.
Krivolutskaya, N.A., 1997. Paragenetic associations of minerals and formation conditions of the Klyuchevsk gold deposit (Eastern Transbaikal Region, Russia). Geology of Ore Deposits 39, 294–310.
Kroner, A., Hegner, E., Lehmann, B., Heinhorst, J., Wingate, M.T.D., Liu, D.-Y., Ermelov, P., 2008. Palaeozoic arc magmatism in the Central Asian Orogenic Belt of Kazakhstan: SHRIMP zircon ages and whole-rock Nd isotopic systematics. Journal of Asian Earth Sciences 32, 118–130.
Kudryavtsev, Y.K., 1996. The Cu–Mo deposits of Central Kazakhstan. In: Shatov, V., Seltmann, R., Kremenetsky, A., Lehmann, B., Popov, V., Ermolov, P. (Eds.), Granite-related Ore Deposits of Central Kazakhstan and Adjacent Areas. GLAGOL Publishing House, St. Petersburg, pp. 119–144.
Kudryavtsev, Y.K., Popov, V.S., 2000. Tectonic setting of Paleozoic copper and gold deposits in the central and eastern Kazakhstan. In: Mezhelovsky, N.V., Morozov, A.F., Gusev, G.S., Popov, V.S. (Eds.), Geodynamics and Metallogeny: Theory and Implications for Applied Geology. GEOKART, Moscow, pp. 359–371.
Lamb, M.A., Badarch, G., 2001. Paleozoic sedimentary basins and volcanic arc systems of southern Mongolia: new geochemical and petrographic constraints. In: Hendrix, M.S., Davis, G.A. (Eds.), Paleozoic and Mesozoic Evolution of Central Asia: From Continental Assembly to Intercontinental Deformation: Geological Society of America Memoir, 194, pp. 117–149.
Lamb, M.A., Cox, D., 1998. New $^{40}Ar/^{39}Ar$ age data and implications for porphyry copper deposits of Mongolia. Economic Geology 93, 521–529.
Laurent-Charvet, S., Charvet, J., Monie, P., Shu, L.-S., 2003. Late Paleozoic strike-slip shear zones in eastern Central Asia (NW China): new structural and geochronological data. Tectonics 22, 1099–1101.
Laverov, N.P., Chernyshev, I.V., Chugaev, A.V., Bairova, E.D., Gol'tsman, Y.V., Distler, V.V., Yudovskaya, M.A., 2007. Formation stage of the large-scale noble metal mineralization in the Sukhoi Log deposit, east Siberia: results of isotope-geochronology study. Doklady Earth Sciences 415, 810–814.
Layer, P.W., Ivanov, V.V., Bundtzen, T.K., 1994. $^{40}Ar/^{39}Ar$ ages from ore deposits in the Okhotsk–Chukotka volcanic belt, Northeast Russia. International Conference on Arctic Margins, September 6–10, 1994. NESC RAS, Magadan, Russia, pp. 64–65 (Abstracts).
Layer, P.W., Newberry, R.J., Fujita, K., Parfenov, L., Trunilina, V., Bakharev, A., 2001. Tectonic setting of the plutonic belts of Yakutia, northeast Russia, based on $^{40}Ar/^{39}$ Ar geochronology and trace element geochemistry. Geology 29, 167–170.
Laznica, P., 1976. Porphyry copper and molybdenum deposits of the U.S.S.R. and their plate tectonic settings. Transactions of the Institution of Mining and Metallurgy 85, B14–B32.
Leng, C.-B., Zhang, X.-C., Hu, R.-Z., Wang, S.-X., Zhong, H., Wang, W.-Q., Bi, X.-W., 2012. Zircon U–Pb and molybdenite Re–Os geochronology and Sr–Nd–Pb–Hf isotopic constraints on the genesis of the Xuejiping porphyry copper deposit in Zhongdian, Northwest Yunnan, China. Journal of Asian Earth Sciences 60, 31–48.
Lepvrier, C., Faure, M., Van, V.N., Vu, T.V., Wei, L., Trong, T.T., Hoa, P.T., 2011. North-directed Triassic nappes in Northeastern Vietnam (East Bac Bo). Journal of Asian Earth Sciences 41, 56–68.
Letinov, F.A., Kotov, A.B., Salnikova, E.B., Shershakova, M.M., Shershakov, A.V., Yakovlena, S.Z., Anisimova, I.V., Fedoseenko, A.M., 2008. On the age of the Stepnyak massif and its related orebody (northern Kazakhstan). Doklady Earth Sciences 423, 1194–1196.
Levitan, G., 2008. Gold Deposits of the CIS. Xlibris Corp.(352 pp.).
Li, H.-Q., Chen, F.-W., 2004. Isotopic Geochronology of Regional Mineralization in Xinjiang, NW China. Geological Publishing House, Beijing 19–42 (in Chinese with English abstract).
Li, Z.-X., Li, X.-H., 2007. Formation of the 1300-km-wide intracontinental orogen and postorogenic magmatic province in Mesozoic South China: a flat-slab subduction model. Geology 35, 179–182.
Li, Z.-X., Powell, C. McA, 2001. An outline of the palaeogeographic evolution of the Australasian region since the beginning of the Neoproterozoic. Earth-Science Reviews 53, 237–277.
Li, H.-Q., Chen, F.-W., Cai, H., Liu, H.-Q., 1999. Study on isotopic chronology of the Mazhuangshan gold mineralization, eastern Xinjiang. Scientia Geologica Sinica 34, 215–256 (in Chinese with English abstract).
Li, J.-W., Vasconcelos, P., Zhang, J., Zhou, M.-F., Zhang, X.-J., Yang, F.-H., 2003. $^{40}Ar/^{39}Ar$ constraints on a temporal link between gold mineralization, magmatism, and continental margin transtension in the Jiaodong gold province, eastern China. Journal of Geology 111, 741–751.
Li, S.-R., Qu, Q.-J., Yuan, W.-M., Deng, J., Hou, Z.-Q., Du, A.-D., 2004a. Re–Os dating of the porphyry copper deposits in southern Gangdese metallogenic belt, Tibet. Extended Abstracts, 19th Himalaya–Karakoram–Tibet Workshop, Niseko, Japan, pp. 192–193.
Li, X.-F., Mao, J.-W., Wang, D., Luo, F., 2004b. Helium and argon isotope systematics in fluid inclusion of gold deposits along the Daduhe River, Sichun Province, southwestern China. Acta Geological Sinica 78, 203–209 (in Chinese).
Li, G.-M., Rui, Z.-Y., Wang, G.-M., Lin, F.-C., Liu, B., She, H.-Q., Feng, C.-Y., Qu, W.-J., 2005. Molybdenite Re–Os dating of Jiama and Zhibula polymetallic copper deposits in Gangdese metallogenic belt of Tibet and its significance. Kuangchuang Dizhi (Mineral Deposits) 24, 481–489.
Li, J.-W., Vasconcelos, P., Zhou, M.-F., Zhao, X.-F., Ma, C.-H., 2006. Geochronology of the Pengjiakuang and Rushan gold deposits, eastern Jiaodong gold province, northeastern China: implications for regional mineralization and geodynamic setting. Economic Geology 101, 1023–1038.
Li, H.-M., Ye, H.-S., Mao, J.-W., Wang, D.-H., Chen, Y.-C., Qu, W.-J., Du, A.-D., 2007a. Re–Os dating of molybdenites from the Dahu Au(Mo) deposit in the Xiaoqinling gold ore district and its geological significance. Mineral Deposits 26, 417–424 (in Chinese with English abstract).
Li, S.-Z., Kusky, T.M., Wang, L., Zhang, G.-W., Lai, S.-C., Liu, X.-C., Dong, S.-W., Zhao, G.-C., 2007b. Collision leading to multiple-stage large-scale extrusion in the Qinling orogen: insights from the Mianlue suture. Gondwana Research 12, 121–143.
Li, X.-F., Mao, J.-W., Wang, C.-Z., Watanabe, Y., 2007c. The Daduhe gold field at the eastern margin of the Tibet Plateau: He, Ar, S, O, and H isotopic data and their metallogenic implications. Ore Geology Reviews 30, 244–256.
Li, X.-F., Wang, C.-Z., Hua, R.-M., Wei, X.-L., 2010. Fluid origin and structural enhancement during mineralization of the Jinshan orogenic gold deposit, South China. Mineralium Deposita 45, 583–597.
Li, J.-X., Qin, K.-H., Li, G.-M., Xiao, B., Zhao, J.-X., Chen, L., 2011a. Magmatic–hydrothermal evolution of the Cretaceous Duolong gold-rich porphyry copper deposit in the Bangongco metallogenic belt, Tibet: evidence from U–Pb and $^{40}Ar/^{39}Ar$ geochronology. Journal of Asian Earth Sciences 41, 525–536.
Li, W.-C., Zeng, P.-S., Hou, Z.-Q., White, N.C., 2011b. The Pulang porphyry copper deposit and associated felsic intrusions in Yunnan province, southwest China. Economic Geology 106, 79–92.
Li, J.-W., Bi, S.-J., Selby, D., Chen, L., Vasconcelos, P., Thiede, D., Zhou, M.-F., Zha, X.-F., Li, Z.-K., Qiu, H.-N., 2012a. Giant Mesozoic gold provinces related to the destruction of the North China craton. Earth and Planetary Science Letters 349–350, 26–37.
Li, J.-X., Qin, K.-Z., Li, G.-M., Cao, M.-J., Xiao, B., Chen, L., Zhao, J.-X., Evans, N.J., McInnes, B.I.A., 2012b. Petrogenesis and thermal history of the Yulong porphyry copper deposit, Eastern Tibet: insights from U–Pb and U–Th/He dating, and zircon Hf isotope and trace element analysis. Mineralogy and Petrology 105, 201–221.
Liang, H.-Y., Xia, P., Wang, X.-Z., Cheng, J.-P., Zhao, Z.-H., Liu, C.-Q., 2007. Geology and geochemistry of the adjacent Changkeng gold and Fuwang silver deposits, Guangdong Province, South China. Ore Geology Reviews 31, 304–318.
Liang, Q.-L., Jiang, S., Wang, S.-H., Li, S., Zheng, F., 2012. Re–Os dating of molybdenite from the Luoboling porphyry Cu–Mo deposit in the Zijinshan ore field of Fujian Province and its geological significance. Acta Geologica Sinica 86, 1113–1118.
Likhanov, I.I., Kozlov, P.S., Popov, N.V., Reverdatto, V.V., Vershinin, A.E., 2006. Collisional metamorphism as a result of thrusting in the Transangara region of the Yensei Ridge. Doklady Earth Sciences 411, 1313–1317.
Lim, C., Cho, M.-S., 2012. Two-phase contractional deformation of the Jurassic Daebo Orogeny, Chungnam Basin, Korea, and its correlation with the early Yanshanian movement of China. Tectonics 31, TC1004. http://dx.doi.org/10.1029/2011TC002909 (23 pp.).
Lin, W., Faure, M., Chen, Y., Ji, W.-B., Wang, F., Wu, L., Charles, N., Wang, J., Wang, Q.-C., 2013. Late Mesozoic compressional to extensional tectonics in the Yiwulushan massif, NE China and its bearing on the evolution of the Yinshan–Yanhshan orogenic belt. Part I: structural analyses and geochronological constraints. Gondwana Research 23, 54–77.
Ling, M.X., Wang, F.Y., Ding, X., Hu, Y.H., Zhou, J.B., Zartman, R.E., Yang, X.Y., Sun, W.D., 2009. Cretaceous ridge subduction along the Lower Yangtze River Belt, Eastern China. Economic Geology 104, 303–321.
Lishnevskii, E.N., Distler, V.V., 2004. Deep structure of the Earth's crust in the district of the Sukhoi Log gold–platinum deposit (eastern Siberia, Russia) based on geological and geophysical data. Geology of Ore Deposits 46, 88–104.

Please cite this article as: Goldfarb, R.J., et al., Phanerozoic continental growth and gold metallogeny of Asia, Gondwana Research (2013), http://dx.doi.org/10.1016/j.gr.2013.03.002

Liu, C., Mu, Z.-G., Liu, R.-X., Huang, B.-L., 1995. $^{40}Ar/^{39}Ar$ laser microprobe dating on hydrothermal minerals from Duobaoshan porphyry copper mining district, Heilongjiang Province, China. Scientia Geologica Sinica 30, 329–337 (in Chinese with English abstract).

Liu, J.-J., Zheng, M.-H., Cook, N.J., Long, X.-R., Deng, J., Zhai, Y.-S., 2007. Geological and geochemical characteristics of the Sawaya'erdun gold deposit southwestern Chinese Tianshan. Ore Geology Reviews 32, 125–156.

Liu, J., Wu, G., Li, Y., Zhu, M.-T., Zhong, W., 2011a. Re–Os sulfide (chalcopyrite, pyrite and molybdenite) systematics and fluid inclusion study of the Duobaoshan porphyry Cu (Mo) deposit, Heilongjiang Province, China. Journal of Asian Earth Sciences 49, 300–312.

Liu, J.-L., Bai, X.-D., Zhao, S.-J., Tran, M.-D., Zhang, Z.-C., Zhan, Z.-L., Zhao, H.-B., Lu, J., 2011b. Geology of the Sandaowanzi telluride gold deposit of the northern Great Xing'an Range, NE China: geochronology and tectonic controls. Journal of Asian Earth Sciences 41, 107–118.

Liu, C.-Z., Liu, Z.-C., Wu, F.-Y., Chu, Z.-Y., 2012. Mesozoic accretion of juvenile subcontinental lithospheric mantle beneath South China and its implications: geochemical and Re–Os isotopic results from Ningyuan mantle xenoliths. Chemical Geology 291, 186–198.

Lu, Y.-J., Ma, D.-M., Jin, H.-T., 1992. Distribution Regularity and Ore-searching Direction of Gold Placers in China. Geological Publishing House, Beijing (107 pp. (in Chinese with English abstract)).

Lu, H.-Z., Wang, Z.-G., Chen, W.-Y., Wu, X.-Y., Hu, R.-Z., Keita, M., 2005a. Turbidite-hosted gold deposits of SE Guizhou, China: their regional setting, mineralizing styles, and some genetic constraints. In: Mao, J.-W., Bierlein, F.P. (Eds.), Mineral Deposit Research: Meeting the Global Challenge. Proceedings of the Eighth Biennial SGA Meeting. Springer, Berlin, pp. 545–548.

Lu, J., Hua, R., Yao, C., 2005b. Re–Os age for molybdenite from the Dexing porphyry Cu–Au deposit of Jiangxi Province, China. Geochimica et Cosmochimica Acta 69 (Suppl. 1), 882.

Lu, Y.-J., McCuaig, C., Kerrich, R., Hart, C.R.J., Cawood, P., Kemp, A.I.S., Li, Z.-X., Hou, Z.-Q., 2010. New types of alkaline porphyry Cu (±Mo, Au) mineral systems of western Yunnan, East Tibet: compositional characteristics, sources, and exploration implications for continental collision metallogeny. Centre for Exploration Targeting Newsletter 14, 16–24.

Luddington, S., Hammarstrom, J.M., Robinson Jr., G.R., Mars, J.C., Miller, R.J., 2010. Porphyry copper assessment of the Tibetan plateau, China. U.S. Geological Survey Scientific Investigations Report 2010-5090-F (74 pp.).

Makrygina, V.A., Belichenko, V.G., Reznitsky, L.Z., 2007. Types of paleoisland arcs and back-arc basins in the northeast of the Paleoasian Ocean (from geochemical data). Russian Geology and Geophysics 48, 107–119.

Manaka, T., Zaw, K., Meffre, S., 2007. Mineralisation characteristics of the Long Chieng track (LCT) gold deposit, Lao PDR. GEOTHAI '07 International Conference on Geology of Thailand: Towards Sustainable Development and Sufficiency Economy, pp. 199–201.

Manaka, T., Zaw, K., Meffre, S., 2008. Geological and tectonic setting of Cu–Au deposits in northern Lao PDF. Proceedings of the International Symposia on Geoscience Resources and Environments of Asian Terranes (GREAT 2008), 4th IGCP 516, and 5th APSEG, November 24–26, 2008, Bangkok, Thailand, pp. 254–257.

Manaka, T., Dinh, S.Q., Zaw, K., Meffre, S., Halpin, J., Hai, T.T., Hai, L.V., Hung, N.B., 2010. Geology and mineralization of the Phuoc Son gold deposits, central Vietnam. Giant Ore Deposits Down-Under, 13th Quadrennial IAGOD Symposium Proceedings, Adelaide, pp. 141–142.

Manini, A., Aquino, J., Gregory, C., Aneka, S., 2001. Discovery of the Sepon gold and copper deposits, Laos. NewGenGold 2001, Conference Proceedings AMF, Adelaide, pp. 93–107.

Mao, J.-W., Wang, Z.-L., 2000. A preliminary study on time limits and geodynamic setting of large-scale metallogeny in east China. Mineral Deposits 19, 289–296 (in Chinese with English abstract).

Mao, J.-W., Zhang, Z.-H., Yang, J.-M., Zhang, Z.-C., 2000. The Hanshan gold deposit in the Caledonian North Qilian orogenic belt, NW China. Mineralium Deposita 35, 63–71.

Mao, J.-W., Goldfarb, R.J., Zhang, Z.-W., Xu, W.-Y., Qiu, Y.-M., Deng, J., 2002a. Gold deposits in the Xiaoqinling–Xiong'ershan region, Qinling Mountains, central China. Mineralium Deposita 37, 306–325.

Mao, J.-W., Qiu, Y., Goldfarb, R.J., Zhang, Z., Garwin, S., Ren, F.-S., 2002b. Geology, distribution, and classification of gold deposits in the western Qinling belt, central China. Mineralium Deposita 37, 352–377.

Mao, J.-W., Konopelko, D., Seltmann, R., Lehmann, B., Chen, W., Wang, Y.-T., Elklung, O., Usubaliev, T., 2004. Postcollisional age of the Kumtor gold deposit and timing of Hercynian events in the Tien Shan, Kyrgyzstan. Economic Geology 99, 1771–1780.

Mao, J.-W., Goldfarb, R.J., Wang, Y.-T., Hart, C.J., Wang, Z.-L., Yang, J.-M., 2005. Late Paleozoic base and precious metal deposits, East Tianshan, Xinjiang, China: characteristics and geodynamic setting. Episodes 28, 23–36.

Mao, J.-W., Wang, Y.-T., Lehmann, B., Yu, J.-J., Du, A.-D., Mei, Y.-X., Li, Y.-F., Zang, W.-S., Stein, H.J., Zhou, T.-F., 2006. Molybdenite Re–Os and albite $^{40}Ar/^{39}Ar$ dating of Cu–Au–Mo and magnetite porphyry systems in the Changjiang valley and metallogenic implications. Ore Geology Reviews 29, 307–324.

Mao, J.-W., Li, X.-F., White, N.C., Zhao, C., Zhang, Z.-H., Wang, Y., Hu, H.-B., 2007. Types, characteristics and geodynamic settings of Mesozoic epithermal gold deposits in Eastern China. Resource Geology 57, 435–454.

Mao, G.-Z., Hua, R.-M., Long, G.-M., 2008. Discussion on the mineralogenetic epoch of the Jinshan gold deposit, Jiangxi Province: based on the quartz fluids inclusion Rb–Sr dating. Acta Geologica Sinica 82, 532–539 (in Chinese with English abstract).

Mao, J.-W., Pirajno, F., Xiang, J.-F., Gao, J.-J., Ye, H.-S., Li, Y.-F., Guo, B.-J., 2011a. Mesozoic molybdenum deposits in the east Qinling–Dabie orogenic belt: characteristics and tectonic settings. Ore Geology Reviews 43, 264–293.

Mao, J.-W., Xie, G.-Q., Duan, C., Pirajno, F., Ishiyama, D., Chen, Y.-C., 2011b. A tectono-genetic model for porphyry–skarn–stratabound Cu–Au–Mo–Fe and magnetite–apatite deposits along the Middle–Lower Yangtze River Valley, Eastern China. Ore Geology Reviews 43, 294–314.

Mao, J.-W., Cheng, Y.-B., Chen, M.-H., Pirajno, F., 2012. Major types and time–space distribution of Mesozoic ore deposits in South China and their geodynamic settings. Mineralium Deposita 1–28. http://dx.doi.org/10.1007/s00126-012-0446-z.

Meert, J.G., Lieberman, B.S., 2008. The Neoproterozoic assembly of Gondwana and its relationship to the Ediacaran–Cambrian radiation. Gondwana Research 14, 5–21.

Meinert, L.D., Dipple, G.M., Nicolescu, S., 2005. World skarn deposits. Economic Geology 100th Anniversary Volume. 299–336.

Mercier, J.L., Hou, M.-J., Vergely, P., Wang, Y.-M., 2007. Structural and stratigraphical constraints on the kinematic history of the southern Tan–Lu fault zone during the Mesozoic, Anhui province, China. Tectonophysics 439, 33–66.

Metcalfe, I., 1984. Stratigraphy, palaeontology and palaeogeography of the Carboniferous of Southeast Asia. Memoirs of the Geological Society of France 147, 107–118.

Metcalfe, I., 2006. Palaeozoic and Mesozoic tectonic evolution and palaeogeography of East Asian crustal fragments: the Korean Peninsula in context. Gondwana Research 9, 24–46.

Metcalfe, I., 2011. Tectonic framework and Phanerozoic evolution of Sundaland. Gondwana Research 19, 3–21.

Miao, L.-C., Qiu, Y.-M., Fan, W.-M., Zhang, F.-Q., Zhai, M.-G., 2005. Geology, geochronology, and tectonic setting of the Jiapigou gold deposits, southern Jilin Province, China. Ore Geology Reviews 26, 137–165.

Miao, L.-C., Qiu, Y.-M., Fan, W.-M., Zhang, F.-Q., 2008. Mesozoic multi-phase magmatism and gold mineralization in the early Precambrian North China craton, eastern Hebei Province, China: SHRIMP zircon U–Pb evidence. International Geology Review 50, 826–847.

Miller, L.D., Goldfarb, R.J., Nie, F.-J., Hart, C.J.R., Miller, M.L., Yang, Y.-Q., Liu, Y.-Q., 1998. North China gold: a product of multiple orogens. Society of Economic Geologists Newsletter 33, 1–12.

Miller, E.L., Katkov, S., Strickland, A., Toro, J., Akinin, V.V., Dumitru, T.A., 2009. Geochronology and thermochronology of Cretaceous plutons and metamorphic country rocks, Anyui–Chukotka Fold Belt, North East Arctic Russia. In: Stone, D.B., Fujita, K., Layer, P.W., Miller, E.L., Prokopiev, A.V., Toro, J. (Eds.), Geology, Geophysics and Tectonics of Northeastern Russia: A Tribute to Leonid Parfenov. Stephan Mueller Special Publication Series, 4. European Geophysical Union, pp. 157–175.

Mirgorodskaya, R.M., 2008. Comparison of Teutedjak and Butarnoe gold–bismuth deposits (the northern Priokhotje). Gold of the North Pacific Rim, International Mining and Geology Forum, Abstracts of the All–Kolyma Mining and Geology Conference, Magadan, September, 10–14, pp. 89–90.

Mironov, A.G., Stein, H., Zimmerman, A., Zhmodik, S.M., 2005. Dating of gold occurrences in the Sayan–Baikal fold belt, southern Siberia, Russian. In: Mao, J.-W., Bierlein, F.P. (Eds.), Mineral Deposit Research: Meeting the Global Challenge: Proceedings of the Eighth Biennial SGA Meeting. Springer, Berlin, pp. 797–800.

Mironov, A.G., Zhmodik, S.M., Kolesov, G.M., Mit'kin, V.N., Damdinov, B.B., Zayakina, S.B., 2008. Platinum group elements in gold-sulfide and base-metal ores of the Sayan–Baikal fold region and possible platinum and palladium speciation in sulfides. Geology of Ore Deposits 50, 41–59.

Mitchell, A.H.G., Ausa, C.A., Deiparine, L., Hlaing, T., Htay, N., Khine, A., 2004. The Modi Taung–Nankwe gold district, Slate belt, central Myanmar: mesothermal veins in a Mezozoic orogeny. Journal of Asian Earth Sciences 23, 321–341.

Mitchell, A.H.G., Htay, M.T., Htun, K.M., Win, M.N., Oo, T., Hlaing, T., 2007. Rock relationships in the Mogok metamorphic belt, Tatkon to Mandalay, central Myanmar. Journal of Asian Earth Sciences 29, 891–910.

Mo, X.-X., Lu, F.-X., Shen, S.-Y., Zhu, Q.-W., Ho, Z.-Q., 1993. Sanjiang Tethyan Volcanism and Related Mineralization. Geological Publishing House, Beijing (267 pp. (in Chinese with English abstract)).

Molchanov, V.P., Moiseenko, V.G., Khomich, V.G., Goryachev, N.A., 2000. Palladium–gold–rare metal mineralization in the Oemku Ore Group, Sikhote Alin Range. Doklady Earth Sciences 375A, 1420–1422.

Morelli, R., Creaser, R.A., Seltmann, R., Stuart, F.M., Selby, D., Graupner, T., 2007. Age and source constraints for the giant Murunatu gold deposit, Ukbekistan, from coupled Re–Os–He isotopes in arsenopyrite. Geology 35, 795–798.

Natal'in, B.A., Sengor, A.M.C., 2005. Late Palaeozoic to Triassic evolution of the Turan and Scythian platforms: the pre-history of the Palaeo-Tethyan closure. Tectonophysics 404, 175–202.

Naumov, E., Borisenko, A., Kovalev, K., Kalinin, Y., Seltmann, R., 2012. Gold deposits of Ob–Zaisan fold zone (western Siberia and eastern Kazakhstan): types and ages of mineralization, correlation with magmatic complexes [abs.]. 34th International Geological Congress, Brisbane, Australia. (Abstract).

Neimark, L.A., Rytsk, E.Y., Ovchinnikova, G.V., Sergeeva, N.A., Gorokhovskii, B.M., Skopintsev, V.G., 1995. Lead isotopes in gold deposits of the Eastern Sayan (in Russia). Geology of Ore Deposits 37, 201–212.

Newberry, R.J., Layer, P.W., Gans, P.B., Goncharov, V.I., Goryachev, N.A., Voroshin, S.V., 2000. Preliminary chronology analysis of Mesozoic magmatism, tectonics and ore mineralization on North-East Russia according to $^{40}Ar/^{39}Ar$ and trace elements data on igneous and ore rocks. Gold Mineralization and Granitoid Magmatism of North Pacific, Proceedings of the All-Russia Meeting Magadan September 4–6, 1999. NEISRI FEB RAS, Magadan, pp. 181–205 (in Russian).

Ni, Z.-Y., Chen, Y.-J., Li, N., Zhang, H., 2012. Pb–Sr–Nd isotope constraints on the fluid source of the Dahu Au–Mo deposit in Qinling Orogen, central China, and implication for Triassic tectonic setting. Ore Geology Reviews 46, 60–67.

Nie, F.-J., 1997. Type and distribution of gold deposits along the northern margin of the North China Craton, People's Republic of China. International Geology Review 39, 151–180.

Nie, F.-J., Jiang, S.-H., Su, X.-X., Wang, X.-L., 2002. Geological features and origin of gold deposits occurring in the Baotou–Bayan–Obo district, south-central Inner Mongolia, People's Republic of China. Ore Geology Reviews 20, 139–169.

Nokleberg, W.J., Parfenov, L.M., Monger, J.W.H., Norton, I.O., Khanchuk, A.I., Stone, D.B., Scotese, C.R., Scholl, D.W., Fujita, K., 2000. Phanerozoic tectonic evolution of the Circum North Pacific. U.S. Geological Survey Profossional Paper, 1626 (122 pp.).

Please cite this article as: Goldfarb, R.J., et al., Phanerozoic continental growth and gold metallogeny of Asia, Gondwana Research (2013), http://dx.doi.org/10.1016/j.gr.2013.03.002

Nokleberg, W.J., Bundtzen, T.K., Eremin, R.A., Ratkin, V.V., Dawson, K.M., Shpikerman, V.I., Goryachev, N.A., Byalobzhesky, S.G., Frolov, Yu.F., Khanchuk, A.I., Koch, R.D., Monger, J.W.H., Pozdeev, A.I., Rosenblum, I.S., Rodionov, S.M., Parfenov, L.M., Scotese, C.R., Sidorov, A.I., 2005. Metallogenesis and tectonics of the Russian Far East, Alaska, and the Canadian Cordillera. U.S. Geological Survey Professional Paper, 1697 (429 pp.).

Nozhkin, A.D., Turkina, O.M., Soretov, Y.K., Travin, A.V., 2007. The Vendian accretionary event in the southwestern margin of the Siberian craton. Doklady Earth Sciences 415A, 869–873.

Oakes, B., Kay, B.D., Arifiev, V., 1998. The Jerooy gold deposit, Kyrgyz Republic. In: Porter, T.M. (Ed.), Porphyry and Hydrothermal Copper & Gold Deposits: A Global Perspective. Conference Proceedings. Australian Mineral Foundation, Glenside, South Australia, pp. 191–196.

Okrugin, V.M., Zelensky, M.E., 2004. Miocene–Quaternary center of volcanic, hydrothermal and ore-forming activity in southern Kamchatka. In: Khanchuk, A.I., Gonevchuk, V.G., Seltman, R. (Eds.), Metallogeny of the Pacific Northwest (Russian Far East): Tectonics, Magmatism and Metallogeny of Active Continental Margins, INTERIM IAGOD Conference Excursion Guidebook. Dalnauka Publ. House, Vladivostok, pp. 147–176.

Oxman, V.S., 2003. Tectonic evolution of the Mesozoic Verkhoyansk–Kolyma belt (NE Asia). Tectonophysics 365, 45–76.

Pan, Y.M., Dong, P., 1999. The Lower Changjiang (Yangzi/Yangtze River) metallogenic belt, East China: intrusion- and wall rock-hosted Cu–Fe–Au, Mo, Zn, Pb, Ag deposits. Ore Geology Reviews 15, 177–242.

Parfenov, L.M., 1995. Tectonics of the Verkhoyansk–Kolyma Mesozoides in context of plate tectonics. Tectonophysics 139, 319–342.

Parfenov, L.M., Kuzmin, M.I. (Eds.), 2001. Tectonics, Geodynamics and Metallogeny of Sakha (Yakutia) Republic. MAIK Nauka/Interperiodika, Moscow (571 pp. (in Russian)).

Parfenov, L.M., Badarch, G., Berzin, N.A., Khanchuk, A.I., Kuzmin, M.I., Nokleberg, W.J., Prokopiev, A.V., Ogasawara, M., Yan, H., 2009. Summary of Northeast Asia geodynamics and tectonics. 4, 11–33.

Peng, B., Frei, R., 2004. Nd–Sr–Pb isotopic constraints on metal and fluid sources in W–Sb–Au mineralization at Woxi and Liaojiaping (Western Hunan, China). Mineralium Deposita 39, 313–327.

Peng, J.-T., Hu, R.-Z., Zhao, J.-H., Fu, Y.-Z., Lin, Y.-X., 2003. Sm–Nd dating on scheelites and Ar–Ar dating quartz from Woxi W–Sb–Au ore deposits in western Hunan. Chinese Science Bulletin 48 (18), 1976–1981 (in Chinese).

Peters, S.G., Huang, J.-Z., Li, Z.-P., Jing, C.-G., 2007. Sedimentary rock-hosted Au deposits of the Dian–Qian–Gui area, Guizhou, and Yunnan Provinces, and Guangxi District, China. Ore Geology Reviews 31, 170–204.

Pirajno, F., Bagas, L., 2002. Gold and silver metallogeny of the South China Fold Belt: a consequence of multiple mineralizing events? Ore Geology Reviews 20, 109–126.

Polzunenkov, G.O., Akinin, V.V., Cherepanova, I.Yu, 2011. New data on the age and composition of Velitkenay and Kuekvun granite–gneiss massifs (Arctic Chukotka): application to elaboration of granite-related mineralization models. Gold of the North Pacific Rim. II Internationl Geology & Mining Forum Dedicated to Yu.A. Bilibin's 110th anniversary, Abstracts of the Geology and Mining Conference. NEISRI FEB RAS, Magadan, pp. 171–172.

Ponomarchuk, V.A., Sorokin, A.A., Travin, A.V., Sorokin, A.P., 2008. Geochronologic correlations of the Mesozoic granitoid magmatism and ore-forming processes. Gold of the North Pacific Rim, International Mining and Geology Forum, Abstracts of the All-Kolyma Mining and Geology Conference, Magadan, September, 10–14, pp. 172–174 (in Russian).

Prokof'ev, V.Y., Zorina, L.D., Kovalenker, V.A., Akinfiev, N.N., Baksheev, I.A., Krasnov, A.N., Yurgenson, G.A., Trubkin, N.V., 2007. Composition, formation conditions, and genesis of the Talatui gold deposit, the eastern Transbaikal region, Russia. Geology of Ore Deposits 49, 31–68.

Prokopiev, A.V., Gamyanin, G.N., Bakharev, A.G., 2004. Tectonics geodynamics and metallogeny in the zone of junction of the Verkhoyansk foldbelt, the Okhotsk terrane and Kolyma–Omolon microcontinent. In: Khanchuk, A.I., Gonevchuk, G.A., Seltmann, R. (Eds.), Metallogeny of the Pacific Northwest: Tectonics, Magmatism, and Metallogeny of Active Continental Margins. Dalnauka, Vladivostok, Russia, pp. 142–145.

Prokopiev, A.V., Toro, J., Miller, E.L., Layer, P.W., Hourigan, J.K., Bakharev, A.G., Zaitsev, A.I., Dumitru, T., Gerels, J.E., Walles, B.L., Tretiyakov, F.F., Tarabukin, V.P., 2006. New U–Pb, $^{40}Ar/^{39}Ar$ and AFT data on North-East Yakutia and their tectonic and geodynamic interpretation. Ore Genesis and Metallogeny of East Asia, DPMI SB RAS. 145–148 (in Russian).

Qiu, Y.-M., Groves, D.I., McNaughton, N.J., Wang, L.-G., Zhou, T.-H., 2002. Nature, age and tectonic setting of granitoid-hosted, orogenic gold deposits of the Jiaodong Peninsula, eastern North China Craton, China. Mineralium Deposita 37, 283–305.

Qu, X.-M., Hou, Z.-Q., Zaw, K., Li, Y.-G., 2007. Characteristics and genesis of Gangdese porphyry copper deposits in the southern Tibetan Plateau: preliminary geochemical and geochronological results. Ore Geology Reviews 31, 205–223.

Ratcliff, J.T., Bercovici, D., Schubert, G., Kroenke, L.W., 1998. Mantle plume heads and the initiation of plate tectonic reorganizations. Earth and Planetary Science Letters 156, 195–207.

Ratkin, V., 1995. Pre- and post-accretionary metallogeny of the southern Russian Far East. Resource Geology Special Issue 18, 127–133.

Ratschbacher, L., Hacker, B.R., Webb, L.E., McWilliams, M., Ireland, T., Dong, S., Calvert, A., Wenk, H., 2000. Exhumation of the ultrahigh-pressure continental crust in east central China: Cretaceous and Cenozoic unroofing and the Tan–Lu fault. Journal of Geophysical Research 105, 13,303–13,338.

Ratschbacher, L., Hacker, B.R., Calvert, A., Webb, L.E., Grimmer, J.C., McWilliams, M.O., Ireland, T., Dong, S.-W., Hu, J.-M., 2003. Tectonics of the Qinling (central China): tectonostratigraphy, geochronology, and deformation history. Tectonophysics 366, 1–53.

Ren, J.-Y., Tamaki, K., Li, S.-T., Junxia, Z., 2002. Late Mesozoic and Cenozoic rifting and its dynamic setting in Eastern China and adjacent areas. Tectonophysics 344, 175–205.

Ren, Y.-S., Ju, N., Zhao, H.-L., Wang, H., Hou, K.-J., Liu, S., 2012. Geochronology and geochemistry of metallogenetic porphyry bodies from the Nongping Au–Cu deposit in the Eastern Yanbian Area, NE China: implications for metallogenic environment. Acta Geologica Sinica 86, 619–629.

Richards, J.P., 2003. Tectono-magmatic precursors for porphyry Cu–(Mo–Au) deposit formation. Economic Geology 98, 1515–1533.

Rodionov, S.M., Fredericksen, R.S., Berndnikov, N.V., 2005. The Kuranakh epithermal gold deposit, East Russia. In: Mao, J.-W., Bierlein, F.P. (Eds.), Mineral Deposit Research: Meeting the Global Challenge. Springer-Verlag, Berlin, pp. 1053–1056.

Rui, Z., Goldfarb, R.J., Qui, Y., Zhou, T., Chen, R., Pirajno, F., Yun, G., 2002. Paleozoic–early Mesozoic gold deposits of the Xinjiang Autonomous Region, northwestern China. Mineralium Deposita 37, 393–418.

Rusinov, V.L., Rusinov, O.V., Kryazhev, S.G., Shchegol'kov, Y.V., Alysheva, E.I., Borisovsky, S.E., 2008. Wall-rock metasomatism of carbonaceous terrigeneous rocks in the Lena gold district. Geology of Ore Deposits 50, 1–40.

Rytsk, E.Y., Makeev, A.F., Glebovitsky, V.A., Fedoseenko, A.M., 2007. Early Vendian age of multiple gabbro-granite complexes of the Karalon–Mamakan zone, Baikal–Muya belt: new U–Pb zircon data. Doklady Earth Sciences 415A, 911–914.

Sakharova, M.S., Krivitskaya, N.N., Ryabov, A.N., 1998. The evolution of the mineral composition of the Au–Ag deposits of the Okhotsk–Chukotsk belt (Russia). Geology of Ore Deposits 40, 30–50.

Sato, K., Rodionov, S.M., Brublevsky, A.A., 2006. Lermontovskoe tungsten skarn deposit: the oldest mineralization in the Sikhote–Alin orogen, Far East Russia. Resource Geology 56, 257–266.

Savva, N.E., Shakhtyrov, V.G., 2011. The Ol'cha gold–silver deposit: tectonic setting, structure, and mineralogy. Geology of Ore Deposits 53, 412–433.

Savva, N.E., Volkov, A.V., Sidorov, A.A., 2007. Specific features of ore formation in the epithermal Kubaka gold–silver deposit, northeast Russia. Doklady Earth Sciences 417, 79–83.

Sayadyan, G.R., 2004. Geology, magmatism and gold mineralization of South Primorye (the Askold strike-slip fault zone, Sergeevka terrane). In: Khanchuk, A.I., Gonevchuk, V.G., Seltman, R. (Eds.), Metallogeny of the Pacific Northwest (Russian Far East): Tectonics, Magmatism and Metallogeny of Active Continental Margins. Interim IAGOD Conference Excursion Guidebook. Dalnauka Publ. House, Vladivostok, pp. 137–146.

Searle, M.P., Yeh, M.-W., Lin, T.-H., Chung, S.-L., 2010. Structural constraints on the timing of left-lateral shear along the Red River shear zone in the Ailao Shan and Diancang Shan ranges, Yunnan, SW China. Geosphere 6, 1–23.

Seedorff, E., Dilles, J.H., Proffett Jr., J.M., Einaudi, M.T., Zurcher, L., Stavast, W.J.A., Johnson, D.A., Barton, M.D., 2005. Porphyry deposits: characteristics and origin of hypogene features. Economic Geology 100th Anniversary Volume. 251–298.

Seltmann, R., Porter, T.M., 2005. The porphyry Cu–Au/Mo deposits of central Eurasia. 1. Tectonic, geologic and metallogenic setting, and significant deposits. In: Porter, T.M. (Ed.), Super Porphyry Copper and Gold Deposits: A Global Perspective, 2. PGC Publishing, Adelaide, pp. 467–512.

Seltmann, R., Konopelko, D., Biske, G., Divaev, F., Sergeev, S., 2011. Hercynian post-collisional magmatism in the context of Paleozoic magmatic evolution of the Tien Shan orogenic belt. Journal of Asian Earth Sciences 42, 821–838.

Sengor, A.M.C., Natal'in, B.A., 1996. Paleotectonics of Asia: fragments of a synthesis. In: Yin, A., Harrison, T.M. (Eds.), The Tectonic Evolution of Asia. Cambridge University Press, Cambridge, pp. 486–640.

Shelton, K.L., So, S.-C., Chang, J.-S., 1988. Gold-rich mesothermal vein deposits of the Republic of Korea: geochemical studies of the Jungwon gold area. Economic Geology 83, 1221–1237.

Shen, Y.-C., Zeng, Q.-D., Xie, H.-Y., 1999. Location time of gold deposits in Jiapigou–Haigou mineralization zone, Jilin Province. Gold Science and Technology 7, 19–26 (in Chinese with English abstract).

Shen, P., Shen, Y.-C., Pan, H.-D., Li, X.-H., Dong, L.-H., Wang, J.-B., Zhu, H.-P., Dai, H.-W., Guan, W.-N., 2012. Geochronology and isotope geochemistry of the Baogutu porphyry copper deposit in the West Junggar region, Xinjiang, China. Journal of Asian Earth Sciences 49, 99–115.

Shicai, S.H.A.O., 2000. Qinling Orogenic Belt: Mesozoic evolution and metallogenesis. Acta Geologica Sinica 74, 452–457.

Shpikerman, V.I., 1998. Pre-Cretaceous Metallogeny of Northeastern Asia. NEISRI FEB RAS, Magadan (333 pp. (in Russian)).

Sillitoe, R.H., 2010. Porphyry copper systems. Economic Geology 105, 3–41.

Simmons, S.F., White, N.C., John, D.A., 2005. Geological characteristics of epithermal precious and base metal deposits. Economic Geology 100th Anniversary Volume. 485–522.

Sinclair, W.D., 2007. Porphyry deposits. In: Goodfellow, W.D. (Ed.), Mineral Deposits of Canada: A Synthesis of Major Deposit-types, District Metallogeny, the Evolution of Geological Provinces, and Exploration Methods: Geological Association of Canada, Mineral Deposits Division, Special Publication, 5, pp. 223–243.

Smelov, A.P., Timofeev, V.F., 2005. The tectonics and metallogeny of the Precambrian of the Aldan–Stanovoy shield. In: Mao, J.-W., Bierlein, F.P. (Eds.), Mineral Deposit Research: Meeting the Global Challenge. Proceedings of the Eighth Biennial SGA Meeting. Springer, Berlin, pp. 53–56.

Smith, S., Olberg, D., Manini, T., 2005. The Sepon gold deposits, Laos: exploration, geology, and comparison to Carlin-type gold deposits in the Great Basin. In: Rhoden, H.N., Steininger, R.C., Vikre, P.G. (Eds.), Window to the World, Symposium Proceedings, 2. Geological Society of Nevada, Reno/Sparks, pp. 899–915.

So, C.-S., Zhang, D.-Q., Yun, S.-T., Li, D.-X., 1998. Alteration–mineralization zoning and fluid inclusions of the high sulfidation epithermal Cu–Au mineralization at Zijinshan, Fujian Province, China. Economic Geology 93, 961–980.

Sokolov, S.D., 2010. Tectonics of northeast Asia: an overview. Geotectonics 44, 60–78.

Sokolov, S.D., Bondarenko, G.Y., Khudoley, A.K., Morozov, O.L., Luchitskaya, M.V., Tuchkova, M.I., Layer, P.W., 2009. Tectonic reconstruction of Uda–Murgal arc and

Please cite this article as: Goldfarb, R.J., et al., Phanerozoic continental growth and gold metallogeny of Asia, Gondwana Research (2013), http://dx.doi.org/10.1016/j.gr.2013.03.002

Late Jurassic and Early Cretaceous convergent margin of northeast Asia–northwest Pacific. Stephen Mueller Special Publication Series 4, 273–288.
Sone, M., Metcalfe, I., 2008. Parallel Tethyan sutures in Southeast Asia: new insights for Palaeo-Tethys closure and implications for the Indosinian orogeny. Comptes Rendus Géoscience 340, 166–179.
Song, B.-J., Jiang, B.-Z., Zhou, D.-Y., Huai, B.-F., 2007. Discussion on the metallogenic condition and ore searching direction of the Shabaosi gold deposit, Northern Daxing'anling Mountains. Contributions to Geology and Mineral Resources Research 2007-02, 5 (in Chinese with English abstract).
Sorokin, A.A., Melnikov, A.V., Ponomarchuk, V.A., Travin, A.V., Sorokin, A.P., 2008. Age and magmatism relationship of Berezitovoye gold-base metal deposit from west part of Selenga–Stanovoy superterrane. Reports of Russian Academy of Sciences, T.421, No.1, pp. 86–89 (in Russian).
Sorokin, A.A., Ostapenko, N.S., Ponomarchuk, V.A., Travin, A.V., 2011. $^{40}Ar/^{39}Ar$ age of adularia from veins of the Tokur gold deposit, the Mongolian–Okhotsk orogenic belt, Russia. Geology of Ore Deposits 53, 264–271.
Sotnikov, V.I., Sorokin, A.A., Ponomarchuk, V.A., Gimon, V.O., Sorokin, A.P., 2007. Porphyry Cu–Mo–(Au) mineralization: the age and relationship with igneous rock complexes of the Borgulikan ore field (upper-Amur region). Russian Geology and Geophysics 48, 177–184.
Spiridonov, E.M., 1996. Granitic rocks and gold mineralization of north Kazakhstan. In: Shatov, V., Seltmann, R., Kremenetsky, A., Lehmann, B., Popov, V., Ermolov, P. (Eds.), Granite-related Ore Deposits of Central Kazakhstan and Adjacent Areas. GLAGOL Publishing House, St. Petersburg, pp. 197–217.
Spiridonov, A.M., Zorin, Y.A., Zorina, L.D., 2005. Gold deposits of Transbaikalia, Russia. In: Mao, J.-W., Bierlein, F.P. (Eds.), Mineral Deposit Research: Meeting the Global Challenge: Proceedings of the Eighth Biennial SGA Meeting. Springer, Berlin, pp. 1189–1191.
Stepanov, V.A., 1998. Gold and mercury of the Amur metallogenic province. Doklady Earth Sciences 359, 190–192.
Stepanov, V.A., 2001. The Bamsk gold deposit, Stanovoi Range, Russia. Geology of Ore Deposits 43, 33–45.
Struzhkov, S.F., Konstantinov, M.M., Aristov, V.V., Ryzhov, O.B., Shergina, Yu.P., 1994. New data on geology and age dates for gold and silver lode deposits in the Omsukchan area of the Okhotsk–Chukotka volcanic belt. Kolyma 9–10, 2–15 (in Russian).
Struzhkov, S.F., Ryjov, O.B., Grugoriev, N.V., Radchenko, Yu.I., Kolesnikov, A.G., Abbott, G.J., 1996. Geological structure and ore mineralogy of the Julietta gold–silver deposit. International Geology Review 38, 625–648.
Su, W.-C., Xia, B., Zhang, H.-T., Zhang, X.-C., Hu, R.-H., 2008. Visible gold in arsenian pyrite at the Shuiyindong Carlin-type gold deposit, Guizhou, China: implications for the environment and processes of ore formation. Ore Geology Reviews 33, 667–679.
Sun, J.-G., Zhao, J.-K., Chen, J.-Q., Keisuke, N., Hirochika, S., Shen, K., Men, L.-J., Chen, L., 2008. Ore-forming mechanism for the Xiaoxinancha Au-rich Cu deposit in Yanbian, Jilin Province, China: evidence from noble gas isotope geochemistry of fluid inclusions in minerals. Science in China Series D: Earth Sciences 51, 216–228.
Sun, X.-M., Zhang, Y., Xiong, D.-X., Sun, W.-D., Shi, G.-Y., Zhai, W., Wang, S.-W., 2009. Crust and mantle contributions to gold-forming process at the Daping deposit, Ailaoshan gold belt, Yunnan, China. Ore Geology Reviews 36, 235–249.
Tafti, R., Mortensen, J.K., Lang, J.R., Rebagliati, M., Oliver, J.L., 2009. Jurassic U–Pb and Re–Os ages for the newly discovered Xietongmen Cu–Au Porphyry District, Tibet, PRC: implications for metallogenic epochs in the Southern Gangdese Belt. Economic Geology 104, 127–136.
Tangwattananukul, L., Ishiyama, D., Matsubaya, O., Mizuta, T., Charusiri, P., Sera, K., 2009. Gold mineralization of Q prospect at Chatree deposit, central Thailand. NMCC Annual Report, 16 70–75.
Tapponnier, P., Lacassin, R., Leloup, P.H., Shärer, U., Zhong, D.-L., Liu, X.-C., Ji, S.-C., Zhang, L.-S., Zhong, J.-Y., 1990. The Ailao Shan–Red River metamorphic belt: Tertiary left lateral shear between Indochina and South China. Nature 343, 431–437.
Tate, N.M., 2005. Discovery, geology and mineralisation of the Phu Kham copper–gold deposit Lao People's Democratic Republic. In: Mao, J.-W., Bierlein, F.P. (Eds.), Mineral Deposit Research: Meeting the Global Challenge: Proceedings of the Eighth Biennial SGA Meeting. Springer, Berlin, pp. 1077–1080.
Tomurtogoo, O., 2005. Tectonics and structural evolution of Mongolia. In: Seltmann, R., Gerel, O., Kirwin, D.J. (Eds.), Geodynamics and Metallogeny of Mongolia With a Special Emphasis on Copper and Gold Deposits: IAGOD Guidebook Series, vol. 11. CERCAMS (Centre for Russian and Central EurAsian Mineral Sudies), Natural History Museum, London, United Kingdom, pp. 5–12.
Tsygankov, A.A., Matukov, D.I., Berezhnaya, N.G., Larionov, A.N., Posokhov, V.F., Tsyrenov, B.Ts., Khromov, A.A., Sergeev, S.A., 2007. Late Paleozoic granitoids of western Transbaikalia: magma sources and stages of formation. Russian Geology and Geophysics 48, 120–140.
United Nations, 1998. Geology and mineral resources of Kyrgyzstan. Atlas of Mineral Resources of the ESCAP Region (163 pp.).
Utkin, V.P., 2012. Tan–Lu and Sikhote–Alin transregional structural paragenesis and its role in continental riftogenesis. Doklady Earth Sciences 444, 687–691.
Utkin, V.P., Mitrokhin, A.N., Nevolin, P.L., Sayadyan, G.R., Sorokin, B.K., 2004. A structural–geodynamic factor in the distribution of gold mineralization in southern Primorye. Doklady Earth Sciences 395, 153–156.
Vakh, A.S., Stepanov, V.A., Avchenko, O.V., 2008. Berezitovoye gold-base metallic deposit: geology and ore composition. Ores and Metals 6, 44–55 (in Russian).
Vernikovsky, V.V., Vernikovskaya, A.E., Kotov, A.B., Sal'nikova, E.B., Kovach, V.P., 2003. Neoproterozoic accretionary and collisional events on the western margin of Siberian craton: new geological and geochronological evidence from the Yenisey Range. Tectonophysics 375, 147–168.
Vernikovsky, V.V., Vernikovskaya, A.E., Wingate, M.T.D., Popov, N.V., Kovach, V.P., 2007. The 880–864 Ma granites of the Yenisey Ridge, western Siberian margin: geochemistry, SHRIMP geochronology, and tectonic implications. Precambrian Research 154, 175–191.
Vielreicher, R.M., Vielreicher, N.M., Hagemann, S.G., 2003. Fault zone evolution and its control on ore-grade distribution at the Jian Cha Ling gold deposit, western Qinling region, central China. Mineralium Deposita 38, 538–554.
Volkov, A.V., Sidorov, A.A., 2001. A Unique Gold Mineral District in Chukotka. NEISRI FEB RAS, Magadan (180 pp. (in Russian)).
Volkov, A.V., Savva, N.E., Sidorov, A.A., Egorov, V.N., Shapovalov, V.S., Prokof'ev, V.Y., Kolova, E.E., 2006. Spatial distribution and formation conditions of Au-bearing porphyry Cu–Mo deposits in the northeast of Russia. Geology of Ore Deposits 48, 448–472.
Volkov, A.V., Savva, N.E., Sidorov, A.A., Prokof'ev, V.Yu., Goryachev, N.A., Voznesensky, S.D., Al'shevsky, A.V., Chernova, A.D., 2011. Shkol'noye gold deposit, the Russian Northeast. Geology of Ore Deposits 53, 1–26.
Voroshin, S.V., Newberry, R.J., 2001. $^{40}Ar/^{39}Ar$ data of gold mineralization in Shturmovskoy ore district. Problems of Geology and Metallogeny of Northeastern Asia at the Boundary of Millenia, Proceedings of XI Session of North-East Branch of All-Russian Mineralogy Society, 2. NEISRI FEB RAS, Magadan, pp. 159–162 (in Russian).
Voroshin, S.V., Newberry, R.J., Layer, P.W., 2004. $^{40}Ar/^{39}Ar$ dating of Au–quartz mineralization in the Upper Kolyma region (Magadan Oblast, Russia). In: Khanchuk, A.I., Gonevchuk, G.A., Seltmann, R. (Eds.), Metallogeny of the Pacific Northwest: Tectronics, Magmatism, and Metallogeny of Active Continental Margins. Dalnauka, Vladivostok, Russia, pp. 568–571.
Wainwright, A.J., Tosdal, R.M., Forster, C.N., Kirwin, D.J., Lewis, P.D., Wooden, J.L., 2011. Devonian and Carboniferous arcs of the Oyu Tolgoi porphyry Cu–Au district, South Gobi region, Mongolia. Geological Society of America Bulletin 123, 306–328.
Wan, B., Xiao, W.-J., Zhang, L.-C., Windley, B.F., Han, C.-M., Quinn, C.D., 2011. Contrasting styles of mineralization in the Chinese Altai and East Junggar, NW China: implications for the accretionary history of the southern Altaids. Journal of the Geological Society of London 168, 1311–1321.
Wang, D.-Z., Shu, L.-S., 2012. Late Mesozoic basin and range tectonics and related magmatism in Southeast China. Geoscience Frontiers 3, 109–124.
Wang, H.-N., Chen, J., Ji, J.-F., Qu, X.-M., 1997. Geological and geochemical characteristics of the Hetai gold deposit, South China: gold mineralization in an auriferous shear zone. International Geology Review 39, 181–190.
Wang, L.-G., Qiu, Y.-M., McNaughton, N.J., Groves, D.I., Luo, Z.-K., Huang, J.-Z., Miao, L.-C., Liu, Y.-K., 1998. Constraints on crustal evolution and gold metallogeny in the northwestern Jiaodong peninsula, China, from SHRIMP U–Pb zircon studies of granitoids. Ore Geology Reviews 13, 275–291.
Wang, X.-Z., Liang, H.-Y., Shan, Q., Cheng, J.-P., Xia, P., 1999. Metallogenic age of the Jinshan gold deposit and Caledonian gold mineralization in South China. Geological Review 45, 19–23 (in Chinese with English abstract).
Wang, Y.-T., Mao, J.-W., Lu, X.-X., Ye, A.-W., 2002. $^{40}Ar–^{39}Ar$ dating and geological implication of the auriferous altered rocks from the middle-deep section of the Q875 gold–quartz vein in the Xiaoqinling area, Henan, China. Chinese Sciences Bulletin 47, 1750–1755.
Wang, E., Meng, Q.-G., Burchfiel, B.C., Zhang, G.W., 2003. Mesozoic large-scale lateral extrusion, rotation, and uplift of the Tongbai–Dabie Shan belt in east China. Geology 31, 307–310.
Wang, Q., Wyman, D.A., Xu, J.-F., Zhao, Z.-H., Jian, P., Zi, F., 2007. Partial melting of thickened or delaminated lower crust in the middle of eastern China: implications for Cu–Au mineralization. Journal of Geology 115, 149–161.
Wang, T., Zheng, Y.-D., Zhang, J.-J., Zeng, L.-S., Donskaya, T., Guo, L., Li, J.-B., 2011. Pattern and kinematic polarity of late Mesozoic extension in continental NE Asia: prospectives from metamorphic core complexes. Tectonics 30, TC6007. http://dx.doi.org/10.1029/2011TC002896.
Watanabe, Y., Stein, H.J., 2000. Re-Os ages for the Erdenet and Tsagaan Suvarga porphyry Cu-Mo deposits, Mongolia, and tectonic implications. Economic Geology 95, 1537–1542.
Wilhem, C., Windley, B.F., Stampfli, G.M., 2012. The Altaids of Central Asia: a tectonic and evolutionary innovative review. Earth-Science Reviews 113, 303–341.
Williams, H.M., Turner, S.P., Pearce, J.A., Kelley, S.P., Harris, N.B.W., 2004. Nature of the source regions for post-collisional, potassic magmatism in southern and northern Tibet from geochemical variations and inverse element modeling. Journal of Petrology 45, 555–607.
Windley, B.F., Alexeiev, D., Xiao, W.-J., Kroner, A., Badarch, G., 2007. Tectonic models for accretion of the Central Asian Orogenic Belt. Journal of the Geological Society 164, 31–47.
Windley, B.F., Maruyama, S., Xiao, W.J., 2010. Delamination/thinning of subcontinental lithospheric mantle under eastern China: the role of water and multiple subduction. American Journal of Science 310, 1250–1293.
Wu, F.-Y., Lin, J.-Q., Wilde, S.A., Zhang, X.-O., Yang, J.-H., 2005. Nature and significance of the Early Cretaceous giant igneous event in eastern China. Earth and Planetary Science Letters 233, 103–119.
Wu, G., Sun, F.-Y., Zhu, Q., Li, Z.-L., Ding, Q.-F., Li, G.-Y., Pang, Q.-B., Wang, H.-B., 2006. Geological characteristics and genesis of gold deposits in Upper Heilongjiang basin. Mineral Deposits 25, 215 (in Chinese with English abstract).
Wu, F.-Y., Sun, D.-Y., Ge, W.-C., Zhang, Y.-B., Grant, M.L., Wilde, S.A., Jahn, B.-M., 2011. Geochronology of Phanerozoic granitoids in northeastern China. Journal of Asian Earth Sciences 41, 1–30.
Xiao, W.-J., Windley, B.F., Hao, J., Zhai, M.-G., 2003. Accretion leading to collision and the Permian Solonker suture, Inner Mongolia, China: termination of the central Asian orogenic belt. Tectonics 22. http://dx.doi.org/10.1029/2002TC001484.
Xiao, W.-J., Han, C.-M., Yuan, C., Sun, M., Lin, S.-F., Chen, H.-L., Li, Z.-L., Li, J.-L., Sun, S., 2008. Middle Cambrian to Permian subduction-related accretionary orogenesis of northern Xinjiang, NW China: implications for the tectonic evolution of central Asia. Journal of Asian Earth Sciences 32, 102–117.
Xiao, W.J., Windley, B.F., Huang, B.-C., Han, C.-M., Yuan, C., Chen, H.-L., Sun, M., Sun, S., Li, J.-L., 2009. End-Permian to mid-Triassic termination of the accretionary

Please cite this article as: Goldfarb, R.J., et al., Phanerozoic continental growth and gold metallogeny of Asia, Gondwana Research (2013), http://dx.doi.org/10.1016/j.gr.2013.03.002

processes of the southern Altaids: implications for the geodynamic evolution, Phanerozoic continental growth, and metallogeny of Central Asia. International Journal of Earth Sciences 98, 1189–1217.
Xiao, W.-J., Mao, Q.-G., Windley, B.F., Han, C.-M., Qu, J.-F., Zhang, J.-E., Ao, S.-J., Guo, G.-G., Cleven, N.R., Lin, S.-F., Shan, Y.-H., Li, J.-L., 2010. Paleozoic multiple accretionary and collisional processes of the Beishan orogenic collage. American Journal of Science 310, 1553–1594.
Xu, J.-H., Ding, R.-F., Xie, Y.-L., Zhong, C.-H., Yuan, X., 2005. Pure CO_2 fluids in the Sarekoubu gold deposit at southern margin of Altai Mountains in Xinjiang, West China. Chinese Science Bulletin 50, 333–340.
Xu, X.-W., Cai, X.-P., Xiao, Q.-B., Peters, S.G., 2007. Porphyry Cu–Au and associated polymetallic Fe–Cu–Au deposits in the Beiya area, western Yunnan Province, south China. Ore Geology Reviews 31, 224–246.
Xue, C.-J., Zhao, Z.-F., Wu, G.-G., Dong, L.-H., Feng, J., Zhang, Z.-C., Zhou, G., Chi, G.-X., Gao, J.-G., 2010. The multi-periodic superimposed porphyry copper mineralization in Central Asian Tectonic Region: a case study of geology, geochemistry and chronology of the Halasu copper deposit, Southeastern Altai, China. Earth Science Frontiers 17, 53–82.
Yakubchuk, A., 2002. The Baikalide–Altaid, Transbaikal–Mongolian and North Pacific orogenic collages: similarity and diversity of structural patterns and metallogenic zoning. Geological Society of London Special Publication 206, 273–297.
Yakubchuk, A., 2008. Re-deciphering the tectonic jigsaw puzzle of northern Eurasia. Journal of Asian Earth Sciences 32, 82–101.
Yakubchuk, A., 2010. Global orogenic gold and related metallogeny through time. Society of Economic Geologists 2010 Conference, Keystone, Colorado (Poster abstract A-52).
Yakubchuk, A.S., Edwards, A.C., 1999. Auriferous Paleozoic accretionary terranes within the Mongol–Okhotsk suture zone, Russian Far East. Australasian Institute of Mining and Metallurgy, PACRIM '99, Bali, Indonesia, pp. 347–358.
Yakubchuk, A., Cole, A., Seltmann, R., Shatov, V., 2002. Tectonic setting, characteristics, and regional exploration criteria for gold mineralization in the Altaid orogenic collage: the Tien Shan province as a key example. Society of Economic Geologists Special Publication 9, 177–201.
Yakubchuk, A.S., Shatov, V.V., Kirwin, D., Edwards, A., Tommurtogoo, O., Badarch, G., Buryak, V.A., 2005. Gold and base metal metallogeny of the central Asian orogenic supercollage. Economic Geology 100th Anniversary Volume. 1035–1068.
Yakubchuk, A., Schloderer, J., Woodcock, J., Wurst, A., 2010. Taldybulak Au–Cu–Mo deposit: a new >5 Moz Au (11.7 Moz Au eq) Ordovican porphyry hosted gold system in Kyrgyzstan, Central Asia. Applied Earth Science, Transactions of the Institute of Mining and Metallurgy, Section B 119, 84.
Yan, F., Qi, J., Guo, J., 2010. Geology and Exploration of Yangshan Gold Deposit in Gansu Province. Geological Publishing House, Beijing (in Chinese with English abstract).
Yang, W., Zhang, H.-F., 2012. Zircon geochronology and Hf isotopic composition of Mesozoic magmatic rocks from Chizhou, the Lower Yangtze Region: constraints on their relationship with Cu–Au mineralization. Lithos 150, 37–48.
Yang, J.-H., Wu, F.-Y., Chung, S.-L., Lo, C.-H., Wilde, S.A., Davis, G.A., 2007. Rapid exhumation and cooling of the Liaonan metamorphic core complex: inferences from $^{40}Ar/^{39}Ar$ thermochronology and implications for Late Mesozoic extension in the eastern North China Craton. Geological Society of America Bulletin 119, 1405–1414.
Yang, F.-Q., Mao, J.-W., Bierlein, F.P., Pirajno, F., Zhao, C.-H., Ye, H.-S., Liu, F., 2009a. A review of the geological characteristics and geodynamic mechanisms of Late Mesozoic epithermal deposits in North Xinjiang, China. Ore Geology Reviews 35, 217–234.
Yang, Z.-S., Hou, Z.-Q., Meng, X.-J., Liu, Y.-C., Fei, R.-C., Tian, S.-H., Li, Z.-Q., Gao, W., 2009b. Post-collisional Sb and Au mineralization related to the South Tibetan detachment system in Himalayan orogen. Ore Geology Reviews 36, 194–212.
Yang, D.-S., Li, X.-H., Li, W.-X., Liang, X.-Q., Long, W.-G., Xiong, X.-L., 2010. U–Pb and $^{40}Ar–^{39}Ar$ geochronology of the Baiyunshan gneiss (central Guangdon, south China): constraints on the timing of early Paleozoic and Mesozoic tectonothermal events in the Wuyun (Wuyi–Yunkai) Orogen. Geological Magazine 147, 481–496.
Yang, S.-Y., Jiang, S.-Y., Li, L., Sun, Y., Sun, M.-Z., Bian, L.-Z., Xiong, Y.-G., Cao, Z.-Q., 2011. Late Mesozoic magmatism of the Jiurui mineralization district in the Middle–Lower Yangtze River Metallogenic Belt, Eastern China: precise U–Pb ages and geodynamic implications. Gondwana Research 20, 831–843.
Yang, S.-J., Duuring, P., Kim, Y.-S., 2012. Structural genesis of the Eunsan and Moisan low-sulphidation epithermal Au–Ag deposits, Seongsan district, Southwest Korea. Mineralium Deposita. http://dx.doi.org/10.1007/s00126-012-0443-2.
Yin, A., Harrison, T.M., 2000. Geologic evolution of the Himalaya–Tibetan orogeny. Annual Review of Earth and Planetary Sciences 28, 211–280.
Yin, A., Nie, S.-Y., 1996. A Phanerozoic palinspastic reconstruction of China and its neighboring regions. In: Yin, A., Harrison, T.M. (Eds.), The Tectonic Evolution of Asia. Cambridge University Press, Cambridge, pp. 442–485.
Yoo, B.-C., Lee, H.-K., White, N.C., 2010. Mineralogical, fluid inclusion, and stable isotope constraints on mechanisms of ore deposition at the Samgwang mine (Republic of Korea): a mesothermal, vein-hosted gold–silver deposit. Mineralium Deposita 45, 161–187.
Yu, C.-T., Jia, B., 1989. Study on the genesis of major types of gold deposits and its mechanism of formation in eastern Hebei. Contributions to the Project of Regional Metallogenetic Conditions of Main Gold Deposit Types in China. 2: Eastern Hebei Province. Geological Publishing House, Beijing, pp. 99–146 (in Chinese with English summary).
Yudovskaya, M.A., Distler, V.V., Rodionov, N.V., Mokhov, A.V., Antonov, A.V., Sergeev, S.A., 2011. Geology of ore deposits: relationship between metamorphism and ore formation at the Sukhoi Log gold deposit hosted in black slates from the data of U–Th–Pb isotopic SHRIMP-dating of accessory minerals. Geology of Ore Deposits 53, 32–64.
Zaw, K., Kamvong, Khositanont, S., Mernagh, T.P., 2011. Oxidized vs reduced Cu–Au skarn formation and implication for exploration, Loei and Troung Son Fold Belts, SE Asia. International Conference on Geology, Geotechnology and Mineral Resources of Indochina (Geoindo 2011), Khon Kaen, Thailand, pp. 97–100.
Zeng, P.-S., Mo, X.-X., Yu, X.-H., Hou, Z.-Q., Xu, Q.-D., Wang, H.-P., Li, H., Yang, C.Z., 2003. Porphyry deposits and porphyry copper of Zhongdian area in northwest Yunnan. Mineral Deposits 22, 325–333 (in Chinese with English abstract).
Zeng, P.-S., Wang, H.-P., Mo, X.-X., Yu, X., Li, W., 2004. Tectonic setting and prospects of porphyry copper deposits in Zhongdian island–arc belt. Acta Geoscientica Sinica 25, 535–540 (in Chinese with English abstract).
Zeng, Q.-D., Liu, J.-M., Yu, C.-M., Ye, J., Liu, H.-T., 2011. Metal deposits in the Da Hinggan Mountains, NE China: styles, characteristics, and exploration potential. International Geology Review 53, 846–878.
Zeng, Q.-T., Evans, N.J., McInnes, B.I.A., Batt, G.E., McCuaig, C.T., Bagas, L., Tohver, H., 2012a. Geological and thermochronological studies of the Dashui gold deposit, West Qinling Orogen, Central China. Mineralium Deposita. http://dx.doi.org/10.1007/s00126-012-0433-4.
Zeng, Q.-T., McCuaig, T.C., Hart, C.J.R., Jourdan, F., Muhling, J., Bagas, L., 2012b. Structural and geochronological studies on the Liba goldfield of the West Qinling Orogen, Central China. Mineralium Deposita. http://dx.doi.org/10.1007/s00126-011-0398-8.
Zhai, W., Li, Z.-H., Sun, X.-M., Huang, D.-L., Liang, J.-L., Miao, L.-C., 2006. SHRIMP zircon U–Pb dating of the Hetai gold deposit in western Guangdong, China and geological implications. Geological Review 52, 690–699 (in Chinese with English abstract).
Zhang, K.-J., Cai, J.-X., 2009. NE–SW-trending Hepu–Hetai dextral shear zone in southern China: penetration of the Yunkai Promontory of South China into Indochina. Journal of Structural Geology 31, 737–748.
Zhang, G.-L., Boulter, C.A., Liang, J.-C., 2001. Brittle origins for disseminated gold mineralization in mylonite: Gaocun gold deposit, Hetai goldfield, Guangdong province, South China. Economic Geology 96, 49–59.
Zhang, D.-Q., She, H.-Q., Li, D.-X., Feng, C.-Y., 2003a. The porphyry–epithermal metallogenic system in the Zijinshan region, Fujian Province. Acta Geologica Sinica 77, 253–261.
Zhang, X.-H., Wang, H., Ma, Y.-J., 2003b. $^{40}Ar/^{39}Ar$ constraints on two NNE-trending ductile shear zones, Yanshan intraplate orogen, North China Craton. International Geology Review 45, 936–947.
Zhang, L.-C., Xiao, W.-J., Qin, K.-Z., Ji, J.-S., Yang, X.-K., 2004. Types, geological features and geodynamic significances of gold–copper deposits in the Kanggurtag metallogenic belt, eastern Tianshan, NW China. International Journal of Earth Sciences 93, 224–240.
Zhang, X.-H., Liu, Q., Ma, Y.-J., Wang, H., 2005a. Geology, fluid inclusions, isotope geochemistry, and geochronology of the Paishanlou shear zone-hosted gold deposit, North China Craton. Ore Geology Reviews 26, 325–348.
Zhang, Y.-H., Zhang, S.-H., Han, Y.-G., Pirajno, F., 2005b. Low-sulphidation epithermal gold-bearing Qiyugou breccia pipes, Xiong'ershan mountains, China. In: Mao, J.-W., Bierlein, F.P. (Eds.), Mineral Deposit Research: Meeting the Global Challenge: Proceedings of the Eighth Biennial SGA Meeting. Springer, Berlin, pp. 1111–1113.
Zhang, H.-Y., Hou, Q.-L., Cao, D.-Y., 2007. Study of thrust and nappe tectonics in the eastern Jiaodong Peninsula, China. Science in China Series D: Earth Sciences 50, 161–171.
Zhang, H.F., Li, S., Li, Z., 2008. Timing of Jinchang porphyry gold deposit, eastern Heilongjian province, Northeast China. Geachimica et Cosmochimica Acta 72, A1082.
Zhang, D.-Q., She, H.-Q., Feng, C.-Y., Li, D.-X., Li, J.-W., 2009a. Geology, age, and fluid inclusions of the Tanjianshan gold deposit, western China: two orogenies and two gold mineralizing events. Ore Geology Reviews 36, 250–263.
Zhang, S.H., Zhao, Y., Song, B., Hu, J.M., Liu, S.W., Yang, Y.H., Chen, F.K., Liu, X.M., Liu, J., 2009b. Contrasting Late Carboniferous and Late Permian-Middle Triassic intrusive suites from the northern margin of the North China craton: geochronology, petrogenesis, and tectonic implications. Geological Society of America Bulletin 121, 181–200.
Zhang, J.-H., Shan, G., Ge, W.-C., Wu, F.-Y., Yang, J.-H., Wilde, S., Li, M., 2010a. Geochronology of the Mesozoic volcanic rocks in the Great Xing'an Range, northeastern China: implications for subduction-induced delamination. Chemical Geology 276, 144–165.
Zhang, Z.-C., Mao, J.-W., Wang, Y., Pirajno, F., Liu, J.-L., Zhao, Z., 2010b. Geochemistry and geochronology of the volcanic rocks associated with the Dong'an adularia–sericite epithermal gold deposit, Lesser Hinggan Range, Heilongjiang Province, NE China: constraints on the metallogenesis. Ore Geology Reviews 37, 158–174.
Zhang, J., Chen, Y.-J., Yang, Y., Deng, J., 2011. Lead isotope systematics of the Weishancheng Au-Ag belt, Tongbai Mountains, central China: implications for ore genesis. International Geology Review 53, 656–676.
Zhang, G.-B., Yang, Y.-C., Wang, J., Wang, K.-Y., Ye, S.-Q., 2013. Geology, geochemistry, and genesis of the hot-spring-type Sipingshan gold deposit, eastern Heilongjiang province, Northeast China. International Geology Review 55, 482–495.
Zhao, Y., Bi, C., Zou, X., Sun, Y., Du, A., Zhao, Y., 1997. The Re-Os isotopic age of molybdenite from Duobaoshan and Tongshan porphyry copper (molybdenum) deposits. Acta Geoscientia Sinica 8, 61–67 (in Chinese with English abstract).
Zhao, Y.-M., Zhang, Y.-N., Bi, C.-S., 1999. Geology of gold-bearing skarn deposits in the Middle and Lower Yangtze River Valley and adjacent regions. Ore Geology Reviews 14, 227–240.
Zhao, J.-H., Zhou, M.-F., Yan, D.-P., Zheng, J.P., Li, J.-W., 2011. Reappraisal of the ages of Neoproterozoic strata in South China: no connection with the Grenvillian orogeny. Geology 39, 299–302.
Zhou, J.-B., Wilde, S.A., 2013. The crustal accretion history and tectonic evolution of the NE China segment of the Central Asian Orogenic belt. Gondwana Research. http://dx.doi.org/10.1016/j.gr.2012.05.012.
Zhou, T.-H., Goldfarb, R.J., Phillips, G.N., 2002. Tectonics and distribution of gold deposits in China: an overview. Mineralium Deposita 37, 249–282.
Zhou, X.-M., Sun, T., Shen, W.-Z., Shu, L.-S., Niu, Y.-L., 2006. Petrogenesis of Mesozoic granitoids and volcanic rocks in South China: a response to tectonic evolution. Episodes 29, 26–33.
Zhou, J.-B., Wilde, S.A., Zhang, X.-Z., Zhao, G.-C., Zheng, C.-Q., Wang, Y.-J., Zhang, X.-H., 2009. The onset of Pacific margin accretion in NE China: evidence from the Heilongjiang high-pressure metamorphic belt. Tectonophysics 478, 230–246.

Please cite this article as: Goldfarb, R.J., et al., Phanerozoic continental growth and gold metallogeny of Asia, Gondwana Research (2013), http://dx.doi.org/10.1016/j.gr.2013.03.002

Zhou, Q., Jiang, Y.-H., Zhao, P., Liao, S.-Y., Jin, G.-D., Liu, Z., Jia, R.-Y., 2012. SHRIMP U-Pb dating on hydrothermal zircons: evidence for an Early Cretaceous epithermal event in the Middle Jurassic Dexing porphyry copper deposit, southeast China. Economic Geology 107, 1507–1514.
Zhu, Y., 2000. Features of minerogenic series related to continental volcanic rocks in the southeastern coastal areas of China: a case study of the Daiyunshan-Shiniushan volcanic depression in Fujian. Acta Geologica Sinica 74, 492–499.
Zhu, D.-C., Zhao, Z.-D., Niu, Y.-L., Dilek, Y., Mo, X.-X., 2011. Lhasa terrane in southern Tibet came from Australia. Geology 39, 727–730.
Zonenshain, L.P., Kuzmin, M.I., Natapov, L.M., 1990. Geology of the USSR: a plate-tectonic synthesis. American Geophysical Union Geodynamic Series, 21 (242 pp.).
Zorin, Y.A., Mazukabzov, A.M., Gladkochub, D.P., Donskaya, T.V., Presnyakov, S.L., Sergeev, S.A., 2008. Silurian age of major folding in Riphean deposits of the Baikal–Patom Zone. Doklady Earth Sciences 423, 1235–1239.
Zorin, Y.A., Sklyarov, E.V., Belichenko, V.G., Mazukabzov, A.M., 2009. Island arc–back-arc basin evolution: implications for Late Riphean–early Paleozoic geodynamic history of the Sayan–Baikal folded area. Russian Geology and Geophysics 50, 149–161.

Richard J. Goldfarb is a senior research geologist with the Minerals Program of the U.S. Geological Survey, where he has been employed for more than 30 years. Rich's major expertise has been on the geochemistry and geology of ore deposits with emphasis on Phanerozoic lode gold. In recent years, Rich has conducted detailed studies on the understanding of the distribution of gold deposits through space and time, compiling the most comprehensive global description of their distribution and evaluating the controlling tectonic/geologic features. He has BSc in geology from Bucknell University (1975), MS in hydrology from MacKay School of Mines (1981), and PhD in geology from the University of Colorado (1988).

Ryan D. Taylor is a research geologist with the Minerals Program of the U.S. Geological Survey and a PhD student at Colorado School of Mines. He obtained his BS (2006) and MS (2008) in geology from Northern Arizona University. His general research interests include geochronology and geochemistry of ore deposits. Much of his work is focused on lode gold deposits and porphyry deposits of the western cordillera of North America, from California to Alaska. This includes correlating the timing of formation of these deposits with the tectonic evolution of the region and the processes that result in ore deposition in a regional framework.

Greg S. Collins is currently the General Manager — Exploration/Chief Geologist for Eldorado Gold in China and has worked in the China/Mongolia region since 2004. Prior to this he worked in the industry throughout Australia, exploring for a wide range of base and precious metal deposits. He has been a professional geologist for more than 20 years, having held senior roles with companies such as North Limited, East Asia Minerals and more recently as China Exploration Manager for Anglogold Ashanti.

N.A. Goryachev (CSEGF, SGA, GSAustralia, Russian Geological and Mineralogical Societies) completed his Ph.D. thesis in 1985 in Moscow State University and his Doctor of Science thesis in 2000. Since 1985 he has been working in NEISRI FEB RAS, Magadan, occupying currently a position of Director. He is a professor of the geological department of North-East State University in Magadan. His principal experience is geology and tectonic setting of gold lode deposits, metallogeny of gold. Publications include more than 200 papers both in Russian and International Journals and Monographs. Field experience is related to researches in Far East Russia, Altay, Transbaikalia, Alaska (USA), Yukon (Canada), Finland, Mongolia. He was co-leader of the long-term international project Tectonics and Metallogenesis Russian Far East, Alaska, western Canada (Russia, USA, Canada). SEG VP Lecturer in 2007. SEG Regional VP on Northern Eurasia 2009–2012.

Omero Felipe Orlandini is pursuing a degree in Geology at the University of Colorado at Boulder. He graduated with a Bachelor's degree of History from the same institution in 2008, and spent the intervening years living and traveling in the People's Republic of China and greater Asia where he discovered an interest in economic geology.

Please cite this article as: Goldfarb, R.J., et al., Phanerozoic continental growth and gold metallogeny of Asia, Gondwana Research (2013), http://dx.doi.org/10.1016/j.gr.2013.03.002